EVALUATION OF PROBIOTICS AND FOOD CONTAMINANTS ON THE GASTROINTESTINAL TRACT INTEGRITY AND IMMUNE HOMEOSTASIS VIA ALTERATION OF GUT MICROBIOME

SHUM TIM FAT

PhD

The Hong Kong Polytechnic University

2022

The Hong Kong Polytechnic University
Department of Applied Biology and Chemical Technology

Evaluation of Probiotics and Food Contaminants on the Gastrointestinal Tract Integrity and Immune Homeostasis via Alteration of Gut Microbiome

Shum Tim Fat

A thesis submitted in partial fulfillment of the requirements for
the degree of Doctor of Philosophy
May 2022

CERTIFICATE OF ORIGINALITY

I hereby declare that this thesis is my own work and that, to the best of my knowledge and belief, it reproduces no material previously published or written, nor material that has been accepted for the award of any other degree or diploma, except where due acknowledgment has been made in the text.

Signature: _____

Name of Student: Shum Tim Fat

Abstract

Gut microbiota is considered as a “forgotten organ” which plays important roles on the health and disease status of human. The composition of microbiota could be affected by various factors such as probiotics, antibiotics, diet, and personal living style. This study aims to determine (1) the beneficial effect of in-house probiotic isolates on the gut integrity and immune homeostasis; and (2) the potential impact of food contaminants on the intestinal epithelium and its subsequent influence on the immune response.

Probiotics have been known to modulate the gut microbiota and involve in promoting barrier function and immunomodulation of gastrointestinal (GI) tract. The first part of this study aims to characterize the ability of GI colonization of probiotics isolated in our laboratory, demonstrate the protective effects on the GI epithelial integrity and ability of immunomodulation from intestinal to systemic regions by the selected novel probiotic isolates. With full length 16S rDNA sequence matching with *Lactobacillus rhamnosus*, S1 was selected for the mentioned investigation using Simulator of Human Intestinal Microbial Ecosystem (SHIME) and Sprague Dawley (SD) rat model. 16S rDNA analyses showed that, S1 treatment to both SHIME and SD rats promoted the relative abundance of commensal genus *Bacteroides*. Several taxa that have been reported associated with inflammatory diseases were reduced by S1 treatment. *Megasphaera* spp. was reduced in distal colon of SHIME, whereas an unclassified genus under family *Prevotellaceae* (*f__Prevotellaceae*), *Clostridia UCG-014* and *Streptococcus* were decreased in SD rats after S1 treatment. These mentioned taxa have been reported associated with inflammatory diseases. The extract of S1-treated SHIME distal colon promoted the trans-epithelial electrical resistance (TEER) (up to 26%) and occludin expression (+39%) of cultural enterocyte (Caco-2), suggesting the enhancement of epithelial integrity. Meanwhile, S1-treated SD rats expressed higher anti-inflammatory cytokine IL-10 in their colonic tissue, mesenteric lymph node cells, and splenic mononuclear cells in *ex-vivo* cultures. The results showed that *L. rhamnosus* S1 can modify the gut original microbiota of both human and murine.

S1 protects intestinal epithelial integrity and modulates immunity, which could serve as a promising probiotic for human health.

Another part of the study was related to food contaminants, microplastics (MP) and plasticizers. Use of plasticware in the daily life has become one of the inevitable essentials for many modern societies due to the convenience and economic reasons. Recent studies have demonstrated that microplastic and plasticizers are present in different food products and drinking water, in which some of those have been shown to interfere the GI microbiota, immunity, endocrine system and reproductive organ developments in the animal models. However, the studies to investigate the impacts of MP and plasticizer on human-origin gut microbiota, and the subsequent influences on the gut barrier function and immunomodulation are rather limited. The second part of this study is to investigate the impact of plasticizers including di(2-ethylhexyl) phthalate (DEHP) and di-iso-nonyl phthalate (DINP), and MPs including polyvinyl chloride (PVC) and polyethylene (PE) on the human gut microbiota. DINP promoted the relative abundance of *Escherichia-Shigella* spp. and *Streptococcus* spp., whereas *Megasphaera* spp. was reduced in the human *in vitro* GI tract. Extracts from the treatment of high DINP dosages (1.68 μg/ml and 16.8 μg/ml) reduced the expression levels of anti-inflammatory genes of RAW264.7, claudin-4, JAM-A and E-cadherin of HT-29, yet the same treatment enriched claudin-2. By contrast, extract from the treatment of DEHP promoted pore-forming claudin-2 in HT-29, and induced microbiota compositional changes similar to those observed in the patients of inflammatory bowel diseases (IBDs). Since plasticizers are commonly used in PVC softening, assessment was expanded to PVC and DEHP/PVC. The distal colon with PVC treatment had a relatively comparable microbiota to that of the control. Augmented relative abundance of pro-inflammatory taxon *Collinsella* spp. was observed in both DEHP and DEHP/PVC fermenters, whereas health-associated short-chain fatty acid producer *Coprococcus* spp. was reduced the most in the gut

microbiota treated with PVC or DEHP. Furthermore, the extract of high dosage of DEHP/PVC decreased occludin by and trans epithelial electrical resistance (TEER) by 13% in Caco-2.

Finally, another MP selected for study is PE as it is widely used in multiple plasticware which leads to high exposure frequency to human. Consistently, the occludin expression was reduced by 23% in the Caco-2 cells treated with the extract from PE batch culture. The SHIME was further adopted to study the effect of PE on the human gut microbiota in this part of study. Though gene expressions of major tight junction and adherens junction remained stable, the extract of PE-treated SHIME distal colon promoted the enterocyte barrier permeability (26%) of cultured Caco-2. The detailed relationships and mechanisms between the biochemical alterations and particular bacterial taxon remains to be elucidated in the future.

Acknowledgements

I wish to express my sincere gratitude to my chief supervisor, Dr. Amber Chiou. She gave me the chance in pursuing my study further in the biotechnology filed, and numerous research and critical thinking skills. I am thankful to my co-supervisor, Prof. Wong Man Sau, who had provided comments and alternatives of research targets when I took the confirmation examination. I am extremely grateful to all the laboratory members in Y1303 and Y1123. Dr. Erin Tse and Dr. Haicui Wu taught me lots of basic bacterial and mammalian cultural techniques, and gene / protein expression comparison assays. Mr. Theo Lam and Ms. Liwen Wang helped me a lot in in-silicon microbiota analysis and batch / SHIME fermenter management.

I would also like to thank all the technicians and Scientific officers in the University Research Facility in Life Sciences (ULS), University Research Facility in Chemical and Environmental Analysis (UCEA) and Department of Applied Biology and Chemical Technology (ABCT) of The Hong Kong Polytechnic University. Their prompt responses and professional trainings helped me to tackle problems in different assays. And finally, my deep appreciation to all my family members. They take care of me and give me emotional support, allow me to focus on my study for these so many years.

Table of contents

List of Figures

Chapter 1

Chapter 2

Chapter 3

Chapter 4

Chapter 5

Chapter 6

List of Tables

Chapter 1

Chapter 2

Chapter 3

Chapter 4

Chapter 5

List of Abbreviations

AC	Ascending colon of SHIME
Ace	Adhesin to collagen
AIEC	Adherent-invasive E. coli
AJ	Adherens junction
AP-1	Activator protein 1
APC	Antigen presenting cell
AS	Aggregation substance
BCA	Bicinchoninic acid
BHI	Brain-heart infusion
cDNA	Complementary DNA
CFU	Colony forming unit
CATC	Citrate azide Tween 80 carbonate
CeD	Celiac disease
Cna	Collagen-binding protein
CRCs	Colorectal cancers
DC	Descending colon of SHIME; Distal colon of SHIME
DEHP	Di(2-ethylhexyl) phthalate

DINP	Di-iso-nonyl phthalate
DMEM	Dulbecco’s modified Eagle’s medium
DnOP	Di-n-octyl phthalate
DSS	Dextran sulfate sodium
EEN	Exclusive enteral nutrition
EFSA	European Food Safety Authority
ELISA	Enzyme-linked immunosorbent assay
EMT	Epithelial–mesenchymal transition
FBS	Fetal bovine serum
FDA	Food and Drug Administration
GC-FID	Gas Chromatograph-Flame Ionization Detection
GI tract	Gastrointestinal tract
GPR	G protein-coupled receptor
GRAS	Generally regarded as safe
IBD	Inflammatory bowel disease
IBS-D	Diarrhea dominant irritable bowel syndrome
IFN-γ	Interferon-γ
IL	Interleukin

IL-1Ra	Interleukin-1 receptor antagonist
IRF4	Interferon regulatory factor-4
LAB	Lactic acid bacterium
LPS	Lipopolysaccharide
LPXTG	Leucine-Proline-(any amino acid)-Threonine-Glycine motif for sortase recognition
M1	Classically activated macrophage
M2	Alternative activated macrophage
mCATC	Modified Citrate azide Tween 80 carbonate
MEHP	Mono-(2-ethylhexyl) phthalate
MLN	Mesenteric lymph node
mMRS	Modified de Man, Rogosa and Sharpe
mMSA	Modified Mannitol salt agar
MP	Microplastic
MRC1	Mannose Receptor C-Type 1
MRS	De Man, Rogosa and Sharpe
MRSA	Methicillin-resistant *Staphylococcus aureus*
MSA	Mannitol salt agar
MSCRAMM	Microbial surface component recognizing adhesive matrix molecules

MTT	3-(4,5-dimethylthiazol-2-yl)-2,5-diphenyltetrazolium bromide
MUB	Mucin-binding protein
MucBP	Mucin-binding protein
NF-κB	Nuclear factor kappa-light-chain-enhancer of activated B cells
OD	Optical density at 600nm
PBS	Phosphate-buffered saline
PCoA	Principal coordinate analysis
PE	Polyethylene
PET	Polyethylene terephthalate
pd	Phylogenetic distance
PP	Peyer's patch
PCR	Polymerase chain reaction
PS	Polystyrene
PVC	Polyvinyl chloride
QPS	Qualified presumption of safety
RCM	Reinforced clostridial medium
rDNA	Ribosomal DNA
RGD-motif	Arginine-Glycine-Aspartate motif

ROS	Reactive oxygen species
SCFAs	Short-chain fatty acids
SD	Sprague Dawley
SHIME	Simulator of the Human Intestinal Microbial Ecosystem
SOD	superoxide dismutase
SpaCBA	Sortase-mediated pilus composed by subunits SpaC, SpaB and SpaA
SpaFED	Sortase-mediated pilus composed by subunits SpaF, SpaE and SpaD
Sob	Observed species
SOCS3	Suppressor of cytokine signaling-3
STAT1	Signal transducer and activator of transcription-1
TBST	Tris buffered saline with 0.1% Tween 20
TC	Transverse colon
TEER	Trans epithelial electrical resistance
TGF-β	Transforming growth factor beta
TGM2	Transglutaminase-2
Th17	T helper 17
TJ	Tight junction
TLR	Toll-like-receptor

TNBS	Trinitrobenzene sulfonic acid
TNF-α	Tissue necrosis factor-alpha
UHMWPE	Ultra-high molecular weight polyethylene
ZO	Zonula occluden

Chapter 1 – Introduction

1. Gut Microbiome

1.1. Gut microbiome

Microbiome describes the overall genetic materials, proteins and metabolites from a particular ecosystem including all the microorganisms within it. Gut microbiome is one of the major microbiological research areas that covers the study of organisms inhabiting the digestive system. Gut microbiota, referring to the microorganisms including bacteria, virus and fungi, is the largest microbiota niche in the human body. Gut flora is composed of approximately 10^{13} to 10^{14} bacteria. In this huge number of bacteria, there are beneficial, commensal and pathogenic microorganisms. Among this ecosystem, colon mucosa has the largest number of microbial colonization, so is the antigen load. With the largest microbiome in human body, the gastrointestinal (GI) tract harbors numerous microorganisms which have been suggested to be closely related to the pathophysiology of different metabolic and inflammatory diseases in human.

Various kinds of bacteria can adhere onto the mucosal layer or even to the epithelial enterocytes, exerting diverse physiological effects to the host. Imbalanced pro-/anti- inflammatory cytokines productions may contribute to the development of chronic inflammation and malignant processes in GI tract. Owing to the ability of altering pro-/anti- inflammatory cytokine expression profile in gut epithelium, dysbiosis in GI tract thus markedly aggravates these health issues. Rapid and dynamic changes can be resulted from host genetics, diet or emotion.

Microbiota metabolites include multiple substances produce and secrete by bacteria according to different environmental stimulations. Soluble substances produced by gut microbiota may influence host cell as they can be absorbed along with nutrients. In the GI tract, bacteria may produce free amino acids (threonine, lysine and glutamate), amino acid metabolites (indole compounds, ornithine and urea), secondary bile salts (deoxycholic acid and lithocholic acid), metabolic products such as acetate, pyruvate, succinate and citrate [1, 2]. Meanwhile, vitamin A and a variety of vitamin B (Thiamine, folate, biotin, riboflavin, and pantothenic acid) could also be synthesized by gut bacteria [3]. Metabolic profiles of a microbial niche are greatly influenced by the composition of bacteria.

A balanced ratio of colonized probiotics, commensals and pathogens in the GI tract is described as gut homeostasis, which when being destroyed would lead to gut dysbiosis and contributes to the onset or progression of various kinds of illnesses such as infection, obesity, diabetes, and cardiovascular diseases, etc. [4-6]. It has been reported that microbiota of obese people have a lower F/B ratio whereas IBDs patients have a higher one [7, 8]. Bacterial phylum *Firmicutes* exerts beneficial effects by metabolites short-chain fatty acids (SCFAs) which has been found promoting central nervous system's health and preventing colorectal cancers (CRCs). Recent studies have started to investigate possibility of treating various kinds of diseases by reversing GI dysbiosis through fecal microbiota transplantation (FMT). There are encouraging results in treating *Clostridium difficile* or inflammatory bowel diseases (IBDs) using FMT [9, 10]. Unfortunately, there is evidence showing possible infection of Severe Acute Respiratory Syndrome Coronavirus 2 (SARS-CoV-2) in the GI tract, which makes FMT treatment processes more complicated and challenging since there is still limited data suggesting whether residual viral remains would be infectious after fecal transplantation [11]. Meanwhile, other therapeutic methods and agents such as antibiotics, probiotics and monoclonal antibody biologics are required to be developed at the same time.

Table 1.1. Role(s) and function(s) of commonly detected bacterial genus and species

Bacteria	**Examples of role(s) or function(s)**
Lactobacillus	Produces anti-microbial substances such as lactic acid and bacteriocin
Bifidobacterium	Strengthens gut barrier function
Akkermansia muciniphila	Ameliorates atherosclerosis, colitis, obesity, diabetes and liver cancer
Bacteroides	Effects on gut barrier function and immune homeostasis are strain-specific
Parabacteroides	Provides anti-inflammatory effect to host enterocytes
Blautia	SCFAs producer mediates anti-inflammation and provides direct energy to enterocyte
Dorea	SCFAs producer mediates anti-inflammation and provides direct energy to enterocyte
Roseburia	Negatively correlated with Crohn's Disease and more abundant in IBDs patients in remission
Faecalibacterium prausnitzii	Negatively correlated with Crohn's Disease
Staphylococcus aureus	Opportunistic pathogen that is able to colonize all mucosal layer in human body
Enterococcus faecalis	Possesses multiple adhesion factor for attachment on endocardium
Campylobacter jejuni	Able to invade epithelial cells and access to bloodstream causing sepsis
Helicobacter pylori	Causes gastric and duodenal ulcer in approximately 30% of Hong Kong people
Prevotella	Positively correlated with diarrhea predominant-irritable bowel syndrome and inflammatory bowel diseases

1.2. Beneficial, commensal and pathogenic bacteria

1.2.1 Beneficial bacteria

Among GI microorganisms, some beneficial microbes have been known to modify the gut microbiota and involve in the immunomodulation in GI tract (Table 1.1). Some of the beneficial bacteria has been recognized as "Probiotics", which by the definition of WHO/FAO is "live strains of strictly selected microorganisms which, when administered in adequate amounts, confer a health benefit on the host"[12]. The idea of probiotic was proposed in early 1900s due to the observation of long-lived lactic acid bacteria. It is suggested that probiotics can provide beneficial effects to human health when taken in an appropriate amount. Some well-known probiotics include *Lactobacilli* and *Bifidobacteria*. Beneficial microbes including probiotics compete with pathogens for adhesion binding sites on the intestinal mucosa, some may also produce anti-pathogenic secretion including lactic acid and bacteriocins [13, 14]. In addition to competitive adhesion, they were also found contributing to the alleviation of diarrhea, ulcers, depression, obesity and cardiovascular disorders, etc. [15-18]. Multiple beneficial effects on human health provided by probiotic species promoted next generation probiotics research in recent years, for example, *Akkermansia muciniphila* was isolated and studied for the safety and feasibility of ameliorating atherosclerosis, colitis, obesity and diabetes [5, 19-21].

1.2.2 Commensal bacteria

Benign commensals inhabit themselves in GI mucosa layer for shelter and obtaining nutrients for survival. Most of their exact roles in GI tract are unclear and remained to be elucidated. The existence of commensals occupies molecular binding sites and resources available on both intestinal mucus and epithelial layers, thus preventing infectious pathogens from settling down and expanding to the minimum number of effective infections. In addition to occupying different cell binding receptors, some *Bacteroides* and *Parabacteroides* species have been demonstrated to harbor anti-inflammatory effect to host [22]. Commensals from genus *Blautia*, *Dorea*, *Roseburia* and *Faecalibacterium* are commonly found SCFA producers in human GI microbiota, in which *Roseburia* spp. and *Faecalibacterium prausnitzii* have been found negatively correlated with Crohn's disease (CD) [20, 23, 24]. Generally, SCFA producers contribute to immunosuppression which helps to maintain immune homeostasis in GI tract. Direct administration of butyrate into colonic region can reduce inflammatory severity of UC by re-balancing IL-10/IL-12 level which contributes to prolong remission of IBDs [25].

1.2.3 Opportunistic pathogens and pathogens

Pathogens in GI tract are infectious agents that can exert harmful effects in host. These bacteria may produce toxins or invade host cells, in turn stimulating humoral or cell-mediated immune responses. Various kinds of infectious bacteria have different pathogenicity causing diseases with different severities. Acute infection may occur when highly invasive pathogens penetrate the circulatory system. To exert certain effects on host, for example, *Staphylococcus aureus*, *Campylobacter jejuni* and *Enterococcus faecalis*, can grow and expand their amount in the GI ecosystem through adhering or even invading to the epithelial cells, then traveling and infecting various organs such as liver, endocardium and brain [26, 27]. *Helicobacter pylori* harbors in the host stomach and duodenum causing acute or chronic inflammation. Such chronic inflammation may result gastric and duodenal ulcer or even gastric cancer. Study estimated that approximate 30% of Hong Kong people and more than half of the population in Asia are *H. pylori* carriers [28]. Meanwhile, gut microbiota harbors pro-inflammatory species that may stimulate pro-inflammatory cytokine produced by immune cells, leading to tissue destruction around the affected area. Chronic low-grade inflammatory has been suggested related to poor prognosis of hypertension, rheumatoid arthritis (RA) and IBDs. Opportunistic pathogen *Prevotella* spp. has been found positively correlated with diarrhea dominant irritable bowel syndrome (IBS-D) and IBDs [29-31]. Crohn's disease (CD) and ulcerative colitis (UC) are two major forms of IBDs affecting different regions in GI tract. CD affects most areas of GI tract, whereas UC is localized at colorectal inner lining region. Complications including anemia, inflammation of joints and even colorectal cancer may be resulted in IBD patients. One of the proposed causes of IBDs is the long-term inflammation brought by dysbiosis which is an unbalanced microbial composition, leading to upset metabolic activities of both microbial community and the host.

1.3 Intestinal mucosa and leaky gut condition

1.3.1 Mucus layer

The intestinal mucosa is one of the locations that gut bacteria can stick themselves onto. If there is not enough probiotics or commensal bacteria occupying the spaces, pathogens may expand their numbers and undergo infection. This may lead to sepsis because the mucosa layer is one of the barriers between gut lumen and the circulatory system. Dysbiosis is the term describing an imbalanced microbiota status or composition. Impairments of mucosa and epithelial barrier may result inflammation and ulcer, leading to leaky gut condition and allowing numerous antigens to penetrate the blood stream and lymph vessels underneath. Mucus secretion is crucial for intestinal health. Deficiency in MUC2 gene expression in GI tract prompted colitis development [32]. Down below the mucus layer, except serving as absorption mediator cells, epithelial cells form a network by connecting each other covering blood stream and lymph vessels which prevent excessive antigens from passing through and triggering immunity.

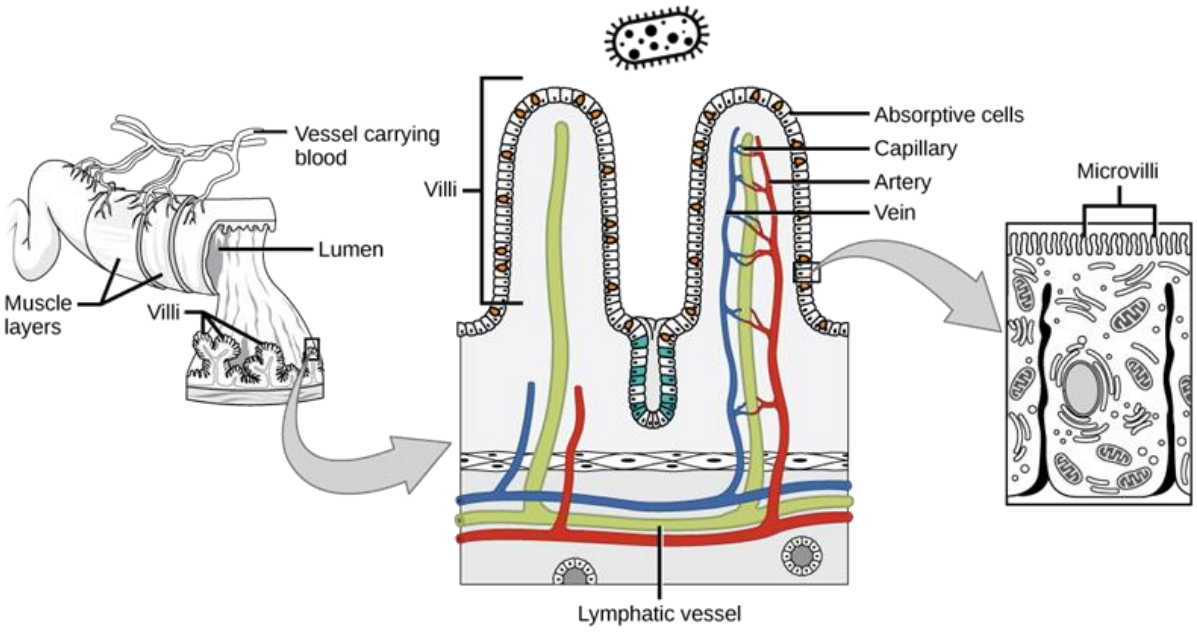

Figure 1.1 Intestinal anatomy, villi structure and epithelial cell [27].

1.3.2 Tight junctions and adherens junctions

Bilateral paracellular junction of the intestinal enterocytes included tight junction (TJ) and adherens junction (AJ), in which TJ positions locate close to the apical region whereas AJ locates are closer to the basolateral region (Figure 1.2). Intestinal TJ consist of transmembrane pore-sealing occludin, claudin-1/-4/-7 and JAM-A in the colonic region of gut. Intestinal epithelial cell permeability can be enhanced by proper expressions of these junction-sealing proteins [33, 34]. Studies also demonstrated that occludin, claudin-1/-4/-7 and JAM-A expressions are reduced, whereas cation channel-forming claudin-2 is enriched in colons of UC patients and experimental dextran sulfate sodium (DSS)-induced colitis animals [35-38]. β-catenin and afadin are AJ adapter proteins linking membrane-integrated E-cadherin or nectin-2/-3 and intracellular actin. On top of bi-cellular junction adhesions, tricellular junction on the apical side of intestinal epithelial cells is composed of tricellulin which also contributes to barrier integrity [39]. These TJ and AJ proteins are connected to intracellular adapter proteins zonula occluden (ZO) -1/-2/-3 directly or indirectly (Figure 1.2). Cytoplasmic F-actin is linked to ZOs in turn holding epithelial cells together. Due to constant flow of chyme and faecal content and active differentiation of epithelial cells, enterocytes shed frequently. Meanwhile, expression profile and remodelling of TJ and AJ proteins will be modified accordingly. Epithelium integrity can be easily modified by the dynamic changes of microbiota compositions.

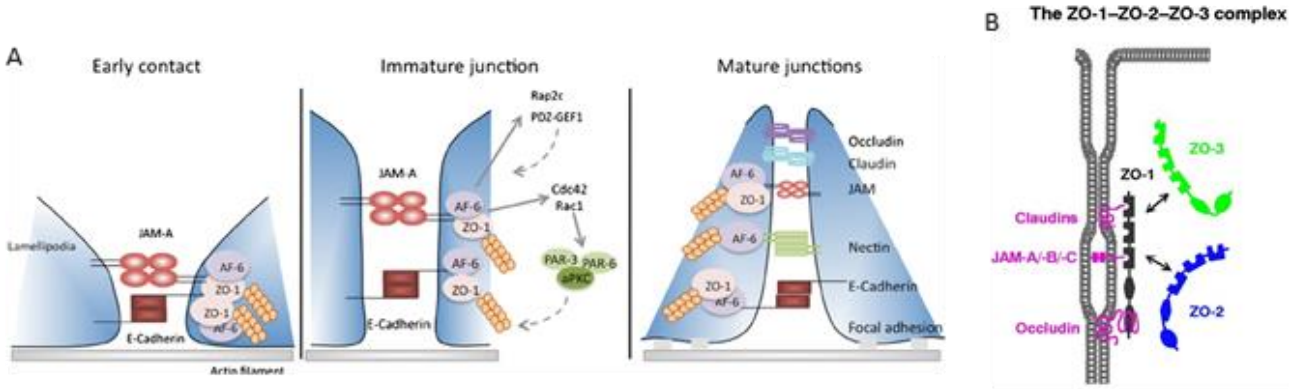

Figure 1.2 Formation of cellular junction (A) and interaction between adapter proteins (B).[40, 41]

1.4 Gut Immunity

1.4.1 Intestinal immunity

Various factors including diet and lifestyle may influence host health directly or indirectly by modifying GI microbiota composition. It has been suggested that a dysbiotic condition in GI tract is related to colon cancer, obesity, inflammatory bowel diseases and pathogen infection. Metabolites derived from an imbalanced ratio of good and bad microorganisms stimulate host cells to behave differently compared to their relatively healthy status. Immune cells are specialized in various kinds of cytokine productions. Peyer's patches (PP) and mesenteric lymph node (MLN) are the major lymphoid tissues in gut. Numerous antigens from different sources may trigger different immune cells which then response according to specific stimulation. Signals from cytokines stimulate other cells to exert particular function by up-/down-regulating certain types of mediators. It is possible that microbiota can influence immunity since GI tract harbors the largest number of immune cells. Among numerous subtypes of immune cells, macrophages serve as one of the antigen-presenting cells (APC) who are specialized in collection of antigens, analyze and execute specific action towards antigens. In addition to exert protective mechanisms for primary response, they also produce a wide spectrum of cytokines to stimulate other immune cells. Under normal situation, immune cells are tightly regulated at rest state to avoid exerting inflammation damaging surrounding tissues. However, the pro-inflammatory to anti-inflammatory immunities could be altered by high level of antigens produced by pathogens or opportunists.

1.4.2 Classically activated macrophage (M1)

Macrophages could be activated by a variety of factors and are usually divided into two categories, namely M1-like and M2-like macrophages (Figure 1.3). Upon receiving specific antigen stimulation such as lipopolysaccharide (LPS), classically activated (M1) macrophage differentiation will be enhanced. Nuclear Factor κB (NF-κB) or Activated Protein-1 (AP-1) mediated pro-inflammatory cytokines, including IL-1β, IL-6, IL-8, IL-12 and TNF-α will be upregulated, in which TNF-α and IL-8 are potent neutrophil chemoattractants, while IL-1β, IL-6 and IL-23 are able to stimulate naïve T cell to differentiate into T helper 17 (Th17) cells which has been shown to be related to poor prognosis of IBDs, RA, hypertension and psoriasis [18, 42, 43]. IL-12 is one of the cytokines produced by both dendritic cells and macrophages in response to microbial stimulants, which can stimulate IFN-γ and TNF-α production from T cell and other macrophages [44-46]. These mentioned pro-inflammatory cytokines can serve as indicators of M1 differentiation, which have also been found contributing to intestinal inflammation severity [47-50].

1.4.3 Alternatively activated macrophage (M2)

Alternative activated macrophage (M2) functions as tissue repairing and immunoregulatory cells after infection clearance. Several anti-inflammatory genes are characterised in M2 macrophages. One of the marker transcription factors, interferon regulatory factor-4 (IRF4), has been demonstrated crucial for M2 differentiation by opposing effects provided by IRF5, NF-κB or AP-1 [14, 51-53]. TGF-β and IL-10 are anti-inflammatory cytokines for growth and development. They also induce Foxp3 expression hindering Th17 differentiation in T cells [42, 54]. In addition to suppressing Th17 population, TGF-β and IL-10 promote immunosuppressive regulatory T cell differentiation [54]. IL-10 is the most studied immunoregulatory cytokines produced by several kind of immune cells [55, 56]. Its importance on intestinal health has been demonstrated by *IL10* or *IL10R* knockout experiments, which IL-10 deficient

and macrophage-restricted IL-10 receptor knockout mice develop spontaneous colitis [57, 58]. Function of suppressor of cytokine signaling 3 (SOCS3) is controversial as it has been shown to have ability to suppress both M1 and M2 macrophage differentiation [59, 60]. Nevertheless, SOCS3 deficiency has been linked to inflammation severity and duration in several murine inflammatory disease models [61-63]. On the other hand, M2 produced mediators and enzyme to neutralized harmful substances. IL-1 receptor antagonist (IL-1Ra) can be produced by tissue-repairing macrophages to neutralize IL-1 cytokines. IL1-Ra polymorphism has been correlated with IBDs, and its balance is crucial for mucosal immunity homeostasis [64-66]. Mannose receptor (MRC1) and transglutaminase-2 (TGM2) are two important M2 markers for debris and inflammatory agents' clearance during resolution in both murine animal model and human. TGM2 is also responsible for transamination crossing or deamination of proteins and efferocytosis. Loss of TGM2 in macrophages promotes pro-inflammatory phenotype [67].

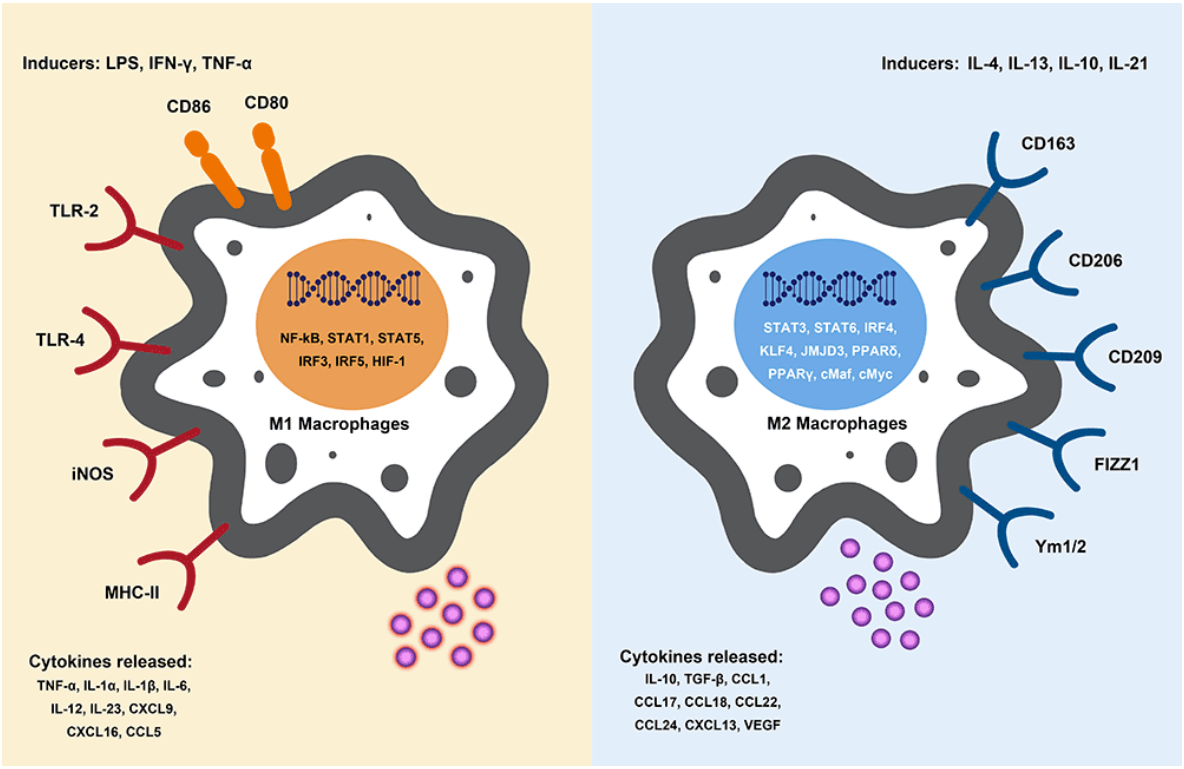

Figure 1.3 General M1/M2 macrophage inducing factors, transcription factors and cytokines [68].

1.5 Microplastics and plasticizers

1.5.1 Microplastics and their direct effect on health

Plastics are widely used for multiple purpose due to its chemical inertness, flexibility and low cost. Most plastics are produced for usages in packaging and construction. Unfortunately, waste management methods are limited for plastic waste while recycling and biodegradation of plastics are rather difficult since these processes are of high costs and time-consuming. Meanwhile, incineration of plastic waste produce greenhouse gases, acidic hydrogen chloride gas and even dioxins. Plastic waste is mainly disposed to landfill. Indiscriminative uses of different types of plastics have produced numerous plastic waste in landfill. It would take hundreds to thousands of years for complete degradation of plastic waste. During this process, secondary microplastic produced by fragmentation and weathering may result in formation of microplastic (MP) which can migrate to various ecosystem. Fragmentation of plastics produces smaller plastic pieces including MPs which have size smaller than 5 mm. In addition to fragmentation, plastic manufacturing, wearing of plastic-based clothes and cosmetics may also release primary MPs to the environment. Plastics persist in different ecosystems such as aquatic and marine environments. MPs have been found in multiple food sources such as tap/bottles water, seafood and package food [69]. Polyethylene (PE), polypropene (PP), polystyrene (PS), polyvinyl chloride (PVC) and polyethylene terephthalate (PET) can be found in different types of drinking water (Table 1.2) [69-72]. MPs can be ingested and accumulated in different organs or tissues within organisms. Research has been indicated that MPs with size smaller than 150 μm can possibly pass through the epithelium by endocytosis, paracellular space, transcytosis and persorption [73]. Study also revealed that major MPs in drinking water are of size smaller than 50 μm, in which PE and PP are the dominant types of plastics [74]. MPs have been found in gut, liver and kidney in mouse fed with microplastics [75]. Translocation of MPs inside body has been found recently. There is study reported that MPs are detected in human blood samples [76]. Direct

influences on body cells by MP particles have been suggested in some studies. Direct contact between MPs and mammalian cells has been demonstrated to trigger pro-inflammatory cytokines IL-1α, Il-1β, IL-6 and TNF-α production by macrophages, fibroblasts or kidney epithelial cells [77-80].

Table 1.2. Different types of microplastic and their sources

Types of plastics	**Sources**
Polyethylene (PE)	Water bottles, detergent bottles, food wrapping films, plastic bags, food wares, food package, water pipes,
Polypropene (PP)	Detergent bottles, water bottle caps, plastic bags, food wares, water pipes, furniture
Polyethylene terephthalate (PET)	Water bottles, detergent bottles, food trays
Polyvinyl chloride (PVC)	Food wrapping films, gloves, blood bags, consumables for injection, water pipes
Polystyrene (PS)	Lunch boxes, foam packaging, disposable cups and caps

1.5.2 Plasticizers and their toxicities

Except direct contact of GI tract cells to MPs, exposure to chemicals leaked from PVC plasticware such as injection tubing, food packages and gloves from the environment, may also pose additional threat on human health. During PVC manufacturing, phthalate ester plasticizers such as di(2-ethylhexyl) phthalate (DEHP) and di-iso-nonyl phthalate (DINP) may have been added to increase the flexibility of plastics. Due to the flexibility, diverse shapes of medical devices and consumables are made from plasticized PVC. However, DEHP has been reported damaging reproductive system by inducing testicular injury and reducing testosterone level in male mouse [81]. On the other hand, DINP administered rodent models have

higher oxidative stress in their liver and kidney cells [82]. Apart from direct influences on mammalian models, more research groups have started to investigate possible detrimental consequences of MP or plasticizer consumptions for human gut health. For example, alteration of *Firmicutes/Bacteroidetes* ratio due to PE exposure have been observed in mice and zebrafish [83, 84]. Studies to investigate the detailed compositional modification of human gut microbiota by these compounds, and the possible health outcome due to the altered microbes would be useful for the general public.

1.5.3 Legislation on control of plasticizers

The use of DEHP in toys is banned in the EU and Japan. DEHP is prohibited in food-handling gloves in Japan as well [85]. The US limits DEHP in plastic below 0.1% by weight, while China and Australia have less stringent policy on DEHP. The percentage of DEHP in children products, food or food wares can be up to 1% [86]. On the other hand, DINP is also banned using in toys in the EU and Japan. <0.1% DINP is allowed in toys and childcare products in the US and China [86]. Currently there is limited legislation regarding the boundary of microplastic in food or cosmetic products in Hong Kong. Voluntary based action was suggested to manufacturers regarding reduction of microplastic-containing products in 2021. WHO suggested daily maximum DEHP exposure as 0.025 mg DEHP per kilogram body weight (maximum 1.75 mg for individual weighted 70kg). Centre for Food Safety (CSF) set standard at maximum 1.5 mg DEHP per kilogram of food [87]. CSF suggests that it is less likely that all consumed foods are contaminated at the maximum DEHP standard, so the exposure to DEHP in general public will not exceed the daily maximum exposure limit set by the WHO.

1.5.4 Summary

MPs have been reported to affect the growth of particular type(s) of bacteria. MPs such as PE, PVC and PS cannot be digested by synthetic secretion from the human GI tract. MPs provide extra surface area

for attachment and biofilm formation. Chen et al. assessed microbiota composition, richness and diversity on waste MPs with different sizes (18 mm, 3 mm and 100 μm) with marine microbiota [88]. Major phylum detected on MPs is *Proteobacteria* which produces biofilm for attachment. Among microbiota on different sized MPs, their composition, richness and diversity are relatively similar. Consistent with the observation in biofilm microbiota in sedimentary samples [89], growth of *Proteobacteria* could be favored. Meanwhile, growth of *Lactobacillus* was inhibited on surface of PS [90]. Modification of microbiota in aquatic lives, sedimentary and soil environments due to the contamination of MPs and plasticizers have been explored in various studies in recent decades. Nevertheless, research on interactions between these contaminants and microbial compositions in rodent or human are relatively limited. Among animal experiments, most published microbiota analyses utilize rodent model since these substances are harmful to human. Utilization of batch culture and GI tract simulator provide platforms for microbiota studies on contaminants-microorganisms interactions. However, there are some differences between human and rodent microbiota compositions. Rodents harbor more *Muribaculum* and *Bacteroidetes* than human, while phylum *Actinobacteria*, which includes probiotic genus *Bifidobacteria*, is generally more abundant in human microbiota [91]. Being a higher consumer in the food chain, it is possible that MP or plasticizers may affect human health by bioaccumulation and biomagnification. Unknown health hazards may affect human after concentration of MPs inside body. Meanwhile, with the advancement on microbiota analysis, multiple studies to investigate the relationships between lifestyle, diet and GI microbiota have been documented. It is possible that different food contaminants may be ingested together with food products, which alters the microbial compositional balance in the GI tract, contributes to intestinal barrier malfunction and low-grade inflammation, and exacerbates inflammatory diseases in human. This urged scientists to investigate more on whether health hazards would be resulted and what possible mediators would be involved in this process in human body.

Chapter 2 – Effect of *Lactobacillus rhamnosus* S1 on intestinal integrity and immunomodulation: from i*n vitro* to *in vivo*

Abstract

Beneficial bacteria are naturally present in the environment, for which some of them inhabit in the mammalian gut while some are commonly used in food products. Twelve probiotic isolates including *Lactobacillus gasseri*, *Lactobacillus paracasei*, *Lactobacillus plantarum*, *Lactobacillus rhamnosus*, *Lactobacillus sakei*, *Leuconostoc mesenteroides*, *Pediococcus acidilactici* and *Pediococcus pentosaceus*, were isolated from infant fecal samples and fermented food products in this study. Characterization of probiotics to assess the acid tolerance, bile salts tolerance, and anti-microbial ability against food-borne pathogens were performed on these isolates. *L. rhamnosus* S1 can grow in acidified cultural medium at pH 4.0, withstand average GI tract bile salt concentration (0.5%). Moreover, S1 reduced *Staphylococcus aureus* and *Enterococcus faecalis* adhesion to cultural intestinal epithelial cells up to 50%. Co-incubation of S1 with *S. aureus*, *Acinetobacter baumannii* and *Enterococcus faecium* reduced the inflammatory cytokine IL-8 production in Caco-2 due to pathogen infections. Together with high beta-glucosidase activity, phenol and salt resistance as described in previous study. S1 was then selected for the subsequent experiments. Supplementation of S1 in the Simulator of Human Intestinal Microbial Ecosystem (SHIME) enriched *Bifidobacterium* and reduced *Megasphaera*, descending colon microbiota derived extract preserved Caco-2 barrier integrity, possibly mediated by the enriched expression of occludin (+39%). S1 also modified fecal microbiota in Sprague Dawley (SD) rats, significantly reduced inflammatory diseases associated taxa (*Streptococcus* and unclassified genus under *Prevotellaceae*), provided immunomodulation effect to colonic/systemic regions by upregulations of IL-10 and TGF-β. These results suggested that *L. rhamnosus* S1 has the potential to be a novel probiotic for the prevention of opportunistic pathogenic infection, amelioration of leaky gut and immunoregulation.

Introduction

1. Legislation about probiotic markets in different countries

Live or inactivated probiotics are present in various kinds of food around the globe. Some strains are added into yogurt, fermented food, candy and chocolate, etc. Different countries have their own regulations on safety and control on probiotic products. The EU has no consistent legal definition on probiotics among different countries, however, it has set health claims regulation to control the promotion and claims listed by the manufacturers. Based on relevant evidence, the European Food Safety Authority (EFSA) revises and publishes Qualified Presumption of Safety (QPS) assessment every 6 months to conclude whether different commonly used probiotic species are safe for human consumption [92]. The US has the most relaxed control on probiotics. Under regulation of Food and Drug Administration, FDA, probiotics can be sold as drug when fulfilled clinical trials; or as biological product, dietary supplement, food or food ingredient under Generally recognized as Safe (GRAS) in different circumstances. Probiotic regulations in China is evolving in recent years. Legislation for registration and safety assessments on probiotics strains is setting up while lists of probiotic species that can be used in food supplements or food supplements for infants had been published, allowing manufacturers to select possible potential strains for their products [93]. In Hong Kong, probiotics can be sold under nutritional supplements or food which is not listed under drug regulatory system. The health claims suggested by the manufacturers are constantly reviewed. In Japan and Taiwan, probiotics can be marketed as general food/food supplement and dietary supplement, respectively [93, 94]. In addition to those classifications, if the probiotics satisfies safety and efficacy tests, it can be registered and approved as Health Food (in Taiwan) or Food for Specified Health Uses (FOSHU) (in Japan), which provide extra information to the general public based on scientific examination.

2. Probiotics and their beneficial effects

Probiotics, namely beneficial bacteria, are microorganisms that confer a health benefit to the host when they are consumed in adequate amounts. These microbes are commonly found in a range of food products such as dairy, pickled vegetables, kimchi, miso and soy sauce, for which foods live probiotic bacteria are often used as the starter culture alone or in mixed culture. In the last 40 years, numerous research have been carried out to investigate the beneficial effects conferred by probiotic bacteria. Bacteria were assessed chemically and metabolically to determine whether they could be a suitable probiotic candidate for therapeutic use. For example, some strains of *E. faecium* were approved for usage in probiotic supplements; *Tetragenococcus halophilus* HmS-129 was suggested to be used as a salted food starter culture for suppressing histamine production during the fermentation process [95]; A vaginal formulation of lyophilized powder containing *Pediococcus pentosaceus* SB83 demonstrated anti-listerial activity inhibiting pathogen attachment [96].

Bifidobacterium and *Lactobacillus* spp. are two of the main probiotic genera that provide physical and physiological protection for the intestinal tract of human. Other than the various beneficial effects of probiotics reported in previous studies, *Lactobacilli* spp. fit the category of generally regarded as safe (GRAS) and qualified presumption of safety (QPS) according to the US Food and Drug Administration (FDA), and European Food Safety Authority (EFSA), respectively. Quite a number of studies to explore the advantages brought by *Lactobacilli* spp. had been conducted. For instance, *L. rhamnosus* GG was found to inhibit several pathogens including *S. aureus*, *Bacillus cereus*, *Escherichia coli* and *Salmonella enterica* serovar Typhimurium from adhering or invading human epithelial Caco-2 cells [15]. Similarly, another *L. rhamnosus* strain LOCK 0908 was found to perform favorably in the competitive adhesion assays, in which the adherence of pathogens *E. faecalis*, *S. aureus*, *Listeria monocytogenes* and *C. difficile* were reduced in the presence of this probiotic [97]. *L. fermentum* MTCC 8711 was shown to reduce the

number of adhered methicillin-resistant *S. aureus* (MRSA) to cultured epithelial Caco-2 cells [98]; whilst a strain of *L. plantarum* was found to possess both cholesterol-lowering, anti-constipation and immuno-regulatory effects demonstrated in rodent models [99-101]. Other than secretion of metabolites that may directly work on the intestinal mucosa or involve in the physiological response of hosts, the ability of a probiotic to colonize itself in the host is one of the crucial features to exert beneficial effects to the hosts.

Intestinal epithelium and mucosal layers are the surfaces for the attachment of microorganisms in the gut, which contribute to the greatest size of microbiota niche in human body, the so-called gut microbiota. Being a barrier between the intestinal cavity and circulatory system, the integrity of intestinal epithelium is important to prevent the body from invading by pathogens and obtain health-promoting substances such as short-chain fatty acids (SCFAs) from symbiotic microorganisms. An unbalanced gut flora status, namely dysbiosis, was found to relate to some chronic metabolic diseases, central nervous system dysfunction and GI inflammatory conditions such as inflammatory bowel disease (IBD). IBD has two major characteristic disease phenotypes, Crohn's disease (CD) and ulcerative colitis (UC), both of which are suggested to attribute to repetitive or constant inflammatory conditions in different parts of the GI tract, which in turn may lead to complications such as inflammation of joints and liver, abscesses and colon cancer. The excessive and unnecessary responses provided by immunity were suggested to be triggered by bacteria. An adherent-invasive *E. coli* (AIEC) was found promoting chronic inflammation in intestinal mucosa by stimulating tissue necrosis factor alpha (TNF-α), causing Crohn's disease [102]. Various attempts have been made to determine the etiological agent for IBD, yet the actual causes of these diseases are not yet confirmed. Except antibiotics and symptomatic treatments, it is suggested that the modification of gut microbiota by fecal microbiota transplantation (FMT) or probiotics could relieve the severity. Though US FDA issued a guidance to adopt FMT to treat IBD attributed to *C. difficile* infection in 2013,

the recent COVID-19 pandemic brought the safety concern of such exercise as the fecal donor could be a potential SARS-CoV-2 carrier [9, 11]. Gut microbiota could be affected by various factors including but not limited to health status, environment, exercise, stress and diets including prebiotics and probiotics. With an array of carbohydrate-metabolizing enzymes and sugar transporter in *Lactobacilli*, this genus of microbes is one of the dominant bacteria in the epithelia of duodenum and jejunum. *Lactobacilli* spp. may possess the ability of GI tract colonization and help to modulate the balance of microbial composition of gut, promoting gut homeostasis.

3. Factors and characteristics required for effective colonization in GI tract

3.1. Adhesion factors in *Lactobacillus*

A considerable amount of bacterial surface appendages has been identified and compared since probiotics' beneficial effects were demonstrated in some studies related to fermented and dairy products. Those bacterial surface macromolecules play an important role in different kinds of bacteria to allow them to obtain nutrient and shelter from the host defensive mechanism. In the meantime, the host GI tract tissues require corresponding ligands to facilitate the colonization of these beneficial bacteria. Some *Lactobacilli* and *Bifidobacteria* have the ability of promoting colonic mucin production by upregulating *MUC2* gene [103, 104]. This allows more binding site for their colonization and promote intestinal barrier function and health of host as it had been demonstrated that genetically modified mice without mucin secretion was found to suffer from spontaneous colitis and developed colorectal cancer [32, 105]. Adhesins expressed by a variety of bacteria were classified as secreted anchorless and cell membrane/ wall-bound adhesion factors. Among all the adhesins reported, bacterial cell membrane/ wall-bound adhesins were considered as more prevalently participating in the mediation of bacterial adherence to mammalian epithelial cells than the others. In *Lactobacillus* spp., there are several types of membrane-bound adhesin

identified to be used by some well-known *Lactobacillus* species. For instance, it was reported that surface 29 kDa protein of L. mucosae ME-340 bound to blood group antigens A and B. Similarly, the mucus adhesion promoting protein and 32 kDa surface protein functioned as cellular adhesins and were responsible for the mucin adhesion ability of *L. reuteri* 104R and *L. fermentum* BCS87, respectively [106-108].

LPXTG motif anchored at the C-termini of adhesins on the cell wall were also discovered in *L. rhamnosus* and *L. plantarum.* In addition to collagen and fibronectin, it was found that *L. rhamnosus* expressed pilus adhesins consisting of subunits SpaCBA or SpaFED for the adhesion of mucin [109]. Moreover, LPXTG anchoring mucin-binding factor for the adhesion of *L. rhamnosus* to mammalian mucosal layer was also reported [110]. Pretzer *et al*. has shown that the adhesin utilized by *L. plantarum* was slightly different from the other bacteria in the *Lactobacilli* species[111]. The factor contributing to the adhesion of *L. plantarum* to mucin was identified to be Mannose-specific adhesin, in which a carbohydrate chain with mannose as receptor was recruited by *L. plantarum* for adhesion [111]. It also has been demonstrated that *L. rhamnosus* GG is able to prevent the damages at tight junction induced by enterohemorrhagic *E. coli* O157:H7 infection [112]. These discoveries provide some insights for the selection of adhesins from probiotic LABs and pathogenic species for further studies and comparisons.

3.2.Adhesion factors in *S. aureus* and *E. faecalis*

S. aureus is one of the commonest bacterial agents of nosocomial infection around the world, posing the greatest threat to humans. MRSA exhibits multi-drug resistance against methicillin, cephalosporin and carbapenem antibiotics. Approximately 20% of humans are persistent carriers of *S. aureus* [113]. *S. aureus* is regarded as an opportunistic pathogen because it can colonize healthy human skin and mucous membranes such as the nasal cavity and GI tract without causing infectious symptoms.

Expressing a variety of virulence factors such as coagulase, hyaluronidase and staphylokinase, *S. aureus* can infect most organs once it has entered the circulatory system [98, 114]. Enterotoxins A, C and D were also reported to be produced by some community-acquired MRSA from time to time, i.e. a gastroenteritis outbreak caused by foodborne MRSA infection in US [115]. The pathogenesis of *S. aureus* depends on the cell surface components of this bacteria and human epithelial cells. Both the endothelial and epithelial tight junction integrities are reported to be disrupted by proteases or alpha toxins produced by *S. aureus* [26, 116, 117]. Adhesion of *S. aureus* involves in the first step of host infection. Multiple surface protein adhesins expressed by *S. aureus* were described in the past few decades, among which five *S. aureus* surface proteins were identified as LPXTG-anchored wall-associated proteins, *Staphylococcus* Protein A, collagen-binding protein, fibronectin-binding protein and clumping factor A ; and non-LPXTG-anchored elastin-binding protein [118].

Another opportunistic infectious agent which also poses a threat to human health is *E. faecalis*. Multidrug-resistant strains, vancomycin-resistant enterococcal species are also emerging rapidly in hospital and general community. *E. faecalis* are commonly found inhabiting in animal large intestine and urinary tracts. This bacterium has an array of virulence factors contributing to its pathogenesis, which includes aggregation substance (AS), gelatinase, hyaluronidase, enterococcal surface protein and cytolysins. Infection of *E. faecalis* may result in urinary tract infection, endocarditis and bacteremia [114].

It has been reported that *E. faecalis* could be internalized in human enterocytes Caco-2 and HT-29, with an augmented cellular invasiveness by overexpressing aggregation substance protein [119]. Furthermore, AS proteins contribute to the adhesion and invasion of this bacteria into the host cells. The Arginine-Glycine-Aspartate (RGD) motif in the AS protein of *E. faecalis* plays a role in the binding of this bacteria to different epithelial cells [27, 120-122]. Adhesin to collagen (Ace) of *E. faecalis* is regarded as microbial surface component recognizing adhesive matrix molecules (MSCRAMM) protein and shares some homology with the *S. aureus* collagen adhesion, Cna. Other than harboring the same ability of binding to collagen type I, Ace was also found binding to collagen IV and laminin [123].

4. Infection/pro-inflammatory stimulation by pathogens and restoration by probiotics

Pathogenic infection at the GI tract not only causes physical damages at the local mucosal lining, but also disrupts the balance of gut microbiota, resulting in gut dysbiosis. Colonization of pathogenic bacteria may alter microbial composition within the host by competing with native gut bacterial species via various mechanisms. For example, presence of the pathogens in the gut could stimulate the secretion of cytokine IL-6 possibly from the proliferation and differentiation of lymphocytes. The anti- or pro-inflammatory characteristic of IL-6 were found to be different in various cell types. Recent research demonstrated that IL-6 increased the permeability of cultured human epithelial cells by destroying the tight junction between adjacent cells [124]. The destruction made by cytokine endangers the intestinal lining to become a niche of entry for pathogenic microbes, which could lead to life-threatening septicemia.

Maintenance of intestinal microbial homeostasis is important in the overall health of human gut. Multiple studies have demonstrated that either one or both of the two main probiotic genera, namely *Bifidobacterium* and *Lactobacillus*, in gut harbor immunomodulation potential for their hosts [125]. Other than IL-6, IL-8 is another important chemokine, which is expressed by macrophages, respiratory smooth muscle cells, epithelial cells and endothelial cells. It signals chemotaxis, the recruitment of immune cells (granulocytes, macrophages and T cells) to the site of infection. The activation of immune cells can impose damage on local tissues. If the immuno-regulation is disturbed, for example, having an imbalanced microbiota composition or pathogenic infection, adjustment of cytokine level is needed for the maintenance of intestine health. A conditioned solution made with *L. plantarum* spent medium inhibited the activation of NF-κB which leads to a downregulation of downstream pro-inflammatory cytokines such as IL-6 and IL-8 [126]. In another study reported by Ren *et al*, two *Lactobacillus* species, *L. salivarius* CICC 23174 and *L. plantarum* CGMCC 1.557 were characterized and compared with a commercially available strain, *L. rhamnosus* GG, for their effect on affecting the immune response. All 3 tested

Lactobacilli were shown to reduce IL-8 expression in Caco-2 cells. Moreover, the pretreatments of these 3 *Lactobacilli* in Caco-2 cells attenuated the upregulation of IL-8 expression triggered by the challenge of *S. enterica* serovar Typhimurium [15]. Induction of $Foxp3^+$ regulatory T cell differentiation for immunomodulation in the gut can also be achieved by anti-inflammatory cytokines produced by other immune cells. Several *Lactobacilli* species were assessed to possess the ability of stimulating IL-10 and TGF-β production in intestinal dendritic cells [127, 128].

In this study, new probiotic isolates were isolated, characterized and selected for the follow-up experiments based on their *in-vitro* characteristics. In addition to acid and bile salt tolerance, S1 has high viability in phenol and salt, and possesses the highest β-glucosidase activity among different probiotic isolates from fermented food, feces and commercially available probiotic drink [129]. The competitive adhesion and excluding pathogens from attaching to host epithelial cells of the isolated *Lactobacillus* spp. has also been performed. In antimicrobial ability, most isolates inhibited growth of acute infectious pathogens including *S. aureus*, *Klebsiella pneumoniae*, *S. enterica* serovar Typhimurium and *B. cereus*. On top of that, 16S rDNA sequencing analysis revealed that *L. rhamnosus* S1 significantly reduced some opportunistic pathogenic taxa including genera *Streptococcus*, unclassified species under *Prevotellaceae*, *Clostridia_UCG-014* in SD rats, and *Megasphaera* in the simulator of human intestinal microbial ecosystem (SHIME). Furthermore, *L. rhamnosus* S1 also promoted epithelial integrity by up-regulation of tight junction (TJ) protein occludin and modulated both intestinal and systemic immunity by up-regulating IL-10 in a cultural epithelial cell model.

Objective

In this study, we aim to determine the following:

1. Characterization of in-house isolated probiotic strains including the tolerance to the digestive condition and antimicrobial potentials.
2. Assessment of the probiotic potential to promote gut homeostasis and immunomodulation of the selected probiotic strain on human *in vitro* GI tract.
3. Initial assessment of the potential of selected probiotic strain to promote gut homeostasis on animals.

Materials and methods

1. Isolation and identification of probiotics

Fecal samples were aseptically homogenized in 10 ml of 0.85% NaCl by using inoculation loop and vortex shaking. Serial dilutions were done in 0.85% NaCl and suspensions were spread on MRS, RCM and M17 plates. Plates were incubated at 37°C in an anaerobic chamber with 5% CO_2 for 48 hours. Single colonies were picked for subculture in respective growth media. Part of the resultant culture was subjected to glycerol stock storage; and the remaining culture was used in genomic DNA extraction.

Identification of fecal isolates was performed by using 16S ribosomal DNA (rDNA) full length amplification and sequencing. Genomic DNA of each isolated bacterium was extracted using the TIANGEN Genomic DNA kit (TIANGEN, Beijing, China) according to the manufacturer's instructions. Polymerase chain reaction (PCR) was performed to amplify the 16S rDNA sequence using the extracted genomic DNA, 16S8F forward primer, 16S1492R reverse primer (primer sequences were listed in supplementary table 2.1), rTaq DNA polymerase and other required PCR reagents. The resulting PCR amplicon was analyzed on a 1% agarose gel. A DNA band corresponding to 1,500 bp in size was excised from the gel; and DNA was extracted from gel by TIANGEN gel extraction kit according to the manufacturer's protocol. The purified PCR product was sent for sequencing. Sequencing data were aligned and compared with DNA sequence on the NCBI 16S rDNA database for bacteria and archaea to identify the bacterial species.

2. Anti-microbial ability against food-borne pathogens

The antimicrobial ability of food-isolated LABs against pathogenic species was assessed by inhibition zone test as described in Halder, et al. [130], with some modification. Probiotic was cultured in MRS broth at 30°C for 24-36 hours, pelleted by centrifugation at 18,626g for 1 minute, washed with PBS pH 7.3 and centrifuged again. Pellet of probiotics was re-suspended in PBS pH 7.3. On each MRS and modified MRS (mMRS) agar (containing MRS ingredients without glucose), 2 µl of probiotic suspension was inoculated at a point at 30°C for another 24-36 hours. Pathogen was cultured in brain-heart infusion (BHI) broth at 37°C overnight with shaking (250 rpm). OD calibration was made in 50°C soft BHI agar. A starting concentration of $1x10^5$ CFU/ml of pathogen was poured onto MRS or mMRS plate with single colony-grown probiotic. Plates with poured soft BHI agars were incubated at 37°C for 24 hours. Common pathogens known to affect the upper respiratory and GI tract were selected for testing, which include *S. aureus, B. cereus, P. aeruginosa, A. baumannii* and *S. enterica* serovar Paratyphi. The antimicrobial zones were determined by measurement of the radius of inhibition zone – radius of LAB colony.

3. Acid tolerance

Acid tolerance of the isolated probiotics was assessed using the protocol as described in Hassanzadazar, et al. [131] with modifications. Initially, probiotics were cultured in MRS broth at 37°C for 24-36 hours, after which point, they were pelleted by centrifugation at 18,626g for 1 min, and then re-suspended in fresh MRS broth. The optical density at 600 nm (OD) of each probiotic was calibrated to 1.1 by the addition of fresh MRS broth. Three hundred microliters of the OD_{600} calibrated probiotic suspension was added into test tube containing 3 ml of MRS with different pH values. probiotics were incubated at 30°C, and the OD was monitored for 48 hours. Duplicate in each pH experimental set were performed. Growth curves of different probiotics in MRS broth with different pH values were plotted for comparison.

4. Bile salts tolerance

The tolerance of bile salts of different LABs were determined using the protocol as in Damayanti, et al. [132], with minor modifications. Initially, LABs were incubated in MRS broth at 30°C for 24-36 hours, and then pelleted by centrifugation at 18,626g for 1 minute. The probiotic pellets were re-suspended in phosphate buffered saline (PBS) (Thermo Fisher Scientific, Waltham, USA) pH 7.3. Probiotic suspension (18 ml) of each strain was calibrated to an OD of 1.1. Six aliquots of 2.7 ml of calibrated probiotic suspensions were prepared. Three hundred microliters of 0%, 3% and 5% of bile salts in PBS pH 7.3 were added into those 2.7 ml aliquots. The bile salts tolerance of probiotics was assessed and compared in 0%, 3% and 5% of bile salts in PBS pH 7.3. All bacterial suspensions were incubated at 37°C for 3 hours. Probiotic percentage survival was determined by calculating the number of CFUs in each bile salts suspension/CFUs in PBS control. Duplicate tests for control and each bile salt concentration were performed.

5. Adhesion to cultural enterocytes and Competitive adhesion against pathogens

The adhesion ability of LABs was investigated according to the experimental design in Ren, et al. [133], with some modifications. To prepare the monolayer, human epithelial Caco-2 cells were seeded in a 24-well plate (Thermo Fisher Scientific, Waltham, USA) with $2x10^4$ cells/well, cultured in Dulbecco's modified Eagle's medium (DMEM) containing 20% fetal bovine serum (FBS) (Thermo Fisher Scientific, Waltham, USA) for 14 to 21 days until a monolayer was formed in each well. On the day of the adhesion assay, a 24-36 hours' culture of LAB culture in MRS broth was centrifuged at 18,626g for 1 minute. The bacterial pellet was washed and re-suspended in PBS pH 7.3. The probiotic suspensions were calibrated with PBS pH 7.3 to OD = 0.5. Caco-2 cells were washed with PBS pH 7.3 twice before infection. To each well of Caco-2 cells, 100 µl of the calibrated bacterial suspension was added. Gentle swirling was provided to facilitate even distribution of bacteria across the monolayer. Cells and bacteria were incubated at 37°C inside an anaerobic chamber (5% CO_2) for 2 hours. After which point, the monolayer was washed twice with PBS pH 7.3 to remove non-adhered bacteria, treated by the addition of 100 µl of 1% Triton-X100 in PBS pH 7.3 for lysis and detachment of Caco-2 cells in plate. After 15 minutes of incubation with the surfactant, 900 µl of PBS pH 7.3 was introduced into each well. Caco-2 cells were homogenized and lysed by pipetting. Serial dilution of the homogenized mixture was performed in 0.85% NaCl. Diluted suspensions were plated on MRS agar for probiotic CFU counting. Adherence was represented and compared as LAB CFU/Caco-2 cell.

The competition adhesion assay was performed according to the protocol adopted from related report Ren, et al. [133]. Pathogen was calibrated to OD of 0.5 while probiotic OD was adjusted to 0.5, 1.0, 2.5 and 5.0 to yield co-incubation ratio of 1:1, 1:2, 1:4 and 1:10, respectively. 100 µl of the bacterial suspensions were added to the Caco-2 monolayer. Cells were incubated at 37°C inside an anaerobic chamber (5% CO2) for 2 hours. After incubation, the Caco-2 cells were lysed and the adhered bacteria in suspensions were plated on selective agars according to the requirement of different bacterial CFU counting. Modified mannitol salt agar (mMSA, containing peptone (10 g/L), beef extract (1 g/L), mannitol (10 g/L), sodium chloride (100 g/L), phenolsulfonphthalein (0.025 g/L), agar (15 g/L)) and modified citrate azide Tween 80 carbonate agar (mCATC, containing peptone (15 g/L), yeast extract (5 g/L), potassium dihydrogen phosphate (5 g/L), sodium citrate (15 g/L), Tween 80 (1 g/L), Agar (15 g/L), sodium carbonate (1 g/L, sterilized solution added after autoclave)) were used as selective agar for the growth of *S. aureus* and *E. faecalis* respectively (recipe can be found in appendix A3). Adherence changes of different bacteria were expressed and compared by the number of CFU adhered to each epithelial cell.

6. SHIME setup

Program and tubing of Simulator of the Human Intestinal Microbial Ecosystem (SHIME) was setup as TWIN-SHIME according to the manufacturer's guideline (ProDigest, Gent, Belgium). Fecal samples were collected from healthy donor who had normal diet and did not intake any probiotics or antibiotics at least 2 weeks before sampling day (Figure 2.1). Fecal material was stored in gas-tight sample bucket with anaerobic sachet (Thermo Fisher Scientific, Waltham, USA) and inoculated within 4 hours after collection. 10% w/v of fecal material was homogenized with anaerobic buffer (autoclave sterilized phosphate buffer: 8.8 g/L K_2HPO_4, 6.8 g/L KH_2PO_4, 0.1 g/L sodium thioglycolate; and supplement solution after autoclave: 15 mg/L sodium dithionite) inside a circulator strainer stomacher bag (Seward, Worthing, UK) for 5 minutes at 200 rpm. Sterilized Adult L-SHIME growth medium (without starch) (composition (g/L): arabinogalactan (1.2), pectin (2), xylan (0.5), glucose (0.4), yeast extract (3), special peptone (1), mucin (3), L-cysteine-HCl (0.5)) (ProDigest, Gent, Belgium) was pH adjusted to pH 5.6-5.9 for ascending colon (AC), pH 6.0-6.3 for transverse colon (TC) and pH 6.6-6.9 for descending colon (DC) mimicking large intestinal environments using 0.5M of HCl and 0.5M NaOH for acid and base adjustment respectively. Filtrate portion obtained after homogenization was inoculated in growth media with volume ratio of 1:10. Starting cultural volumes in each AC, TC and DC were 500 ml, 800 ml and 600 ml respectively. All chambers were maintained at 37°C by warm water circulation. When microbiota had been reached stability, which was indicated by SCFAs concentrations, S1 treatment was delivered in 5 ml saline at dosage of 10^{10} CFUs daily directly into AC1 chamber (Figure 2.1). Anaerobic condition was maintained by nitrogen purging after introduction of probiotic. Quality control including pH meter calibration and SCFAs concentration were monitored throughout the whole experiment period. SHIME pump action was verified and calibrated every week to ensure proper volume transitions between chambers. After treatment

period, luminal culture and biofilm on inner wall from all chambers were collected and stored at -20°C until assay.

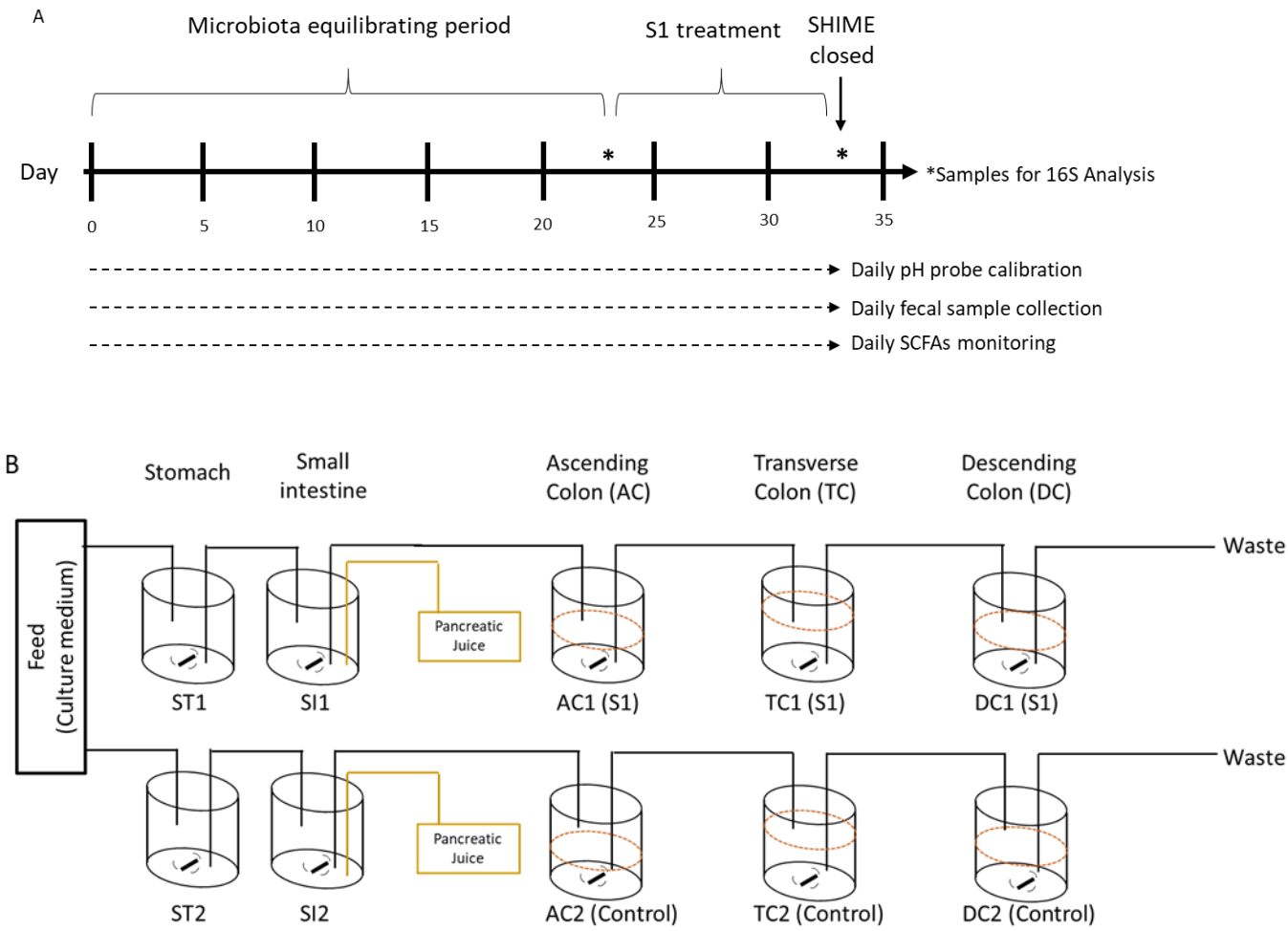

Figure 2.1. TWIN-SHIME timeframe (A) and setup (B) including SHIME-1 (top) with probiotic treatment (AC1-TC1-DC1) and SHIME-2 control (bottom, AC2-TC2-DC2).

7. Preparation of luminal extracts

Resultant fermentation culture was defrosted from -20°C and centrifuged at 15,000g for 30 minutes at 4°C. Supernatant from centrifugation was filter-sterilized by 0.22 μm syringe filter. Filtrate was then aliquoted into 2 ml micro-centrifuge tubes and stored at -20°C as luminal extract.

8. Cell culture and viability assay

Human intestinal epithelial cell line Caco-2 were maintained in complete medium (Dulbecco′s Modified Eagle′s Medium (DMEM) with 10% fetal bovine serum (FBS)) in a 5% CO_2, 37°C humidified incubator. For Caco-2, cells were sub-cultured by tryptic digestion when they reached 80-90% confluence. Enterocyte monolayers were differentiated in 24-well flat bottom cell culture plate starting at $2x10^4$ cell/well for 12-14 days before treatment or viability assay.

Viabilities of cells after incubating with a range of luminal extracts were determined by 3-(4,5-dimethylthiazol-2-yl)-2,5-diphenyltetrazolium bromide (MTT, Sigma, St. Louis, USA) assay. Treatment media containing different concentrations of luminal extracts from no plasticizer control chambers of each experiment in complete medium were incubated with differentiated Caco-2 monolayer for 24 hours. Cells were washed by phosphate buffered saline pH 7.3 (PBS) and incubated with 0.5 mg/ml MTT solution for 1-1.5 hours in triplicate. Luminal extract concentrations (v/v%) were employed as treatment percentage for gene expression assay, which preserved >90% cell viability mimicking a sub-lethal chronic exposure of to each cell-line.

9. RNA extraction, reverse transcription, and real-time PCR gene expression analysis

Caco-2 cells were treated with 1 ml of 20% and 5% v/v filter-sterilized extracts in DMEM for 48 and 24 hours inside a cell culture incubator, respectively. Total RNA was extracted using RNAiso PLUS (Takara, Kusatsu, Japan). RNA concentration was determined by NanoDrop spectrophotometer (Thermo Fisher Scientific, Waltham, USA). cDNA was reverse transcribed using PrimeScript reverse transcription kit (Takara, Kusatsu, Japan) according to the manufacturer's protocol. Real-time PCR was performed on Applied Biosystems QuantStudio 7 Flex Real-Time PCR System (Thermo Fisher Scientific, Waltham, USA) with TB Green Premix Ex Taq II (Takara, Kusatsu, Japan) reagent. Relative quantification of target gene expression was calculated by 2^(-ΔΔCt). Ribosomal protein lateral stalk subunit P0 (*RPLP0*) was used as housekeeping genes for Caco-2gene expression calculation, respectively. Primers for specific mRNA amplification are listed in supplementary information (Supplementary Table 2.2).

10. Western blot

Western blot was employed for comparison of tight junction and adherens junction protein expressions after fermenter extract treatment. Caco-2 cells were seeded at $2x10^4$ cell/well in 24-well plate. Cells were cultured for 14 days before treatment. Cells was incubated with 20% extracts for 48 hours prior to protein quantification. After treatment, cells were washed with PBS and then incubated in 200 µl RIPA buffer (Merck Millipore, Burlington, US) with protease inhibitor cocktail (Sigma, St. Louis, USA) for 2 hours at 4°C. Total protein was obtained in supernatant after centrifugation at 20,000g for 10 minutes. Protein samples were stored at -80°C before protein concentration quantification by BCA assay (Thermo Fisher Scientific, Waltham, USA). For SDS-PAGE, 10 µg of total protein from each sample was mixed with sample buffer, heated at 95°C for 5 minutes before loading. SDS-PAGE with 4% stacking and 10% resolving gels was used for electrophoresis. Western blot transfer was done in wet condition with 80V for 90 minutes at 4°C. PVDF (GE Healthcare, Chicago, US) after transfer was blocked with blocking solution (5% skimmed milk in TBST) for 2 hours, and then incubated with primary antibody in blocking solution overnight at 4°C. Primary antibodies used for this study were: mouse monoclonal anti-β-actin (1:2000, Sigma, St. Louis, USA), rabbit polyclonal anti-E-cadherin (1:1000, ABclonal, Woburn, US), rabbit polyclonal anti-occludin (1:2000, ABclonal, Woburn, US) and rabbit polyclonal anti-F11R (1:2000, ABclonal, Woburn, US). Horseradish peroxidase-conjugated goat anti-rabbit IgG (H+L) secondary antibody (1:2000, Novus Biologicals, Centennial, US) and goat anti-mouse IgG (H+L) secondary antibody (1:2000, Thermo Fisher Scientific, Waltham, USA) were used for chemiluminescent signal generation during image capture. Densitometry of chemiluminescent signal was analyzed using Image J. Relative expression of target protein was calculated by dividing its signal to β-actin signal. Normalized expression of target in each sample was generated by dividing relative expression to average relative

expression in control fermenter extract group. Target protein expression in control fermenter treatment group was normalized as 1.

11. Measurement of epithelial integrity by trans-epithelial electrical resistance (TEER)

Epithelial tight junction integrity of Caco-2 monolayer was estimated by TEER assay. Resistances of transwell membrane and transwell with differentiated monolayer were measured by epithelial voltohmeter (EVOM2; WPI, Sarasota US). Caco-2 cells were seeded at $2x10^4$ cell/transwell and allowed to differentiate for 21-28 days until stable TEER was obtained (>600 Ωcm^2). 20% v/v of luminal extracts in DMEM were loaded on the apical chamber while complete medium was placed in the basolateral region. Initial TEER was recorded as $TEER_o$, and TEER values at time t = 0, 24, 48, 72, 96, 120, 144 hours were used for the calculation of percentage TEER change by $(TEER_t\text{-}TEER_o)/TEER_o$ x100%.

12. Animal study

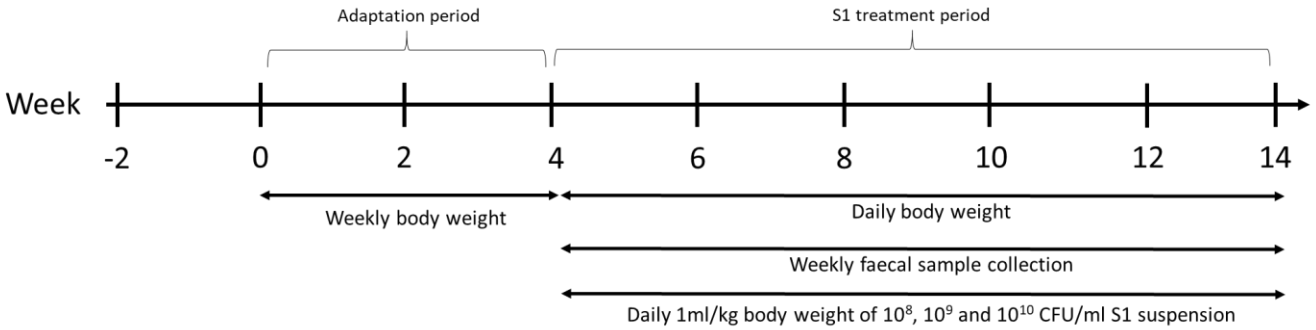

Figure 2.2. Timeframe of S1 treatment on SD rats

Sprague Dawley (SD) rats were bred by the Centralized Animal Facilities (CAF) at The Hong Kong Polytechnic University. Six-week-old male rats weighing approximately 200 g were used for animal experiment with the approval and strict accordance to the Code of Practice - Care and Use of Animals for Experimental Purposes prepared by the Agriculture, Fisheries and Conservation Department in Hong Kong. Animal experiment procedures and licenses were permitted and granted by Hong Kong Department of Health (Reference number: (18-3) in DH/SHS/8/2/4 Pt.3). All experimental procedures were performed humanely and efficiently to minimize unnecessary discomfort and pain to the animal during the process. All animals were maintained in CAF at a temperature of 21 ± 2°C, relative humidity of 55% ± 10%, and with 12-hour light/dark cycle. Standard diet and water were constantly supplied to all animals. Before starting the experiment, all rats were maintained in experimental environment for 2 weeks to allow them to adapt to the experimental conditions. Probiotic treatment dosages were set in a range adopted from Li, 2014 [101]. After two weeks' adaptation period, SD rats will be subjected to 10 ml/kg rat body weight of 10^7, 10^8, or 10^9 CFU/ml probiotic suspension in 0.85% NaCl, whilst the same volume of 0.85% NaCl will be fed to the rats in control group by oral gavage. All rats will be sacrificed 10 weeks after the probiotic introduction to the GI tracts (Figure 2.2). Fecal and blood samples of rats will be collected weekly and immediately after sacrifice, to perform microbiota and biochemical analyses, respectively.

13. 16S rDNA Sequencing and Analysis

Total genomic DNA from collected rat fecal and SHIME luminal or biofilm samples were extracted by using TIANamp stool DNA kit (TIANGEN, Beijing, China) according to the manufacturer's protocol. The V3-V4 region of 16S rDNA were sequenced by using 16S338F forward primer and 16S806R reverse primer. 16S rDNA sequencing was performed by MajorBio using Illumina HiSeq 2000 sequencer. For sequence analysis, primer sequences will be trimmed, and raw data was analyzed by using QIIME2 with HPC provided by Information Technology Services Office, The Hong Kong Polytechnic University. Paired-end sequences with quality data were denoised by DADA2 plugin, and taxonomy was assigned according to SILVA database. Alpha-diversity indices, beta-diversity weighted UniFrac PCoA plots were generated by using pipelines within QIIME2. Taxonomy heatmaps and barplots were generated by RStudio with gplots and ggplot2 packages.

14. Analysis of short-chain fatty acids (SCFAs)

Method for quantification of SCFA concentrations was adopted from Song, et al., 2018 and Zhao, et al., 2006 [134, 135]. Fecal samples were defrosted from -80ºC and weighted. About 0.15 g of solid samples was transferred to a new Eppendorf tube and were centrifuged to the bottom of tube at 13,684g for 1 minutes at 4ºC. Samples were then homogenized in 600 µl sterilized Milli-Q water by using an inoculation loop. Fecal suspensions were vortexed briefly, placed in ice for 10 minutes. Suspensions were centrifuged at 13,684g for 1 minute at 4ºC. 270 µl of supernatants were transferred to a new tube and its pH was adjusted to pH 2-3 by 27 µl of 1M HCl (tested by pH paper). 3 µl of internal standard (100 mM 2-Ethyl-butyric acid) was added into each mixture. All mixtures were centrifuged at 2,376g for 20mins at 4ºC. Supernatant was filtered and transferred to a sample vial with insert for GC-FID analysis equipped with Agilent GC column DB-FFAP (123-3232). Oven temperature was set at: 80ºC for 2 minutes followed by ramping 6ºC per minute until 180ºC and then hold for 2 minutes. Concentration of different SCFAs were calculated from standard curves and respective dilution factor.

15. Isolation of lymphocytes from Mesenteric lymph node (MLN)

MLNs were excised and extra fat tissue was removed. By using a syringe plunger, total cells from MLNs were gently dissociated against a 70-um cell strainer. Cells passed through the strainer were washed and collected in a total of 4 ml PBS. Cells were wash by centrifugation at 400g for 5 minutes. Cell pellet was then re-suspended in RPMI with 1X penicillin/streptomycin (Thermo Fisher Scientific, Waltham, USA), counted by using hemocytometer with trypan blue exclusion. Total MLNs cells were seeded at 50 x 10^4 cell/well and incubated at 37ºC in 5% CO_2 for 24 hours. Cultural medium was collected by centrifugation at 20000g for 10 minutes at 4ºC. Supernatant was stored at -80ºC until assay.

16. Isolation of mononuclear cells from spleen

Spleen was excised and its weight was measured. By using a syringe plunger, total cells from spleen were gently dissociated against a 70-um cell strainer. Cells passed through the strainer were washed and collected in a total of 4 ml PBS. Cells were wash by centrifugation at 400g for 5 minutes. Cell pellet was re-suspended into 4 ml PBS and layered on 5 ml of Ficoll Paque Plus (GE Healthcare, Chicago, US) slowly. Density gradient separation was done by centrifugation at 400g for 30 minutes at room temperature. Top layers were carefully removed and discarded. Buffy-coat was collected and washed by PBS. Cell pellet was re-suspended in 1ml RPMI with 1X penicillin/streptomycin (Thermo Fisher Scientific, Waltham, USA), counted by using hemocytometer with trypan blue exclusion. Mononuclear cells were seeded at 50 x 10^4 cell/well and incubated at 37ºC in 5% CO_2 for 24 hours. Cultural medium was collected by centrifugation at 20000g for 10 minutes at 4ºC. Supernatant was stored at -80ºC until assay.

17. *Ex-vivo* distal colon tissue culture

Colon was excised and its length was measured. Two 1 cm segments of distal colon from the rectal end were dissected and washed by PBS. Weights of these segments were measured to the closest milligram and recorded. Each segment was placed into separated well in 24-well cell culture plate with 1 ml RPMI with 1X penicillin/streptomycin (Thermo Fisher Scientific, Waltham, USA). Tissue was incubated at 37ºC in 5% CO_2 for 24 hours. Cultural medium was transferred to an Eppendorf tube and centrifuged at 20000g for 10 minutes at 4ºC. Supernatant was stored at -80ºC until assay.

18. Enzyme-linked immunosorbent assay (ELISA)

Total protein extracts and cultural supernatants were defrosted from -80ºC. Cytokine productions by various kinds of tested cells were assessed by ELISA according to the manufacturer's manual. Duplicate assay wells were used for all samples' quantification. Rat IL-10 (R&D System), rat TGF-β (ExCell, Shanghai, China) and human IL-8 (Novus Biologicals, Centennial, US) ELISA assay kits were used in this study.

19. Statistical analysis

Statistical comparisons were performed using GraphPad Prism 5. All results are shown as mean +/- SEM from the replicates. Statistical analysis, t-test or one-way ANOVA was used with 95% confidence.

Results

1. Isolation and determination of probiotics

Total twelfth potential probiotics were isolated from Hong Kong local infant feces and different fermented foods including kimchi, soy-paste, and Kombucha (Table 2.1). The probiotic isolates were identified by sequencing the housekeeping gene 16S rDNA. The full length of 16S rDNA sequencing results were analyzed and compared with matches at the NCBI database. Probiotics isolates named S1, S2, S5, S9, S11, S12, S13, S14, MM1, MM2, 96B2 and E96, matched with *L. rhamnosus*, *L. sakei*, *Leu. mesenteroides*, *L. plantarum*, *P. acidilactici*, *P. pentosaceus*, *L. paracasei* and *L. gasseri* respectively (Table 2.1). All the isolates were included in the Qualified Presumption of Safety (QPS) list by European Food Safety Authority (EFSA). These probiotics were then subjected to further characterization to determine the potential of being used in the subsequent studies.

Table 2.1. Probiotic isolates used in this study

Isolate	Identity based on 16S rDNA sequences	Source of isolation
MM1	*P. acidilactici*	Soy-paste from local wet market
MM2	*P. pentosaceus*	Soy-paste from local wet market
S1	*L. rhamnosus*	Infant feces
S2	*L. sakei*	Korean kimchi
S5	*Leu. mesenteroides*	Korean kimchi
S9	*L. plantarum*	Kombucha
S11	*L. plantarum*	Taiwanese kimchi
S12	*L. plantarum*	Taiwanese kimchi
S13	*L. plantarum*	Taiwanese kimchi
S14	*L. plantarum*	Taiwanese kimchi
96B2	*L. paracasei*	Infant feces
E96	*L. gasseri*	Infant feces

2. *In-vitro* characteristics of in-house probiotic isolates

2.1. Acid tolerance

After 48-hours incubation in MRS broth with different pH values, acid tolerance of probiotic was determined by the ability of reaching a comparable OD value with that in ordinary MRS broth, and the time required to enter log-growth phase and stationary phase. Growth curves in different probiotics inoculated in pH 5.7 were found similar with those cultured in MRS with ordinary pH value (pH 6.2), and the growth of most isolated probiotics was found to be inhibited by acid in MRS with pH 2.0 (data not shown). To compare the acid tolerance abilities of all isolated probiotics, growth curves in MRS pH 4.0 were overlaid and compared (Figure 2.3). It was observed that, though S1, S9, S11, S12, S13 and S14 required a different time for entering log-growth phases, they still reached OD > 2.0 after 48 hours of incubation in MRS of pH 4.0. Among these probiotics, S12 and S14 entered their log-growth phases within the shortest time. This indicated that these two probiotics had the best acid tolerance among all the probiotics being tested. For S2 and MM2, they had a similar growth trend and entered the stationary phase at OD around 1.2. For MM1, its growth in acidified MRS was retarded but able to reach OD = 1.5 after 48 hours of incubation. S5 showed the minimum acid as tolerance indicated by its inhibited growth in the whole period of incubation time.

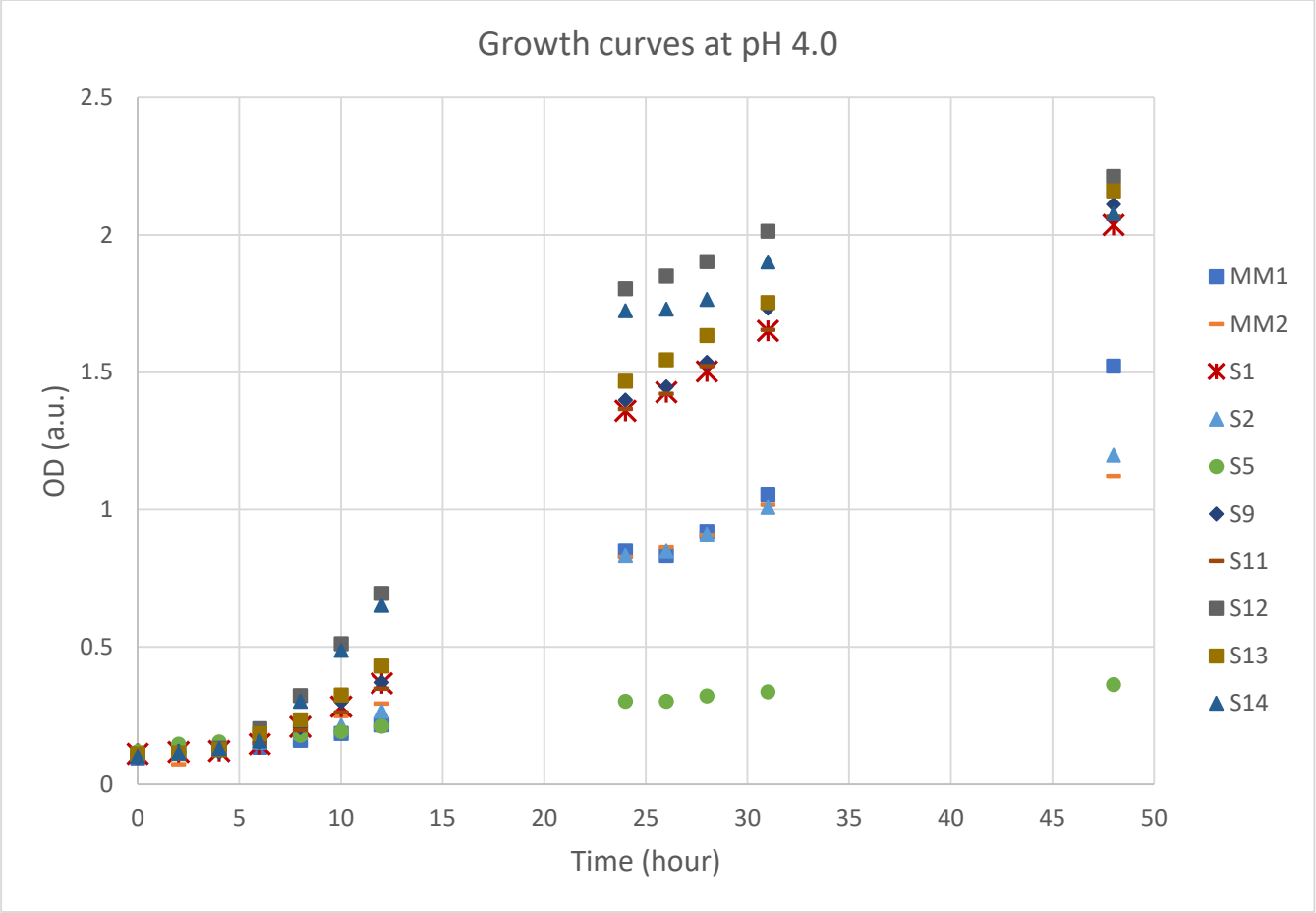

Figure 2.3. Probiotic growth curves in MRS pH 4.0

2.2.Bile salt tolerance

Percentage survival rate of each probiotic isolate tested was determined by the CFU recovered after 3 hours of incubation in the PBS supplemented with 0.3% or 0.5% bile salts, followed by plating on the MRS agar. CFUs on MRS agars were counted and back calculated to CFU remaining in the bacterial suspensions after incubation with or without bile salts. When probiotic isolates were co-incubated with bile salts, S1 and S11 showed 80-100% survival rate which had better bile salts tolerance than all the other tested LABs (Figure 2.4). S12 was found to be able to stay alive with 60% survival rate in 0.3% bile salts, while reduced to 30% in 0.5% bile salts. The survival rates of S9 and S13 in media containing bile salts were around 30-40%, while only 10% of S14 were recovered after incubating with 0.3% or 0.5% bile salts. Probiotic isolates MM1, MM2, S2, S5 and 96B2 were found to have <1% survival calculated by CFU and were sensitive to bile salts.

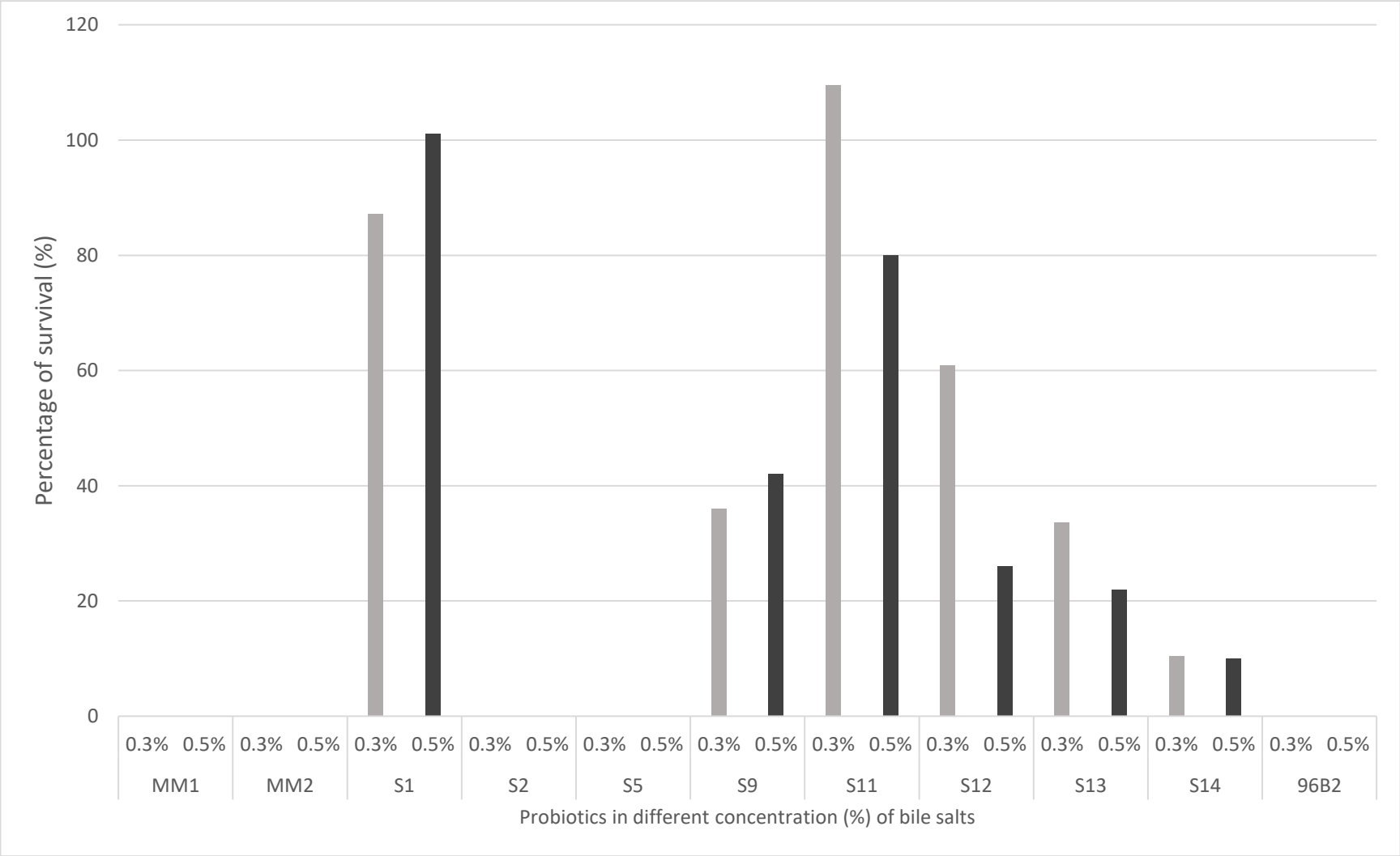

Figure 2.4. Percentage survival of probiotics in different concentration of bile salts.

2.3.Antimicrobial ability

With plenty of glucose supply in the MRS agar, production of lactic acid and alcohol by homo-fermentative and hetero-fermentative metabolisms were able to inhibit certain kinds of pathogen adjacent to the probiotic colony formed on the MRS agar. Among all the inhibition zone radii for *S. aureus* and *P. aeruginosa*, S5 on MRS agar was observed to have the highest anti-pathogenic growth ability. In the inhibition zone radii for *B. cereus*, S12 was found to inhibit the growth of *B. cereus* the most when compared with other LABs. With inhibition zone radius of 1.90 cm, S5, S12 and S13 showed the best and same anti-pathogenic growth ability towards *A. baumannii*. Probiotic MM1 gave the highest inhibitory effect to the growth of *S. enterica* serovar Paratyphi. Among the probiotics tested, S5 on MRS agar, followed by S11, S12 and S13, showed an overall and relatively high antibacterial capacity toward the pathogens tested in this study (Table 2.2).

With limited sugar supply in the mMRS agar, anti-microbial effects were mainly based on bactericidal substances other than lactic acids generated from glucose fermentation (Table 2.3). S2, S12 and S13 showed a relatively bigger inhibition zone on the growth of *S. aureus* than the other tested LABs. All tested LABs failed to inhibit the growth of *B. cereus* except S13 and S14. MM1, S5, S12 and S14 shared the same anti-microbial ability towards *P. aeruginosa*. Furthermore, MM1 and S12 also shared the same capability in impeding the growth of *A. baumannii*. With inhibition zone radius of 0.7 cm, S5 suppressed the growth of tested *S. enterica* serovar Paratyphi. Generally, S12 and S5 had the strongest antimicrobial effects against some selected pathogens among all the tested probiotics even in the limitation of lactic acid or alcohol produced by sugar fermentation. Pathogens in the poured soft BHI agar were unable to grow or even killed by the bactericidal substances produced by probiotics.

Table 2.2. Radii of inhibition zones by probiotics cultured with different pathogens on MRS agar

Probiotic isolate	Radius of inhibition zone on MRS (cm)				
	S. aureus	***B. cereus***	***P. aeruginosa***	***A. baumannii***	***S. enterica* serovar Paratyphi**
MM1	0.63	0.80	0.83	1.20	2.10
MM2	0.80	1.03	0.73	1.40	1.70
S1	0.47	0.87	0.97	1.40	1.90
S2	0.40	0.33	0.37	0.70	1.10
S5	1.13	0.93	1.47	1.90	1.60
S9	0.57	0.87	0.87	1.50	1.60
S11	1.07	1.00	1.27	1.80	1.40
S12	0.80	1.67	0.97	1.90	0.80
S13	0.77	1.17	0.93	1.90	1.30
S14	0.93	1.13	0.90	1.50	1.20

Table 2.3. Radii of inhibition zones by probiotics cultured with different pathogens on mMRS agar

Probiotic isolate	Radius of inhibition zone on mMRS (cm)				
	S. aureus	***B. cereus***	***P. aeruginosa***	***A. baumannii***	***S. enterica* serovar Paratyphi**
MM1	0.10	n.d.	0.40	0.70	0.10
MM2	0.10	n.d.	0.30	0.40	0.10
S1	0.10	n.d.	0.30	0.30	0.30
S2	0.20	n.d.	0.20	0.20	0.50
S5	0.10	n.d.	0.40	0.30	0.70
S9	0.10	n.d.	0.20	0.40	0.40
S11	0.10	n.d.	0.20	0.20	0.50
S12	0.20	n.d.	0.40	0.70	0.30
S13	0.20	0.10	0.30	0.30	0.20
S14	0.10	0.10	0.40	0.50	0.20

(n.d., not determined)

2.4.Probiotics adhesion and competitive adhesion ability

Adhesiveness to cultured human epithelial Caco-2 cells of different isolated probiotics were examined. It was observed that S1, S9, S11, S12, S13 and S14 demonstrated a relatively higher adhesiveness to Caco-2 compared with MM1, MM2, 92B2, S2 and S5. Among these LABs with better Caco-2 adhesion, S1 performed well in both acid and bile salt tolerance. With some other biochemical characterization done previously, for instance, the soymilk fermented by S1 had higher free amino acids content and showed higher beta-galactosidase activity than the other tested LAB isolates (data not shown), this novel isolate was selected for further testing in the competitive adhesion against *S. aureus* and *E. faecalis*. Adhesion of S1 onto the enterocytes was determined using human intestinal epithelial Caco-2 and HT-29 cells in the absence and presence of pathogenic bacteria. Adhesions of *S. aureus* and *E. faecalis* were higher toward Caco-2 cells than that to HT-29. It was found that adhesion of both *S. aureus* and *E. faecalis* toward both secretive HT-29 and absorptive Caco-2 were reduced in a S1 dose-dependent manner when co-incubation with S1 (Figure 2.5). Approximately half of the pathogens were unable to bind to Caco-2 monolayer when 4-times of S1 was introduced to the mixture.

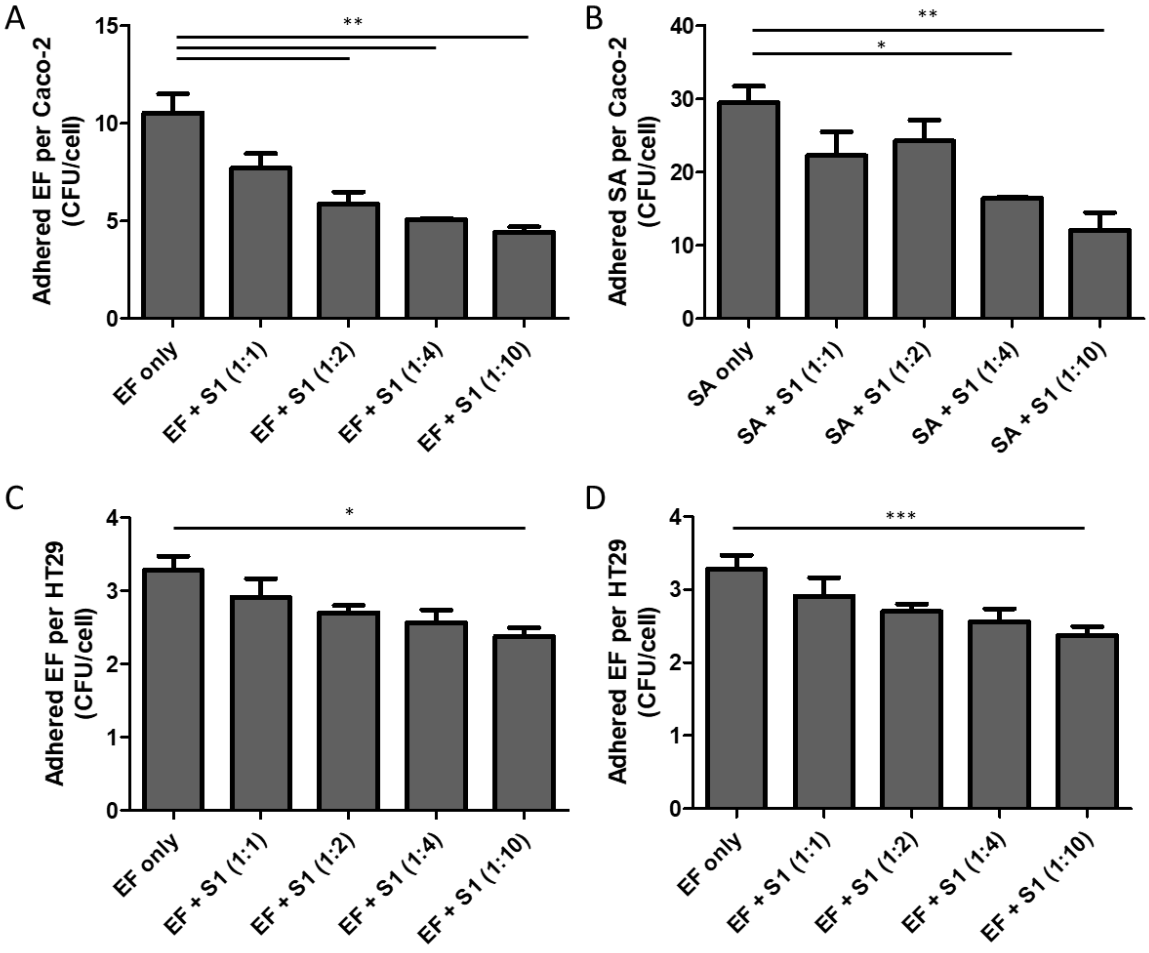

Figure 2.5. Average adhered pathogens on Caco-2 or HT-29 cell with or without S1 co-incubation. SA: *S. aureus* EF: *E. faecalis*. OD ratio of pathogen load to S1 was indicated in bracket. ANOVA, data shown as mean +/- SEM; n=2; *$p<0.05$, **$p<0.01$ and ***$p<0.005$.

2.5.Immunoregulatory effects on cultural epithelial cells

Changes of pro-inflammation cytokine IL-8 upon pathogen infections were determined in the absence and presence of selected probiotic isolate S1. When Caco-2 was incubated with S1, IL-8 level in cultural supernatant was reduced slightly comparable to those from Caco-2 cultured in DMEM only. Six to eight-fold secretion of pro-inflammatory cytokine IL-8 by Caco-2 cells was stimulated by *S. aureus*, *A. baumannii* and *E. faecium* compared to DMEM control. Co-incubation with S1 reduced the production of IL-8 triggered by *S. aureus*, *A. baumannii* and *E. faecium* back to no stimulation state (Figure 2.6).

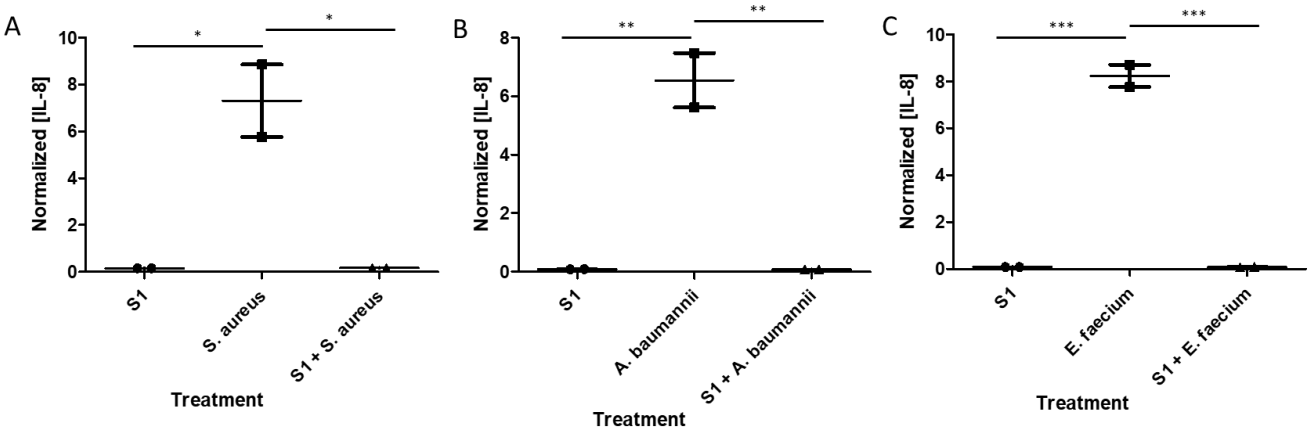

Figure 2.6. Normalized IL-8 production in Caco-2 cells after incubated with S1 and mixes of S1 + *S. aureus* (A), S1 + *A. baumannii* (B) and S1 + *E. faecium* (C). IL-8 concentration in DMEM-treated Caco-2 cultural supernatant was normalized to be 1. ANOVA, data shown as mean +/- SEM; n=2; *p<0.05, **p<0.01 and ***p<0.005.

3. Effect of *L. rhamnosus* S1 on the gut microbiota of *in vitro* human GI tract (SHIME)

3.1. Preparation of SHIME for the experiment

After inoculation of fecal slurry into each SHIME chambers, concentrations of SCFAs in each chamber were quantified by GC-FID, which were used as indicators reflecting microbiota compositional stability between same regions of SHIME-1 and SHIME-2 (ACs, TCs and DCs). As suggested in the protocol of ProDigest SHIME, treatment can be started when SCFA levels had been stabilized with similar concentrations in each colon regions. S1 treatment was started 24 days after inoculation, since SCFAs levels had been stably established (Figure 2.7).

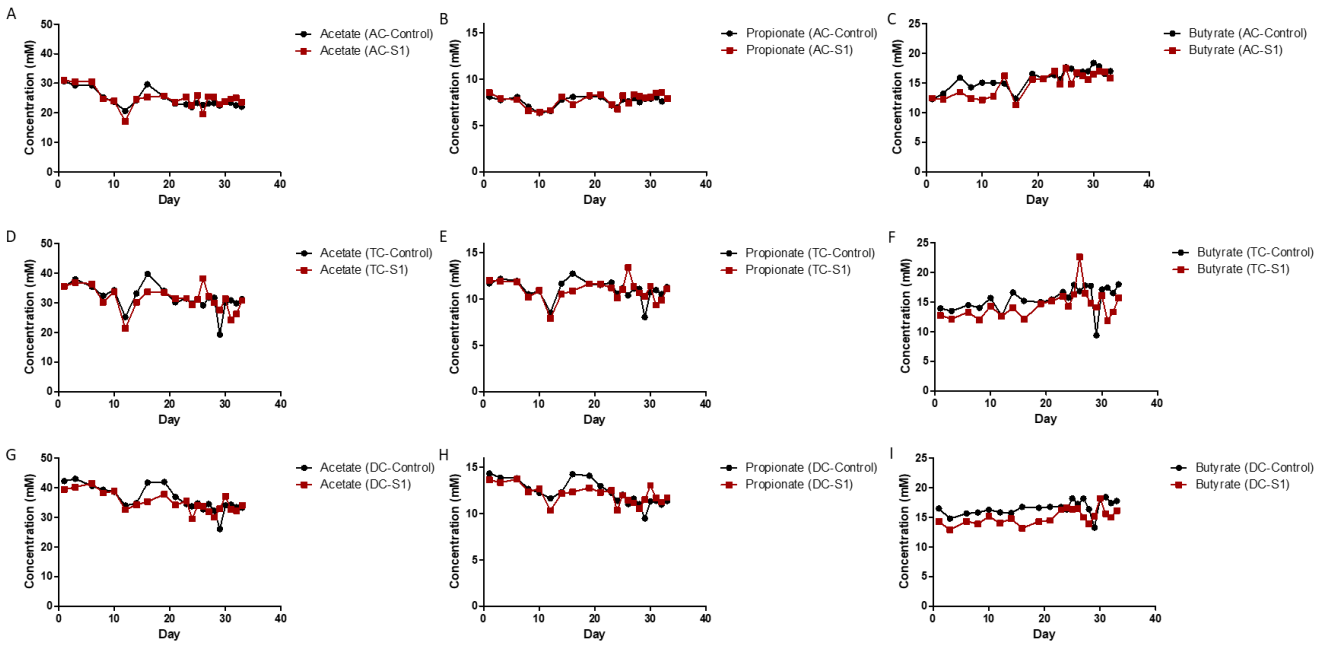

Figure 2.7. Concentrations of SCFAs in different SHIME chambers (ACs: A-C, TCs: D-F and DCs: G-I)

3.2.Luminal phase microbiota

All extracted genomic DNA from SHIME samples were characterized by 16S rDNA gene (V3-V4 regions) using Illumina sequencer. A total of 716,009 qualified reads from 18 samples passing through DADA2 pipeline within QIIME2 were used for subsequent analysis. In the SHIME experiment, the gut microbiota treated with or without S1 treatment were compared and indicated as S1 and control, respectively, throughout the results and discussion. The microbial composition and abundance of ascending colon (AC), transverse colon (TC) and distal colon (DC) were analyzed using 16S rDNA sequencing. Similar baseline microbiota in ACs, TCs and DCs at day-0 were established before S1 treatment as indicated in unweighted UniFrac PCoA (Figure 2.8A). The beta-diversities between AC-S1 and AC-control, TC-S1 and TC-control, were clustered closer to each other after 10-day S1 treatment period regardless abundance of taxa as indicated in both unweighted and weight UniFrac PCoA (Figure 2.8). However, it was observed that DC-S1 community deviated from DC-control after the treatment. Compositional differences became more significant if phylogenetic distance was considered (Figure 2.8B). *Megasphaera* spp. under phylum *Firmicutes* and family *Veillonellaceae* was the dominant genus in this experiment. The drop of genus *Megasphaera* (-9%) also contributed to the reduction of these phylum and family in DC-S1 when compared to DC-control after the 10-days of treatment. From AC to DC, the relative abundance of genus *Bacteroides* was enriched by more than 2-folds when the system was treated with S1. On the other hand, *Blautia* spp. and *Subdoligranulum* spp. were reduced in TC-S1 and DC-S1 comparing to their controls. *Bifidobacterium* spp. was reduced in AC-S1 but increased in TC-S1 and DC-S1 (Figure 2.9).

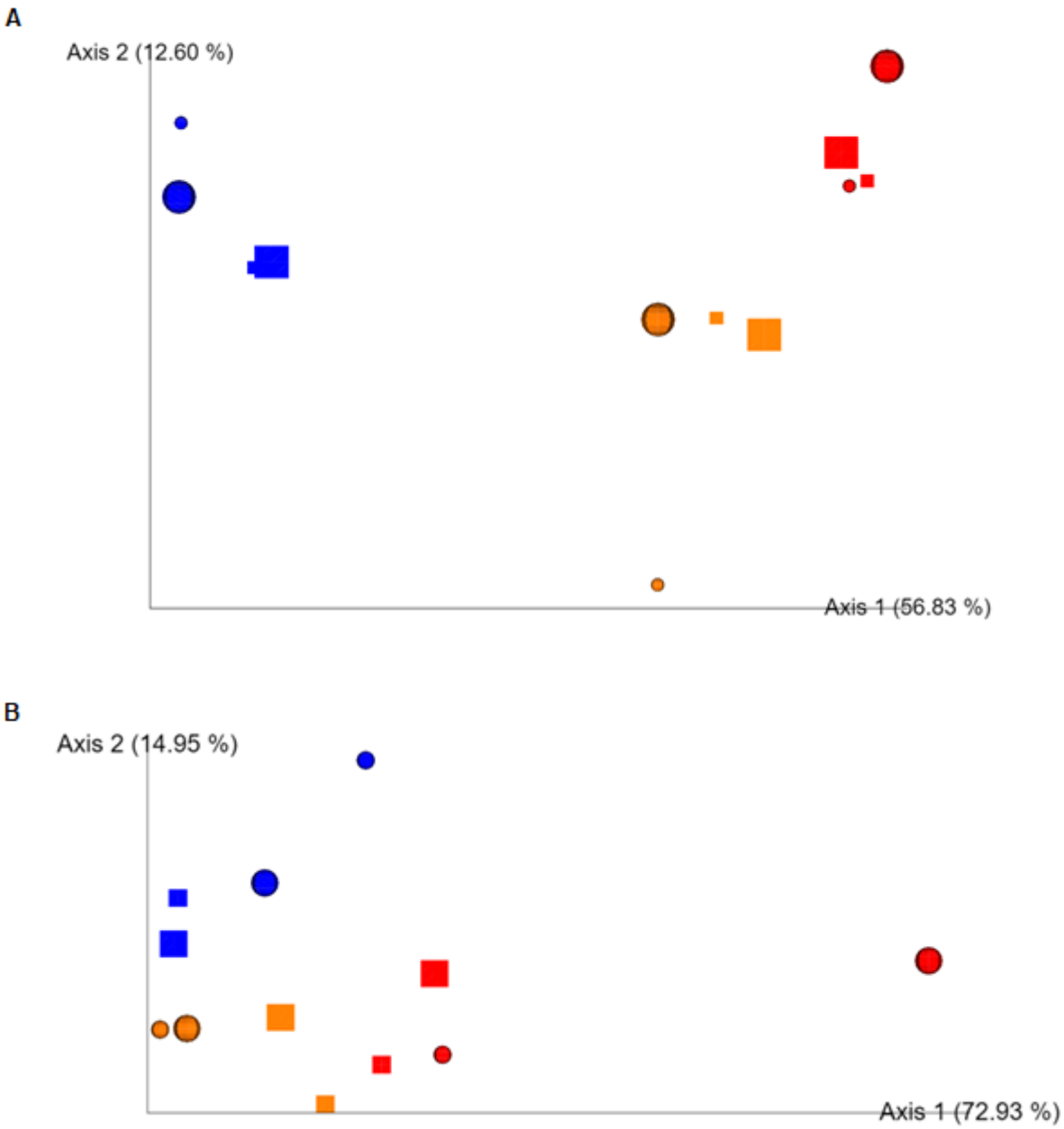

Figure 2.8. Unweighted (A) and Weighted (B) UniFrac PCoA analysis for the microbiota compositions in different parts of SHIME. AC: blue, TC: orange and DC: red. Square and sphere indicated control SHIME and S1 SHIME, respectively. Day-0 and day-10 were indicated by small and large labels.

Figure 2.9. Taxonomy heatmaps showing relative abundance of all taxa in luminal contents on phylum (A), family (B) and genus (C) levels.

3.3.Biofilm microbiota

Resultant biofilm microbiota was also analyzed. Beta-diversities of the whole community deviation revealed that, implicated in unweighted UniFrac PCoA, higher community taxa variation between DC-control and DC-S1 was observed (Figure 2.10A). However, abundance weighted compositions were similar in respective colon regions. Microbiota of TC-S1 and TC-control were more comparable than that between AC-S1 and AC-control, DC-S1 and DC-control (Figure 2.10B). *Firmicutes* was the dominant phylum in AC and TC microbiota, while *Proteobacteria* contributed to over 50% of relative abundance in DC fermenters. Compared with respective controls, bacteria under phylum *Bacteroidetes* were reduced in AC-S1 but increased in TC-S1 and DC-S1. *Firmicutes* in S1-administing chamber AC-S1 was increased. Family *Bacteroidaceae* and Genus *Bacteroides* were reduced in AC-S1. Interestingly, relative abundance of *Lactobacillus* spp. under family *Lactobacillaceae* was smaller in AC-S1 than that in the control. 10% more *Veillonellaceae* was detected in AC-S1 than AC-control. Furthermore, *Pseudomonadaceae* was suppressed in AC-S1. *Tyzzerella* spp. was reduced in AC-S1 and TC-S1, and even depleted in DC-S1 in the resultant microbiota. More *Megasphaera* spp. was found in AC and TC chambers' biofilm, and it was the dominant genus within these communities. 10% more *Megasphaera* was detected on AC-S1 biofilm, while relative abundance of this genus remained stable in other samples. Under phylum *Proteobacteria*, an unclassified genus (*f__Enterobacteriaceae;__*) from family *Enterobacteriaceae* was detected in DC-control with over 50% relative abundance. However, *Escherichia-Shigella* in DC-S1 dominated the community with 57% relative abundance. Relative abundance of *Klebsiella* spp. in DC-S1 biofilm was less than one-third of that in DC-control (Figure 2.11).

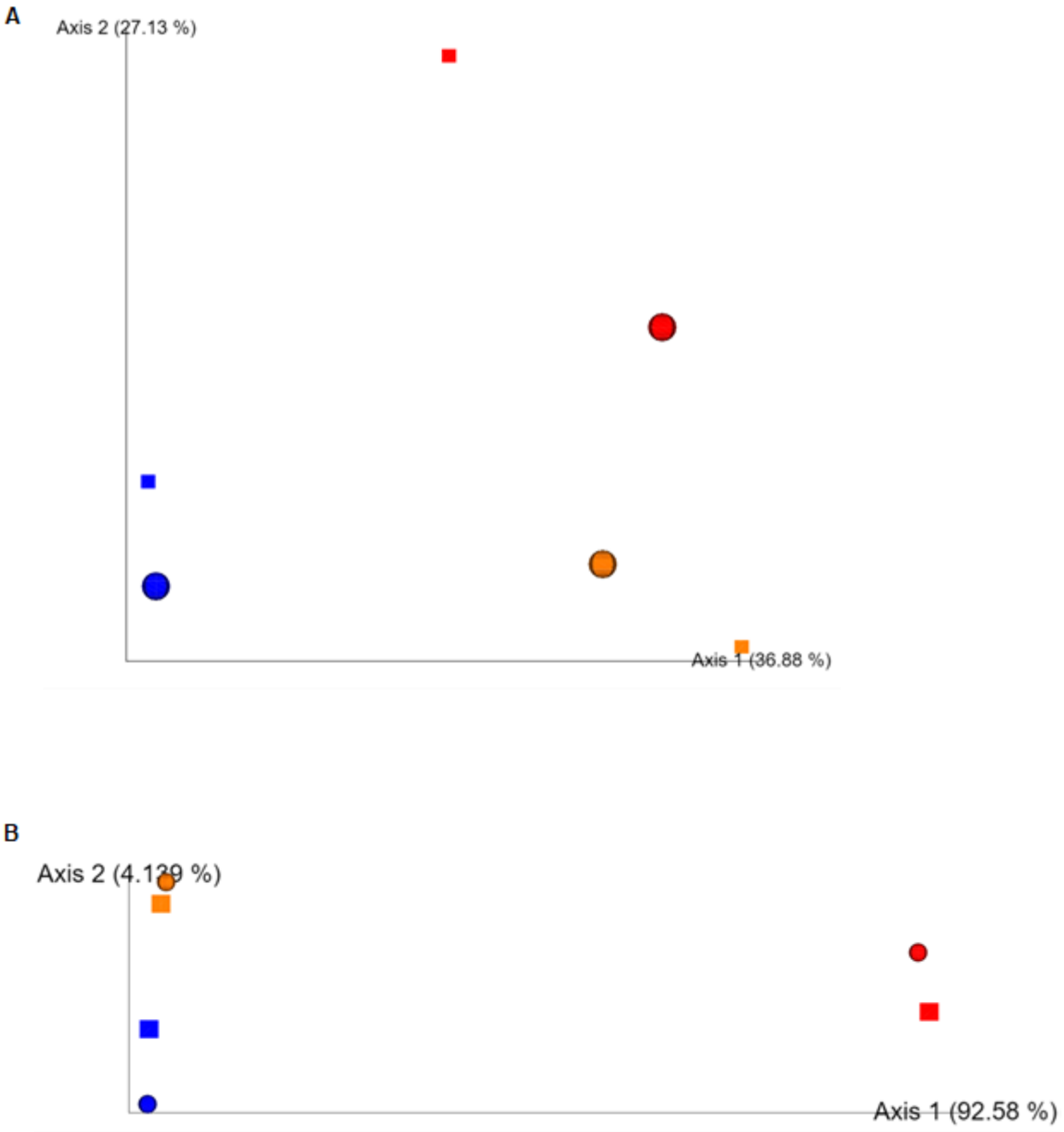

Figure 2.10. Unweighted (A) and weighted (B) UniFrac PCoA for biofilm microbiota compositions. AC: blue, TC: yellow and DC: red. Square and sphere indicated control and S1 SHIME, respectively.

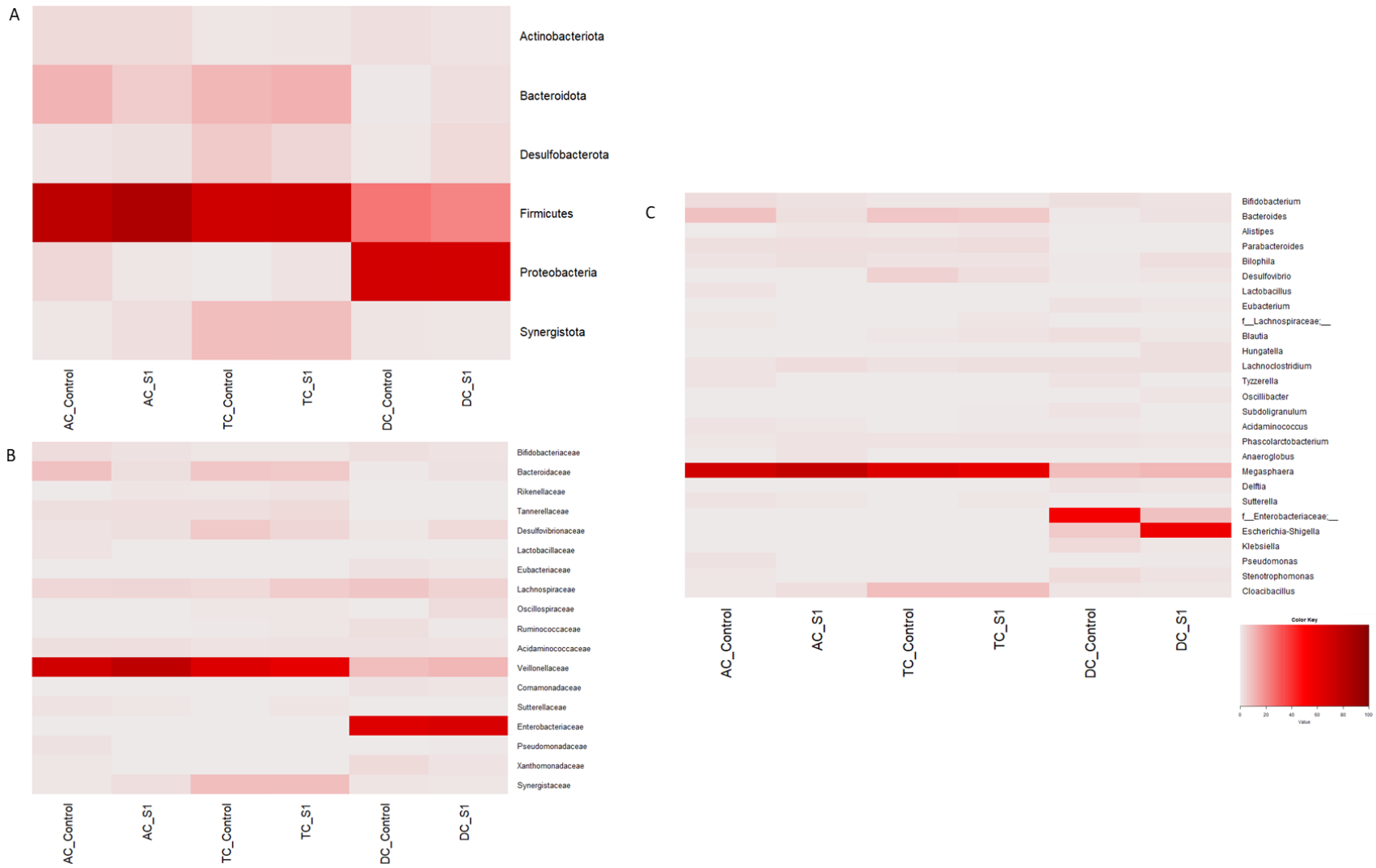

Figure 2.11. Taxonomy heatmaps showing relative abundance of all taxa in biofilm on phylum (A), family (B) and genus (C) levels.

3.4.Epithelial integrity assays by TEER

Filter-sterilized luminal microbiota derived metabolites from each chamber were incubated with differentiated Caco-2 monolayer for epithelial integrity test. Luminal extract concentration (20% v/v in cultural medium) were employed as treatment percentage, which preserved >90% cell viability for both ACs, TCs and DCs' extracts treatments mimicking a sub-lethal chronic exposure of to each cell-line (Figure 2.12). TEERs in monolayers treated with AC and TC microbiota extracts remained comparable. It was observed that TEER dropped with a more rapid rate in Caco-2 monolayers treated with DC-control extract than those incubated with DC-S1 extract (Figure 2.13). Significant increases of TEERs were detected after Caco-2 had been treated with DC-S1 extract for 72 hours. Up to 26% more TEER percentage growth was observed after 144-hour incubation (Figure 2.13).

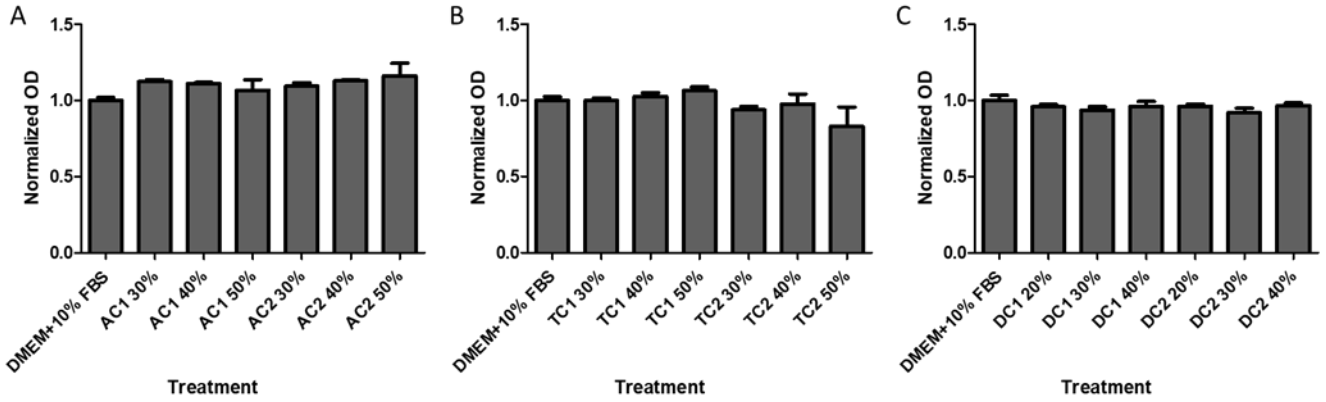

Figure 2.12. Normalized viability of Caco-2 cells in different concentrations of luminal extracts of AC (A), TC (B) and DC (C) compared to those incubated in complete medium.

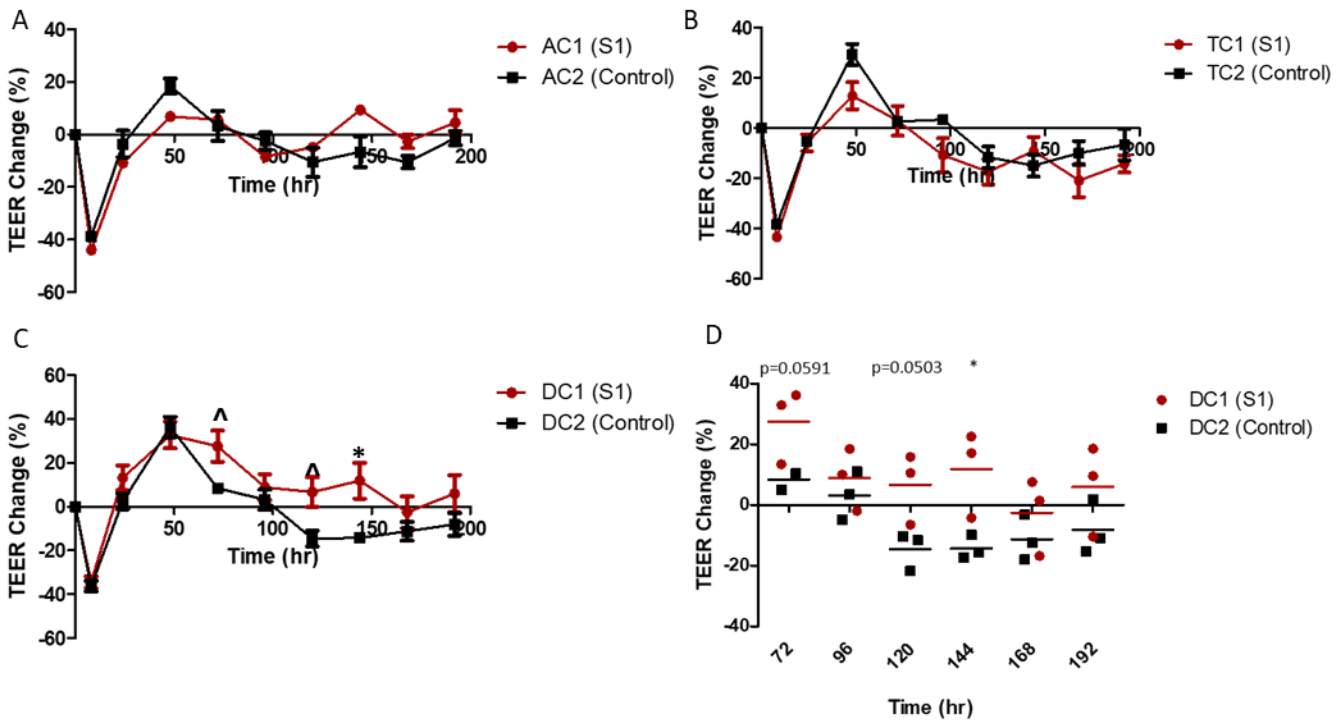

Figure 2.13. Changes of TEER after treatment of SHIME luminal extracts. The TEER of Caco-2 cells treated with AC (A), TC (B) and DC (C) microbiota derived metabolites were shown. SHIME-1 (AC1-TC1-DC1) indicated S1 SHIME treatment group while SHIME-2 (AC2-TC2-DC2) indicated control SHIME setup. Statistical analysis of TEER changes between monolayer treated with DC-control (black) and DC-S1 extracts (red) from 72-hour onwards (D). t-test, data shown as mean +/- SEM; n=3; ^0.05<p<0.06, *p<0.05, **p<0.01 and ***p<0.005.

3.5.TJ/AJ gene expression in Caco-2

From TEER assay, the permeability of Caco-2 monolayer was reduced by DC-S1 extract. RT-qPCR was employed to further assess mRNA expression of major TJ and AJ genes in Caco-2 cells treated with DC-control and DC-S1 extracts (Figure 2.14). After normalizing relative quantification of expression levels to DC-control, the expression of *CDH1* was enriched by 10% in DC-S1 extract-treated Caco-2 cells, though the difference was not statistically significant. Moreover, *OCLN* expression was up-regulated by 77% in Caco-2 treated with DC-S1 extract compared to the control ($p<0.05$).

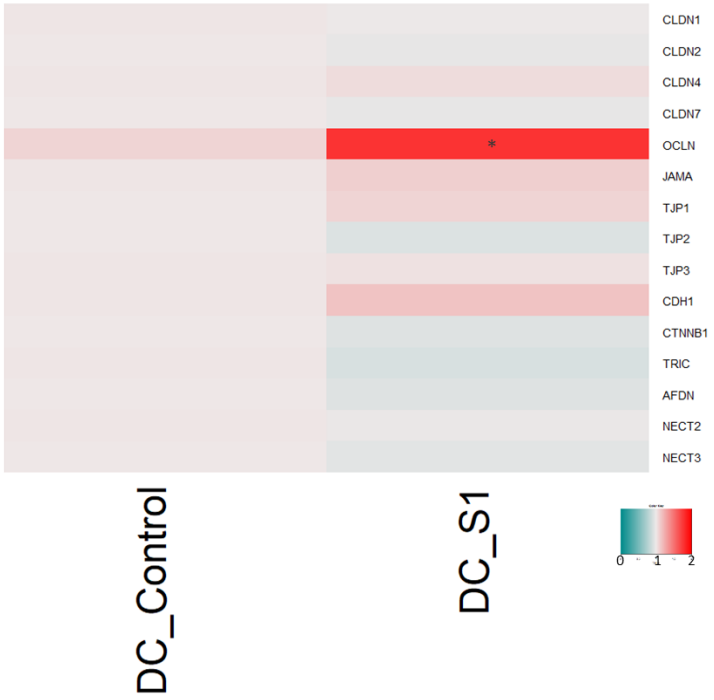

Figure 2.14. Normalized expressions of TJ/AJ genes in Caco-2 cells. t-test. Data shown as mean +/- SEM; minimum n=3, *$p<0.05$, **$p<0.01$ and ***$p<0.005$.

3.6.DC-S1 extract promoted occludin expression in Caco-2

Protein expression of occludin in Caco-2 was then assessed by western blot (Figure 2.15). After treatment of different DC regions' extracts, occludin protein level was 39% higher in Caco-2 incubated with metabolites from DC-S1 ($p<0.05$) than that from DC2.

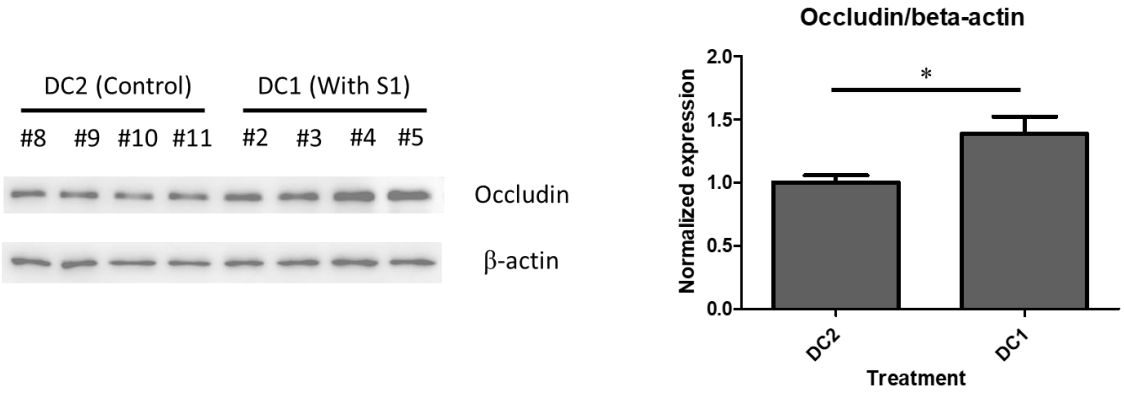

Figure 2.15. Effect of DC extracts on the expression levels of occludin in Caco-2 cells by western blot analysis. Data shown as mean +/- SEM. t-test, n=4, *p<0.05, **p<0.01 and ***p<0.005.

4. Effect of *L. rhamnosus* S1 on SD rat

4.1. Changes of gut microbiota by supplementation of *L. rhamnosus* S1 in SD rat

Fecal DNA extracted from 20 rats were sequenced for 16S rDNA (V3-V4 regions) on Illumina platform. A total of 233,737 high quality reads resulted from DADA2 denoising pipeline within QIIME2 were used for analysis. In the animal experiment, healthy SD rats were treated with S1 at different dosages and their resultant fecal microbiota compositions were analyzed by 16S rDNA sequencing. *Firmicutes* to *Bacteroidetes* (F/B) ratio showed gradual drops across S1 treatment dosages to rats yet not statistically significant (Figure 2.16). Beta-diversities unweighted and weighted UniFrac PCoA showed that the microbiota communities of rats from the control group were clustered which partially align with the gut microbiota of rats fed with the lowest dosage, 10^7 CFU/ml, suggesting that they share a relatively similar microbial composition (Figure 2.17A). However, microbial compositions from rats treated with dosages 2 and 3 of S1 were deviated from both control and dosage 1. More significant variation was observed in abundance-weighted UniFrac PCoA which indicated that most rats from S1-D3 group had microbial community differed from all the other groups of rats (Figure 2.17B).

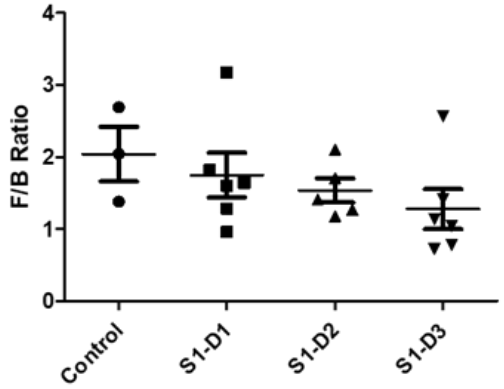

Figure 2.16 *Firmicutes* to *Bacteroidetes* ratio in the GI microbiota of SD rats.

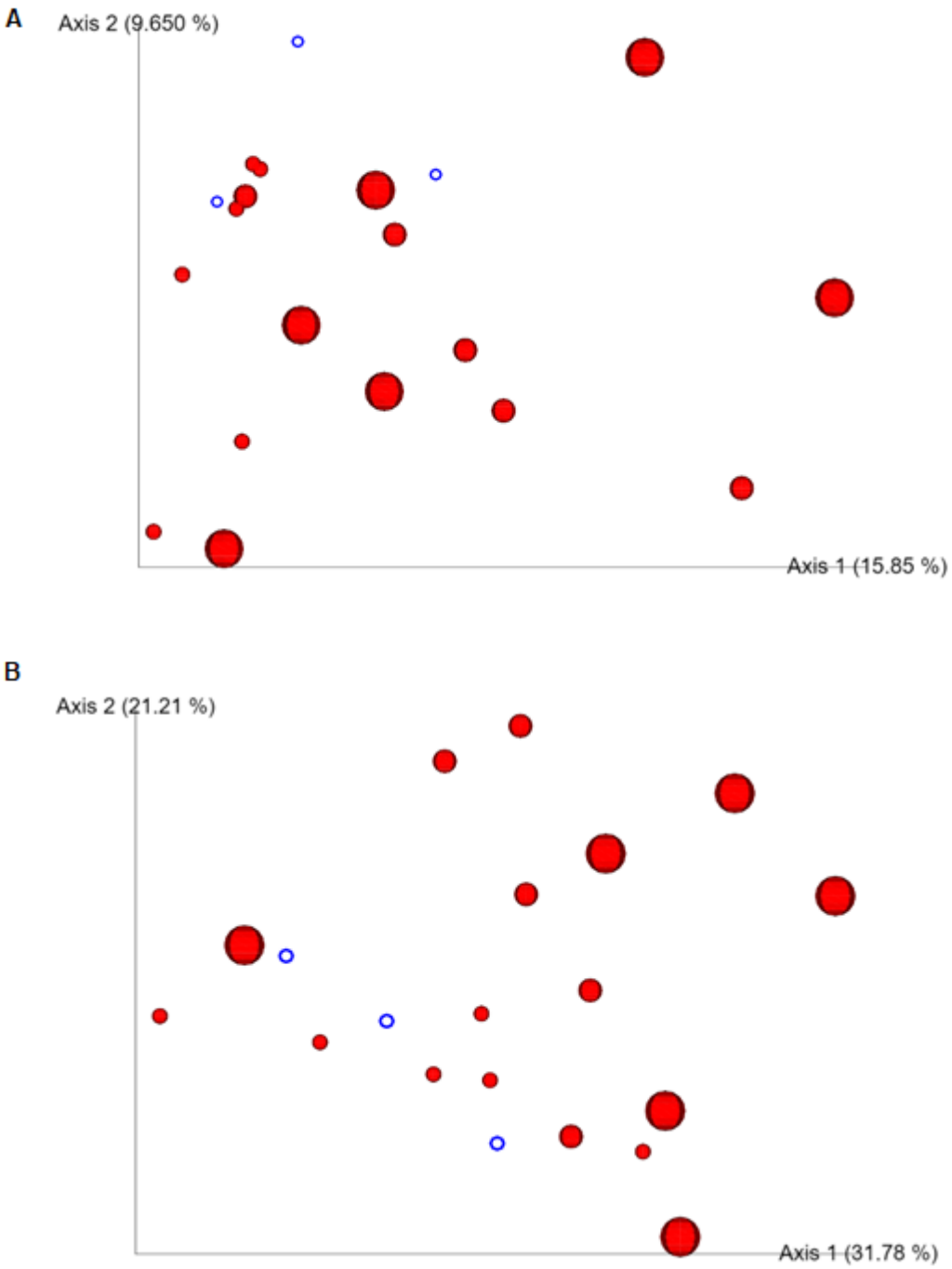

Figure 2.17. Unweighted (A) and weighted (B) UniFrac PCoA for SD rat microbiota compositions. No treatment: blue circles, S1-treated rats: red spheres. Sizes of spheres indicated S1 dosages 1, 2 and 3, which correspond to 10^7, 10^8, or 10^9 CFU/ml probiotic suspension in 0.85% NaCl respectively.

Administration of S1 induced several intestinal microbiota compositional changes (Figure 2.18). *Firmicutes* was the dominate phylum within each rat microbiota, which contributed approximately 50-60% of total abundance (Figure 2.18A). After S1 treatment, enrichment of *Lactobacillus* spp. was detected in S1-D1 to S1-D3 groups but not significant (Figure 2.18C). Genus *Bacteroides* under phylum *Bacteroidetes* and family *Bacteroidaceae* contributed 30-40% of total microbial compositions in all rats (Figure 2.18B). Although not statistically significant, there was a dose-dependent trend of increase in this genus as the S1 treatment increased. Except *Bacteroidaceae*, mean relative abundance of family *Erysipelotrichaceae* also showed an S1-dose-dependent increase. Under this family, *Turicibacter* spp. was observed significantly increased in S1-D2 and S1-D3 treatment groups ($p<0.05$). An unclassified genus under family *Prevotellaceae* (*f__Prevotellaceae*) was detected reduced in S1-D2 group ($p<0.01$). Relative abundance of this genus was depleted in S1-D3 group ($p<0.01$). *Romboutsia* spp. was enriched in all S1-treated groups, while Genus *Family_XIII_AD3011_group* under family *Anaerovoracaceae*, and *Candidatus_Saccharimonas* under family *Saccharimonadaceae* were reduced by high dosages S1 treatments. *Streptococcus* spp. under family *Streptococcaceae*, and genus/family *Clostridia_UCG-014* were significantly reduced in S1-treatment groups ($p<0.05$) (Figure 2.18C). Relative abundance of SCFA producers was not observed altered after treatments. Fecal SCFAs remained stable in various groups of rats (Figure 2.19)

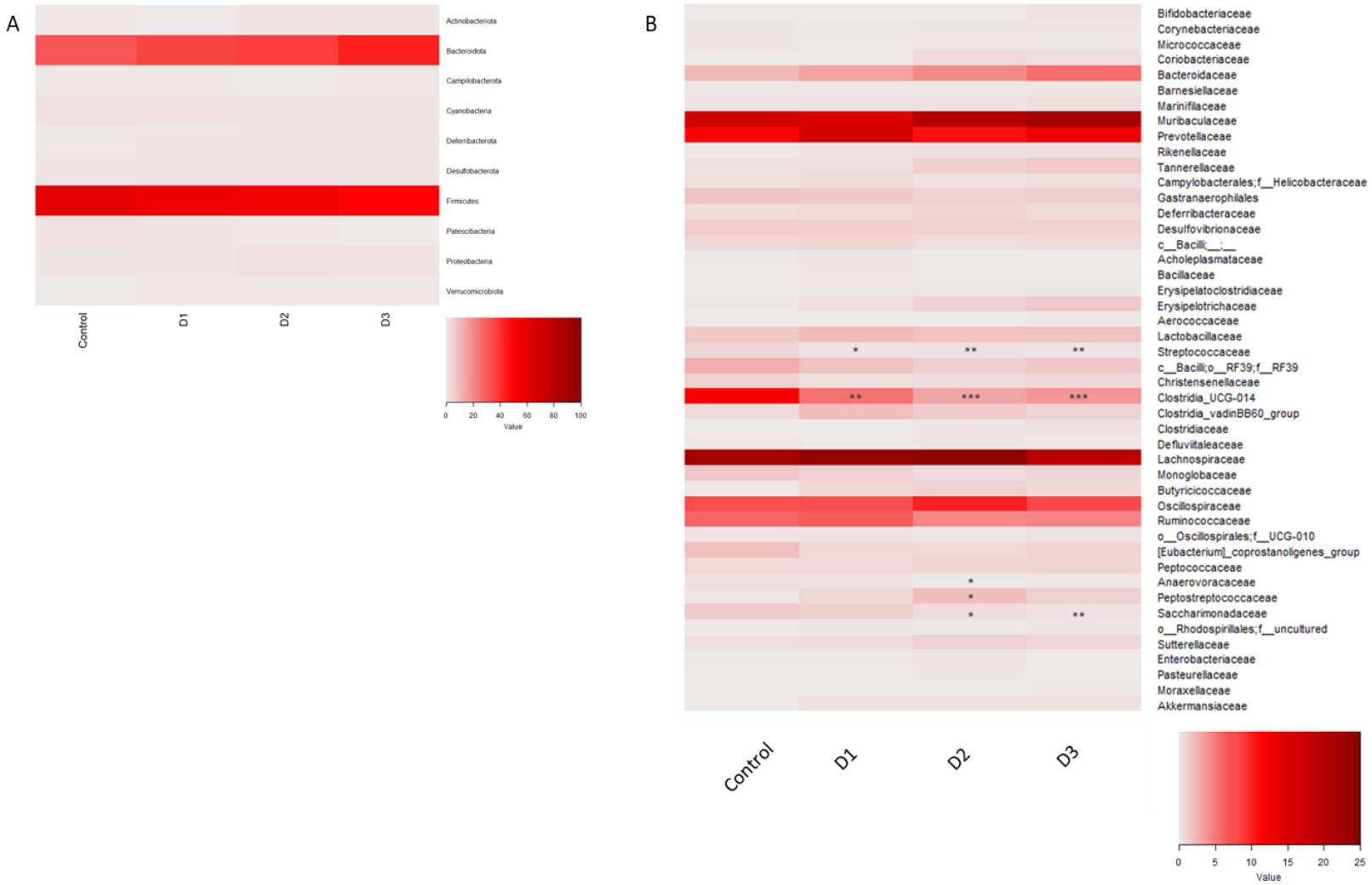

Figure 2.18. Taxonomy heatmaps of gut microbiota at phylum (A), family (B) and genus (C) levels in the SD rats. Dosage 1-3 of S1 were labels as D1 to D3 respectively. Data shown as mean +/- SEM. ANOVA; control n=3, D1 n=6, D2 n=5 and D3 n=6; *p<0.05, **p<0.01 and ***p<0.005.

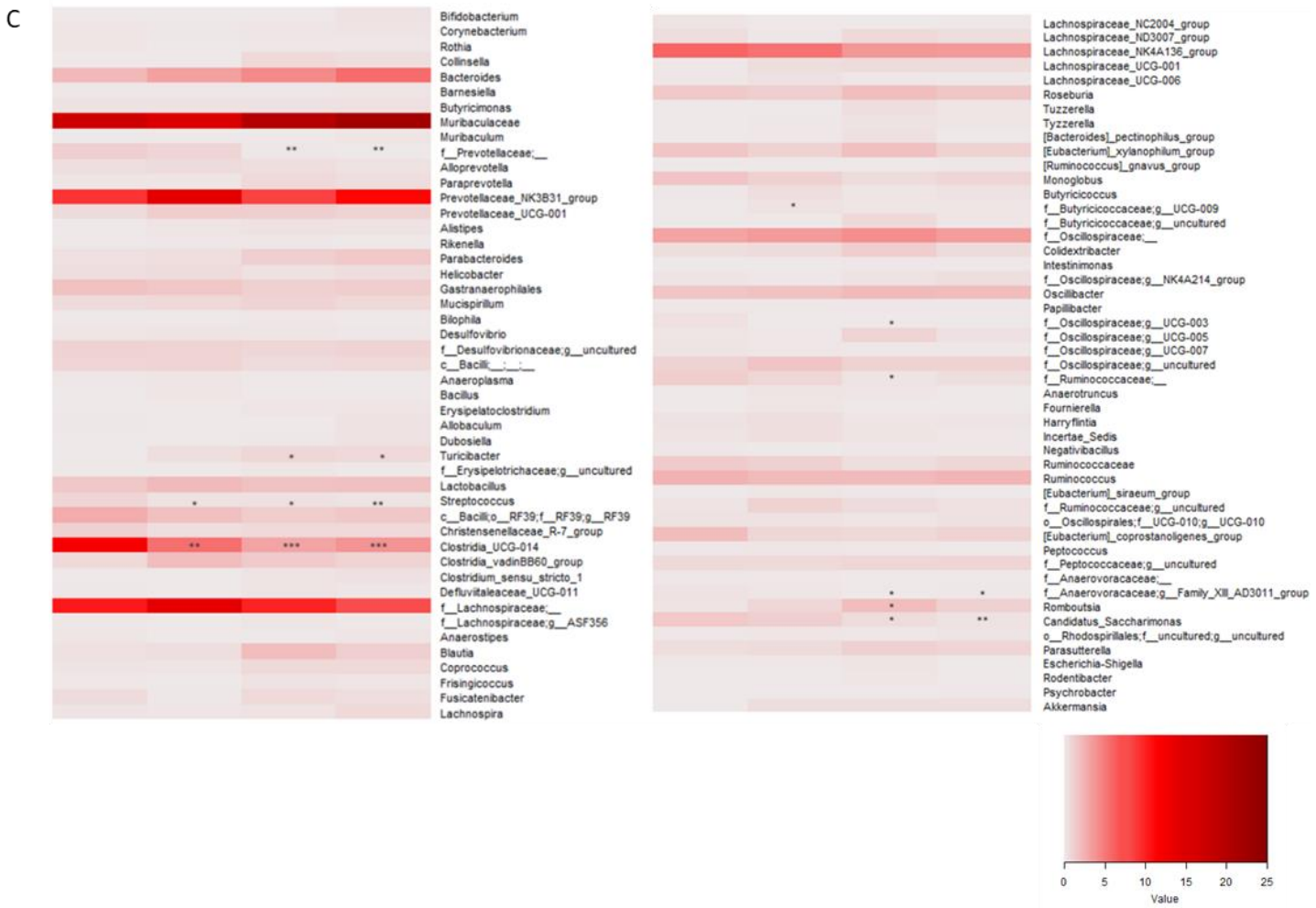

Figure 2.18. Taxonomy heatmaps of gut microbiota at phylum (A), family (B) and genus (C) levels in the SD rats. Dosage 1-3 of S1 were labels as D1 to D3 respectively. Data shown as mean +/- SEM. ANOVA; control n=3, D1 n=6, D2 n=5 and D3 n=6; *p<0.05, **p<0.01 and ***p<0.005 - continued.

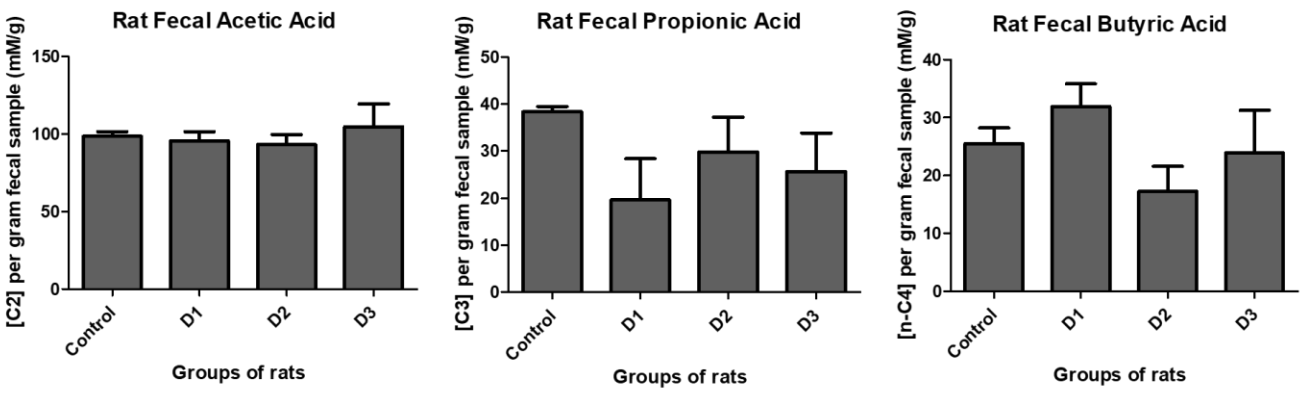

Figure 2.19. Mean concentrations of short-chain fatty acids in rat fecal samples (in mM per gram feces). Data shown as mean +/- SEM.

4.2.Cytokines in rat *ex-vivo* colon tissue, MLN cells and splenic mononuclear cells cultures

Secretions of anti-inflammatory cytokine IL-10 and TGF-β from colon tissues were quantified by ELISA. Compared with no S1 treatment, IL-10 production from colon tissues in rats received different dosages of S1 was higher than no treatment control rats. S1-D3 rats' colon tissue secreted more TGF-β compared to control (p=0.072). Ex-vivo cultures of MLN and splenic mononuclear cells from S1-D3 produced more IL-10 (p=0.089 and p=0.202, respectively). Significant increases in IL-10 generation were detected in spleen mononuclear cell cultures from S1-D1 and S1-D2 (p<0.05) (Figure 2.20). Except minor reduction of liver weight was observed at high dosage groups, most organ weights remained stable (Figure 2.21)

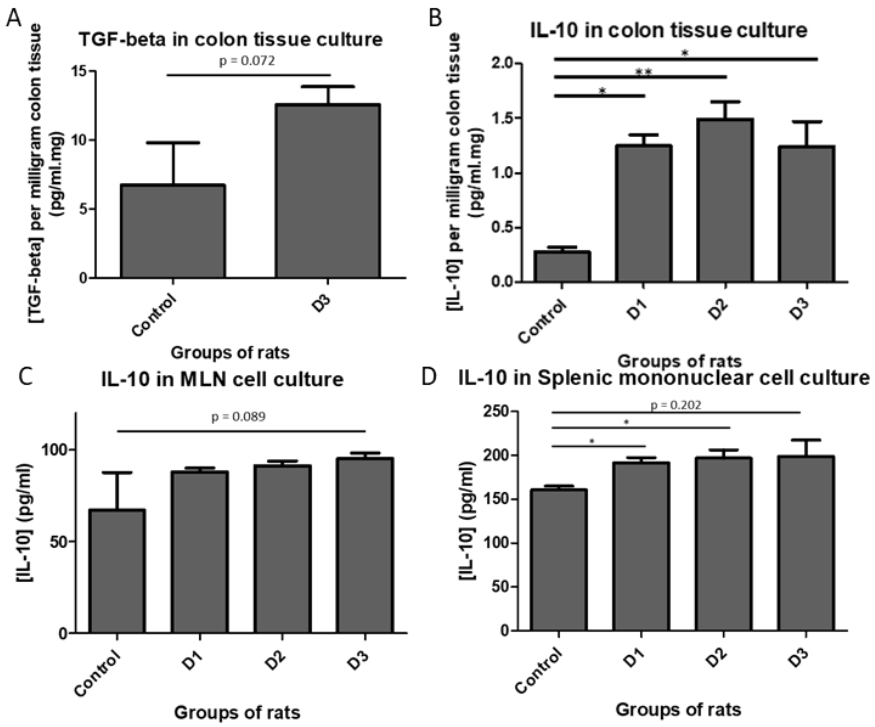

Figure 2.20. Concentrations of TGF-β and IL-10 in *ex-vivo* colon tissue culture (A and B). Concentrations of IL-10 in MLN total cell and splenic mononuclear cell cultures (C and D). Data shown as mean +/- SEM. ANOVA; control n=3, D1 n=6, D2 n=5 and D3 n=6; *p<0.05, **p<0.01 and ***p<0.005.

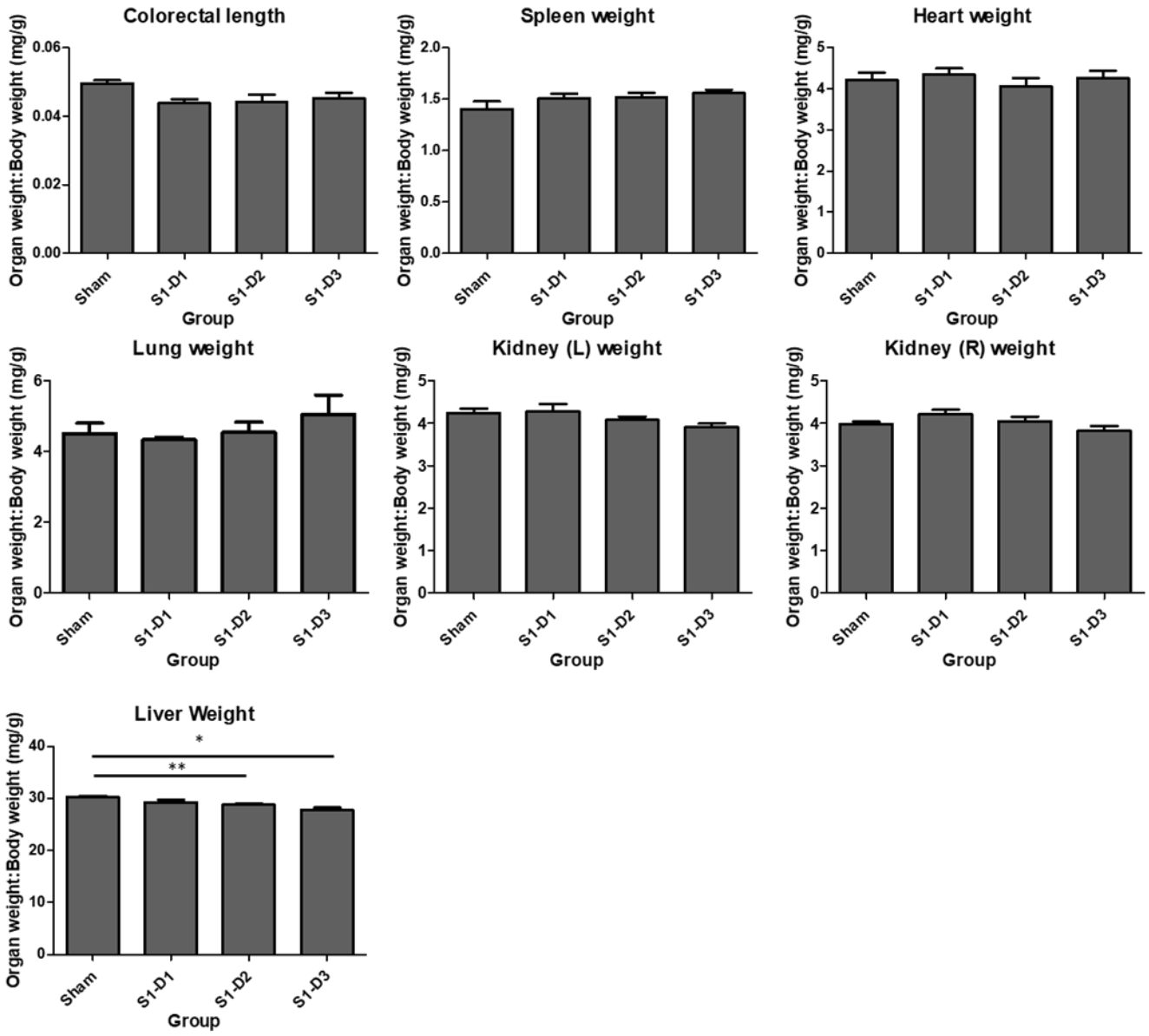

Figure 2.21. Mean rat organ weights per unit body weights. Data shown as mean +/- SEM. ANOVA; control n=3, D1 n=6, D2 n=5 and D3 n=6; *p<0.05, **p<0.01 and ***p<0.005.

Discussion

1. Selection of probiotic isolate by *in-vitro* characterization assays

LABs are commonly isolated beneficial bacteria from the environment. Typically, they could be acid resistant due to the production of lactic acid that serves as natural anti-microbial compound in multiple mucosal surfaces within hosts. Among all the isolates in this study, *Lactobacillus* spp. obtained from various sources performed better in acid and bile tolerance which facilitate their survival and colonization within the GI tract. Lactic acid and acetic acid produced during carbohydrate metabolism, as well as bacteriocins secretion, are major anti-microbial substances produced by these LABs for competing nutrients or colonization within hosts [13, 136, 137]. The beneficial microbes isolated from a particular origin are often the best-fit isolates that could survive within that host origin.

L. rhamnosus is one of the most studied LABs. *L. rhamnosus* GG had multiple adhesion molecules such as teichoic acids, LPXTG-like protein, and pili, all of which enable them to bind to mammalian cells [109, 110, 138, 139]. Differentiated Caco-2 monolayer mimics the epithelial lining under the mucus layer of enterocytes in the gut. Extracellular matrix proteins and surface receptors can be found at the apical side receiving antigen signals and bacterial adhesions. In the adhesion assay of this study, the isolate S1 originated from human feces performs well in attaching to cultural enterocytes Caco-2 and HT-29 cells, though S1 has a relatively weaker adhesiveness towards these cell lines compared to *S. aureus* and *E. faecalis.* Upon simultaneous colonization, S1 can compete binding sites with these opportunist pathogens. This protective effect of S1 reduces the chance of infection as both *S. aureus* and *E. faecalis* could invade epithelial cells and get into the bloodstream underneath the epithelium, leading to the possibilities of sepsis and endocarditis. In addition to occupying binding sites, S1 produces anti-microbial substances inhibiting growth of some common food-borne pathogens such as *S. aureus*, *P. aeruginosa*, *Sal. enterica* serovar Paratyphi and *B. cereus*, which further reduced the chance of getting gastroenteritis.

L. rhamnosus S1 had an average performance in terms of acid and bile tolerances, and it also showed moderate abilities against foodborne pathogens. However, this probiotic isolate possessed high epithelium adhesion and protection against the adhesions of opportunistic pathogens, namely *S. aureus* and *E. faecalis*, towards epithelial cells. It also reversed the pro-inflammatory stimulation triggered by *S. aureus*, *A. baumannii* and *E. faecium* as indicated by IL-8 secretion. These factors made S1 outcompeting others as a potential probiotic for preventing pathogenic infection, ameliorating dysbiosis, promoting epithelium integrity and regulating immunity in host GI tract. Administrating alive S1 isolate to the *in-vitro* GI tract / animals, and then monitor its effects on the epithelium permeability in cultural intestinal epithelial Caco-2 and secretion of anti-inflammatory cytokines in various organs were carried out for assessing probiotic effects of S1.

2. *L. rhamnosus* S1 changed human-origin microbiota in SHIME

The simulator of human intestinal microbial ecosystem (SHIME), namely *in- vitro* GI tract, is an ideal and alternative approach to study the effect of target of interest, i.e., probiotics, supplements, food contaminants, toxicants, and drug, on the gut microbial community and its derived metabolites in human. Furthermore, the whole system runs continuously from oral to fecal and the researchers could opt to include an absorption unit, for which setting the whole system runs uninterrupted as many other similar in-house settings in different research institutions. SHIME had been employed in multiple assessments in these research areas [140-144]. Luminal phase of the SHIME mimics the ingested food flow across the GI tract from stomach, small intestine, ascending colon, transverse colon and finally descending colon to waste.

Colonic microbiota is the largest community within human body. The effect of S1 administration to this ecosystem was studied by 16S rDNA sequencing analysis. Beta diversity PCoA (Weighted UniFrac) showed that community deviation was observed between DC-control and DC-S1 after 10-days of treatment. S1 changed the microbiota of DC and increased the phylogenetic distance between DC-S1 and DC-control.

Among these modification, *Bacteroides* spp. increased in luminal microbiota of all three colon regions (AC, TC and DC) in SHIME which received S1 treatment. *Bacteroides* is commonly found in human microbiota but less abundant in IBS and UC patients [22]. Some species from this genus were able to regulate immunity of GI tract [29, 145]. DC-S1 possessed 9% less *Megasphaera* spp. within its community. Though *Megasphaera elsdenii* was found to be able to reverse damages caused by lactate in the rumen gut, and produce SCFAs including acetate, propionate, butyrate and valerate, previous studies related to this genus are scarce. [146, 147]. Two studies published in 2020 reported the correlation between this *Megasphaera* spp. and cancers, yet it remained largely unclear if it is a causal or consequential relationship

[148, 149]. *Megasphaera elsdenii* was also found promoting pro-inflammatory status of blood monocyte-differentiated dendritic cells and stimulating proinflammatory cytokine productions by these cells [150]. Suppressive effect on relative abundance of genus *Megasphaera* may provide less inflammatory stimulation to both mucosal epithelium and local immune cells.

3. Metabolites from *L. rhamnosus* S1-modified gut microbiota promoted the epithelium integrity

Total microbial metabolites were collected from the distal colon regions of SHIME and used as extracts for the treatment of cultural epithelial cells. The epithelium integrity was assessed by TEER test and further confirmed with qPCR and western blot for the TJ/AJ proteins being affected in this process. The permeability of Caco-2 monolayer increased more rapidly when treated with DC-control extract compared to DC-D1 extract in a TEER assay. Together with the major microbiota compositional deviation in DCs, Caco-2 cells were used for TJ and AJ gene expression assay to identify which major component was affected. When Caco-2 cells were incubated with DC-S1 extracts, mRNA level of OCLN was enriched by 77% ($p<0.05$). This up-regulation was also translated to protein level. Occludin protein in Caco-2 cells was also enriched by 39%. Occludin is one of the most important tight junction proteins in cell-cell junction for the formation of epithelium [33]. Except maintaining epithelium integrity by reducing pore size between cell junctions, its expression also indicates the epithelial characteristic in the epithelial cells as tumor and metastatic cells undergoing epithelial–mesenchymal transition (EMT) produces fewer adhesive proteins such as E-cadherin and occludin [151, 152].

4. *L. rhamnosus* S1 reduced opportunistic pathogens in the gut microbiota of SD rats

In addition to the complete test on digestive juice tolerance, animal model provided a more realistic mucosal surface than that in the cultural Caco-2 monolayer as there is proper mucus secretion between bacteria and epithelial cells. Body weights, food and water intakes of rats receiving different dosages of S1 were stable and comparable to the control group receiving no treatment (data not shown). Colon lengths and organ weights were similar except liver. Reduction of relative liver weight was observed in S1-treated rats and the reason for this phenomenon remained to be elucidated. Though numerous *Lactobacilli* spp. can promote intestinal SCFA levels in experiment animals, fecal SCFAs including acetic acid, propionic acid and butyric acid concentrations in this study remained similar across different groups of rats in this study.

Total microbiota compositional analysis is also available in this animal experiment. Consistent with the findings in the SHIME experiment, increase in the relative abundance of commensal genus *Bacteroides* in S1 treated rat microbiota were observed, though the difference is not statistically significant. *Romboutsia* spp. and *Turicibacter* spp. were also enriched in high dosages S1-treated rats. An unclassified taxon under family *Prevotellaceae* (*f__Prevotellaceae*) and *Clostridia UCG-014* were reduced significantly after S1 treatment in a dose-dependent manner. Studies on the correlation between microbiota composition and metabolic diseases found that, family *Prevotellaceae* was positively related to CD, diarrhea-predominant irritable bowel syndrome (IBS-D) and risk of cardiovascular diseases [29, 153, 154]. Our results showed that S1 also reduced *Streptococcus* spp. in the gut microbiota of rats. This genus of bacteria was observed to be positively correlated with joint inflammation and can be found in biofilm of atherosclerosis plaque and endocarditis [31, 155, 156]. It is possible that the up-regulations of immunoregulatory IL-10 and TGF-β were due to the reduction of these taxa with pro-inflammatory profile. Yet the exact mediators and mechanisms remained to be further investigated.

5. Immunoregulatory effect of *L. rhamnosus* S1 on colon, MLN and systemic regions of SD rats

Modification in microbial community alters metabolites and antigens that diffuse through the mucosa into circulatory and lymphatic systems. IL-10 and TGF-β in the colon tissue was increased in the rats administered with S1. Other than local cytokine levels, MLNs in the mesentery located closely together with blood, lymph and nerve supplies, which harbor multiple immune cells for GI immunity. The resultant microbiota shifted by S1 treatment also regulates these immune cells. Primary total MLN cells from the rats treated with S1 produced over 4-fold more IL-10 than that from the Sham rats. IL-10 expression is not only stimulated in MLN but also in the largest lymphatic organ and spleen. Primary culture of splenic mononuclear cells from rats treated with S1 also showed enriched IL-10 expression. IL-10 are produced by tissue repairing M2 macrophages, dendritic cells, regulatory T cells and T helper 1 cells when they receive anti-inflammatory signals such as GPCR43 or GPCR109 mediated short-chain fatty acid bindings [157]. Both IL-10 and TGF-β are signals to stimulate regulatory T cell differentiation to maintain immune tolerance. This indicates that metabolites from S1-treaed rats' GI microbes can modulate local (MLN) and systemic lymphatic systems.

Summary

Different LABs were isolated from infant feces and various fermented food samples, which were verified by 16S rDNA sequencing to be classified in the genera of *Lactobacillus*, *Leuconostoc* and *Pediococcus*. All the tested probiotics from the *Lactobacillus* genera were found to have better acid tolerance than the isolated *Pediococcus* species. *L. rhamnosus* S1 showed relatively higher resistance to acid and bile salt, and moderate antimicrobial strength against *S. aureus, P. aeruginosa, A. baumannii* and *S. enterica* serovar Paratyphi on both MRS and mMRS plates, and *B. cereus* on MRS. Moreover, S1 showed high adhesion compared with other isolates in this study and was able to compete with *S. aureus* and *E. faecalis* for the binding to cultured human epithelial Caco-2 and HT-29 cells. In addition to anti-microbial ability, this isolate can also regulate inflammatory stimulation triggered by *S. aureus, A. baumannii* and *E. faecium in-vitro*.

Our previous findings showed that S1 has good tolerance on extreme conditions in the GI tract, and high activity of β-glucosidase for antioxidant ability when compared with various probiotic strains from food and commercially available probiotic drink in the previous study [129]. *L. rhamnosus* S1 was selected for further analysis in SHIME and animal model. S1 altered DC microbiota derived metabolites, which reduced the permeability of cultural epithelium by up-regulating *OCLN* and the protein occludin. Suppressing opportunists from family *Prevotellaceae*, *Streptococcus* spp. and *Clostridia_UCG-014* while promoting *Turicibacter* spp. and *Romboutsia* spp., S1 altered the GI microbial compositions of SD rats. Furthermore, treatment of S1 promoted anti-inflammatory cytokines IL-10 and TGF-β in the colon tissue of rats. Immunomodulation effect was also detected in both local and systemic lymphatic organs, namely MLN and spleen respectively. S1 possesses these characteristics which make it a good candidate to be used as a novel mucosal probiotic for oral or topical usages.

Supplementary information

Supplementary Table 2.1. Primers used for 16S sequence amplification and 16S rDNA sequencing

Primers names	Sequences (5'-3')
16S8F	AGAGTTTGATCCTGGCTCAG
16S1492R	CGGTTACCTTGTTACGACTT
16S341F	CCTACGGGAGGCAGCAG
16S806R	ATTAGATACCCSBGTAGTCC
16S338F	ACTCCTACGGGAGGCAGCA

Supplementary Table 2.2. Primers for RT-qPCR on gene expressions in Caco-2 (Adopted from [1]Putt, 2017 and [2]Suzuki, 2011 [33, 124])

Gene	Protein	Forward sequence (5'-3')	Reverse sequence (5'-3')
RPLP0	Ribosomal protein P0	ACTTCCTTAAGATCATCCAACT	TATGAGGCAGCAGTTTCTCCA
OCLN[1]	Occludin	CCAATGTCGAGGAGTGGG	CGCTGCTGTAACGAGGCT
CLDN1	Claudin-1	TGGTGGTTGGCATCCTCCTG	AATTCGTACCTGGCATTGACTGG
CLDN2[2]	Claudin-2	CTCCCTGGCCTGCATTATCTC	ACCTGCTACCGCCACTCTGT
CLDN4	Claudin-4	ATCATCGTGGCTGCTCTGG	ACACCGGCACTATCACCATAA
CLDN7	Claudin-7	TTTCATCGTGGCAGGTCTTG	CTCATACTTAATGTTGGTAGGG
JAMA	JAM-A	GATCACAGCTTCCTATGAGGA	ATGGAGGCACAAGCACGAT
CDH1	E-cadherin	AAGAGGACCAGGACTTTGACTT	CAGCCGCTTTCAGATTTTCATC
CTNNB1	Beta-catenin	GGAATGAGACTGCTGATCTTGG	ATCATCCTGGCGATATCCAAGG
TJP1[1]	ZO-1	CAAGATAGTTTGGCAGCAAGAGATG	ATCAGGGACATTCAATAGCGTAGC
TJP2	ZO-2	GCACAGAATGCAAGGATCGA	GTCTGGAACTCGTGTGCTGG
TJP3	ZO-3	GCGAGAAGCCAGTTTCAAGC	GTCCTGGACACAGTCTCTGCGA
TRIC	Tricellulin	GGCAAAATACCCTGTGATTCAGACAG	CATGGATTCTTGAAATTCTCTCATG
AFDN	Afadin	ACCGACAAGCAAGAGCACCACTAG	TGCCTGCGATAATCTGGCTGCTG
NECT2	Nectin-2	CAGAGTCATAGCCAAGCCCAAGAAC	GTCCAGGGATGAGAGCCAGGAG
NECT3	Nectin-3	TCTCCAGGCTCTGTGGTGCC	ATGGTGAACTGCAACAGTCTGTGAA

Chapter 3 – Potential impact of plasticizer on the integrity and tissue-repairing ability of human enterocytes via altering gut microbiome

Abstract

Plasticizers can be found in both environmental and food samples. Toxicological research on different organs has been numerously reported in the past few decades. Effects of such contamination on microbiota composition shift and T helper cells homeostasis in zebrafish have also been studied recently. However, there is limited investigation regarding impact on human microbiota by plasticizer. In this study, we aimed to determine the effect of 2 plasticizers, namely Di(2-ethylhexyl) phthalate (DEHP) and di-iso-nonyl phthalate (DINP), on the gut integrity and enterocyte repairing ability via altering gut microbiota. Healthy human fecal microbiota was co-incubated with different concentrations of DEHP and DINP

Microbial diversity is reduced by DEHP treatment in a dose-dependent manner. DEHP treatment reduced phyla *Firmicutes/Bacteroidetes* ratio, while DINP treatment promoted *Proteobacteria*. Enriched (*Collinsella*, *Alloprevotella* and *Prevotella*) and reduced (*Bifidobacterium, Dorea*, *Faecalibacterium*, *Coprococcus* and *Roseburia*) taxa from the DEHP-treated fermenters were similar to those observed in the gut microbiota of IBD patients. Expressions of tight/adherens junction genes in HT-29 cells and anti-inflammatory genes in RAW264.7 were down-regulated by the metabolites from plasticizer-co-incubated microbiota. Extracts from DEHP-modified microbiota stimulated pore-forming claudin-2 expression in HT-29 cells by up to 2.4-fold. Interestingly, DINP modified microbiota-derived extract reduced claudin-2. However, TJ/AJ sealing proteins E-cadherin (-20%), JAM-A (-30%) and claudn-4 (-17%) were reduced by high dosage DINP-modified microbiota extract. Overall, it is observed that selected plasticizers at high dosages induce compositional changes of gut microbiota. Metabolites from such altered microbiota may affect tight junction integrity of intestinal epithelium and upset macrophage differentiation homeostasis in

proximity. Chronic exposure to these plasticizers may promote risks of dysbiosis, leaky gut or exacerbation of inflammatory bowel diseases (IBDs).

Introduction

Phthalates are one of the major groups of environmental contaminants with global occurrence. They have been ubiquitously found in human urine and blood and posed potential health issues [158]. Di(2-ethylhexyl) phthalate (DEHP) and di-iso-nonyl phthalate (DINP) are widely used as plasticizers to soften poly-vinyl chloride (PVC) plastics for flexibility [159]. The primary concern is that DEHP can be metabolized into different toxic metabolites such as Di-n-octyl phthalate (DnOP), and mono-(2-ethylhexyl) phthalate (MEHP) when it enters the human body. Studies have shown that it can induce reproductive toxicity and endocrine disruption. It is best known as an endocrine disruptor that disrupts the regulation and action of thyroid hormones [160]. In addition, DEHP and its metabolites have the potential to induce testicular, ovarian, renal, neuro, and cardiovascular toxicity [161]. Both occupational and environmental routes of exposure to DEHP are of concern for human health [162]. Due to the toxic effect of DEHP, another phthalate, DINP is used as an alternative to DEHP during PVC production. It is suggested that DINP has lower cytotoxicity and carcinogenicity compared with DEHP, however, some studies have demonstrated that DINP can also disrupt immune homeostasis and cause spleen, liver, and kidney damages [158, 159]. In addition to alteration of metabolisms by DEHP/DINP or their derivatives, recent study has demonstrated that DEHP is able to modify microbiome-gut-immune axis upset gastrointestinal homeostasis. Transcriptomic and metagenomic analysis reveal that gene expressions of intestine associated T helper cell subsets and tight junction proteins are changed after DEHP exposure in zebrafish [163], however, studies regarding effects of plasticizer on human microbiota is relatively limited.

Earlier findings suggested that bacterial isolates from environmental sources or GI tract may degrade plasticizers DEHP and DINP. *Proteus mirabilis, Desulfitobacterium hafniense* and *Paenibacillus barengoltzii* isolated from gut could grow on culture plate with DINP as sole carbon source [164]. In addition to these isolates, genera *Pseudomonas, Methylobacillus* and *Achromobacter* have been reported growing on DINP-containing medium. Possible mechanisms of energy utilization from DINP includes de-esterification and beta-oxidation [164, 165]. Genera *Rhodococcus* and *Achromobacter* have also been found degrading DEHP through de-esterification [166, 167]. Among these bacteria, genus *Pseudomonas* can be found various mucosal surfaces in human and possesses multiple antibiotic resistance genes. These studies related to how DINP is utilized as carbon source which supports the growth of certain types of bacteria are published in recent years. It is possible that DINP could affect and favor the growth of some bacteria in gut microbial ecosystem.

Since oral intake is the major exposure pathway for DEHP and DINP to enter human body, and their systemic availabilities were verified to be about 7% and 50% in rats, respectively [168-170], we hypothesize that such plasticizer can shift microbial composition of human microbiota, in turn affect intestinal tight junction integrity and macrophage differentiation (pro-inflammatory M1/tissue repairing M2). We adopt a batch culture model which consists of fermenters simulating the human intestinal ecosystems of colons to investigate the alteration of microbiota by a wide range of plasticizer concentrations. Fecal microbiota was cultured anaerobically with different concentrations of DEHP and DINP for 24 hr. Resultant microbiota compositions were analyzed by 16S rDNA sequencing. Influence of microbial metabolites from luminal extracts on the cultural enterocytes and macrophage were investigated. It is observed that microbial compositional changes in plasticizer containing niches towards dysbiosis. Gene expressions involved in the epithelial junction integrity of HT-29 cells were affected, which may lead to a “leaky gut” profile. Down-regulation of reactive oxygen species (ROS) neutralizing

machinery related genes were also observed. Moreover, anti-inflammatory, tissue repairing macrophage M2 signature genes were reduced in cultural macrophage cell-line. These results indicated that over consumption of plasticizer could induce changes of microbiota in a way which produces metabolites upsetting intestinal epithelial integrity and immune homeostasis, contributing to progression of leaky gut or even exacerbation of inflammatory bowel diseases (IBDs).

Objective

In this study, we aim to determine:

1. If DEHP or DINP alters the microbial diversity and compositions of human gut microbiota *in vitro*;
2. Gene expressions of TJ, AJ and cytokines in HT-29 and RAW264.7 cells after treatments of luminal extracts of gut microbiota exposed to DEHP and DINP;
3. Whether the affected TJ and AJ gene expressions were translated to proteins level.

Materials and methods

1. Batch Culture

Fecal samples were collected from healthy donor who had normal diet and did not intake any probiotics or antibiotics at least 2 weeks before sampling day. Fecal material was stored in gas-tight sample bucket with anaerobic sachet (Thermo Fisher Scientific, Waltham, USA) and inoculated within 4 hours after collection. Final concentration of 10% w/v of fecal material was homogenized with anaerobic buffer (autoclave-sterilized phosphate buffer: 8.8 g/L K_2HPO_4, 6.8 g/L KH_2PO_4, 0.1 g/L sodium thioglycolate; and supplement solution after autoclave: 15 mg/L sodium dithionite) inside a stomacher bag with filter (Seward, Worthing, UK) for 5 minutes at 200 rpm. Sterilized Adult L-SHIME growth medium (without starch) (ProDigest, Gent, Belgium) was adjusted to pH 6.9 mimicking distal colon environment. Filtrate portion obtained after homogenization was inoculated in growth medium with volume ratio of 1:10. Starting cultural volume in each chamber was at 200 ml (10% of daily fluid intake 2000 ml). One of the four inoculated chambers was used as no treatment control (D0). Three dosages of DEHP or DINP (Sigma, St. Louis, USA), were introduced into each treatment cultural chamber (Figure 3.1). The starting amounts of plasticizers were set at: 0.21 mg DEHP (D1 = 0.21 mg, D2 = 2.1 mg and D3 = 21 mg) and 33.6 μg DINP (D1 = 33.6 μg, D2 = 336 μg and D3 = 3360 μg) according to possible daily exposures detected from previous studies on either food contamination testing or daily exposure of workers in plasticware manufacturing and cosmetic fields [85, 162, 169, 171, 172]. Culture chamber was purged by nitrogen for 10 minutes after inoculation and maintained at 37°C by water circulation. pH values and culture mixtures in different chambers were recorded and collected at 0, 4, 8 and 24 hours after inoculation, respectively.

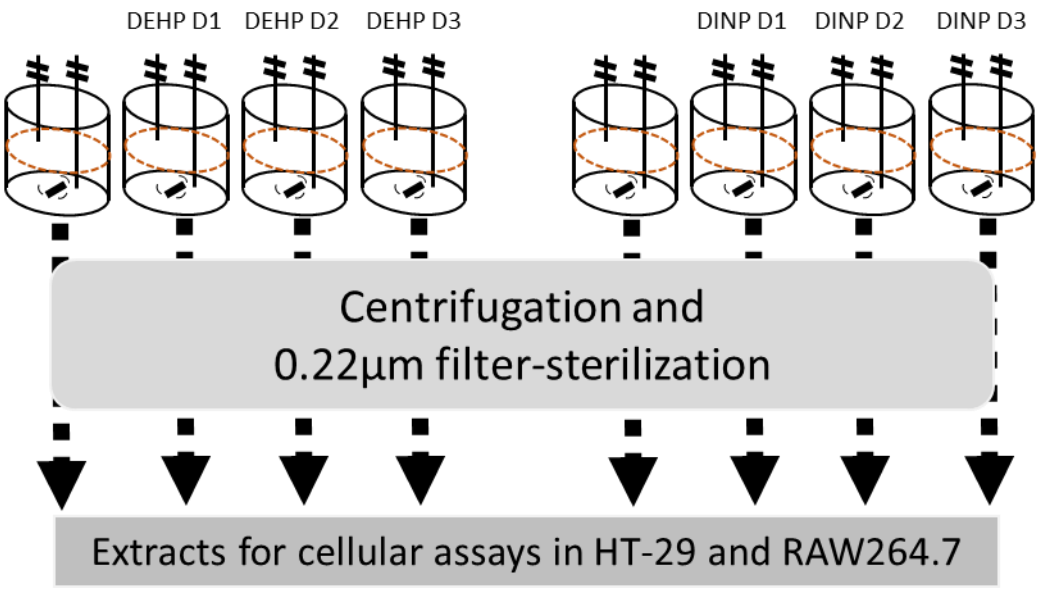

Figure 3.1. Setup of batch culture fermenter and experiment flow chart.

2. DNA Extraction, 16S rDNA gene sequencing and microbial composition analysis

16S rDNA analysis was performed for assessment of microbial composition and diversity of fecal microflora. Samples were centrifuged at 13,684g for 5 minutes. DNA extractions form the pellet were carried out by using stool DNA extraction kit (TIANGEN, Beijing, China) according to the manufacturer's manual. Extracted DNA concentration was determined by NanoDrop 2000 (Thermo Fisher Scientific, Waltham, USA). Bacterial 16S rDNA sequencing of V3-V4 region (336F-806R) was conducted by MajorBio (Shanghai, China). Microbiota analysis was performed by using MajorBio analysis platform.

3. Analysis of SCFAs

SCFAs in the fecal cultures were analyzed by Gas Chromatograph-Flame Ionization Detection (GC-FID) using Agilent 7980B GC system (Agilent, Santa Clara, US) with a fused silica capillary column (Agilent, Santa Clara, US) as described previously [134, 135]. Collected samples were centrifuged at 2,376g for 2 minutes. 930 µl of supernatant and 60 µl of 1 M HCl was mixed to yield a pH 2–3 mixture. An internal standard (2-ethylbutyric acid) was added at final concentration of 1 mM before injection into the GC system. Nitrogen gas was applied as the mobile phase flowing at 0.6 ml/min. The initial oven temperature was maintained at 80°C for 2 minutes and raised gradually to 180°C at 6°C/min and maintained for 4 minutes. The injection volume was 1 µl. The inlet temperature was controlled at 200°C; and the detector temperature was set at 220°C. Four SCFA standards (Sigma, St. Louis, USA), including acetic acid, propionic acid, n-butyric acid, and i-butyric acid, were used for identification and quantification.

4. Preparation of luminal extracts

Resultant fermentation culture was defrosted from -20°C and centrifuged at 15,000g for 30 minutes at 4°C. Supernatant from centrifugation was filter-sterilized by 0.22 µm syringe filter. Filtrate was then aliquoted into 2 ml micro-centrifuge tubes and stored at -20°C as luminal extract.

5. Cell culture and viability assay

Human intestinal epithelial cell line HT-29 and murine macrophage RAW264.7 were maintained in complete medium (Dulbecco′s Modified Eagle′s Medium (DMEM) with 10% fetal bovine serum (FBS)) in a 5% CO_2, 37°C humidified incubator. For HT-29, cells were sub-cultured by tryptic digestion when they reached 80-90% confluence. Enterocyte monolayers were differentiated in 24-well flat bottom cell culture plate starting at $2x10^4$ cell/well for 12-14 days before treatment or viability assay. RAW264.7 passaging was performed by using a cell scrapper and seeded at $20x10^4$ cell/well in a 24-well flat-bottom plate 24 hours before treatment or viability assay.

Viabilities of cells after incubating with a range of luminal extracts were determined by 3-(4,5-dimethylthiazol-2-yl)-2,5-diphenyltetrazolium bromide (MTT, Sigma, St. Louis, USA) assay. Treatment media containing different concentrations of luminal extracts from no plasticizer control chambers of each experiment in complete medium were incubated with differentiated HT-29 monolayer or RAW264.7 cells for 24 hours. Cells were washed by phosphate buffered saline pH 7.3 (PBS) and incubated with 0.5 mg/ml MTT solution for 1-1.5 hours in triplicate. Luminal extract concentrations (v/v %) were employed as treatment percentage for gene expression assay, which preserved >90% cell viability mimicking a sub-lethal chronic exposure of to each cell-line.

6. RNA extraction, reverse transcription, and real-time PCR gene expression analysis

HT-29 and RAW264.7 cells were treated with 1 ml of 10% and 5% v/v luminal extracts in complete medium for 24 hours inside a cell culture incubator, respectively. Total RNA was extracted using RNAiso PLUS (Takara, Kusatsu, Japan). RNA concentration was determined by NanoDrop spectrophotometer (Thermo Fisher Scientific, Waltham, USA). Complementary DNA (cDNA) was reverse transcribed using PrimeScript reverse transcription kit (Takara, Kusatsu, Japan) according to the manufacturer's protocol. Real-time PCR was performed on Applied Biosystems QuantStudio 7 Flex Real-Time PCR System (Thermo Fisher Scientific, Waltham, USA) with TB Green Premix Ex Taq II (Takara, Kusatsu, Japan) reagent. Relative quantification of target gene expression was calculated by 2^(-ΔΔCt). Ribosomal protein lateral stalk subunit P0 (*RPLP0*) and hydroxymethylbilane synthase (*HMBS*) were used as housekeeping genes for HT-29 and RAW264.7 gene expression calculation, respectively. Primers for specific mRNA amplification are listed in supplementary information (Supplementary Table 3.1-3.2).

7. Measurement of intracellular ROS

Intracellular ROS content was reflected by ROS-sensitive compound 2',7-dichlorofluorescin diacetate (H_2DCFDA; Sigma, St. Louis, USA) measured by a flow cytometry (Accuri C6, BD). HT-29 cells were seeded at $30x10^4$ cell/ml/well in 6-well plate overnight before treatment. Cells were incubated in 10% v/v luminal extracts in complete medium for 24 hours inside a cell culture incubator. Treatment medium was removed, and cells were washed by PBS and further incubated with 1 ml of 1 μM H_2DCFDA in PBS for 15 minutes. Stained HT-29 was pelleted by centrifugation and washed by PBS again. Washed cells were re-suspended in PBS with 5 mg/L propidium iodide for flow cytometry.

8. Lipopolysaccharide concentration quantification by ELISA

Lipopolysaccharide (LPS) concentration in luminal extracts was assessed by general lipopolysaccharide ELISA Kit (ABclonal, Woburn, US) according to the manufacturer's manual. Duplicate assay wells were used for each luminal extracts' LPS quantification.

9. Western blot

Western blot was employed for comparison of tight junction and adherens junction protein expressions after fermenter extract treatment. HT-29 cells were seeded at $2x10^4$ cell/well in 24-well plate. Cells were cultured for 14 days before treatment. HT-29 was incubated with 20% extracts for 48 hours prior to protein quantification. Cells were washed with PBS and then incubated in 200 µl RIPA buffer (Merck Millipore, Burlington, US) with protease inhibitor cocktail (Sigma, St. Louis, USA) for 2 hours at 4°C. Total protein was obtained in supernatant after centrifugation at 20,000g for 10 minutes. Protein samples were stored at -80°C before protein concentration quantification by BCA assay (Thermo Fisher Scientific, Waltham, USA).

For SDS-PAGE, 20 µg of total protein from each sample was mixed with sample buffer, heated at 95°C for 5 minutes before loading. SDS-PAGE with 4% stacking and 10% resolving gels was used for electrophoresis. Western blot transfer was done in wet condition with 80V for 90 minutes at 4°C. PVDF (GE Healthcare, Chicago, US) after transfer was blocked with blocking solution (5% skimmed milk in Tris buffered saline with 0.1% Tween 20 (TBST)) for 2 hours, and then incubated with primary antibody in blocking solution overnight at 4°C. Primary antibodies used for this study were: mouse monoclonal anti-β-actin (1:2000, Sigma, St. Louis, USA), rabbit polyclonal anti-ZO-1 (1:1000, ABclonal, Woburn, US), rabbit polyclonal anti-E-cadherin (1:1000, ABclonal, Woburn, US), rabbit polyclonal anti-occludin (1:2000, ABclonal, Woburn, US), rabbit polyclonal anti-F11R (1:2000, ABclonal, Woburn, US), rabbit

polyclonal anti-claudin-4 (1:1000, ABclonal, Woburn, US) and rabbit polyclonal anti-histone-H3 (1:2000, Proteintech, Rosemont, US). Horseradish peroxidase-conjugated goat anti-rabbit IgG (H+L) secondary antibody (1:2000, Novus Biologicals, Centennial, US) and goat anti-mouse IgG (H+L) secondary antibody (1:2000, Thermo Fisher Scientific, Waltham, USA) were used for chemiluminescent signal generation during image capture. Densitometry of chemiluminescent signal was analyzed using Image J. Relative expression of target protein was calculated by dividing its signal to Histone-H3 signal. Normalized expression of target in each sample was generated by dividing relative expression to average relative expression in control fermenter extract group. Target protein expression in control fermenter treatment group was normalized as 1.

10. Immunofluorescence

Immunofluorescence was used for validation of changes in claudin-2 expression in HT-29 cells. HT-29 cells were seeded at $2x10^4$ cell/well in 6-well plate with coverslip. Cells were cultured for 14 days before treatment. Same extract concentration and incubation duration were employed as mentioned in real-time PCR section. Cells were washed thrice with PBS and fixed by 4% PFA for 10 minutes. Followed by removal of PFA and three PBS washes, cells were permeabilized with 0.1% Triton X-100 for 10 minutes. Permeabilized cells were washed with PBS again, and then blocked by blocking buffer (10% FBS and 1% BSA in PBS) for 30 minutes. Cells were incubated with rabbit polyclonal anti-claudin-2 (ABclonal, Woburn, US) primary antibody diluted in blocking buffer (1:200) overnight at 4°C. Following three PBST (0.1% Tween 20 in PBS) washes, cells were incubated with goat anti-rabbit IgG (H+L) Alexa Fluor 488 (Thermo Fisher Scientific, Waltham, USA) secondary antibody (1:500 in blocking buffer) for 2 hours at 4°C. After incubation with secondary antibody, coverslip was removed from well and invertedly placed onto one drop of fluoroshield mounting medium with DAPI (abcam) on glass slide, and then sealed with nail polish. Fluorescence signals were captured by ZEISS Axio Vert. A1 with objective magnification of 40x. Width of images was 330 microns. Exposure time for FITC and DAPI channels were 300 ms and 150 ms, respectively. Fluorescence intensities were analyzed using Image J. Relative expression of claudin-2 was calculated by dividing claudin-2 signal to DAPI signal. Normalized expression of claudin-2 in each sample was generated by dividing each relative expression to average relative expression of control fermenter extract group. Claudin-2 expression in control fermenter treatment group was normalized as 1.

11. Statistical analysis

Statistical comparisons were performed using GraphPad Prism 5. All results are shown as mean +/- SEM from the replicates. Statistical analysis, t-test, was used with 95% confidence.

Results

1. Concentration of SCFAs and LPS

Three types of SCFAs including acetic acid (C2), propionate acid (C3) and n-butyrate acid (n-C4), often observed in human gut were measured (Figure 3.2A-3.2C and 3.2E-3.2G for DEHP and DINP experiments, respectively). Among these tested SCFAs, C2 accounted for the highest concentration, which had a significant increase after 24-hour incubation. Increases in SCFAs implied the growth of SCFA-producing bacteria. Propionate acid was the second most abundant SCFA produced during fermentation. Resultant propionate and butyrate concentrations in high dosages DEHP microbiota reduced slightly. ELISA also demonstrated that LPS concentrations among different fermenters in both DEHP and DINP experiments remained similar (Figure 3.2D and 3.2H).

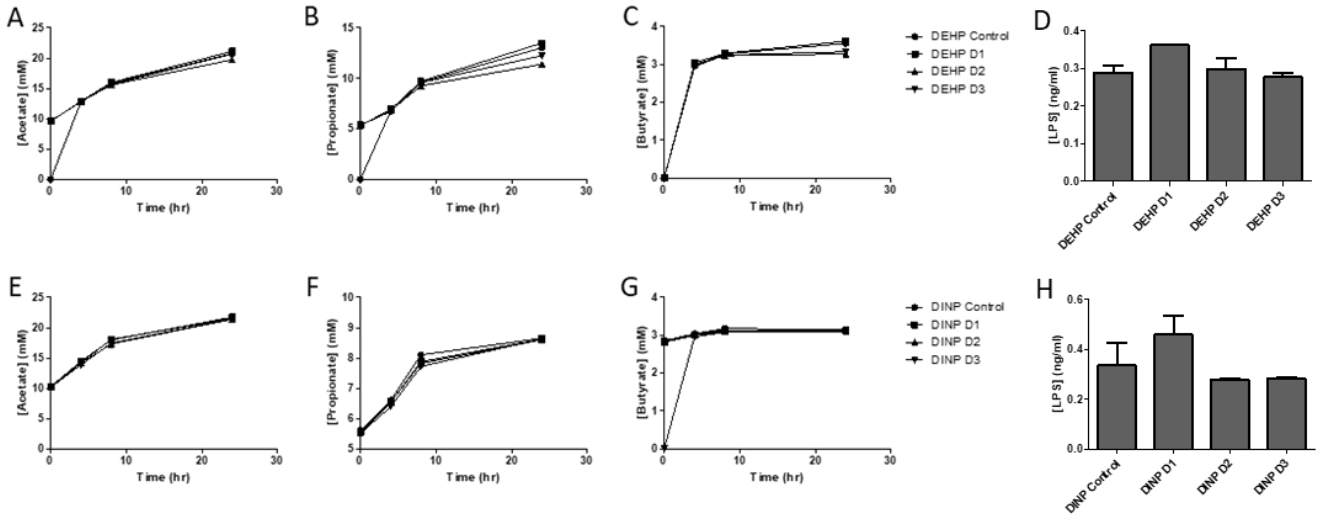

Figure 3.2. The SCFAs, acetic acid (A/E), propionic acid (B/F) and butyric acid (C/G) concentrations in DEHP (A-C) and DINP (E-G) experiment fermenters. Resultant LPS concentrations in different fermenters (D: DEHP experiment / H: DINP experiment). Error bars indicate standard error mean on duplicate ELISA results.

2. 16S sequencing analysis on the microbiota compositions in different anaerobic fermenters

Fermenter microbial genomic DNA was extracted and sequenced on Illumina platform. A total of 315,669 qualified reads in 8 resultant fermenters was used for detailed diversity and taxonomy analysis on Majorbio online analysis platform. DEHP contamination altered microbial diversity and composition as showed in alpha-, beta-diversities and taxonomy in various microbiota communities (Figure 3.3). The dissimilarity among different fermenters showed that the microbiota compositions of DEHP experiment at the beginning (DE_0 to DE_3) were clustered together, indicating all 4 fermenters have similar initial microbial composition. After 24-hour incubation, DEHP containing fermenters (DE_5 to DE_7) were clustered away from no DEHP chamber (DE_4) (Figure 3.3A). Shannon indices of DEHP-dosed microbiota were increased while Simpson's indices were reduced. Other alpha diversity indices such as observed species (Sobs), ACE, Chao1 and phylogenetic distance (pd) were all reduced in DEHP-D1 to DEHP D3 comparing with the control (DE_0, no DEHP) (Table 3.1).

Table 3.1. Alpha diversity indices for DEHP experiment

	Indices			
Alpha diversities	DEHP Control	DEHP D1	DEHP D2	DEHP D3
Community richness				
Sobs	85	79	73	74
ACE	99.1	90.6	78.9	80.4
Chao1	105	92.1	77.5	83.0
Community diversity				
Shannon	1.88	1.91	2.04	2.25
Simpson	0.28	0.22	0.2	0.16
pd	13.24	12.69	12.39	12.07

Overall phyla *Firmicutes* and *Actinobacteria* were reduced while phylum *Bacteroidetes* was found to be more abundant in DEHP-dosed fermenters (Figure 3.3B). Compared to control fermenter without any DEHP treatment, DEHP-dosed fermenters had an enriched family *Coriobacteriaceae* population, particularly in the DEHP-D3 fermenter microbiota with almost 3 times more in relative abundance compared with D0 (Figure 3.3C). In addition to that, more abundant *Prevotellaceae* was also observed in dosed microbiota. Relative abundance of families *Bifidobacteriaceae*, *Erysipelotrichaceae*, *Lachnospiraceae*, *Ruminococcaceae* and *Veillonellaceae* were all reduced in DEHP-dosed fermenters (Figure 3.3C). At genus level, among the five enriched genera, *Alloprevotella*, *Collinsella*, *Megasphaera*, *Prevotella_9* and unclassified_f__*Veillonellaceae* (Figure 3.3D) were enriched. On the other hand, relative abundance of genera *Bifidobacterium, Catenibacterium, Dorea, Faecalibacterium, Holdemanella, Mitsuokella* and *Prevotella_2* was all reduced when DEHP was present in the fermentation mixture (Figure 3.3D).

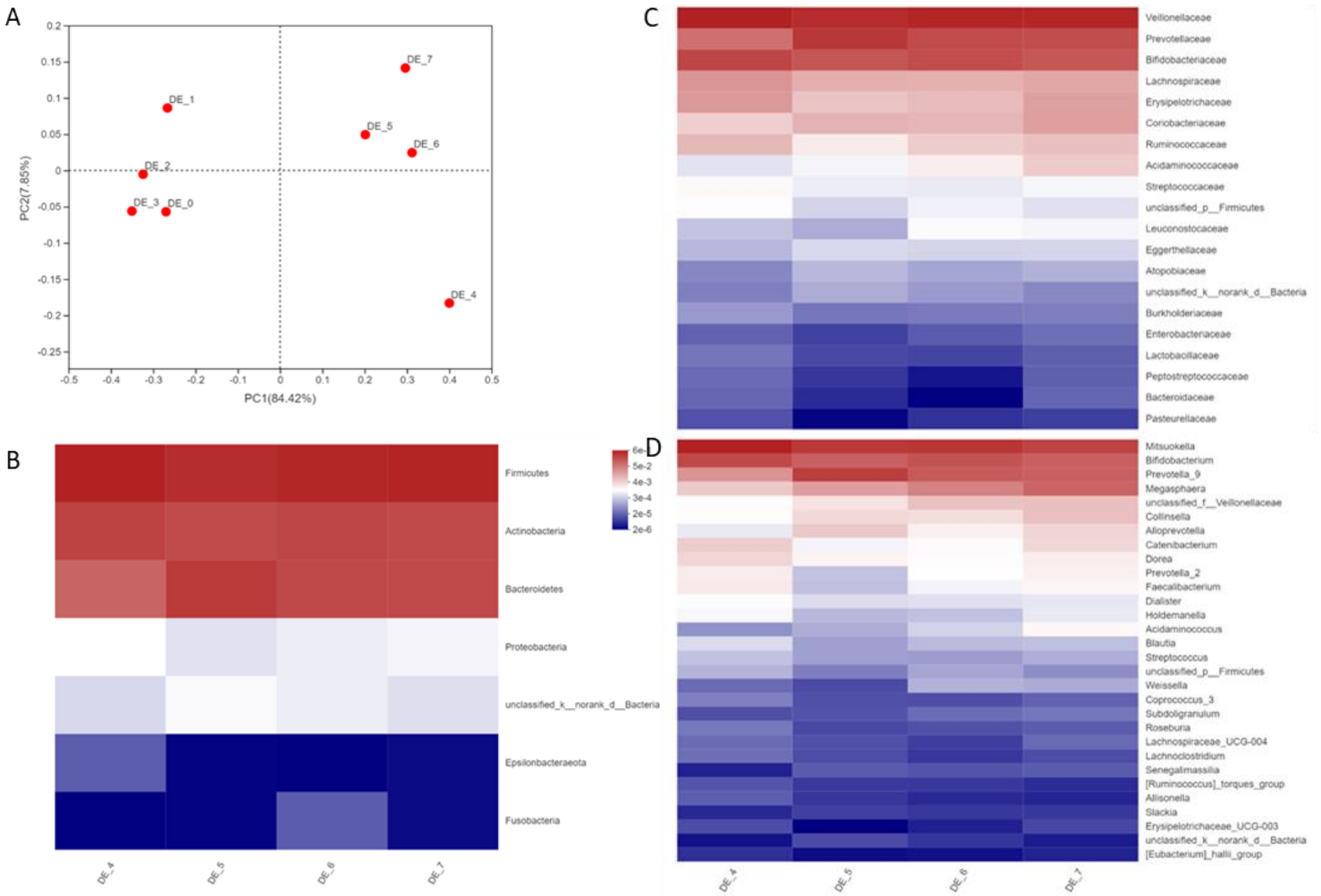

Figure 3.3. PCoA plot for community distances at 0-hour (DE_0 to DE_3 for DEHP D0-D3) and 24-hour (DE_4 to DE_7 for DEHP D0-D3) by Bray Curtis analysis at OTU level (A). Comparative heatmap assigned according to phylum (B), family (C) and genus (D) levels.

Similar to the initial time point of DEHP, the starting microbiota compositions (DI_0 to DI_3) in the anaerobic fermenters with DINP were clustered together (Fig. 3.4A). After 24-hour incubation, control (DI_4), DINP dosage 1 and 2 (DI_5 and DI_6), were clustered in PCoA plot while DINP dosage 3 (DI_7) community was differed from all others (Figure 3.4A). Sobs, ACE and Chao1 were increased slightly in DINP-D1 to DINP-D3 comparing to no DINP control. Fluctuation in Shannon, Simpson and pd indices were recorded in DINP-D1 and DINP-D2 comparing with control. At high dosage group, Shannon index was increased slightly while Simpson and pd were remained stable (Table 3.2).

Table 3.2. Alpha diversity indices for DINP experiment

	Indices			
Alpha diversities	DINP Control	DINP D1	DINP D2	DINP D3
Community richness				
Sobs	99	110	105	106
ACE	103.3	121.6	118.8	118.1
Chao1	104.1	123.3	122.0	126.0
Community diversity				
Shannon	2.59	2.44	2.52	2.72
Simpson	0.13	0.17	0.15	0.12
pd	15.53	16.49	16.54	15.53

Dose-dependent increases in relative abundance of phyla *Actinobacteria* and *Proteobacteria* were detected (Figure 3.4B). Comparing the microbiota compositions of DINP-D0 and DINP-D3 at family level, *Bifidobacteriaceae*, *Enterobacteriaceae*, *Erysipelotrichaceae*, *Lachnospiraceae*, *Streptococcaceae* were more abundant in the DINP-D3 fermenter, of which *Enterobacteriaceae* and *Streptococcaceae* possessed a DINP dose-dependent expansion (Figure 3.4C). Though fluctuations were observed in DINP-D1 and DINP-D2 microbiota, relative abundance of *Coriobacteriaceae* and *Prevotellaceae* were reduced in DINP-D3 microbiota (Figure 3.4C). Dose-dependent drop was only observed in family *Veillonellaceae* across different dosages of DINP. Similar variations were also observed on genus level, relative abundance of *Streptococcus* spp. and *Lactococcus* spp. were increased in DINP-D1 and DINP-D3 fermenters while they stayed relatively stable in DINP-D2 (Figure 3.4D). Moreover, relative abundance of *Blautia* spp., *Catenibacterium* spp., *Dorea* spp., *Escherichia-Shigella* spp., *Holdemanella* spp. and *Prevotella_2* spp. in DINP-D3 fermenter were around 2-fold of that in DINP-D0 fermenter (Figure 3.4D). Though increases in *Prevotella_2* spp. was observed in the DINP-D3 group, relative abundance of *Prevotella_9* spp. was reduced by about 40% comparing with control. Finally, dramatic shrink of *Megasphaera* spp. abundance was detected in DINP-D3 community (Figure 3.4D).

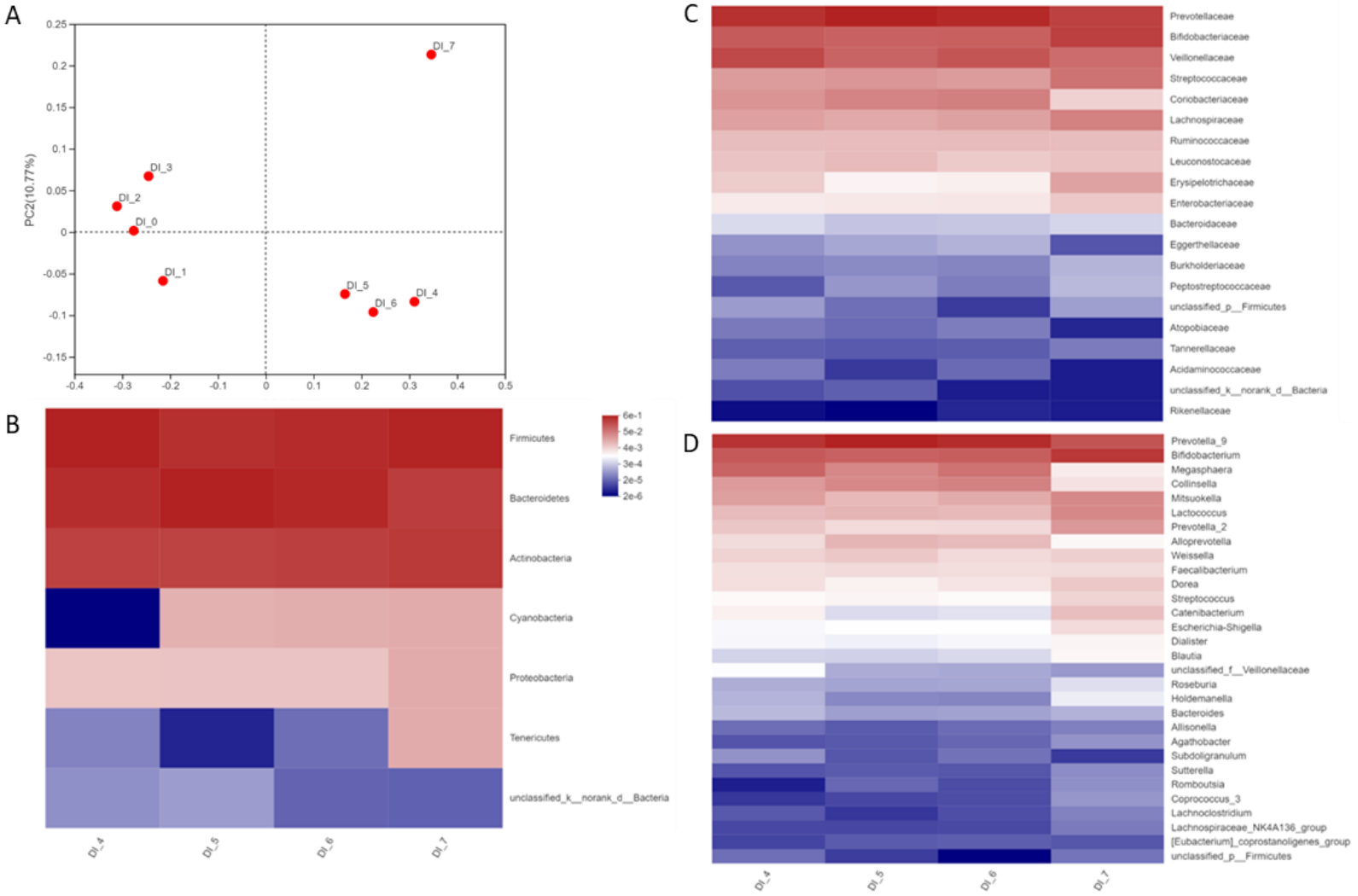

Figure 3.4. PCoA plot for community distances at 0-hour (DI_0 to DI_3 for DINP D0-D3) and 24-hour (DI_4 to DI_7 for DINP D0-D3) by Bray Curtis analysis at OTU level (A). Comparative heatmap assigned according to phylum (B), family (C) and genus (D) levels.

3. Effect of luminal extracts co-incubated with DINP and DEHP on the mRNA levels of enterocyte and macrophage

Treatment percentages of extracts were set at 10% and 5% v/v for HT-29 and RAW264.7 cells, respectively, in cultural medium as cells preserved high viability (Figure 3.5). HT-29 and RAW 264.7 cells were treated with luminal extracts from human gut microbiota after co-incubated with DEHP or DINP, followed by RT-qPCR to check the expression levels of tight junction and adherens junction proteins. Changes of the TJ/AJ protein expressions in HT-29 cells treated with luminal extracts from DEHP fermenter were limited, among which the most significant being the *CLDN2* expression in all extract treatment groups enhanced by >35% (Figure 3.6A). Expression changes of other TJ proteins *OCLN*, *JAMA*, *CLDN1*, *CLDN4* and *CLDN7* were less than 10% even in the highest dosage D3 comparing to the no treatment control. Changes in TJ and AJ adaptor proteins *TJP1*, *TJP2* and *TJP3* were less than 5%. Expressions of AJ related proteins, *CDH1* and *CTNNB1*, were close to that of the control sample. Expressions of ROS generating and neutralizing proteins, *ALOX5*, *NOX1* and *SOD1* to *SOD3*, remained stable in HT-29 treated with luminal extracts from different DEHP-dosed fermenters.

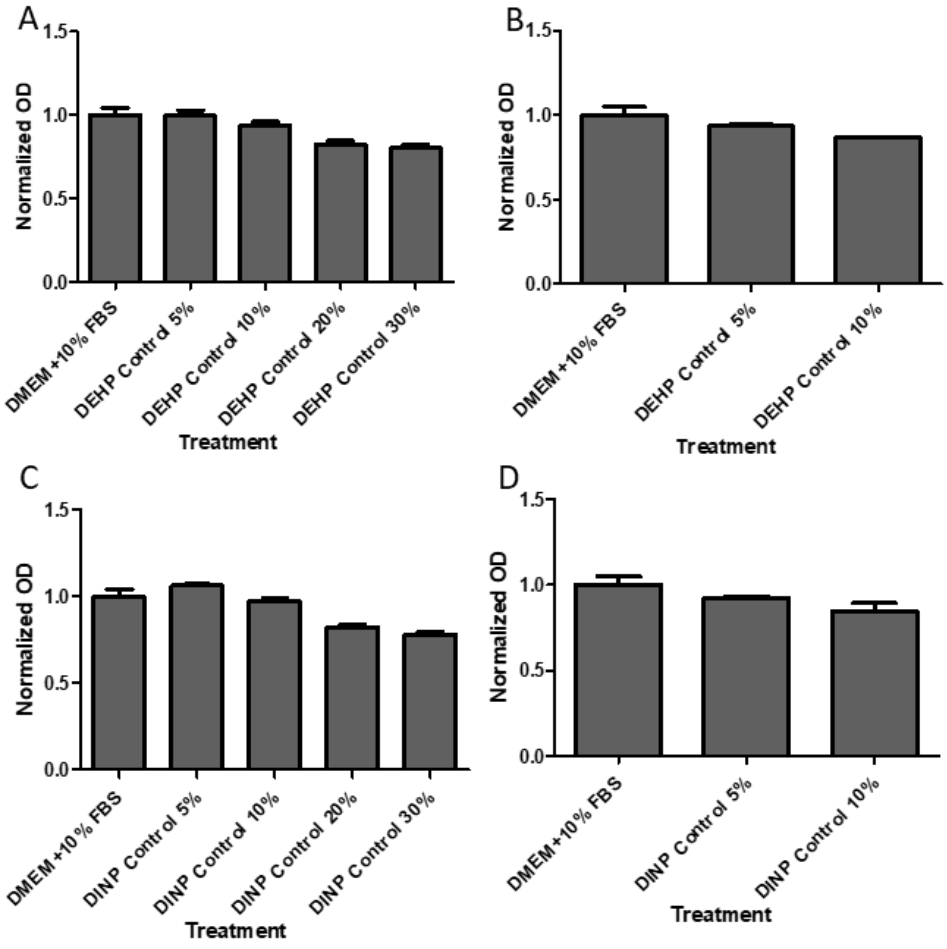

Figure 3.5. Viability of HT-29 and RAW264.7 after treatment of control fermenter extracts from DEHP experiment (A-B) and DINP experiment (C-D), respectively. Data represent mean with SEM from at least repeats of 3.

Adherens junction protein E-cadherin (encoded by *CDH1*), trans-membrane tight junction proteins and their intracellular adaptor proteins were down-regulated in HT-29 treated with high DINP-dosed fermenter luminal extracts. Significant reductions in adherens junction *CDH1* mRNA levels were observed in DINP-D2 and DINP-D3 fermenter luminal extracts treated HT-29 (by 12% and 20%, respectively). Tight junction *OCLN* expression level was dropped by 10% when HT-29 exposed to DINP-D2 or DINP-D3 extracts (Figure 3.6B). Decreases in expressions of *CLDN2* and *CLDN4* were found in DINP-D3 luminal extract treated HT-29 (by 24% and 19% respectively). Around 15% drop in *JAMA* expression was also observed in the highest DINP-dosed extract treated HT-29 (p=0.0528). *TJP1* coding for ZO-1 was down-regulated by more than 40% in the same dosed extract treated HT-29. No significant changes in expressions of *CTNNB1*, *CLDN1*, *CLDN7*, *TJP2* and *TJP3* were observed. For ROS related gene expressions at the highest DINP-dosed extract treatment, significant alterations in *ALOX5*, *NOX1* and *SOD1* were not observed, while *SOD2* and *SOD3* were diminished by 7% and 21%, respectively.

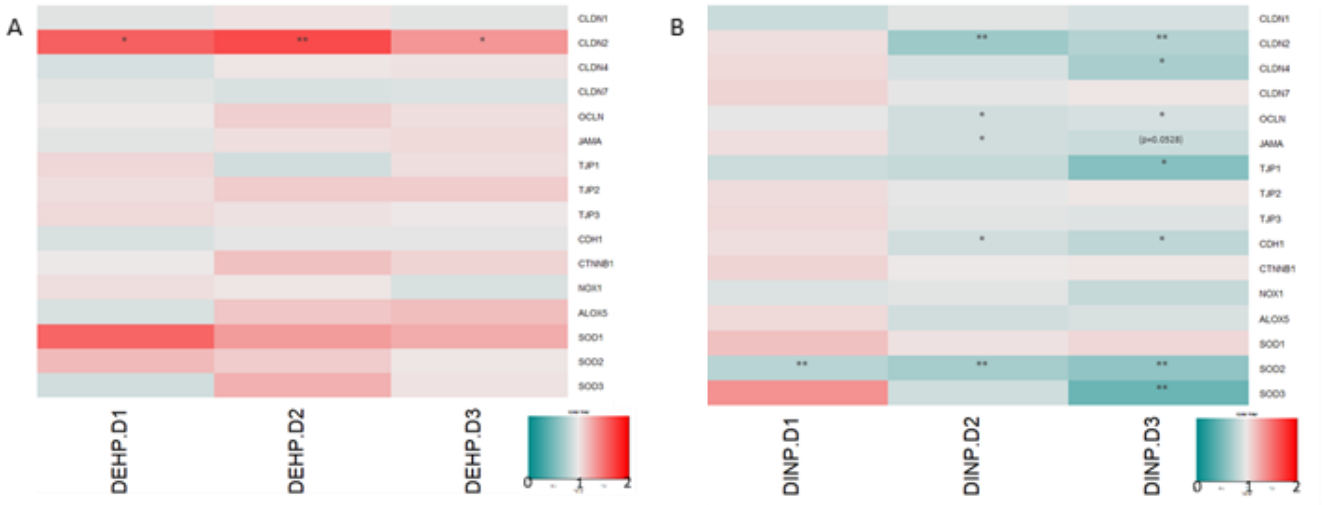

Figure 3.6. Normalized expressions of TJ/AJ genes in HT-29 after treatment of fermenter extracts from DEHP (A) and DINP (B) experiments. t-test, n=3, *p<0.05, **p<0.01 and ***p<0.005.

Cytokine and cytokine receptors in RAW264.7 cells treated with different DEHP dosed-luminal extracts remained similar. Comparing to those treated with luminal extract from DEHP-D0 fermenter, changes of pro-inflammatory cytokine expressions, *TNFA*, *IL1B*, *IL6*, *KC*, *IL12p40* and *IL23p19* in RAW264.7, were maintained similar without significant variation. No significant differences were observed in expressions of *TGFB1*, *IL1RA*, *IL10* and its receptor units. However, among selected alternative activated M2 genes, expression of suppressor of cytokine signaling 3 (*SOCS3)* was reduced in macrophage treated with DEHP fermenter extracts (Figure 3.7A).

Anti-inflammatory mediators in RAW264.7 were downregulated while pro-inflammatory cytokine expressions were remained unchanged. IL-1 receptor antagonist (encoded by *IL1RA*) mRNA level in RAW264.7 cells was decreased by about 17% in DINP-D1 and DINP-D3 extracts treatment groups. More than 15% and around 17% drops in *IL10* and *IL10R2* expressions were detected in all DINP-dosed luminal extract treated RAW264.7 samples. DINP-fermented microbial contents induced suppressions in Interferon regulatory factor-4 (*IRF4*) and *SOCS3*. Significant downregulations of Transglutaminase-2 (*TGM2*) were detected in the RAW264.7 treated with luminal extracts of DINP-D2 and DINP-D3. Expressions of pro-inflammatory cytokines (TNF-α, IL-1β, IL-6, KC, IL-12p40, IL-23p19) and tissue-repairing TGF-β1 were remained stable after the treatment of DINP-dosed luminal extracts (Figure 3.7B).

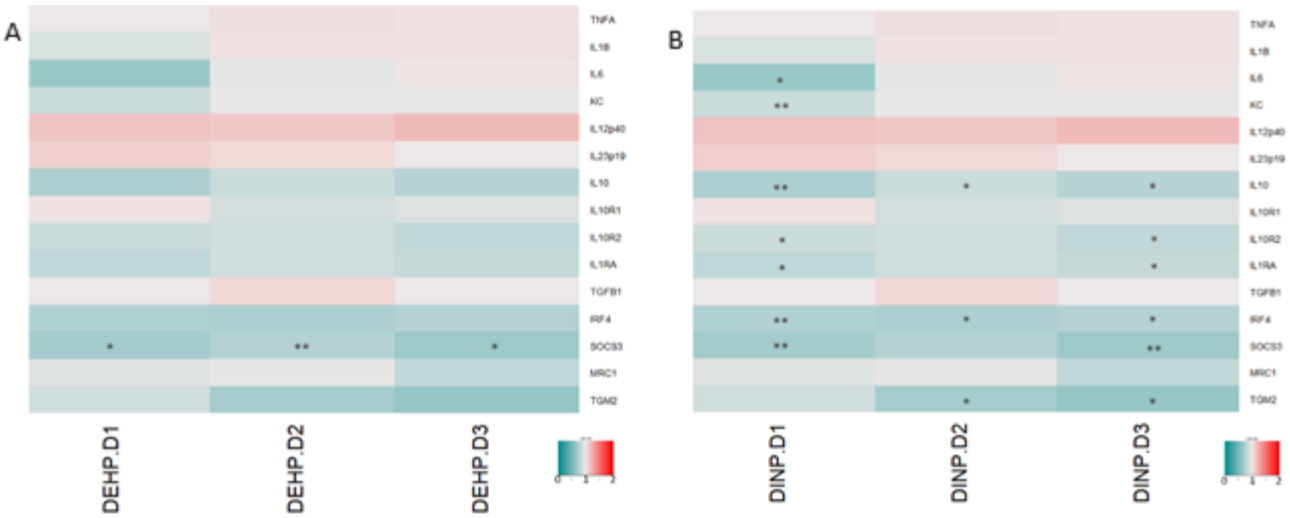

Figure 3.7. Normalized expressions of cytokine and M2 maker genes in RAW264.7 after DEHP (A) and DINP (B) fermenter extracts' treatments. t-test, n=3, *p<0.05, **p<0.01 and ***p<0.005.

4. Effect of luminal extracts co-incubated with DINP and DEHP on the protein expression levels of enterocyte

The level of mRNA coding for adherens junction protein E-cadherin (*CDH1*) in HT-29 was reduced by 20% after treatment of DINP-D3 extract comparing to DINP-D0 control extracts. Consistently, the protein level of E-cadherin in HT-29 was also reduced by almost 20% (Figure 3.8A). Claudin-4 protein was also reduced by 17% after DINP-D3 incubation (Figure 3.8C). Consistent reductions of both *JAMA* mRNA and its protein were observed after treatment of DINP-co-incubated fermenter extracts. From western blot, more than 30% of JAM-A proteins were lost after DINP-D3 extract treatment (Figure 3.8B). Although reductions of *TJP1* and *OCLN* mRNA levels in HT-29 treated with DINP-dosed fermenter extracts were observed, proteins levels of ZO-1 and occludin in HT-29 were remained similar after the treatment (Figure 3.8D-3.8E).

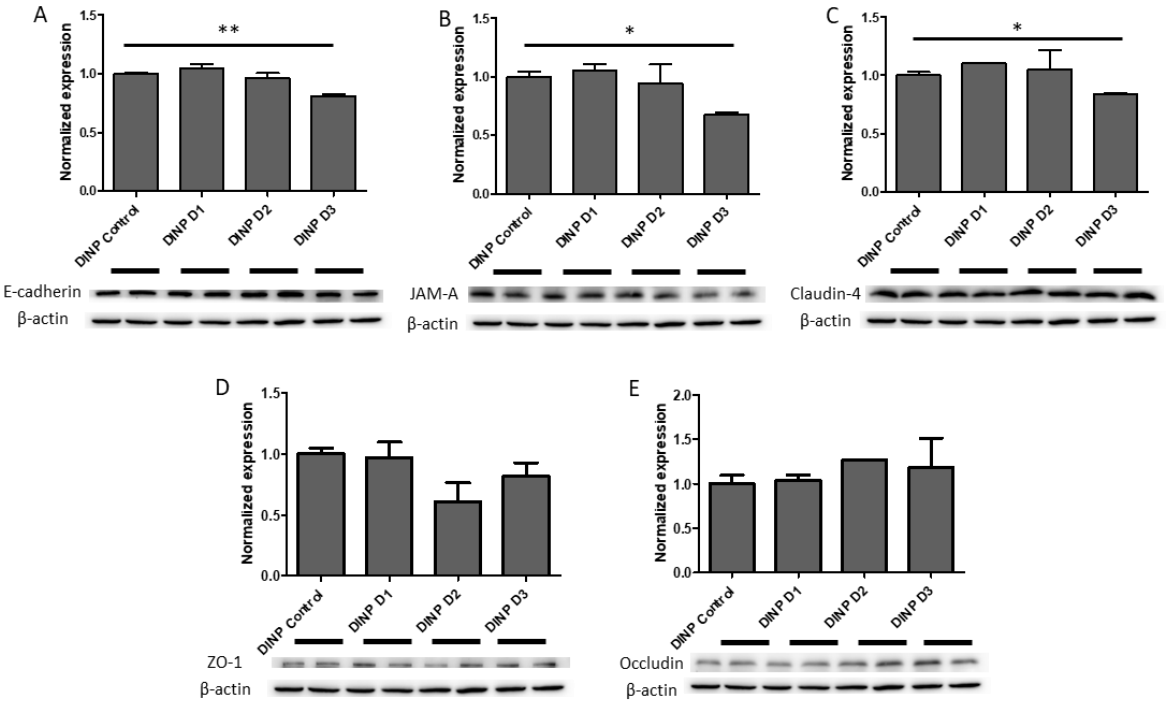

Figure 3.8. Quantification of E-cadherin (A), JAM-A (B), claudin-4 (C), ZO-1 (D) and occludin (E) in HT-29 after treatment of DINP fermenter extracts. t-test, n=2, *p<0.05, **p<0.01 and ***p<0.005.

The expression level of claudin-2 in HT-29 was further confirmed using fluorescent-tagged anti-claudin-2. Treatment of luminal extracts co-incubated with DEHP showed limited effect on the morphology of HT-29, though DEHP-D1 and DEHP-D2 extracts treatments increased the levels claudin-2 by 50%. Average enrichment of cladin-2 was up to 2.4-fold from HT-29 treated with DEHP-D3 extracts compared to that of no DEHP fermenter extract ($p=0.08$) (Figure 3.9A). Consistent with the percentage drops obtained in *CLDN2* RT-qPCR results, claudin-2 in HT-29 treated with DINP-D2 and DINP-D3 extracts was down-regulated by about 30% and 20% (Figure 3.9B).

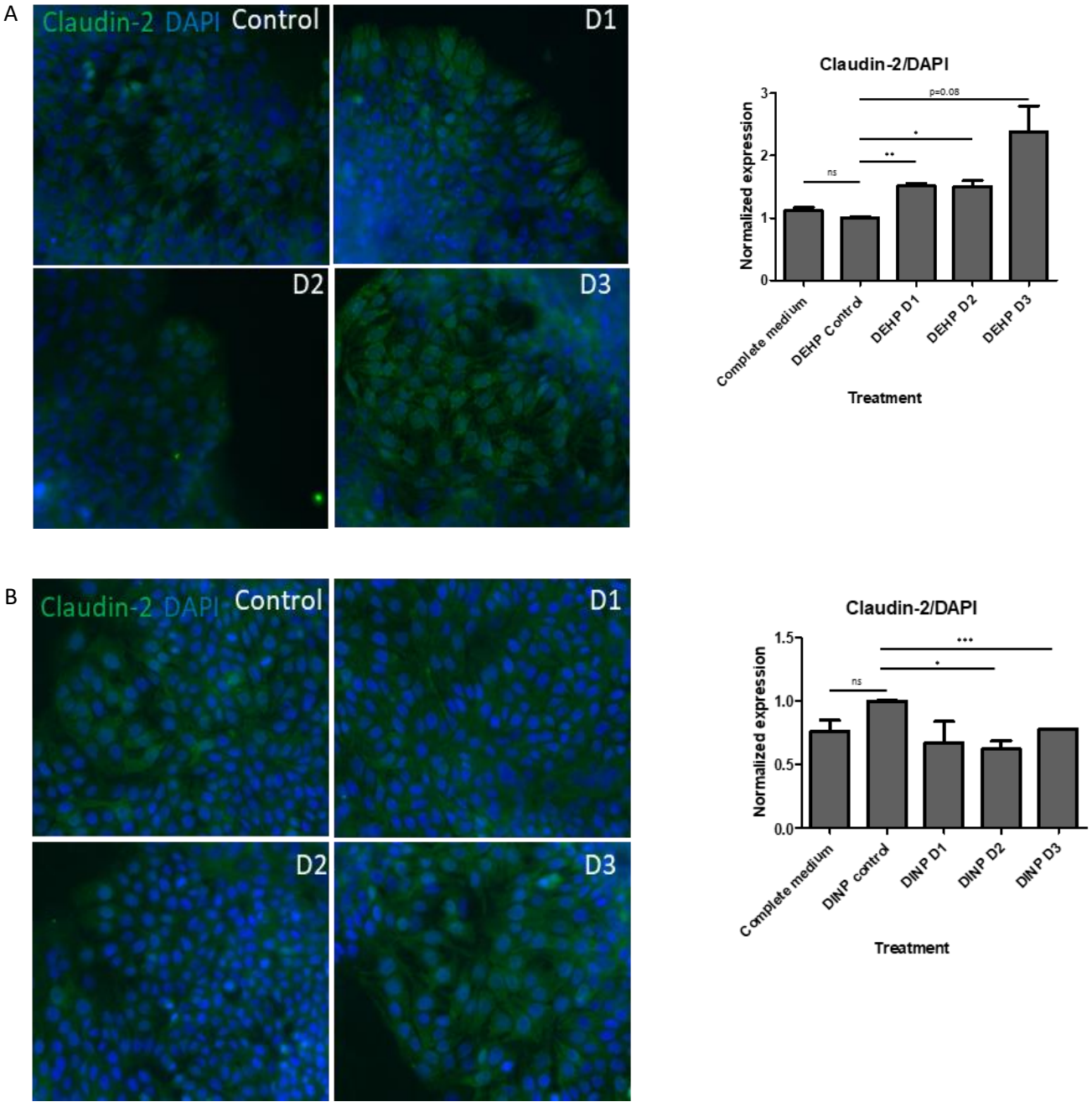

Figure 3.9. Immunofluorescence staining of claudin-2 in HT-29 after DEHP (A) and DINP (B) extracts' treatments (image width=330µm). Normalized expressions of claudin-2 in HT-29. t-test, n=2, *p<0.05, **p<0.01 and ***p<0.005.

Gene expressions of SOD2 and SOD3 in high dosage DINP-treated HT-29 were reduced by about 40% and 55%, respectively. Intracellular ROS levels of HT-29 after treatments of different extracts were compared. In the flow cytometry analysis, mean fluorescence, which reflected the intracellular ROS level, remained stable across different treatments (Figure 3.10).

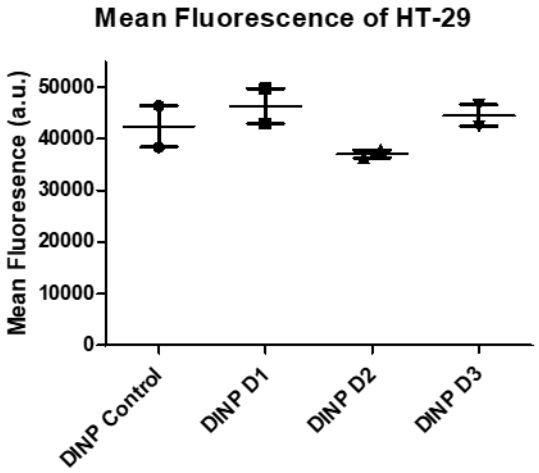

Figure 3.10. Mean fluorescence of HT-29 exposed to DINP extracts. Data represent mean with SEM from triplicate.

Discussion

1. Exposure to DEHP/DINP altered the microbial compositions of human gut *in vitro*

In this study, we aimed to determine if exposure to plasticizers DEHP or DINP lead to an aberrant gut microbiota and its possible effects on human enterocytes and immune cells. The gut microbiota co-incubated with DEHP exhibited a decrease in community richness indices (ACE and Chao1) and community phylogenetic diversity index pd. Interestingly, Shannon index, another community diversity index, was promoted along the increase of DEHP dosages. This deviation may be caused by the loss of rare species that had a low abundance originally, which has higher impact on the Shannon index than the Simpson index. Consistently, observed species indicated by Sobs index reflected that there was a decreasing trend in species numbers when DEHP dosage was added. On the other hand, in DINP experiment, Sobs, ACE and Chao1 were enriched in DINP-dosed communities. This suggested higher species richness; and more low-abundant OTUs were observed. However, Shannon and Simpson indices indicated that DINP-D1- and DINP-D2-treated resultant microbiota became less diverse comparing with no treatment control. Phylogenetic diversity was increased in low dosage groups (DINP-D1 and DINP-D2) and reduced back to the level shared with control. Overall, DINP-D3-dosed community had a relatively higher alpha diversity. For beta-diversity, all starting communities in DEHP or DINP experiments were clustered together, this indicated they have a relatively similar starting microbiota as baseline. After 24-hour incubation, DEHP-treated fermenter communities (DE_5, DE_6 and DE_7) were all clustered away from the no treatment community (DE_4) as shown in the PCoA plot, while DINP-D3 fermenter microbiota composition was deviated from DINP control, DINP-D1 and DINP-D2 communities. This implied that all three DEHP treatments and the highest DINP dosage significantly modified the baseline microbiota.

Biochemical and molecular functions derived by different and specific species are important hallmarks to determine whether such community could be considered as health or not. MP is generated during plastic processing, detachment of micro-particles from plastic packages and degradation of plastics by microbes. MPs are the carriers of plasticizers and have a large surface area which facilitate the formation of biofilm. Chung et. al. have indicated that major biofilm colonizers were from phyla *Proteobacteria*, followed by *Bacteroidetes*, *Firmicutes*, *Acidobacteria* and *Actinobacteria* [89]. Not only MPs, but plasticizers also contribute to the changes of gut microbial compositions. Studies on zebrafish treated with DEHP revealed that such plasticizer shifted the gut community by reducing the overall diversity and enriching phyla *Fusobacteria*, *Bacteroidetes* and *Verrucomicrobia* [163]. Consistent observation was obtained in this study. Human gut microbiota treated with DEHP showed an increase of phylum *Bacteroidetes* in all DEHP-containing fermenters but not in the no treatment control. On the other hand, dosage-dependent growth of phylum *Proteobacteria* was noted in DINP treatment groups. Similar observations were reported in comparative studies related to IBDs [173].

Intestinal microbiota comparisons in healthy and IBD individuals had been intensively studied in recent decade. DEHP or DINP altered the microbial composition, which shared some similarities with IBD patients' microbiomes. Families *Erysipelotrichaceae*, *Lachnospiraceae* and *Ruminococcaceae* under phylum *Firmicutes,* and *Bifidobacteriaceae* under phylum *Actinobacteria*, were commonly observed decreased in CD patients [173]. Members from these families were all detected to be less abundant in each DEHP-treated microbiota comparing to no treatment control. Meanwhile, more abundant *Coriobacteriaceae* under phylum *Actinobacteria* was identified in DEHP-treated microbiome. Number of bacteria from this family were also reported increased in CD patients' mucosa and submucosa microbiomes [174]. On the other hand, though microbial compositions on family level in DINP-treated fermenters fluctuated, enrichment of *Enterobacteriaceae* and *Streptococcaceae* were observed in DINP-

treated microbiomes. Members from these families were also associated with inflammatory conditions in CD patients [173, 175, 176].

Several genera were enriched in DHEP-treated fermenter including *Alloprevotella* spp., *Collinsella* spp., *Megasphaera* spp., *Prevotella* spp. and an unclassified genus under family *Veillonellaceae*. *Prevotellaceae* were observed enriched in diarrhea-predominant irritable bowel syndrome (IBS) patients' microbiota. Members of such family can generate hydrogen and methane gases through carbohydrate fermentation causing pain in the abdominal region [29]. Studies also found that *Prevotella* spp. were related to pro-inflammatory responses exacerbating colitis in DSS-induced animal model by impairing the repair mechanisms of the mucosa [30]. Clinically, *Prevotella* spp. was reduced in microbiota of exclusive enteral nutrition (EEN)-treated CD patients in remission [177]. Relative abundance of *Alloprevotella* spp. and *Prevotella_9* spp. was enhanced in all DEHP-treated microbiota, whereas decrease in *Prevotella_2* was observed simultaneously. Collectively, the increase of *Prevotellaceae* was contributed to the major expansion of *Prevotella_9*. Inflammatory status and microbiota in UC patients were shown to be different. *Collinsella* spp. was found to be enriched in UC patients' microbiota [17, 175]. DEHP also favored the expansion of *Collinsella* spp. which was the only taxon under family *Coriobacteriaceae.* In DINP experiment, *Escherichia-Shigella* spp. and *Streptococcus* spp. accounted for most abundance of families *Enterobacteriaceae* and *Streptococcaceae.* These genera were detected more abundant in IBD patients [173, 175]. In addition, CD post-operative recurrence was found associated with the relative abundance of *Streptococcus* spp. [17].

Abundance and changes of phylum *Actinobacteria* and family *Bifidobacteriaceae* were composed largely of genus *Bifidobacterium* spp. in DEHP experiment. Decreases in relative abundance of members from this genus were found in all DEHP-treated microbiota, with the greatest drop observed in DEHP D3 fermenter. Reduction of *Bifidobacterium* spp. was detected in onset CD patients' microbiota and its

supplementation had been demonstrated improving intestinal barrier function leading to a lower plasma endotoxin level [173, 175, 178]. SCFAs induced APCs such as dendritic cells and macrophages can stimulate regulatory T cell differentiation to maintain immune homeostasis [179]. Apart from regulatory T cells, it was reported that SCFAs can also stimulate anti-inflammatory IL-10 production by T helper I cell through GPR43 [55]. Butyrate was also proved to enhance intestinal barrier integrity by repression of cation-leaky claudin-2 in cultural enterocyte [157]. Propionate and butyrate concentrations in high dosages DEHP fermenters showed slight decreases, and SCFAs producers' abundance was observed adjusted in plasticizer treated microbiota. SCFAs producers in genera *Blautia* spp., *Dorea* spp., *Lachnospira* spp., *Roseburia* spp. and *Faecalibacterium* spp. were observed less abundant in microbiota of CD patients [17, 173, 179]. DEHP-treated microbiota had a reduced *Dorea* spp. and *Faecalibacterium* spp. abundance. *Faecalibacterium prausnitzii* is one of *Faecalibacterium* spp. that produces SCFAs regulating immune cells by acting on mentioned APCs, and its loss had been frequently described as a marker of IBDs. In DINP treated fermenters, changes of *Dorea* spp. and *Faecalibacterium* spp. were limited and not associated with the dosages of plasticizer. Interestingly, butyrate producers, *Megasphaera* spp. were enriched in DEHP treated microbiota while *Mitsuokella* spp. were reduced. Opposite changes were obtained in DINP treated fermenters.

2. DEHP- and DINP-altered microbiota derived metabolites interfered epithelial integrity

Intestinal epithelial cells beneath mucus layer contribute forming a barrier separating bacteria in the gut lumen from blood vessels. Epithelium integrity is crucial in preventing external antigens from contacting immune cells trigging inflammation responses. Influences brought by the dynamic changes of microbiota affect claudin remodeling which occurs within several days due to the short life span of IECs [180]. TJ and AJ proteins are devoted to constructing epithelial barrier, which connects epithelial cells together limiting solute passages through the paracellular space. Claudin-1, claudin-4 and claudin-7 were observed reduced in both acute colitis, CD and UC patients, which are normally expressed in colon for tight junction sealing [35, 37, 181]. Deterioration of TJ proteins such as occludin and junction adhesion molecule A were also shown to upset barrier functions leading to leaky-gut and endotoxemia [34, 181]. AJ E-cadherin and its adapter protein β-catenin support junction stability. Moreover, ZO-1, ZO-2 and ZO-3 (encoded by *TJP1*, *TJP2* and *TJP3*) are main intracellular adapter proteins interacting both transmembrane TJ proteins and cytoskeletal proteins [181]. Though DEHP altered microbiota towards dysbiosis, most selected target genes encoding tight junction sealing proteins were found to be remained stable in HT-29 cells. However, mRNA levels of *CLDN4*, *OCLN*, *JAMA*, *TJP1* and *CDH1* were detected down-regulated (by 10-43%) in DINP-D3 luminal extract treated HT-29 cells. Significant reduction (12%) in expressions of *OCLN*, *JAMA* and *CDH1* were observed even when the cells were incubated with DINP-D2 luminal extracts. Since TJ/AJ proteins are generated by epithelial cells constitutively, only some of these losses of TJ/AJ expressions were translated to observable protein levels. Western blot verified that significant reduction of E-cadherin, JAM-A and claudin-4 were observed at protein level after DINP-D3 fermenter treatment.

Apart from proteins promoting paracellular integrity, participating in nutrient absorption, cation-leaky pore-forming claudin-2 expression is localized in duodenum and ileum. However, studies demonstrated claudin-2 can also increase IEC paracellular permeability leading to diarrhea, and is highly expressed in UC patients' colon [182]. Enhanced claudin-2 expression can be induced by microbial metabolites; and may intend to result an osmotic imbalance between epithelium to remove unwanted contents such as pathogens and their products from the lumen [36, 183]. In addition to the suppression of TJ and AJ sealing proteins expressions, *CLDN2* was enhanced by 35-67% in HT-29 treated with different DEHP fermenters extracts. Consistent results were obtained in subsequent immunofluorescence assays. Interestingly, consistent down-regulations in both mRNA and protein of claudin-2 in DINP-D2/DINP-D3 extracts treated HT-29 were detected. This may be due to the enrichment of taxon *Bifidobacterium* in DINP-containing fermenters.

3. ROS-neutralization gene in enterocytes was changed by DEHP/DINP luminal extracts

Apart from TJ and AJ gene expressions, antioxidant and antioxidant enzymes have been demonstrated in reducing the severities of dextran sulfate sodium (DSS)-/ trinitrobenzene sulfonic acid (TNBS)-induced ulcerative colitis in murine animal model [184, 185]. High oxidative stress in inflamed tissues were recently observed and such status was considered as one of the pathogeneses of colitis [186]. Several types of superoxide dismutase (SOD) produced by cells catalyze the disproportionation of reactive oxygen species superoxide ions to oxygen and less harmful hydrogen peroxide. Dismutations of superoxide ions by SODs were reduced in experimental colitis animal drastically; and SOD activity-elevating antioxidant treatment was found to be effective in relieving such disease [184]. In this study, though minor enrichment of *SOD1* was observed, gene expressions of *SOD2* and *SOD3* in high dosage DINP-treated HT-29 were reduced by about 40% and 55%, respectively. In subsequent flow cytometry analysis, mean fluorescence, which reflected the intracellular ROS level, was remained stable across different treatments.

4. Plasticizer fermenter extracts skewed macrophages away from M2 differentiation

Most pro-inflammatory cytokines (*TNFA, IL1B, IL6, KC, IL12p40 and IL23p19*) expressions were remained stable after the treatment of DEHP or DINP co-incubated microbial extracts. In contrast, M2 alternative activated macrophages not only participates in T help 2 responses on helminth infection, but also the repairing of inflammatory damages brought by constant stimulation of luminal antigens. One of the M2-polarization markers, IL-1 receptor competitive ligand, *IL1RA* expression was reduced in macrophages treated with different dosages of DINP fermenter extracts. On the other hand, efferocytosis enzyme transglutaminase (*TGM2*), another M2 expressed gene which is shared by both humane and murine macrophages [187], was also diminished in those cells.

IL-12/IL-10 ratio is a general indicator of M1/M2 polarization. IL-10 signaling axis is an important regulator in colitis. Spontaneous colitis will be resulted if IL-10 is deleted; and DSS-induced colitis in animal with macrophage-specific deletion of *IL-10R1* developed disease severity shared with *IL-10* or *IL-10R1* knot-out mice [56]. *IL-10* and *IL-10R2* expressions were downregulated in macrophages treated with extracts from all DINP-treated fermenters. Except autocrine stimulation, significant downregulation of *SOCS3* was observed in almost all plasticizer treated microbial extract-treated macrophages. Enhanced *SOCS3* signaled by *IL-10* promotes alternative activation of macrophages inhibiting nitric oxide synthesis and blocking inflammatory cytokine expression [59]. IFN-γ- and LPS-stimulated signal transducer and activator of transcription-1 (STAT1) pathway was prolonged in SOCS3 deficient macrophages [60].

Macrophage alters intracellular signaling according to different extracellular stimulants and responds by expressing different genes with specific functions. Transcription factors in M2-polarized macrophage have been intensively studied to identify treatment targets for autoimmune diseases in recent years. IRF-4 deficient macrophage was found to be more sensitive to toll-like-receptor (TLR) ligand stimulation and expressed more pro-inflammatory cytokines [51]. Induced *IRF4* expression promoted M2-polarization and ameliorated LPS-induced M1 cytokine secretion, alleviating DSS-induced colitis in mice [188]. Macrophages may display pro-inflammatory phenotype with these expression changes.

Summary

Plasticizers can easily be detected in processed or packaged foods. Utilizing human intestinal epithelial and murine macrophage cell lines, herein we observed that, microbial compositions could be modified within one day of high dosage co-incubation. This altered microbiota shifted the luminal substances which can lead to transcriptional changes in cells located at proximity. DEHP reduced the overall microbiota compositional diversity, metabolites from these communities promoted *CLDN2* which may impair epithelial barrier functions. Major TJ and AJ gene expression reductions (*CLDN2*, *CLDN4*, *OCLN*, *JAMA*, *CDH1 and TJP1*) were observed in HT-29 cells treated with DINP D2 and/or D3 extracts. Compared to those treated with health microbial extracts, RAW264.7 cells expressed less *SOCS3* when treated with DEHP-/DINP-treated fermentation extracts. DINP-co-incubated microbial extracts further suppressed anti-inflammatory genes *IL10*, *IL10R2* and *IRF4*, which may skew macrophage differentiation balance.

Although study has indicated that limited DINP was persisted in organs of rodent, its metabolites absorbed into human circulatory system, liver and kidney were not all excreted within 48 hours [169, 170]. In general, the average daily phthalate intakes in Asian areas such as Taiwan, Japan and Hong Kong are not as high as the dosages used in current study [85, 171, 172], however, their accumulation within human body through repetitive intakes are remained to be elucidated. It would be better to avoid using too much plastic during food processing so that people could limit their exposure to such artificial chemicals.

Supplementary information

Supplementary Table 3.1. Primers for real-time PCR on gene expressions in HT-29 (Adopted from [1]Putt, 2017 and [2]Suzuki, 2011 [33, 124])

Gene (*Homo sapiens*)	Protein	Forward sequence (5'-3')	Reverse sequence (5'-3')
RPLP0	Ribosomal protein P0	ACTTCCTTAAGATCATCCAACT	TATGAGGCAGCAGTTTCTCCA
OCLN[1]	Occludin	CCAATGTCGAGGAGTGGG	CGCTGCTGTAACGAGGCT
CLDN1	Claudin-1	TGGTGGTTGGCATCCTCCTG	AATTCGTACCTGGCATTGACTGG
CLDN2[2]	Claudin-2	CTCCCTGGCCTGCATTATCTC	ACCTGCTACCGCCACTCTGT
CLDN4	Claudin-4	ATCATCGTGGCTGCTCTGG	ACACCGGCACTATCACCATAA
CLDN7	Claudin-7	TTTCATCGTGGCAGGTCTTG	CTCATACTTAATGTTGGTAGGG
JAMA	JAM-A	GATCACAGCTTCCTATGAGGA	ATGGAGGCACAAGCACGAT
CDH1	E-cadherin	AAGAGGACCAGGACTTTGACTT	CAGCCGCTTTCAGATTTTCATC
CTNNB1	Beta-catenin	GGAATGAGACTGCTGATCTTGG	ATCATCCTGGCGATATCCAAGG
TJP1[1]	ZO-1	CAAGATAGTTTGGCAGCAAGAGATG	ATCAGGGACATTCAATAGCGTAGC
TJP2	ZO-2	GCACAGAATGCAAGGATCGA	GTCTGGAACTCGTGTGCTGG
TJP3	ZO-3	GCGAGAAGCCAGTTTCAAGC	GTCCTGGACACAGTCTCTGCGA
NOX1	NADPH Oxidase 1	TTCCCAGGATTGAAGTGGATGG	GAGGTTGTGGTCTGCACACTGG
ALOX5	Arachidonate 5-lipoxygenase	AGGAGGTCCAGCAAGGGAAC	GATTTGGTTGAGCTGGATGGCA
SOD1	Superoxide dismutase 1	ACAGCAGGCTGTACCAGTGCAG	TTCATGGACCACCAGTGTGC
SOD2	Superoxide dismutase 2	CCAAAGGGGAGTTGCTGGAA	AGGCCTGTTGTTCCTTGCAGTG
SOD3	Superoxide dismutase 3	GCTGGAAAGGTGCCCGACTC	ACCTTGGCGTACATGTCTCGGA

Supplementary Table 3.2. Primers for real-time PCR on gene expressions in RAW264.7

Gene (*Mus musculus*)	**Protein**	**Forward sequence (5'-3')**	**Reverse sequence (5'-3')**
HMBS	Hydroxymethylbilane synthase	ATGGGCAACTGTACCTGACT	ACCATCTTCTTGCTGAACAG
TNFA	Tumor necrosis factor-α	AAGGGATGAGAAGTTCCCAA	CTTGGTGGTTTGCTACGACGT
IL1B	Interleukin-1 beta	AGGATGAGGACATGAGCACC	GGAGAATATCACTTGTTGGTTG
IL6	Interleukin-6	CTGATGCTGGTGACAACCAC	GCCATTGCACAACTCTTTTCTC
KC	CXCL1	CCGAAGTCATAGCCACACTCAA	CCGTTACTTGGGGACACCTTTTAG
IL12p40	Interleukin-12 p40	AGAGCAGTAGCAGTTCCCCTGA	GGTTTGATGATGTCCCTGATGA
IL23p19	Interleukin-23 p19	CCAGCGGGACATATGAATCTAC	GCAAGCAGAACTGGCTGTTGTC
IL10	Interleukin-10	GCAGGACTTTAAGGGTTACTTGG	AATCGATGACAGCGCCTCAG
IL10R1	Interleukin-10 receptor 1	GTGGATGAAGTGATTCTGACAG	GGTTGCATTCTTTAGTTCTGAG
IL10R2	Interleukin-10 receptor 2	CGTGGAAGACACCATCATTG	CGGAGACACAACTTGAAACTTC
TGFB1	Transforming growth factor beta	CGCAACAACGCCATCTATGA	TATTTCTGGTAGAGTTCCACATG
IL1RA	Interleukin-1 receptor antagonist	GCCTTCAGAATCTGGGATAC	CCAGACTTGGCACAAGACAG
IRF4	Interferon regulatory factor 4	CTCTCAGACTGCCGGCTGCA	CTGGTCCAGGTTGCTAACATCA
SOCS3	Suppressor of cytokine signaling 3	GCTTCGGGACTAGCTCCCCGG	TTGGAGCTGAAGGTCTTGAGGC
MRC1	Mannose Receptor C-Type 1	GAGCAAGCATTTGTTACCTATCAC	CTTCTTCTTCCACCAGGATAGC
TGM2	Transglutaminase 2	GAGCGCCATGGTCAACTGCA	AGCGCCGCAGAATGTCCACA

Chapter 4 – Microplastic PVC and its plasticizer DEHP modified human intestinal microbiota compositions which promoted permeability in cultural intestinal epithelium

Abstract

Polyvinyl chloride (PVC, $(C_2H_3Cl)_n$) and one of its plasticizers di(2-ethylhexyl) phthalate (DEHP, $C_{24}H_{38}O_4$) are commonly found in medical consumables and food packaging. Detachment of microplastic (MP) through fragmentation and dissolution DEHP from PVC plasticware into high lipid or alcohol content substances may contaminate foods inside the package. In addition to that, as a high consumer in the food chain, it is also possible for human to receive the biomagnified health hazard from these chemicals through ingestion. Research has demonstrated MP can change aquatic organisms' gastrointestinal (GI) microbiota and triggered inflammatory responses. However, assessments of GI bacterial community modification by MPs and plasticizers in human origin microbiota, and alterations on GI epithelium and immunity brought by the modified ecosystem are limited.

In this study, we extended the investigation on alteration of microbiome by microplastic PVC, and the mix of it and its plasticizer DEHP. 16S rDNA sequencing revealed less healthy individual associated *Coprococcus* was detected in all PVC or DEHP treated communities. *Collinsella*, a genus that has been showed positively correlated with inflammatory bowel disease (IBDs), was enriched in DEHP-contaminated microbiota. High dosage PVC and DEHP+PVC contaminated fermenter extracts reduced mRNA level of several anti-inflammatory genes including *IL10*, *IL1RA* and *IRF4* in cultural macrophages. Gene expressions of intestinal junction proteins, occludin, JAM-A and E-cadherin were also reduced in Caco-2 after different contaminated fermenter extracts by up to 54%. Consistent reduction of JAM-A (-27%) on protein level was observed in Caco-2 when treated with extract from high dosage PVC contaminated microbiota. Interestingly, although mRNA level was stable, protein level of occludin in Caco-2 after treatment of extract from high DEHP+PVC contaminated microbiota was reduced by 13%.

Oral intake of these chemicals may impair barrier function of GI epithelium and upset immune homeostasis through modification of overall microbial communities.

Introduction

1. Microplastics PVC

Plastics degradation takes hundreds to thousands of years due to their chemical inertness. Fragmentation during this degradation process produces different small-sized MP which has been showed harmful to aquatic and marine ecosystems [71]. Except damaging the environment, recent studies have indicated that bioaccumulation of MP is observed in higher consumers in the food chain. This implied human could have ingested certain amount of MP, and studies have demonstrated that there is bioaccumulation of MPs along the food chain [71, 189].

Polyethylene, polymethylpentene, polyvinylidene chloride and PVC are common plastics used in food wrap. In which PVC and PVDC plastics contain chlorine atoms and are often produced with plasticizers for better flexibility. Other than food wrapping film, consumables of medical devices, gloves and food packages may also contain PVC. Small MP fragments could be ingested together with the food. Studies on degradation of MPs by human digestive secretions suggested that the surface of MPs could be affected, but hardly be eliminated. However, it has been reported certain bacteria in the environment and human GI tract have the ability of degrading PVC. A strain under genus *Klebsiella*, EMBL-1 has been found to be able to utilize PVC as energy source [190]. These suggest that PVC could modify gut microbiota composition by favoring certain types of bacteria, however, limited studies provide comprehensive or systematic insights in this area.

Except direct intake from package food, we may have consumed MP indirectly through eating seafood. After disposal of plastic waste, due to the lack of recycling capacity, landfill is a common method in waste management in Hong Kong. Landfill of plastics undergoes fragmentation and weathering detaching various sizes of microplastic, whereas acidic hydrogen chloride gas, carbon dioxide and even dioxins will be emitted during incineration of these chlorinated polymers. MPs may be transferred from site of landfill

to water source or ocean and ingested by aquatic organisms. This makes plastic waste, especially chlorinated types, difficult to be handled appropriately. There are limited methods for plastic waste management, while frequency of indiscriminative usages of plastic elevates every day. More MP will be generated and released to the environment.

2. Plasticizer DEHP

DEHP is one of the most frequent used phthalate ester plasticizers adding to PVC to increase softness. It can be found in food processing plastics and medical devices and consumables such as intravenous injection solution packs, dialysis and fluid delivery tubing, surgical masks and gloves, etc. [85, 162]. During food processing, the food wrapping film, gloves, and food packages may contain various kind of plasticizers. On top of that, package food nowadays usually has a long shelf-life prolonging migration of plasticizer into content materials. Since DEHP is hydrophobic and not covalently bound to PVC polymer chain, they can be translocated from PVC to substances through direct contact, especially food and drinks with low pH, high fat or alcohol contents. Studies also demonstrated that heating food with plasticware increase DEHP content in package foods [191, 192].

Toxicity of DEHP has been diversely studied and reproductive system is the major organ that DEHP affects the most. It has been reported that DEHP can induce testicular injury and reduced testosterone level in male mouse [81]. Though its usage is gradually reduced due to its harmful effects on health, it is still detected in common food and drink selling in Hong Kong, especially those with multiple plastic food packaging materials. Possible linkages have been suggested between DEHP and cancer, development of fetus and male reproductive system health. Pregnant mouse exposed to DEHP reproduced male descendants with lower fertility, spermatogenesis and testicular steroid generation [193]. Recent correlation study also indicated that maternal exposure to DEHP is associated with reduced descendant testicular volume [194]. DEHP even promotes proliferation and drug resistance of breast and colon cancer cells [195-198]. Meanwhile, mediating by the microbiome, DEHP has been found to stimulate leaky gut and intestinal inflammation in zebrafish model through activation of several helper T cell subsets [163].

3. PVC/DEHP and health of GI tract

Evidence on how PVC and DEHP affect health is gradually established as more studies have been working on these contaminants. These compounds can stimulate antigen presenting cells and adaptive helper T cells causing inflammation. Recent study has demonstrated that PVC particles treatment augmented IL-1β production in IFN-γ stimulated cultural human macrophage THP-1 [199]. Chronic exposure of DEHP altered GI microbiota composition of zebrafish, leading to obesity. Taxonomic diversity and species richness were disrupted. Among treatment group, male fish intestinal villus length and goblet cell number were reduced, whereas inflammatory cytokine gene *IL8* expression was increased [200]. Another study with transcriptomic analysis on DEHP-treated zebrafish model revealed that expressions of GI pro-inflammatory cytokines categorized in helper T cells specific pathways were significantly promoted [163].

Detrimental effects on intestinal barrier function and immunity were demonstrated with cultural cell models and aquatic animal models in some published studies. Yet little investigation was performed based on human origin microbiota. In this study, we collected fecal samples from one healthy donor on separated dates, utilizing batch culture systems, co-cultured PVC, DEHP+PVC with the same starting microbiota in anaerobic fermenters, leaving 1 fermenter un-treated as control. Together with DEHP batch culture performed in previous study, we expanded the microbiota compositional analysis, barrier integrity test and gene expression assays in Caco-2/RAW264.7 cells by comparing alteration provided by different treatments.

Objective

In this study, we aim to:

1. Compare the changes of microbiota community diversity and compositions by DEHP, PVC and the mix of DEHP+PVC
2. Determine the gene expressions of TJ, AJ, pro-/anti-cytokines in Caco-2 and RAW264.7 cells after treatments of microbiota extracts from all mentioned batch culture experiments
3. Assessment of whether affected TJ and AJ gene expressions translate to proteins or phenotypic levels

Materials and methods

1. Batch Culture

Fecal samples were collected from healthy donor who had normal diet and did not intake any probiotics or antibiotics at least 2 weeks before sampling day. Fecal material was stored in gas-tight sample bucket with anaerobic sachet (Thermo Fisher Scientific, Waltham, USA) and inoculated within 4 hours after collection. Final concentration of 10% w/v of fecal material was homogenized with anaerobic buffer inside a stomacher bag with filter (Seward, Worthing, UK) for 5 minutes at 200 rpm. Sterilized Adult L-SHIME growth medium (without starch) (ProDigest, Gent, Belgium) was adjusted to pH 6.9 mimicking distal colon environment. Filtrate portion obtained after homogenization was inoculated in growth medium with volume ratio of 1:10. Starting cultural volume in each chamber was at 200 ml. One of the four inoculated chambers was used as no treatment control (D0). Three dosages of DEHP, PVC and DEHP+PVC (Sigma, St. Louis, USA), were introduced into each treatment cultural chamber. The starting amounts of plasticizers were set at: 0.21 mg DEHP (D1 = 0.21 mg, D2 = 2.1 mg and D3 = 21 mg) and 0.7 mg PVC (D1 = 0.7 mg, D2 = 7 mg and D3 = 70 mg) according to possible daily exposures detected from previous studies [85, 162, 171, 201]. For mixed DEHP+PVC batch culture, D1 to D3 treatment groups contained both D1 to D3 dosages of DEHP and PVC, respectively. Culture chamber was purged by nitrogen for 10 minutes after inoculation and maintained at 37°C by water circulation. pH values and culture mixtures in different chambers were recorded and collected at 0, 4, 8 and 24 hours after inoculation, respectively.

2. Preparation of luminal extracts

Resultant fermentation culture was defrosted from -20°C and centrifuged at 15,000g for 30 minutes at 4°C. Supernatant from centrifugation was filter-sterilized by 0.22 μm syringe filter. Filtrate was then aliquoted into 2 ml micro-centrifuge tubes and stored at -20°C as luminal extract.

3. Analysis of SCFA concentrations

Method for quantification of SCFA concentrations was adopted from Song, et al., 2018 and Zhao, et al., 2006 [134, 135]. Suspensions were centrifuged at 13,684g for 1 minutes at 4ºC. 270 μl of supernatants were transferred to a new tube and its pH was adjusted to pH 2-3 by 27 μl of 1M HCl (tested by pH paper). 3 μl of internal standard (100 mM 2-Ethyl-butyric acid) was added into each mixture. All mixtures were centrifuged at 2,376g for 20mins at 4ºC. Supernatant was filtered and transferred to a sample vial with insert for GC-FID analysis equipped with Agilent GC column DB-FFAP (123-3232). Oven temperature was set at: 80ºC for 2 minutes followed by ramping 6ºC per minute until 180ºC and then hold for 2 minutes. Concentration of different SCFAs were calculated from standard curves and respective dilution factor.

4. Lipopolysaccharide concentration quantification

Lipopolysaccharide (LPS) concentration in luminal extracts was assessed by general lipopolysaccharide ELISA Kit (ABclonal, Woburn, US) according to the manufacturer's manual. Duplicate assay wells were used for each luminal extracts' LPS quantification.

5. 16S rDNA Sequencing and Analysis

Total genomic DNA from luminal fraction pellets after centrifugation were extracted by using TIANamp stool DNA kit (TIANGEN, Beijing, China) according to the manufacturer's protocol. V3-V4 for DEHP and PVC experiments' samples, and V4 region for DEHP+PVC experiment samples were sequenced. The V3-V4 region of 16S rDNA were sequenced by using 16S338F forward primer and 16S806R reverse primer, while primer pair 16S515F and 16S806R was used in V4 region sequencing (Supplementary Table 4.1). 16S rDNA sequencing was performed by MajorBio (V3-V4) and BGI (V4) using Illumina HiSeq 2000 sequencer. For sequence analysis, primer sequences will be trimmed, and raw data was analyzed by using QIIME2 with HPC provided by Information Technology Services Office, The Hong Kong Polytechnic University. Paired-end sequences with quality data were denoised by DADA2 plugin, and taxonomy was assigned according to SILVA database. Alpha-diversity indices, beta-diversity weighted UniFrac PCoA plots were generated by using pipelines within QIIME2. Taxonomy heatmaps and barplots were generated by RStudio with gplots and ggplot2 packages.

6. Measurement of trans-epithelial electrical resistance (TEER)

Epithelial tight junction integrity of Caco-2 monolayer was estimated by TEER assay. Resistances of transwell membrane and transwell with differentiated monolayer were measured by epithelial voltohmeter (EVOM2; WPI, Sarasota US). Caco-2 cells were seeded at $2x10^4$ cell/transwell and allowed to differentiate for 21-28 days until stable TEER was obtained (>600 Ωcm^2). 10% v/v of luminal extracts in DMEM were loaded on the apical chamber while complete medium was placed in the basolateral region. Initial TEER was recorded as $TEER_o$, and TEER values at time t = 0, 24, 48, 72, 96, 120, 144 and 168 hours were used for the calculation of percentage TEER change by $(TEER_t\text{-}TEER_o)/TEER_o$ x100%.

7. RNA extraction, reverse transcription, and real-time PCR gene expression analysis

Caco-2 and RAW264.7 cells were treated with 1 ml of 20% and 5% v/v filter-sterilized extracts in DMEM for 48 and 24 hours inside a cell culture incubator, respectively. Total RNA was extracted using RNAiso PLUS (Takara, Kusatsu, Japan). RNA concentration was determined by NanoDrop spectrophotometer (Thermo Fisher Scientific, Waltham, USA). cDNA was reverse transcribed using PrimeScript reverse transcription kit (Takara, Kusatsu, Japan) according to the manufacturer's protocol. Real-time PCR was performed on Applied Biosystems QuantStudio 7 Flex Real-Time PCR System (Thermo Fisher Scientific, Waltham, USA) with TB Green Premix Ex Taq II (Takara, Kusatsu, Japan) reagent. Relative quantification of target gene expression was calculated by 2^(-ΔΔCt). Ribosomal protein lateral stalk subunit P0 (*RPLP0*) and hydroxymethylbilane synthase (*HMBS*) were used as housekeeping genes for Caco-2 and RAW264.7 gene expression calculation, respectively. Primers for specific mRNA amplification are listed in supplementary information (Supplementary Table 4.2-4.3).

8. Western blot

Western blot was employed for comparison of tight junction and adherens junction protein expressions after fermenter extract treatment. Caco-2 cells were seeded at $2x10^4$ cell/well in 24-well plate. Cells were cultured for 14 days before treatment. Cells was incubated with 20% extracts for 48 hours prior to protein quantification. After treatment, cells were washed with PBS and then incubated in 200 µl RIPA buffer (Merck Millipore, Burlington, US) with protease inhibitor cocktail (Sigma, St. Louis, USA) for 2 hours at 4°C. Total protein was obtained in supernatant after centrifugation at 20,000g for 10 minutes. Protein samples were stored at -80°C before protein concentration quantification by BCA assay (Thermo Fisher Scientific, Waltham, USA). For SDS-PAGE, 10 µg of total protein from each sample was mixed with sample buffer, heated at 95°C for 5 minutes before loading. SDS-PAGE with 4% stacking and 10% resolving gels was used for electrophoresis. Western blot transfer was done in wet condition with 80V for 90 minutes at 4°C. PVDF (GE Healthcare, Chicago, US) after transfer was blocked with blocking solution (5% skimmed milk in TBST) for 2 hours, and then incubated with primary antibody in blocking solution overnight at 4°C. Primary antibodies used for this study were: mouse monoclonal anti-β-actin (1:2000, Sigma, St. Louis, USA), rabbit polyclonal anti-E-cadherin (1:1000, ABclonal, Woburn, US), rabbit polyclonal anti-occludin (1:2000, ABclonal, Woburn, US) and rabbit polyclonal anti-F11R (1:2000, ABclonal, Woburn, US). Horseradish peroxidase-conjugated goat anti-rabbit IgG (H+L) secondary antibody (1:2000, Novus Biologicals, Centennial, US) and goat anti-mouse IgG (H+L) secondary antibody (1:2000, Thermo Fisher Scientific, Waltham, USA) were used for chemiluminescent signal generation during image capture. Densitometry of chemiluminescent signal was analyzed using Image J. Relative expression of target protein was calculated by dividing its signal to β-actin signal. Normalized expression of target in each sample was generated by dividing relative expression to average relative expression in

control fermenter extract group. Target protein expression in control fermenter treatment group was normalized as 1.

9. Statistical analysis

Statistical comparisons were performed using GraphPad Prism 5. All results are shown as mean +/- SEM from the replicates. Statistical analysis, t-test or one-way ANOVA was used with 95% confidence.

Results

1. 16S rDNA sequencing analysis

Fermenter microbial genomic DNA was extracted and sequenced on Illumina platform. A total of 271,716 qualified reads in 12 resultant fermenters was used for detailed diversity and taxonomy analysis on Majorbio online analysis platform. Beta-diversity PCoA (weighted UniFrac) showed that different dosages of PVC treatments did not alter community compositions. Microbiota cultured with or without PVC shared similar community similarity (Figure 4.1). On the other hand, high/medium dosage DEHP+PVC slightly modified the whole community away from control (Figure 4.2). Biodiversity in DEHP experiment fermenters were mentioned in chapter 3 (Figure 3.2G and Table 3.1). There were drops in observed OTU number and taxa phylogenetic distance in all DEHP-co-incubated communities (DEHP-D1 to DEHP-D3). These observations were not in PVC experiment fermenters but DEHP+PVC treated communities (Table 4.1). Trends of increasing Shannon, shrinking observed OTU counts and Faith's pd were consistently observed in both DEHP- and DEHP+PVC-treated microbiota communities comparing to their respective no treatment controls (Table 4.1). Consistent drops of OTU number and Faith's pd were detected in DEHP+PVC-D1 to DEHP+PVC-D3 chambers compared to control. Though fluctuated, Shannon, Simpson and Faith's pd in PVC experimental fermenters remained similar. Interestingly, number of observed OTUs was enriched in PVC-treated communities.

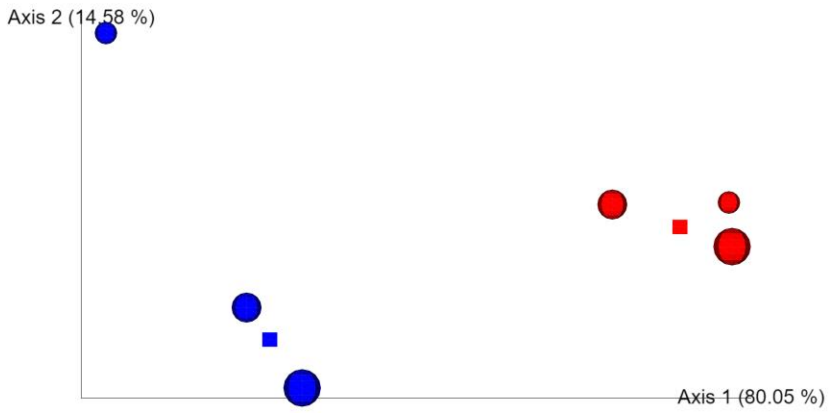

Figure 4.1. Weighted UniFrac PCoA analysis of PVC experiment fermenters at time 0-hour (blue) and 24-hour (red) microbiota compositions. No treatment: square, PVC-treated fermenters: spheres. Sizes of spheres indicated dosages 1, 2 and 3.

Figure 4.2. Weighted UniFrac PCoA for DEHP+PVC experiment fermenters at time 0-hour (blue) and 24-hour (red) microbiota compositions. No treatment: square, DEHP+PVC-treated fermenters: spheres. Sizes of spheres indicated dosages 1, 2 and 3.

Table 4.1 Alpha diversity indices of PVC and DEHP+PVC resultant fermenters' communities.

Fermenters	Indices			
	Observed OTUs	Shannon	Simpson	Faith's pd
PVC-D0	112	4.45	0.92	6.98
PVC-D1	117	4.10	0.90	6.20
PVC-D2	153	4.43	0.92	7.37
PVC-D3	165	4.48	0.91	7.01
DEHP+PVC D0	140	6.03	0.98	9.52
DEHP+PVC D1	110	6.24	0.98	8.76
DEHP+PVC D2	105	6.14	0.98	8.65
DEHP+PVC D3	97	6.19	0.98	8.05

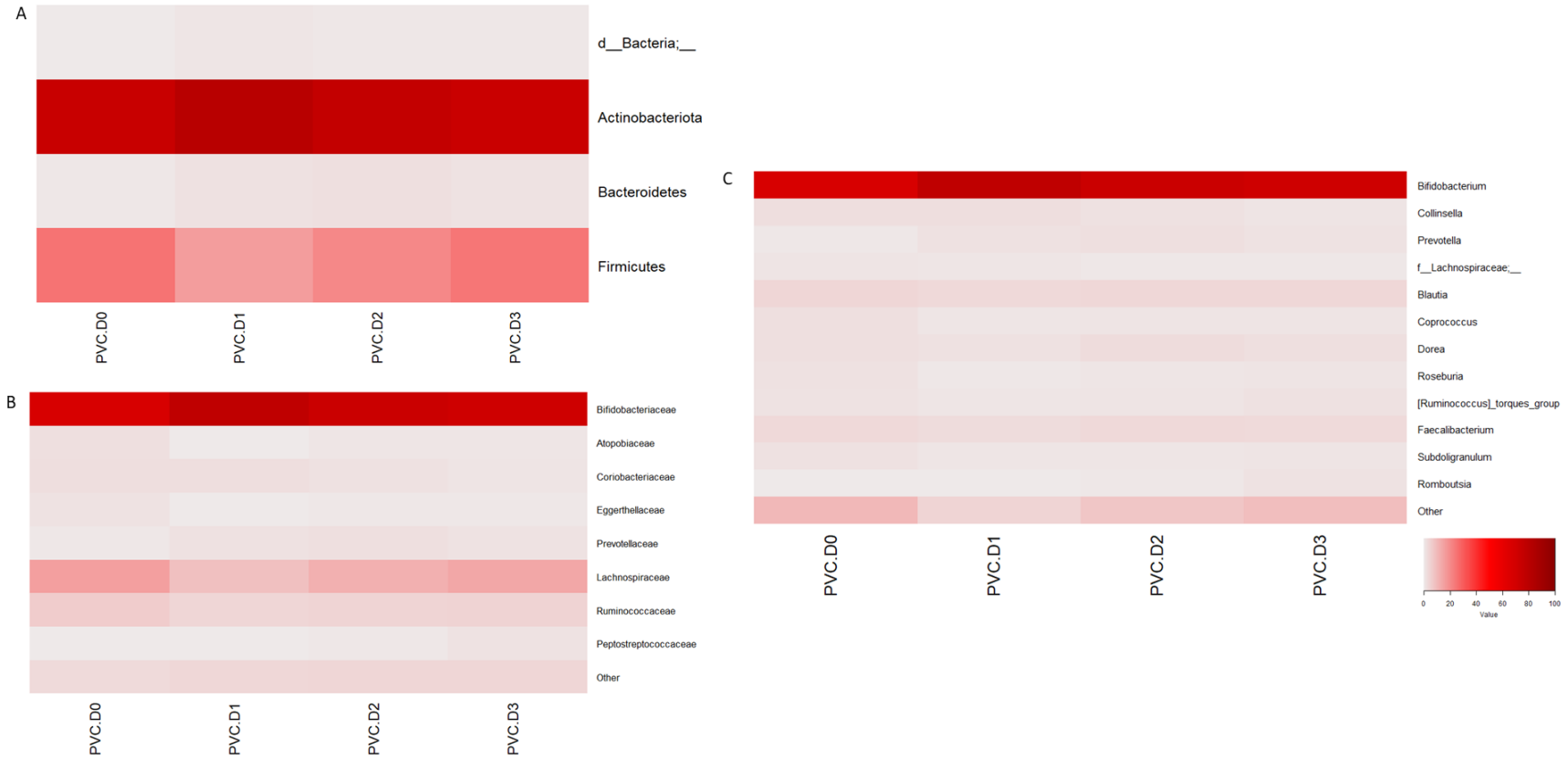

Figure 4.3. Taxonomy heatmaps showing relative abundance of all taxa in PVC experiment (A: phylum, B: family and C: genus) and DEHP+PVC experiment (D: phylum, E: family and F: genus).

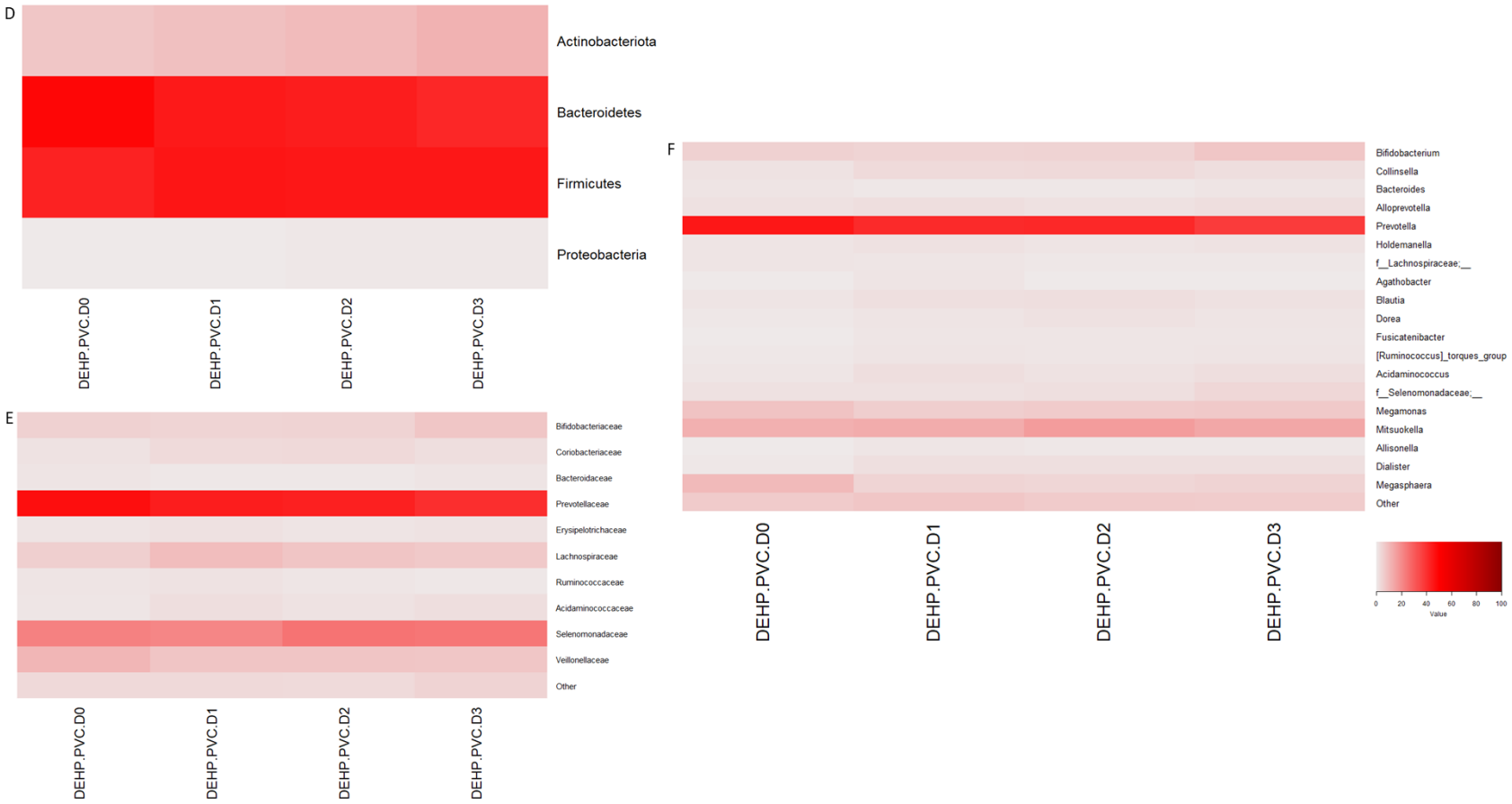

Figure 4.3. Taxonomy heatmaps showing relative abundance of all taxa in PVC experiment (A: phylum, B: family and C: genus) and DEHP+PVC experiment (D: phylum, E: family and F: genus) - continued.

As described in the previous chapter, phyla *Firmicutes* and *Actinobacteria* were reduced while phylum. *Bacteroidetes* was found to be more abundant in DEHP-containing fermenters (Figure 3.3B). In PVC co-incubated microbiota, relative abundance of *Bacteroidetes* was higher in PVC-treated communities (>1.35%) than that in control community (0.45%) (Figure 4.3A). On the other hand, modest increases of *Actinobacteria* in DEHP+PVC-treated microbiota were observed (Figure 4.3D). On family level, more abundant *Prevotellaceae* were observed in PVC contaminated fermenters (Figure 4.3B). Being the dominant family in the microbiota of DEHP+PVC experiment, such adjustment was not observed in DEHP+PVC fermenters (Figure 4.3F). Relative abundance of *Coriobacteriaceae* was shrunk in from 2.58% (in control community) to 1.06% (in PVC-D3 community) along with increasing PVC dosage, however, consistent with DEHP batch culture experiment, DEHP+PVC-treated fermenters had *Coriobacteriaceae* enriched comparing to respective no treatment fermenters (Figure 3.3C and 4.3E).

On genus level, less abundant *Bifidobacterium*, *Dorea*, *Coprococcus_3*, *Roseburia* and *Faecalibacterium*, and enriched *Prevotella_9*, *Collinsella* and *Alloprevotella* were detected in DEHP-treated microbiota (Figure 3.3D). *Roseburia* population was decreased in both DEHP and PVC-treated microbiota (Figure 3.3D and 4.3C). In DEHP and DEHP+PVC batch cultures, more *Collinsella* spp. under family *Coriobacteriaceae* was detected in the microbiota treated with high dose of DEHP+PVC (Figure 4.3F). Overall, comparing to control, though only small amount of *Coprococcus* was detected in DEHP+PVC D0 and D1 microbiota with relative abundance of 0.27% and 0.46%, respectively, *Coprococcus* was detected less abundant in almost all microbiota treated with three sets of contaminants (Figure 3.3D, 4.3C and 4.3F). D2 and D3 DEHP+PVC treatments depleted *Coprococcus* population. Finally, enrichment in genera *Dialister* and *Acidaminococcus*, and reduction of *Megamonas* and *Megasphaera* were only observed in DEHP-PVC-treated fermenters (Figure 4.3F).

With the mentioned modification in microbiota composition, PVC-D3 fermenter had propionate concentration reduced comparing to control and D1-D2. In DEHP+PVC experiment, consistent with DEHP experiment reported previously (Figure 3.2B-3.2C) propionate and butyrate concentrations were reduced at high dosages contaminated groups (D2-D3) comparing to their respective no treatment controls (Figure 4.4E-4.4F). Concentration of acetate remained stable in different fermenters (Figure 4.4A, 4.4D). LPS concentration was stable in each fermentation experiment with no significant difference (Figure 4.5).

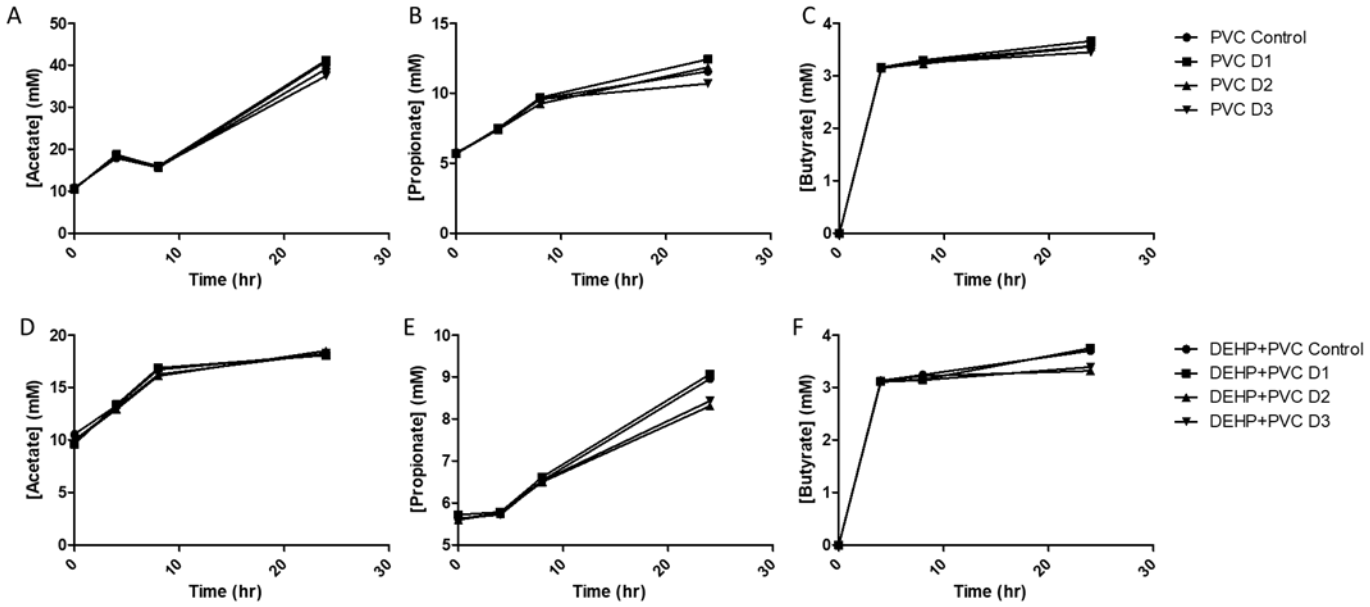

Figure 4.4. Concentrations of SCFAs in various chambers at different time points. A: acetate, B: propionate and C: butyrate.

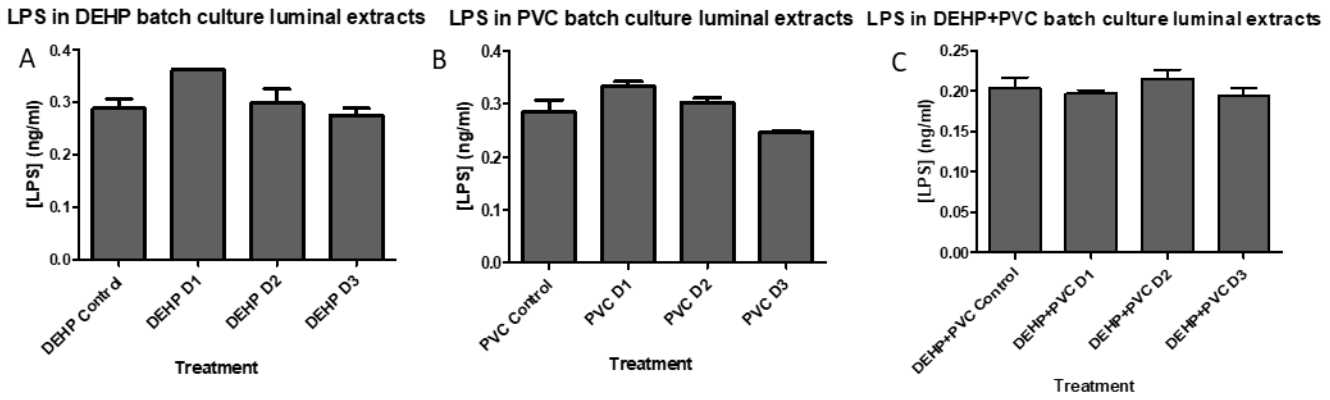

Figure 4.5. Concentrations of LPS in all resultant fermenters (A: DEHP experiment; B: PVC experiment; C: DEHP+PVC experiment). Data represent mean with SEM from at repeats of 2.

2. RT-qPCR gene expression assays on TJ/AJ genes in Caco-2 and M1/M2 markers in RAW264.7

20% v/v and 5% v/v of extracts were added in the cultural medium as the treatment for Caco-2 and RAW264.7 cells respectively as these percentages preserved high viabilities (Figure 4.6). Selected major tight junction and adherens junction genes were found reduced after treatment of extracts derived from fermenters with DEHP, PVC, and DEPH+PVC (Figure 4.7). Comparing to those treated with extracts from the control fermenter, *OCLN* mRNA level of Caco-2 cells was reduced by almost 30% after DEHP-D3 extract treatment. Though *OCLN* expression in DEHP-D2 treatment group remained similar as control, 12-15% drop *CLDN1*, *CLDN7*, *TJP1*, *TJP3* and *CTNNB1* mRNA levels were detected in DEHP-D2 extract-treated Caco-2. Epithelial marker gene *CDH1* expression was decreased when treated with DEHP-D1 to DEHP-D3 extracts in a dose-dependent manner. *TRIC*, coding for tricellulin, was observed slightly enriched by 14% by DEHP-D3 extract.

When Caco-2 incubated with extracts from PVC experiment fermenters, most selected TJ and AJ genes remained stable except *JAMA* and NECT2. It was observed that *JAMA* was down-regulated from 12% to almost 50% in PVC-dose-dependent manner. *NECT2* expressions were decreased by 14-43% in Caco-2 co-incubated with PVC-fermented microbial extracts, however, marginal statistically significant drop ($p=0.0542$) was only observed in the highest PVC dosage group.

In DEHP+PVC mixed batch cultures, though not significant in D1-D2 groups, *JAMA* down-regulation was consistently observed in Caco-2 treated with DEHP+PVC-D3 extracts. Deceasing trend of *CDH1* expression detected in DEHP experiment was also showed in Caco-2 cells incubated with DEHP+PVC D2-D3 extracts, which had values of -23% and -26%, respectively. In addition to *CDH1*, *TRIC* expression was reduced by 24% after DEHP+PVC-D2 extract treatment.

M1/M2 cytokines and markers in RAW264.7 after DEHP fermenter extract treatment was described in previous chapter. Enrichment of pro-inflammatory cytokine genes such as *TNFA*, *IL1B*, *IL6*, *KC*, *IL12p40* and *IL23p19* in cultural macrophages were not significant, however, down-regulation of *SOCS3* was observed after treatments. This reduction was not observed in both PVC and DEHP+PVC experiments, yet some other tissue repairing M2 markers were suppressed (Figure 4.8). *IL10*, *IL10R1* and *TGM2* expressions were reduced by 11-17% in PVC-D3 treated RAW264.7 comparing to those treated with PVC-D0 control fermenter extracts. *Il10R1* expression was affected similarly even when treated with PVC-D2 extract. Anti-inflammatory genes transcription factor *IRF4* was significantly down-regulated after DEHP+PVC-D1 and D3 extracts' treatments. *IL10* in DEHP+PVC-D3 extract-treated RAW264.7 cells was almost reduced by half. In addition to this immune-regulating cytokine, *IL1RA* expression was also suppressed by more than 40% after the treatment.

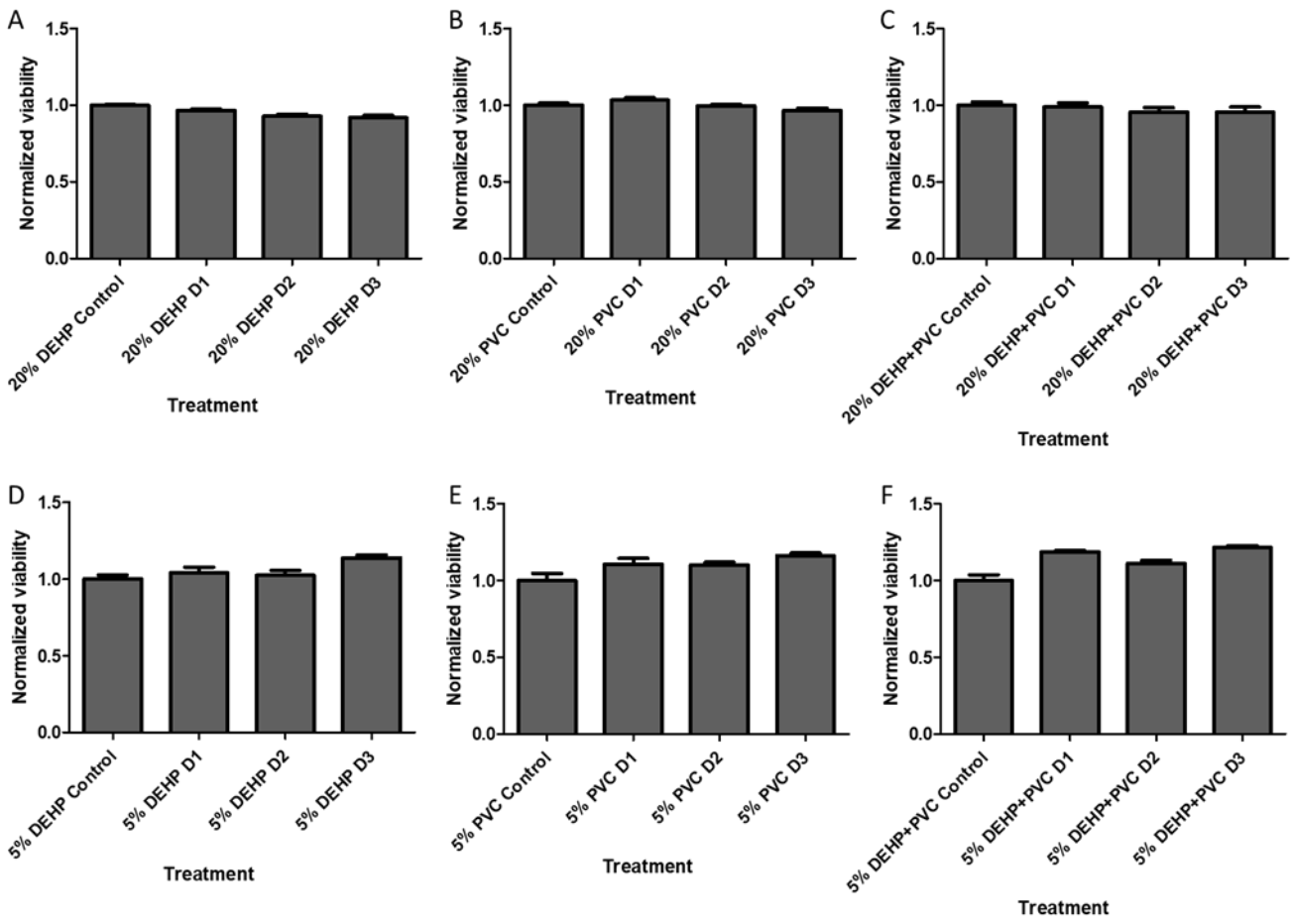

Figure 4.6. Viability of Caco-2 (A-C) and RAW264.7 (D-F) cells after different fermenter extract treatments. Data represent mean with SEM from at repeats of 3.

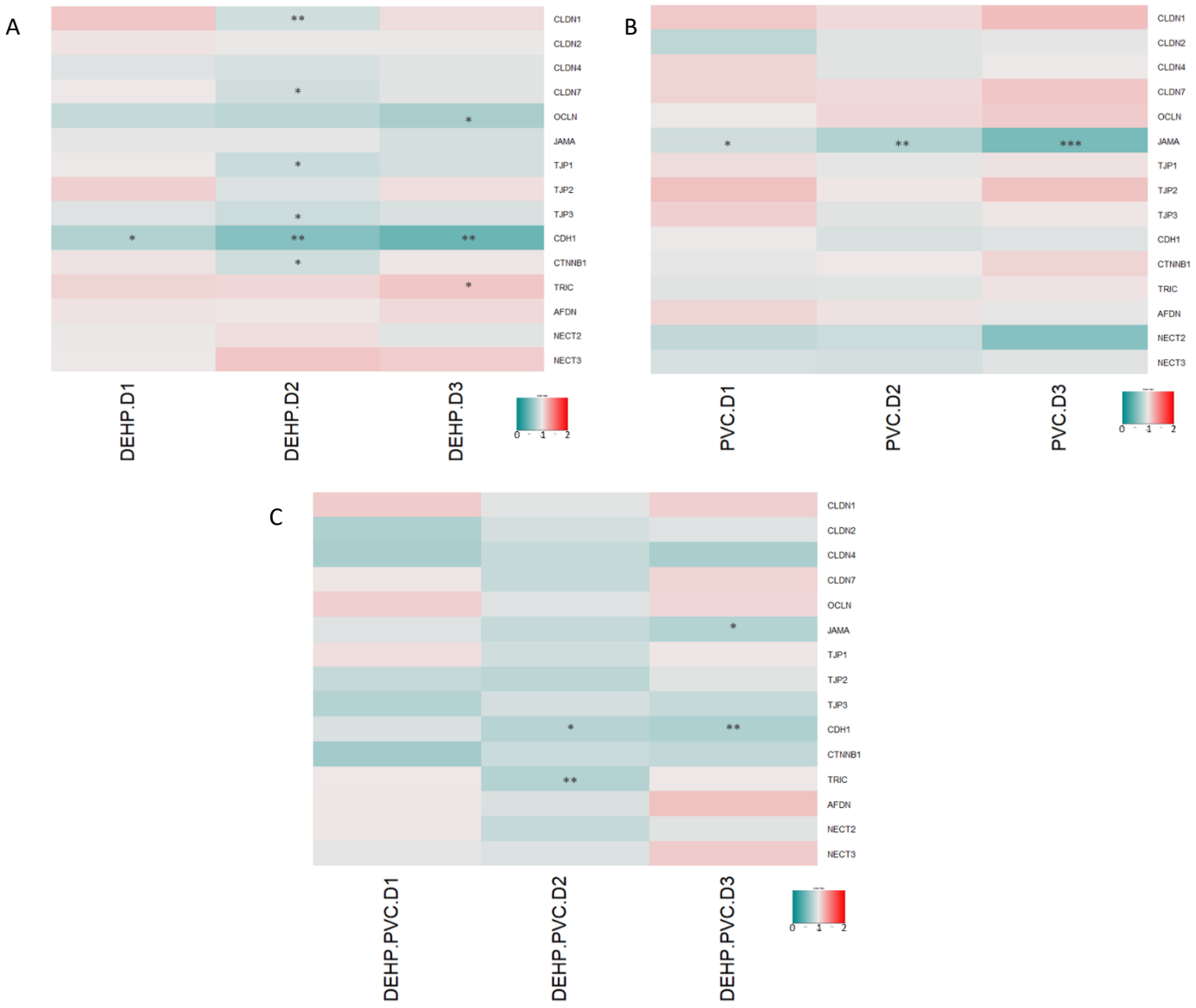

Figure 4.7. Normalized expressions of TJ/AJ associated genes in Caco-2 after extract treatments (A: DEHP experiment, B: PVC experiment and C: DEHP+PVC experiment). Gene expressions in Caco-2 after respective control fermenter extract treatment was normalized as 1. t-test, n=3, *p<0.05, **p<0.01 and ***p<0.005.

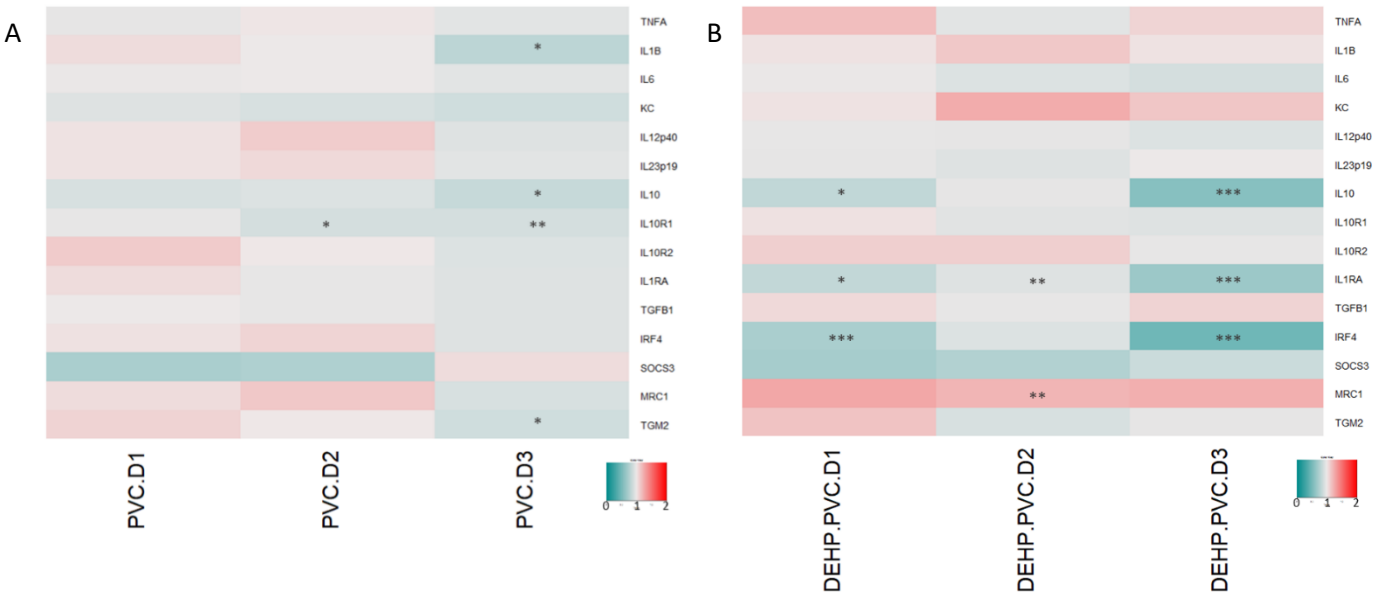

Figure 4.8. Normalized expressions of cytokine and M2 maker genes in RAW264.7 (A: PVC experiment and B: DEHP+PVC experiment). Gene expressions in RAW264.7 after respective control fermenter extract treatment was normalized as 1. t-test, n=3, *p<0.05, **p<0.01 and ***p<0.005.

3. TEER assay

TEER (which reflected cultural Caco-2 epithelium integrity) was monitored for at least 6 days after introduction of extracts. There were significant drops of TEER by 15% and 19% in DEHP-D1 extract-treated Caco-2 monolayer after 24 and 48 hours, respectively (Figure 4.9A), however, TEERs in monolayers treated with DEHP-D0, DEHP-D2 and DEHP-D3 remained similar. Though PVC-fermenter extracts induced larger percentage drop of TEER in Caco-2 than those treated with control extract, the differences were not statistically significant (Figure 4.9B). In DEHP+PVC experiment, fermenter extract from D3 chamber stimulated more rapid drop in TEER comparing to those treated with control, D1 and D2 extracts (Figure 4.9C). 10% and 13% more TEER drops were detected after treatments for 72 and 96 hours, respectively (Figure 4.9D).

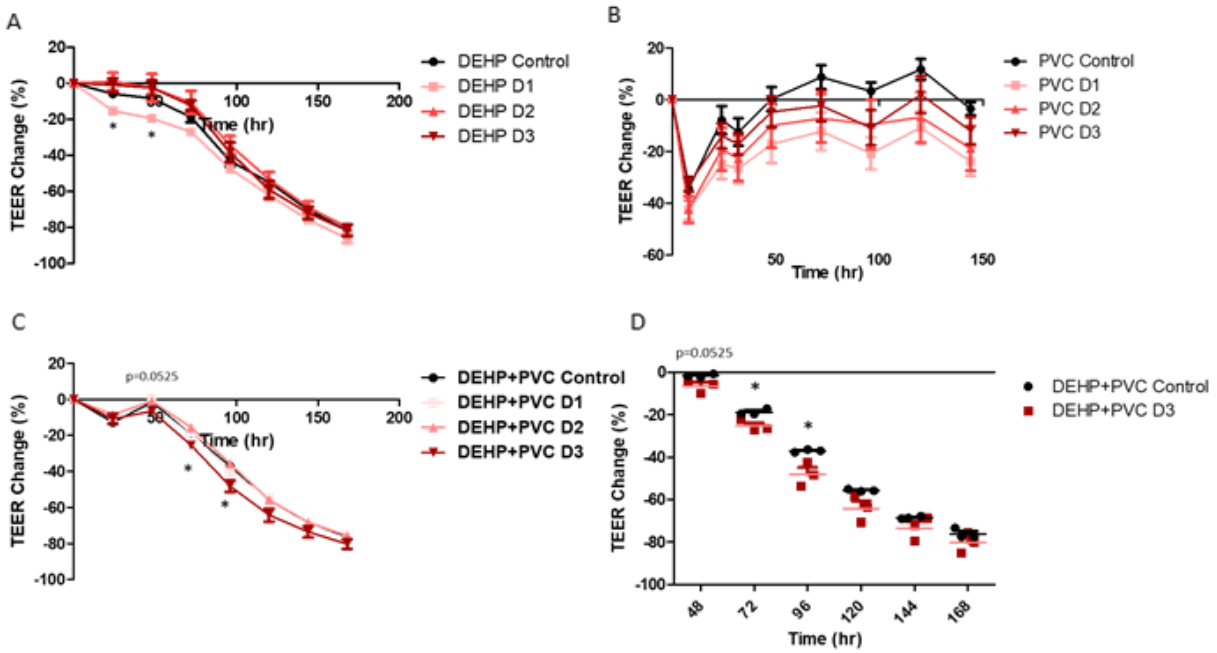

Figure 4.9. Percentage Caco-2 monolayer TEER changes in different treatments (A: DEHP fermenter extracts, B: PVC fermenter extracts and C: DEHP+PVC fermenter extracts). TEER changes comparisons of DEHP+PVC-D0 and DEHP+PVC-D3 treatment groups at different time-points (D). t-test, *p<0.05, **p<0.01 and ***p<0.005.

4. Western blot occludin protein level comparison

Western blot assays were employed to compare the expressions of various TJ/AJ proteins in Caco-2 cells after treatment with different fermenter extracts. Although DEHP-fermenter extracts did down-regulate the *CDH1*, *JAMA* and *OCLN* to a certain level, western blot assays showed that E-cadherin, occludin and JAM-A proteins remained stable after treatment of different fermenter extracts (Figure 4.10A-4.10D). Consistent with the drop of mRNA level, JAM-A protein in Caco-2 treated with PVC-D3 fermenter extract was reduced by 26% ($p<0.005$) (Figure 4.10E and 4.10H). Interestingly, E-cadherin was observed slightly enriched after PVC-D2 extract treatment (Figure 4.10F). In DEHP+PVC test, Significant down-regulation of *CDH1* mRNA expressions were detected in Caco-2 treated with DEHP+PVC- D2 and D3 extracts, and *JAMA* after DEHP+PVC-D3 treatment. However, only DEHP+PVC-D3 extract reduced occludin protein level in Caco-2 cells (Figure 4.10I and 4.10K).

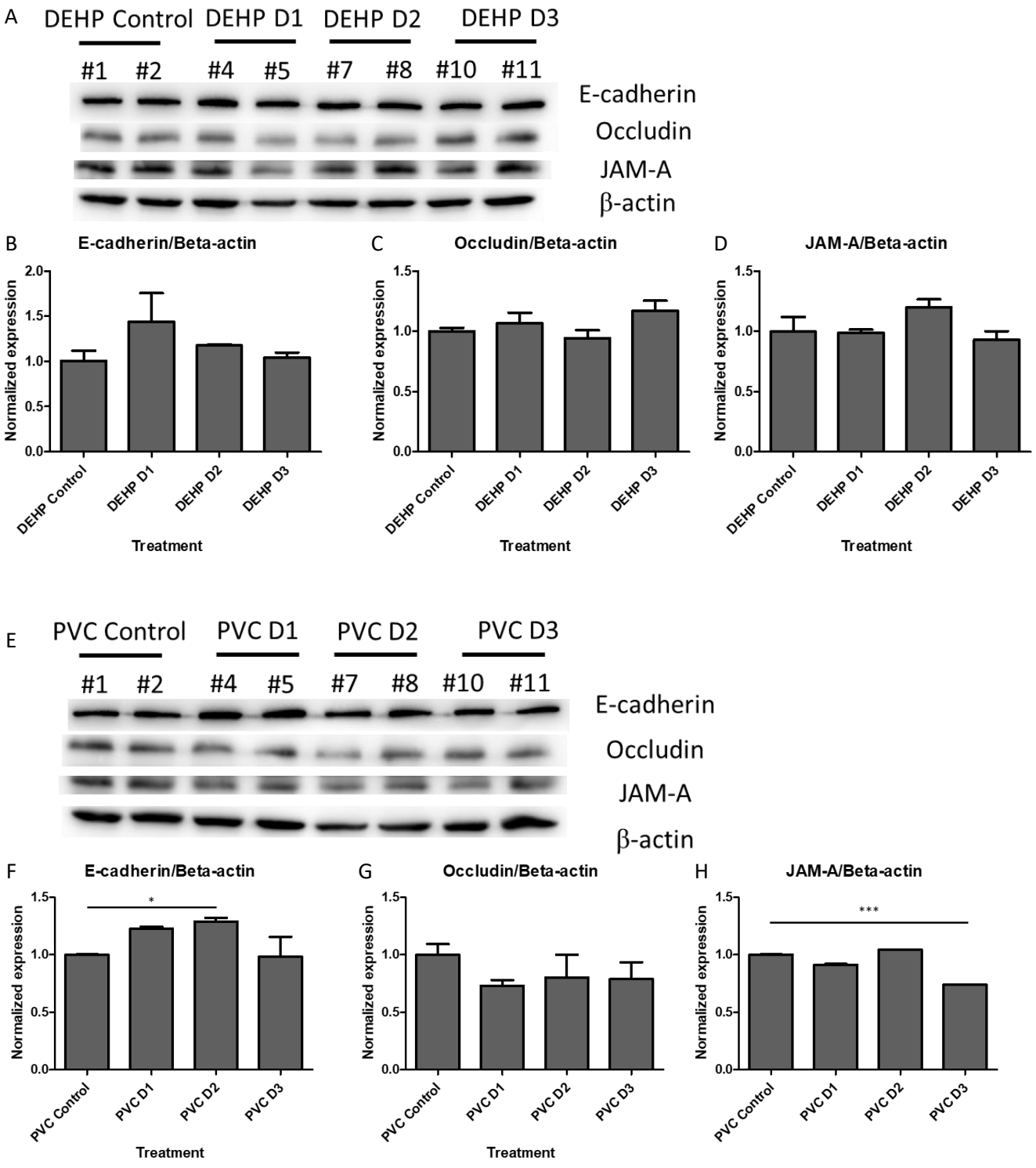

Figure 4.10. Comparison of protein levels of occludin, JAM-A and E-cadherin in Caco-2 cells after treatments (A-D: DEHP experiment, E-H: PVC experiment and I-L: DEHP+PVC experiment). t-test, n=2, *p<0.05, **p<0.01 and ***p<0.005.

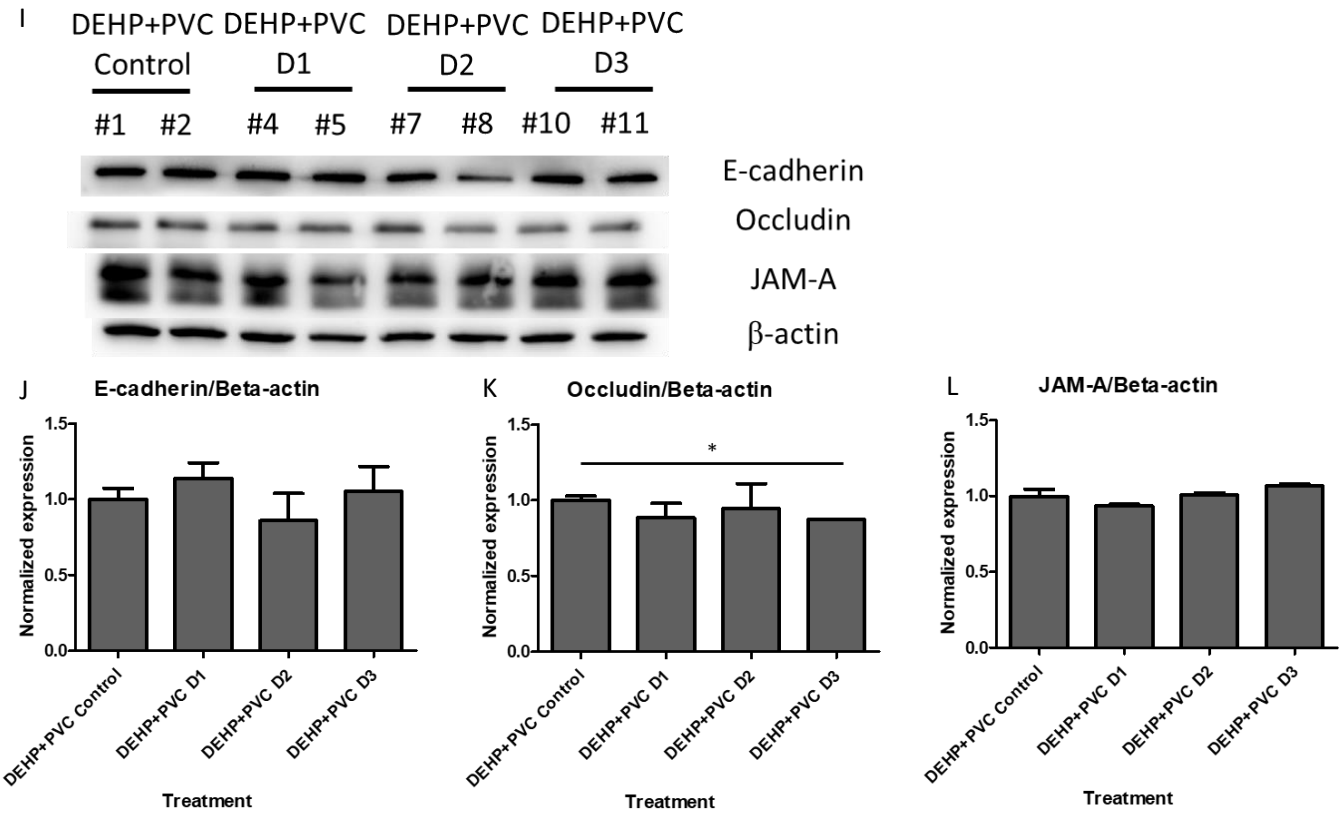

Figure 4.10. Comparison of protein levels of occludin, JAM-A and E-cadherin in Caco-2 cells after treatments (A-D: DEHP experiment, E-H: PVC experiment and I-L: DEHP+PVC experiment). t-test, n=2, *p<0.05, **p<0.01 and ***p<0.005 - continued.

Discussion

1. DEHP treatment reduced community phylogenetic diversity

Three different sets of human fecal microbiota were collected for DEHP, PVC and DEHP+PVC batch cultures. The shift of any taxon relative abundance was compared to the microbiota without any treatment (control fermenter) to observe possible changes brought by these substances independently. After that, it is still possible to compare any similar modification on taxonomy among batch cultures of DEHP versus DEHP+PVC, and PVC versus DEHP+PVC. Alpha diversities observed OTU count and Faith's pd were dropped in DEHP-treated microbiota in both DEHP and DEHP+PVC batch cultures. In addition to that, in weighted UniFrac PCoA, both DEHP-treated and DEHP+PVC-treated microbiota had clustered and shifted away from their respective controls. Such relative phylogenetic deviation was not observed in sole PVC experiment instead. This implied DEHP can alter different certain types of bacterial growth. Nevertheless, the functional characteristics of these modified microbiota could have been changed by DEHP, since phylogenetic information was considered during weighted UniFrac PCoA calculation,

As indicated in alpha- and beta-diversity analyses, PVC-fermenter possessed communities similar to that in control fermenter PVC-D0. Relative abundance of only several taxa were changed. Genus *Roseburia* was detected reduced in sole PVC-treated microbiota. Several SCFA producer genera such as *Bifidobacterium*, *Dorea*, *Roseburia* and *Faecalibacterium* were found to be reduced in DEHP fermenters. Resultant propionate and butyrate concentrations in high dosages DEHP microbiota reduced slightly, while only mild drop in propionate was observed in high dose PVC extracts. Consistent with sole DEHP experiment, DEHP+PVC-treated community extracts contained less propionate and butyrate. SCFAs, especially butyrate, has been showed bearing beneficial effects as direct energy supply to enterocytes, and immune-regulation mediated by G protein-coupled receptors (GPR41, GPR43 and GPR109) [157, 202]. Another anaerobic butyrate producer, *Coprococcus* spp., was detected reduced in all DEHP- or PVC-

containing fermenters. *Coprococcus* has been observed less abundant in IBD patients' mucosa [24, 176, 203]. Together with *Roseburia*, their existence can be used as an indication of IBD remission signature in the microbiota [204].

More abundant *Collinsella* spp. was observed consistently in high dosages DEHP- and DEHP+PVC-co-incubated communities comparing with their respective no treatment controls. Studies comparing bacteria in IBD and healthy mucosa revealed that *Collinsella* spp. was more frequently found in those IBDs' samples [205]. *Collinsella* spp. was found to be related to some inflammatory and metabolic diseases. Patients with nonalcoholic steatohepatitis had high *Collinsella* abundance in their GI microbiota [206]. Chen et al. reported that *Collinsella* spp. was found more abundant in rheumatoid arthritis patient GI microbiota. Follow-up study on epithelium integrity assays on Caco-2 cell revealed that *Collinsella aerofaciens* promoted Caco-2 barrier permeability by down-regulating ZO-1 and occludin. Besides reducing tight junction protein levels, IL-17A expression was also enriched by this bacterium [207]. More *Dialister* spp. was detected in DEHP+PVC co-fermented community. *Dialister* was correlated with some inflammatory status. This genus was found more abundant in CD patient's ileum and colon biopsy samples, its relative abundance was also positively correlated with spondyloarthritis [208].

2. Extracts from altered microbiota due to DEHP+PVC downregulated immunoregulatory genes

In cultural murine macrophage, slightly down-regulation of *SOCS3* was observed in DEHP+PVC groups, though not significant. Mild reduction in pro-inflammatory *IL1B* and anti-inflammatory *IL10*, *IL10R1* and *TGM2* was observed in PVC-D3-treated RAW264.7. Percentage reduction of mRNA levels of *IL10*, *IL1RA* and *IRF4* were higher than those observed in PVC experiment. The drops in IL-10-IL-10R autocrine loop genes could be resulted from the reductions of propionate and butyrate concentrations. On the other hand, several pro-inflammatory taxa were enriched in the communities treated with dosages 2-3 of DEHP+PVE. Mediators from these bacteria could stimulate immune homeostasis skewing RAW264.7 cells away from M2 tissue-repairing profile.

3. High-dose of DEHP+PVC fermenter extract affected Caco-2 epithelium integrity

Extracts from high dosages DEHP or PVC treatment groups among three different batch cultures suppressed *JAMA* expression in Caco-2, in which PVC extracts reduced both mRNA and protein levels of JAM-A significantly. Starting from dosage 2, DEHP and DEHP+PVC extracts repressed *CDH1* expression. In addition to *CDH1*, *OCLN* coding for occludin, also down-regulated significantly in DEHP-D3 extract treatment group. JAM-A protein in PVC-D3 extract treatment group reduced significantly. And high dosage DEHP+PVC extract decreased occludin protein expression in Caco-2. Occludin has been showed to be important for maintenance of intestinal paracellular barrier function preventing excessive antigen from passing through the epithelium towards bloodstream [33, 34, 206]. It is possible that the downregulated occludin contributed to the rapid drop in TEER of Caco-2.

Summary

Phylogenetic distance of community became further apart between health and DEHP-dosed batch cultures. Similar phenomenon was also observed in subsequent DEHP+PVC batch culture experiment. In addition to that, consistently, resultant propionate and butyrate concentrations were slightly reduced. Relative abundance of *Collinsella*, which has been linked to severity of intestinal inflammation, was enriched in these DEHP-containing fermenters. On the contrary, genus *Coprococcus*, a health-associated taxon, was observed suppressed in all PVC/DEHP included microbiota. Such extracts interfered *OCLN*, *JAMA* and *CDH1* expressions in Caco-2 cells; and *IL10*, *IL1RA* and *IRF4* in RAW264.7 cells. Though limited studies were performed on accumulation and biomagnification of PVC and DEHP in human body, these substances may pose threats on epithelial integrity and immune homeostasis in GI tract.

Modification on PVC polymers by physical and chemical measures have been suggested as alternative plasticizing method other than using phthalates [209]. Internal plasticization of PVC polymers prevents plasticizers from leaking out of the plastic via covalent bonds. Plasticizing molecules are covalently bound onto the PVC polymer chain to increase chain-chain distance and minimize the interaction among them. These molecules to be bound onto PVC chains includes phthalate derivatives or replacement of chlorine atom on polymer chain with propargyl ether cardanol. Other than chemical modification on the polymer chain, several methods with lower costs have also been proposed as replacement of phthalates. Hyper-branched polyglycerol and vegetable oil derivatives have also been suggested as plasticizers for PVC. These polymeric plasticizers or macromolecule plasticizers have been suggested as replacement for low molecular weight plasticizers (DEHP and DINP) as they have been demonstrated to harbor low migration and extractability in tests [210]. Migration of plasticizers can be reduced by surface plasma treatment or UV irradiated modifications. Surface plasma treatment with thiosulfate, sodium azide and sodium sulfides improve migration resistance of plasticizers within the plastic.

PVC plastics are widely used in medical consumables, food processing chain and daily plasticware due to its low price and convenience. Reduce usage of plastics dose decrease plasticizer contamination as indicated in the mentioned literature about terminating usages in food processing in Japan [85]. Reduce usages of plastics, plan medical processes so that minimum plastics will be used. Since the exposure route of PVC and DEHP are mainly oral intake, it is always good to wash hands after contact with plastics to reduce intake of contaminants from mouth. Besides avoiding intake, it has been demonstrated that certain *Lactobacillus* species can prevent plasticizer absorption by bio-binding and retaining these compounds in the GI tract [211]. Maintaining a balanced gut microbiota may prevent us from absorbing plasticizers. The Hong Kong government tends to control the usage of plastics through public education to encourage using reusable alternatives and reduce unnecessary plastics. It may be more effective if the government could provide incentive measures to promote usage of lunch box and food-wares made from glass or metal, and support manufacturers to switch from traditional plastics to bio-degradable plastics. On the other hand, Taiwan and France governments have and will ban the use of plastic food-wares in 2020 and 2030, respectively, which the relevant legislation could be good references for Hong Kong to investigate and develop one that suits the need of local community.

Supplementary information

Supplementary Table 4.1. Primers used for 16S sequence amplification and 16S rDNA sequencing

Primers names	Sequences (5'-3')
16S341F	CCTACGGGAGGCAGCAG
16S806R	ATTAGATACCCSBGTAGTCC
16S338F	ACTCCTACGGGAGGCAGCA

Supplementary Table 4.2. Primers for RT-qPCR on gene expressions in Caco-2 (Adopted from [1]Putt, 2017 and [2]Suzuki, 2011 [33, 124])

Gene	Protein	Forward sequence (5'-3')	Reverse sequence (5'-3')
RPLP0	Ribosomal protein P0	ACTTCCTTAAGATCATCCAACT	TATGAGGCAGCAGTTTCTCCA
OCLN[1]	Occludin	CCAATGTCGAGGAGTGGG	CGCTGCTGTAACGAGGCT
CLDN1	Claudin-1	TGGTGGTTGGCATCCTCCTG	AATTCGTACCTGGCATTGACTGG
CLDN2[2]	Claudin-2	CTCCCTGGCCTGCATTATCTC	ACCTGCTACCGCCACTCTGT
CLDN4	Claudin-4	ATCATCGTGGCTGCTCTGG	ACACCGGCACTATCACCATAA
CLDN7	Claudin-7	TTTCATCGTGGCAGGTCTTG	CTCATACTTAATGTTGGTAGGG
JAMA	JAM-A	GATCACAGCTTCCTATGAGGA	ATGGAGGCACAAGCACGAT
CDH1	E-cadherin	AAGAGGACCAGGACTTTGACTT	CAGCCGCTTTCAGATTTTCATC
CTNNB1	Beta-catenin	GGAATGAGACTGCTGATCTTGG	ATCATCCTGGCGATATCCAAGG
TJP1[1]	ZO-1	CAAGATAGTTTGGCAGCAAGAGATG	ATCAGGGACATTCAATAGCGTAGC
TJP2	ZO-2	GCACAGAATGCAAGGATCGA	GTCTGGAACTCGTGTGCTGG
TJP3	ZO-3	GCGAGAAGCCAGTTTCAAGC	GTCCTGGACACAGTCTCTGCGA
TRIC	Tricellulin	GGCAAAATACCCTGTGATTCAGACAG	CATGGATTCTTGAAATTCTCTCATG
AFDN	Afadin	ACCGACAAGCAAGAGCACCACTAG	TGCCTGCGATAATCTGGCTGCTG
NECT2	Nectin-2	CAGAGTCATAGCCAAGCCCAAGAAC	GTCCAGGGATGAGAGCCAGGAG
NECT3	Nectin-3	TCTCCAGGCTCTGTGGTGCC	ATGGTGAACTGCAACAGTCTGTGAA

Supplementary Table 4.3. Primers for real-time PCR on gene expressions in RAW264.7

Gene	Protein	Forward sequence (5'-3')	Reverse sequence (5'-3')
HMBS	Hydroxymethylbilane synthase	ATGGGCAACTGTACCTGACT	ACCATCTTCTTGCTGAACAG
TNFA	Tumor necrosis factor-α	AAGGGATGAGAAGTTCCCAA	CTTGGTGGTTTGCTACGACGT
IL1B	Interleukin-1 beta	AGGATGAGGACATGAGCACC	GGAGAATATCACTTGTTGGTTG
IL6	Interleukin-6	CTGATGCTGGTGACAACCAC	GCCATTGCACAACTCTTTTCTC
KC	CXCL1	CCGAAGTCATAGCCACACTCAA	CCGTTACTTGGGGACACCTTTTAG
IL12p40	Interleukin-12 p40	AGAGCAGTAGCAGTTCCCCTGA	GGTTTGATGATGTCCCTGATGA
IL23p19	Interleukin-23 p19	CCAGCGGGACATATGAATCTAC	GCAAGCAGAACTGGCTGTTGTC
IL10	Interleukin-10	GCAGGACTTTAAGGGTTACTTGG	AATCGATGACAGCGCCTCAG
IL10R1	Interleukin-10 receptor 1	GTGGATGAAGTGATTCTGACAG	GGTTGCATTCTTTAGTTCTGAG
IL10R2	Interleukin-10 receptor 2	CGTGGAAGACACCATCATTG	CGGAGACACAACTTGAAACTTC
TGFB1	Transforming growth factor beta	CGCAACAACGCCATCTATGA	TATTTCTGGTAGAGTTCCACATG
IL1RA	Interleukin-1 receptor antagonist	GCCTTCAGAATCTGGGATAC	CCAGACTTGGCACAAGACAG
IRF4	Interferon regulatory factor 4	CTCTCAGACTGCCGGCTGCA	CTGGTCCAGGTTGCTAACATCA
SOCS3	Suppressor of cytokine signaling 3	GCTTCGGGACTAGCTCCCCGG	TTGGAGCTGAAGGTCTTGAGGC
MRC1	Mannose Receptor C-Type 1	GAGCAAGCATTTGTTACCTATCAC	CTTCTTCTTCCACCAGGATAGC
TGM2	Transglutaminase 2	GAGCGCCATGGTCAACTGCA	AGCGCCGCAGAATGTCCACA

Chapter 5 – Effect of polyethylene on human gut microbiome and its associated influences on gut permeability in vitro and Simulator of Human Intestinal Microbial Ecosystem (SHIME)

Abstract

Polyethylene (PE) is one of the most utilized plastics in daily life. Fragmentation of plastics produces smaller pieces microplastics (MPs) ranged from millimeter to nanometers. Studies have been conducted to investigate MP and their plasticizers on aquatic lives and murine models. Yet, there was limited study performed on assessing the effects of MP on human microbiota and cultural cells. In this study, we employed batch culture and Simulator of Human Intestinal Microbial Ecosystem (SHIME) to detected possible shift of microbiota composition due to exposure to PE. Total metabolic extracts derived from the microbiota exposed to PE were tested to determine if they would compromise the intestinal epithelial permeability via up- or down-regulation tight junction (TJ) and adherens junction (AJ) proteins.

In the batch culture of human fecal microbiota co-incubated with PE, several inflammation-correlated gut bacteria taxa including *Holdemanella, Collinsella* and *Allisonella* were enriched in the PE treatment groups. Moreover, SCFA-producing bacteria, such as *Dorea*, *Roseburia* and *Faecalibacterium* were less abundant in the PE-treated microbiota. Though beneficial (*Bifidobacterium*) genus was enriched in the PE-treated groups, the overall microbial extracts from PE fermenters reduced occludin expression up to 23% in the cultural enterocytes.

In the SHIME setting, more abundant pro-inflammatory diseases associated taxa, *Bilophila* and *Acidaminococcus* were detected in PE-treated distal colon (DC) than the control. Extract from PE-contaminated distal colon stimulated a more rapid drop of TEER in Caco-2 monolayer (up to 26%), suggesting PE particles may alter human microbiota leading to leaky gut condition.

Introduction

1. Microplastic PE

Fragmentation and weathering of landfill plastic waste, plastic manufacturing, food packaging, and cosmetics waste may produce unwanted MPs. Due to the migration of small sized MPs, they can be transferred to different environments. MPs have been found in various kind of foods and drinks including sugar, seafood and tap/bottled water, etc., and the top five most frequently found microplastic in drinking water are PE, polypropene (PP), polystyrene (PS), polyvinyl chloride (PVC) and polyethylene terephthalate (PET) [69-72]. Over 400 microplastic particles per liter drinking water can be detected in China, which includes mainly PE and PP fragments with size smaller than 50 μm [74]. Most studies have been reported on biodegradation, recycling and re-using plastics to minimize plastic waste production. In addition to the damages to aquatic organisms, bioaccumulation of these substances occurs in higher consumers of food chain including human, more researchers have started to investigate whether these waste particles would bring consumers any health hazards recently.

2. Effect of direct PE treatment on experiment animal and cultural cells

Most studies on potential harmful effects of PE were based on animal models and cancer cell lines through direct contact with PE particles. Powell et al. has suggested that MPs with size smaller than 150 μm could possibly pass through the epithelium by endocytosis, paracellular space, transcytosis and persorption in a review [73]. MP particles can be phagocytosed directly by cultural macrophages *in-vitro*. Such treatment also promoted significant increases of pro-inflammatory cytokines IL-1α, Il-1β, IL-6 and TNF-α production by the macrophages [77-79]. Furthermore, direct PE particles are able to induce TNF-α production in murine fibroblast L929 and canine kidney epithelial cell (MDCK).[80].

3. PE and the GI microbiota

There is limited study about the effects of PE consumption on microbial composition in GI tract. A PE intake experiment showed that *Firmicutes*/*Bacteroidetes* ratio was reduced in the gut microbiota of a murine model, and mucin-2 levels was decreased in the PE-treated mouse [84]. Consistent with a study on microbiome modification in a zebrafish model, phylum *Bacteroidetes* was enriched after the larval zebrafish was exposed to polyethylene MP of 20 mg/L [83]. A recent study has been demonstrated that a biofilm producing pathogen, namely *Pseudomonas aeruginosa* under *Gammaproteobacteria*, is able to degrade PE particles [212]. This implies that MPs may provide support on the growth of particular type(s) of bacteria affecting the homeostasis of gut microbiota.

In this study, batch culture and SHIME system utilizing health human origin microbiota were adopted. Different dosages of PE particles were incorporated into the one-day batch community and long-term continuous *in-vitro* GI tract system to assess if any modification of microbial compositions will be resulted. Final extracts from the culture supernatants were collected to investigate whether the shifted microbial community produced substances affecting gut permeability, TJ/AJ gene and protein expressions in cultural Caco-2 monolayer.

Objective

In this study, we aim to determine:

1. The effect of PE on alteration of human gut microbiota;
2. The potential influences of PE-treated gut microbiota derived metabolites on the TJ/AJ proteins of enterocytes and inflammation;
3. Whether luminal extracts of human microbiota retrieved from SHIME and exposed to PE pose detrimental effects on intestinal epithelial permeability.

Materials and methods

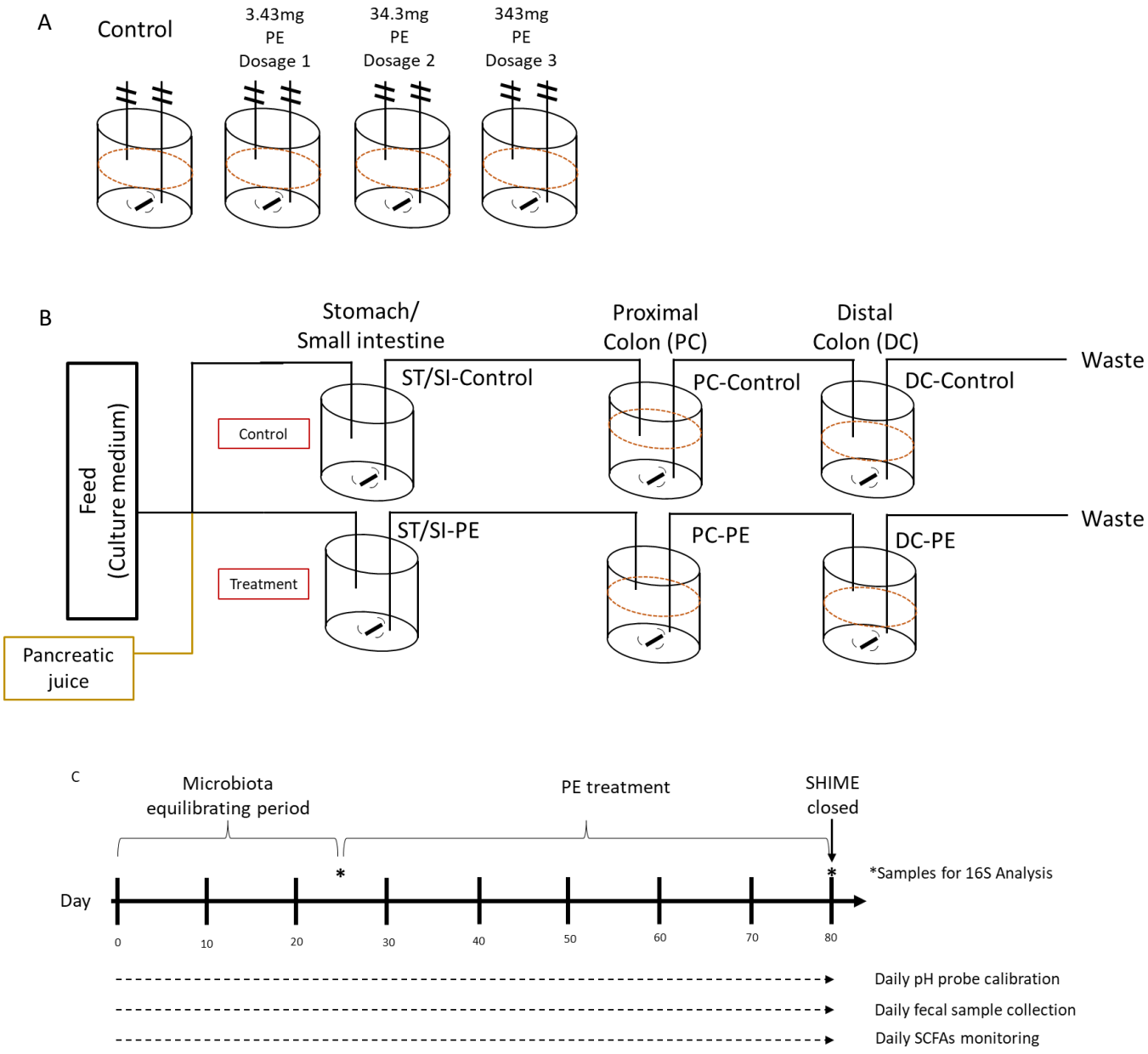

Figure 5.1. Experimental setups of batch culture (A) and SHIME (B). Timeframe of SHIME (C).

1. Batch Culture

Fecal samples were collected from healthy donor who had normal diet and did not intake any probiotics or antibiotics at least 2 weeks before sampling day. Fecal material was stored in gas-tight sample bucket with anaerobic sachet (Thermo Fisher Scientific, Waltham, USA) and inoculated within 4 hours after collection. Final concentration of 10% w/v of fecal material was homogenized with anaerobic buffer inside a stomacher bag with filter (Seward, Worthing, UK) for 5 minutes at 200 rpm. Sterilized Adult L-SHIME growth medium (without starch) (ProDigest, Gent, Belgium) was adjusted to pH 6.9 mimicking distal colon environment. Filtrate portion obtained after homogenization was inoculated in growth medium with volume ratio of 1:10. Starting cultural volume in each chamber was at 200 ml. One of the four inoculated chambers was used as no treatment control (D0). Three dosages of PE (Alfa Aesar, Haverhill, US) were introduced into each treatment cultural chamber. Middle dosage (D2) was calculated by using possible weekly microplastic intake (5 gram) and percentage of PE in total tap water microplastic contamination from published studies (47% PE in total microplastic) [74, 201]. Total 3 dosages, namely D1/D2/D3 at 3.43 mg, 34.3 mg, and 343 mg were added into the batch culture pre-inoculated with human fecal samples, respectively (Figure 5.1A). Culture chamber was purged by nitrogen for 10 minutes after inoculation and maintained at 37°C by water circulation. pH values and culture mixtures in different chambers were recorded and collected at 0, 4, 8 and 24 hours after inoculation, respectively.

2. SHIME setup

Program and tubing of Simulator of the Human Intestinal Microbial Ecosystem (SHIME) was setup as Twin SHIME according to the manufacturer's guideline (ProDigest, Gent, Belgium) with stomach and small intestine combined as ST/SI (Figure 5.1B). Fecal samples were collected from healthy donor who had normal diet and did not intake any probiotics or antibiotics at least 2 weeks before sampling day. Fecal material was stored in gas-tight sample bucket with anaerobic sachet (Thermo Fisher Scientific, Waltham, USA) and inoculated within 4 hours after collection. 10% w/v of fecal material was homogenized with anaerobic buffer inside a circulator strainer stomacher bag (Seward, Worthing, UK) for 5 minutes at 200 rpm. Sterilized Adult L-SHIME growth medium (ProDigest, Gent, Belgium) was pH adjusted to pH 5.6-5.9 for proximal colon (PC) and pH 6.6-6.9 for distal colon (DC) mimicking large intestinal environments. Filtrate portion obtained after homogenization was inoculated in growth media with volume ratio of 1:10. Starting cultural volumes in each PC and DC were 500ml and 800ml, respectively. All chambers were maintained at 37°C by warm water circulation. Ultra-high molecular weight polyethylene (UHMWPE) sized 40-48 μm (Sigma, St. Louis, USA) at dosage 0.714 g/day was introduced into ST/SI-PE mimicking ingestion of microplastic according to the estimated dosage (5 gram weekly) from published studies [74, 201]. After treatment period, luminal culture from all chambers were collected and stored at -20°C until further analysis.

3. Analysis of SCFA concentrations

Method for quantification of SCFA concentrations was adopted from Song, et al., 2018 and Zhao, et al., 2006 [134, 135]. Suspensions were centrifuged at 13,684g for 1 minutes at 4ºC. 270 µl of supernatants were transferred to a new tube and its pH was adjusted to pH 2-3 by 27 µl of 1M HCl (tested by pH paper). 3 µl of internal standard (100 mM 2-Ethyl-butyric acid) was added into each mixture. All mixtures were centrifuged at 2,376g for 20mins at 4ºC. Supernatant was filtered and transferred to a sample vial with insert for GC-FID analysis equipped with Agilent GC column DB-FFAP (123-3232). Oven temperature was set at: 80ºC for 2 minutes followed by ramping 6ºC per minute until 180ºC and then hold for 2 minutes. Concentration of different SCFAs were calculated from standard curves and respective dilution factor.

4. Preparation of luminal extracts

Resultant fermentation culture was defrosted from -20°C and centrifuged at 15,000g for 30 minutes at 4°C. Supernatant from centrifugation was filter-sterilized by 0.22 µm syringe filter. Filtrate was then aliquoted into 2 ml micro-centrifuge tubes and stored at -20°C as luminal extract.

5. 16S rDNA Sequencing and Analysis

Total genomic DNA from luminal fraction pellets after centrifugation were extracted by using TIANamp stool DNA kit (TIANGEN, Beijing, China) according to the manufacturer's protocol. The V4 region of 16S rDNA were sequenced by using 16S515F forward primer and 16S806R reverse (Supplementary Table 5.1). 16S rDNA sequencing was performed by BGI using Illumina HiSeq 2000 sequencer. For sequence analysis, primer sequences will be trimmed, and raw data was analyzed by using QIIME2 with HPC provided by Information Technology Services Office, The Hong Kong Polytechnic University. Paired-end sequences with quality data were denoised by DADA2 plugin, and taxonomy was assigned according to SILVA database. Alpha-diversity indices, beta-diversity weighted UniFrac PCoA plots were generated by using pipelines within QIIME2. Taxonomy heatmaps and barplots were generated by RStudio with gplots and ggplot2 packages.

6. Cell culture and viability assay

Human intestinal epithelial cell line Caco-2 was maintained in complete medium (Dulbecco′s Modified Eagle′s Medium (DMEM) with 10% fetal bovine serum (FBS)) in a 5% CO_2, 37°C humidified incubator. For Caco-2, cells were sub-cultured by tryptic digestion when they reached 80-90% confluence. Enterocyte monolayers were differentiated in 24-well flat bottom cell culture plate starting at $2x10^4$ cell/well for 12-14 days before treatment or viability assay.

Viabilities of cells after incubating with a range of luminal extracts were determined by 3-(4,5-dimethylthiazol-2-yl)-2,5-diphenyltetrazolium bromide (MTT, Sigma, St. Louis, USA) assay. Treatment media containing different concentrations of luminal extracts from no plasticizer control chambers of each experiment in complete medium were incubated with differentiated Caco-2 monolayer for 24 hours. Cells were washed by phosphate buffered saline pH 7.3 (PBS) and incubated with 0.5 mg/ml MTT solution for 1-1.5 hours in triplicate. Luminal extract concentrations (v/v%) were employed as treatment percentage for gene expression assay, which preserved >90% cell viability mimicking a sub-lethal chronic exposure of to each cell-line.

7. Measurement of trans-epithelial electrical resistance (TEER)

Epithelial tight junction integrity of Caco-2 monolayer was estimated by TEER assay. Resistances of transwell membrane and transwell with differentiated monolayer were measured by epithelial voltohmeter (EVOM2; WPI, Sarasota US). Caco-2 cells were seeded at $2x10^4$ cell/transwell and allowed to differentiate for 21-28 days until stable TEER was obtained (>600 Ωcm^2). 10% v/v of luminal extracts in DMEM were loaded on the apical chamber while complete medium was placed in the basolateral region. Initial TEER was recorded as $TEER_o$, and TEER values at time t = 24, 48, 72, 96, 120 and 144 hours were used for the calculation of percentage TEER change by $(TEER_t\text{-}TEER_o)/TEER_o$ x100%.

8. RNA extraction, reverse transcription, and real-time PCR gene expression analysis

Caco-2 cells were treated with 1 ml of 20% filter-sterilized extracts in DMEM for 48 hours inside a cell culture incubator, respectively. Total RNA was extracted using RNAiso PLUS (Takara, Kusatsu, Japan). RNA concentration was determined by NanoDrop spectrophotometer (Thermo Fisher Scientific, Waltham, USA). cDNA was reverse transcribed using PrimeScript reverse transcription kit (Takara, Kusatsu, Japan) according to the manufacturer's protocol. Real-time PCR was performed on Applied Biosystems QuantStudio 7 Flex Real-Time PCR System (Thermo Fisher Scientific, Waltham, USA) with TB Green Premix Ex Taq II (Takara, Kusatsu, Japan) reagent. Relative quantification of target gene expression was calculated by 2^(-ΔΔCt). Ribosomal protein lateral stalk subunit P0 (*RPLP0*) was used as housekeeping genes for Caco-2 gene expression calculation. Primers for specific mRNA amplification are listed in supplementary information (Supplementary Table 5.2).

9. Western blot

Western blot was employed for comparison of tight junction and adherens junction protein expressions after fermenter extract treatment. Caco-2 cells were seeded at $2x10^4$ cell/well in 24-well plate. Cells were cultured for 14 days before treatment. Cells was incubated with 20% extracts for 48 hours prior to protein quantification. After treatment, cells were washed with PBS and then incubated in 200 µl RIPA buffer (Merck Millipore, Burlington, US) with protease inhibitor cocktail (Sigma, St. Louis, USA) for 2 hours at 4°C. Total protein was obtained in supernatant after centrifugation at 20,000g for 10 minutes. Protein samples were stored at -80°C before protein concentration quantification by BCA assay (Thermo Fisher Scientific, Waltham, USA). For SDS-PAGE, 10 µg of total protein from each sample was mixed with sample buffer, heated at 95°C for 5 minutes before loading. SDS-PAGE with 4% stacking and 10% resolving gels was used for electrophoresis. Western blot transfer was done in wet condition with 100V for 120 minutes at 4°C. PVDF (GE Healthcare, Chicago, US) after transfer was blocked with blocking solution (5% skimmed milk in TBST) for 2 hours, and then incubated with primary antibody in blocking solution overnight at 4°C. Primary antibodies used for this study were: mouse monoclonal anti-β-actin (1:2000, Sigma, St. Louis, USA) and rabbit polyclonal anti-occludin (1:2000, ABclonal, Woburn, US). Horseradish peroxidase-conjugated goat anti-rabbit IgG (H+L) secondary antibody (1:2000, Novus Biologicals, Centennial, US) and goat anti-mouse IgG (H+L) secondary antibody (1:2000, Thermo Fisher Scientific, Waltham, USA) were used for chemiluminescent signal generation during image capture. Densitometry of chemiluminescent signal was analyzed using Image J. Relative expression of target protein was calculated by dividing its signal to β-actin signal. Normalized expression of target in each sample was generated by dividing relative expression to average relative expression in control fermenter extract group. Target protein expression in control fermenter treatment group was normalized as 1.

Results

1. Effect of PE on the composition and diversity of gut microbiota in batch culture and SHIME

Fermenter microbial genomic DNA was extracted and sequenced on Illumina platform. A total of 366,255 reads in 16 samples was qualified after DADA2 denoising pipeline withing QIIME2 and used for diversity and taxonomy analysis on Majorbio online analysis platform. In the batch culture experiment, community variation among starting microbiota was small as indicated in weighted UniFrac PCoA (Figure 5.2). After 24-hour incubation, the communities of microbiota in the presence of PE, regardless of the dosages, clustered together and away from the no treatment control microbiota. Moreover, their variations were not shifted according to the dosages of PE. There was less OTUs observed in the control resultant community than those treated with PE. Together with Shannon diversity, Faith's pd in the control community also had a lower value compared to PE batch communities.

As indicated in weighted UniFrac PCoA (Figure 5.3), overall resultant community phylogenetic diversities of DC-control and DC-PE clustered together before or after treatment. Unexpectedly, two original PCs phylogenetic diversities were deviated, however, community diversities clustered together at the end stage of experiment. For alpha diversity, although two PCs shared similar observed OTU count and Faith's pd, PC-PE chamber in the SHIME had a slightly higher Shannon diversity than PC-control. In the region of descending colon, PE-treated SHIME had more observed OTU and higher Shannon diversity (Table 5.1).

The overall abundances of *Actinobacteria* (24.5%) and *Firmicutes* (20%) in microbial community of control fermenter were increased to >30% in PE-treated microbiota. Meanwhile, *Bacteroidetes* was less abundant in PE-treated microbiota (<40%) than microbial community of control (54.6%) (Figure 5.4A). On family level, *Prevotellaceae* and *Erysipelatoclostridiaceae* were reduced in all PE-co-fermented

microbiota, while 5 families (*Bifidobacteriaceae*, *Coriobacteriaceae*, *Erysipelotrichaceae*, *Lachnospiraceae*, *Selenomonadaceae* and *Veillonellaceae*) were enriched (Figure 5.4B). Genus *Collinsella*, which contributed to all family *Coriobacteriaceae* abundance, was detected in all PE batch fermenters. *Alloprevotella*, *Prevotella* and *Catenibacterium*, were less abundant in PE-treated microbiota. Relative abundance of *Roseburia* was halved in PE-D1 and PE-D2 communities and nearly non-exist in PE-D3 fermenter. *Faecalibacterium* contributed to 2.84% of control community, however, it was less abundant in all PE-treated microbiota (at 1.64-1.80%). On the other hand, *Bifidobacterium*, *Blautia* and *Mitsuokella* were increased in PE batch microbiota. *Holdemanella* was detected in PE contaminated fermenters only. Its relative abundance was higher as PE dosage increased (1.38%, 1.74% and 3.17% in D1, D2 and D3 microbiota, respectively). In addition to *Holdemanella*, *Allisonella* was another genus detected in PE-contaminated communities but not in the control community. Its relative abundance also grew with PE dosage (0.73%, 0.90% and 1.51% in D1, D2 and D3 fermenters, respectively.) (Figure 5.4C).

Different from the batch culture, fecal microbiota underwent dynamic changes in the SHIME system and may reflect different influences of PE on the changes of gut microbiota. In the SHIME experiment, from 16S sequencing analysis, phylum *Firmicutes* was enriched while *Bacteroidetes* was reduced in both PE-treated PC and DC (Figure 5.5A). On family level, *Prevotellaceae* was reduced in PE-treated PC and DC. *Desulfovibrionaceae* and *Acidaminococcaceae* were enriched in PE-treated DC (Figure 5.5B). Genera *Bilophila* and *Acidaminococcus* were enriched in both PC and DC of SHIME in the presence of PE (Figure 5.5C). On the other hand, genera *Prevotella* and *Megasphaera* were reduced. Taxa *Alloprevotella* and *Megamonas* were reduced in PE-treated PC but increased in the subsequent DC. It was observed that genus *Prevotella* was dominant in proximal colons, while in distal colons, *Mitsuokella* was dominant genus. Comparing to PCs and DCs without treatment, relative abundances of *Prevotella* spp. were reduced in PE-treated microbiota. Such reduction of taxon *Prevotella* was also observed in PE batch

culture mentioned above. Overall microbiota modification did not alter SCFAs concentrations (Figure 5.6).

Figure 5.2. Weighted UniFrac PCoA of PE batch culture of starting and resultant microbiota (0-hour in blue and 24-hour in red; PE Control: ring; PE D1: square; PE D2: triangle; PE D3: sphere).

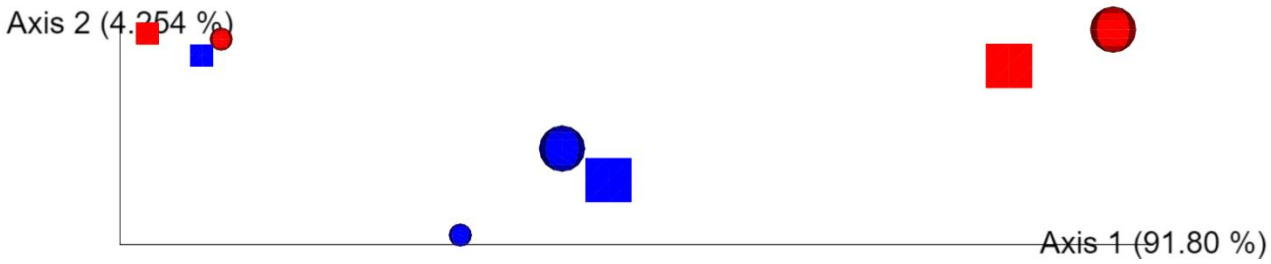

Figure 5.3. Weighted UniFrac PCoA of PE SHIME resultant microbiota. Day-0 in blue and Day-50 in red; Control: square; PE: sphere; PC and DC fermenters were labeled with small and large symbols, respectively.

Table 5.1 Alpha diversity indices of PE batch culture and SHIME microbiota.

		Indices		
Fermenters	Observed OTUs	Shannon	Simpson	Faith's pd
Batch culture				
PE-D0	28	4.26	0.93	4.20
PE-D1	122	6.10	0.98	7.13
PE-D2	119	6.14	0.98	6.77
PE-D3	99	5.92	0.98	6.43
SHIME				
PC-Control	62	4.57	0.94	3.37
PC-PE	60	4.80	0.95	3.30
DC-Control	96	5.66	0.97	5.95
DC-PE	108	5.87	0.97	5.95

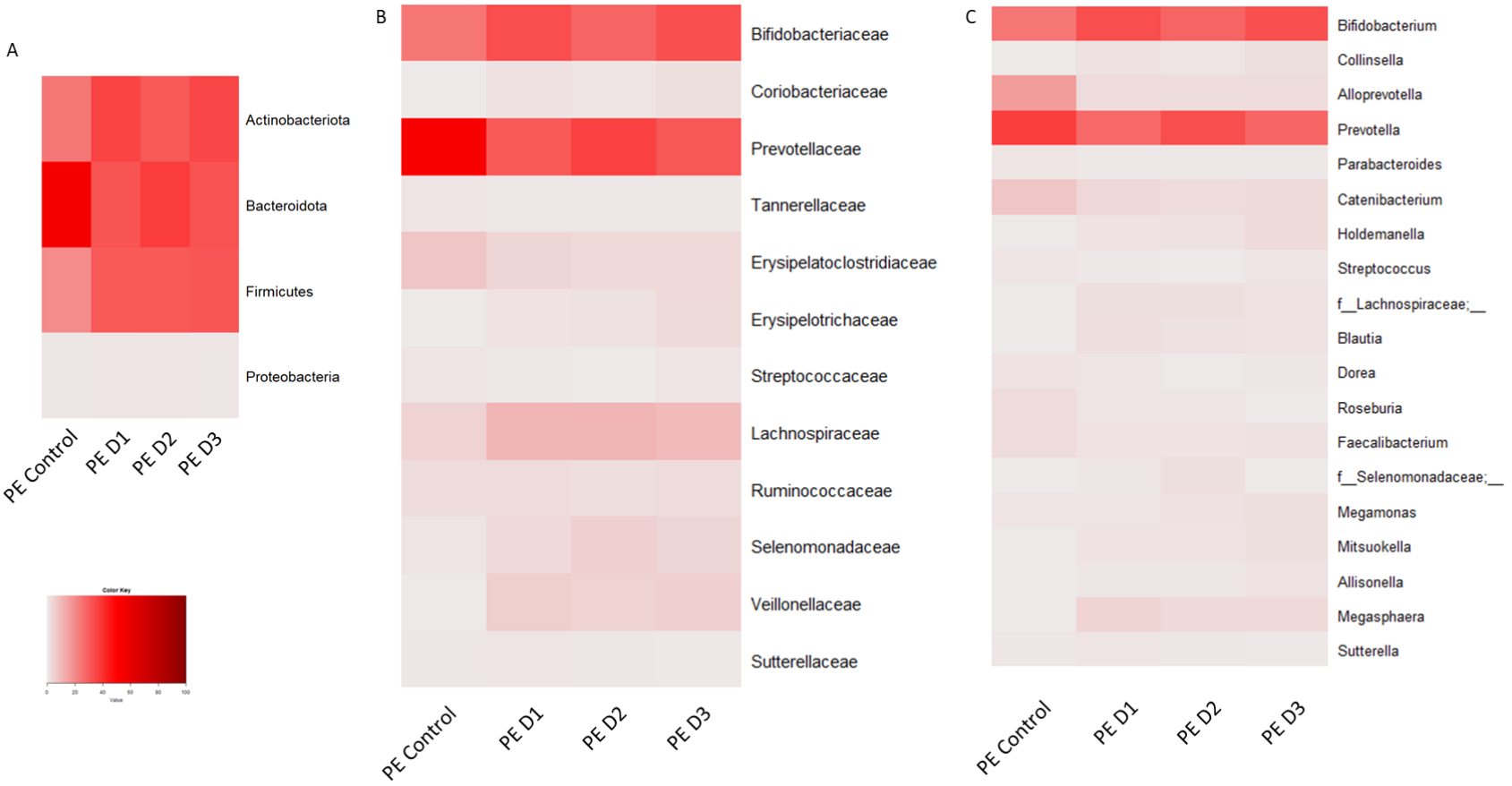

Figure 5.4. Taxonomy heatmaps showing taxa with relative abundance >1% on phylum (A), family (B) and genus (C) levels in batch culture in the presence of PE.

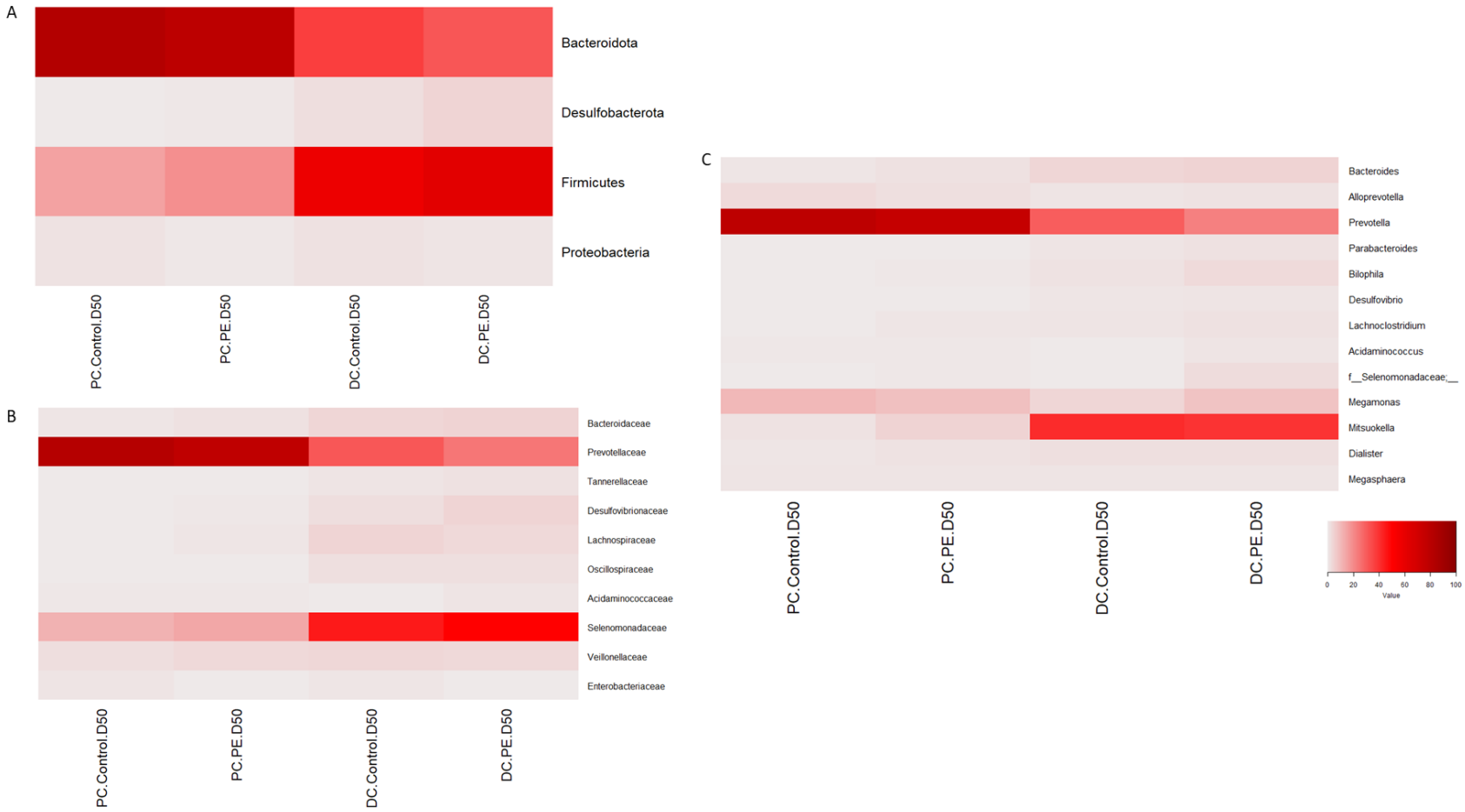

Figure 5.5. Taxonomy heatmaps showing taxa with relative abundance >1% on phylum (A), family (B) and genus (C) levels in the microbiota of control, PE-treated PC and PE-treated DC chambers in the SHIME.

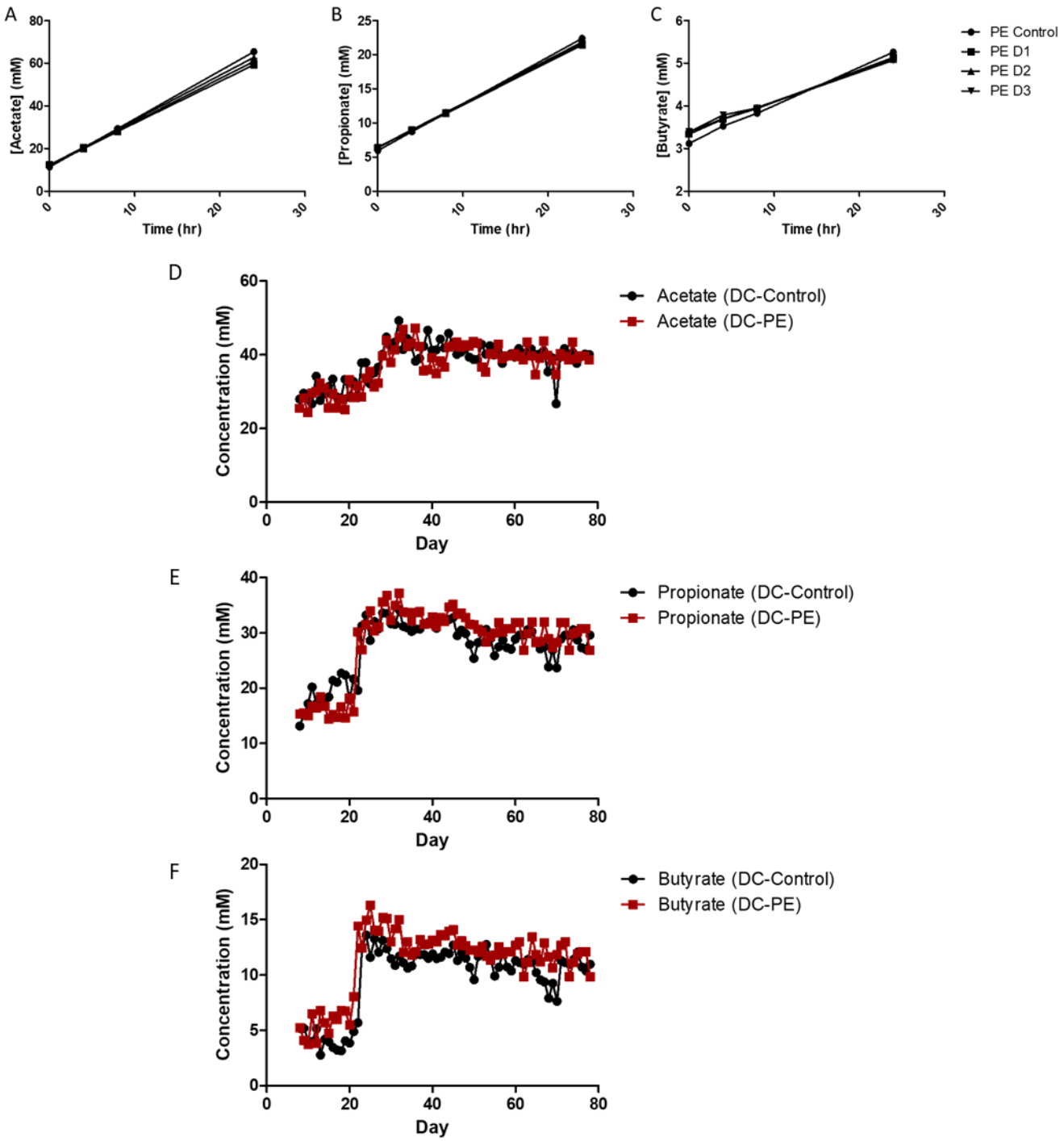

Figure 5.6. Concentrations of SCFAs in different fermenter extracts (A: acetate, B: propionate and C: butyrate in batch culture; D: acetate, E: propionate and F: butyrate in SHIME).

2. Effect of gut microbiota-derived metabolites on the TEER of enterocytes after PE exposure

20% v/v extracts in cultural medium was selected as the treatment media for Caco-2 as Caco-2 cells remained highly viable under this concentration (Figure 5.7). The TEER of Caco-2 allows determination of potential permeability of intestinal epithelial cells. Caco-2 epithelium TEER changes were similar when they were incubated with extracts from PE batch culture microbiota (Figure 5.8A).

TEER of Caco-2 monolayer varied with similar trend and no significant difference was observed between PC-Control and PC-PE treatments (Figure 5.8B). Percentage drops of TEER in DC-PE treatment group showed significant rapid decreases in several time points (Figure 5.8C). Difference of TEER changes diverged when Caco-2 cells were treated with DC extracts for 48 hours. Maximum difference (26%, $p<0.01$) between DC-Control and DC-PE treatments was observed after 96 hours (Figure 5.8D).

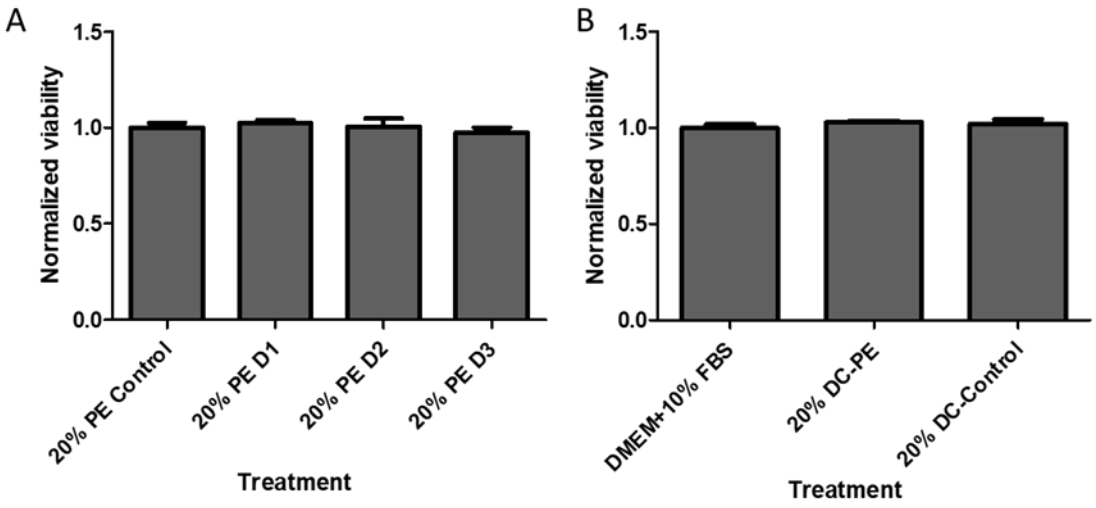

Figure 5.7. Viability of Caco-2 cells (A: batch culture; B: SHIME DC extracts) cells in PE batch culture or SHIME extracts.

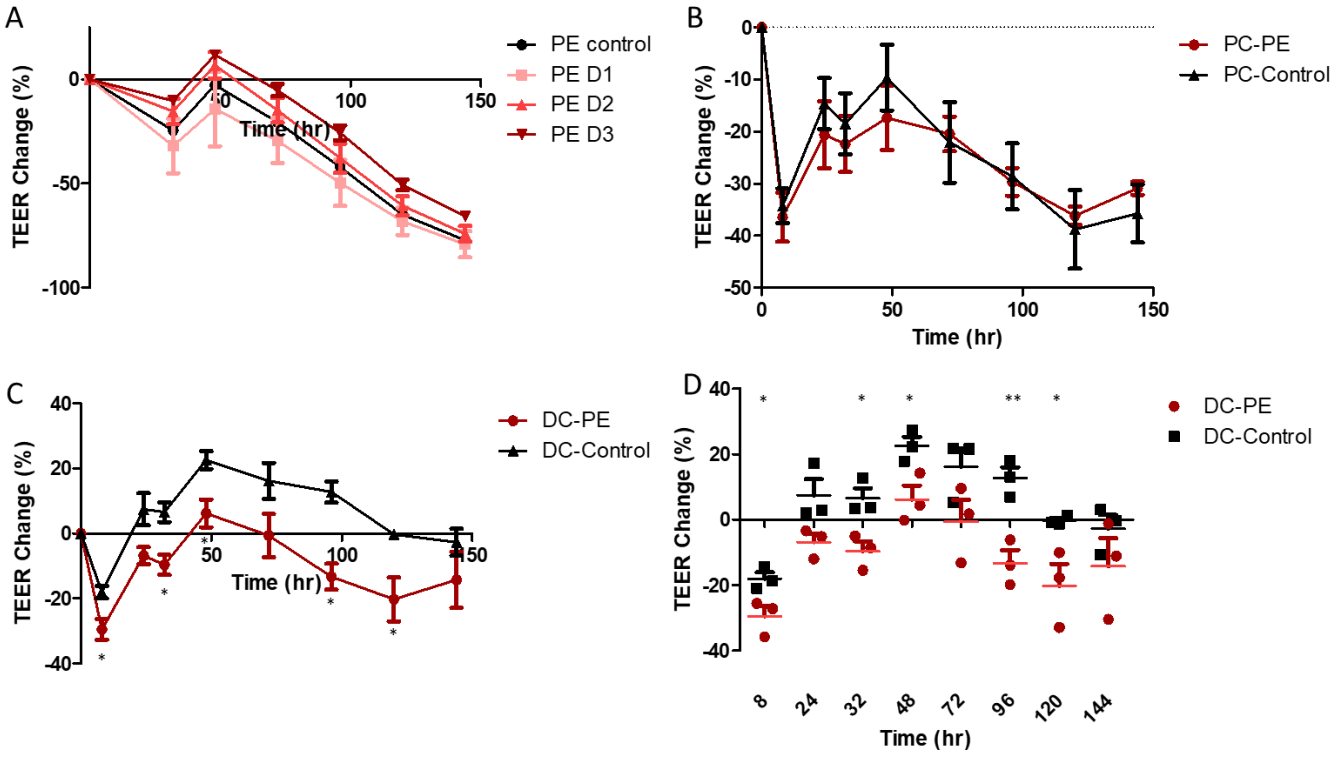

Figure 5.8. Changes of TEER in Caco-2 monolayers after treatment of batch culture extracts (A), SHIME PC extracts (B), SHIME DC extracts (C), and statistical analysis of mean TEER changes in DC TEERs (D). Data shown as mean +/- SEM with n=3. t-test, *p<0.05, **p<0.01 and ***p<0.005.

3. Effect of gut microbiota-derived metabolites on the TJ/AJ gene expressions after PE

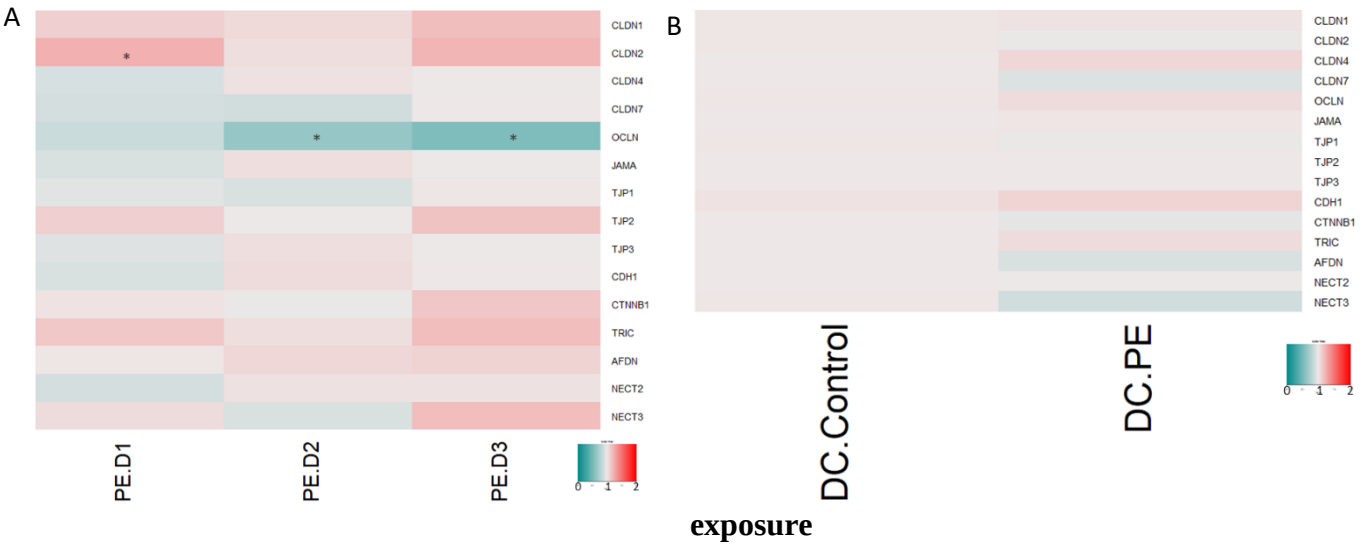

Figure 5.9. Normalized expressions of TJ/AJ genes in Caco-2 cells (A: batch culture and B: SHIME DC extracts). Gene expressions in Caco-2 treated with batch culture PE Control extract or DC-Control extract were normalized as 1 (A). t-test, n=3, *p<0.05, **p<0.01 and ***p<0.005.

After co-incubation of microbiota-derived extracts exposed to PE dosages 2 and 3, the mRNA levels of *OCLN* in the Caco-2 cell were decreased significantly by 36% and 46%, respectively (p<0.05) (Fig. 5.9A). Reduction of *OCLN* expression was PE-dose-dependent (Figure 5.9A) in the presence of PE in the batch culture setting.

By contrast, though the TEER was significantly reduced in cultural epithelium after DC-PE extract treatment, the mRNA levels of major TJ and AJ genes remained stable (Figure 5.8C-5.8D and 5.9B).

4. Effect of gut microbiota-derived metabolites on the occludin protein levels after PE exposure

Caco-2 occludin protein levels in different batch culture extract treatment groups were assessed by western blot. Consistent with the RT-qPCR results, 17%-23% occludin was lost in PE batch culture extract treatment groups (Figure 5.10).

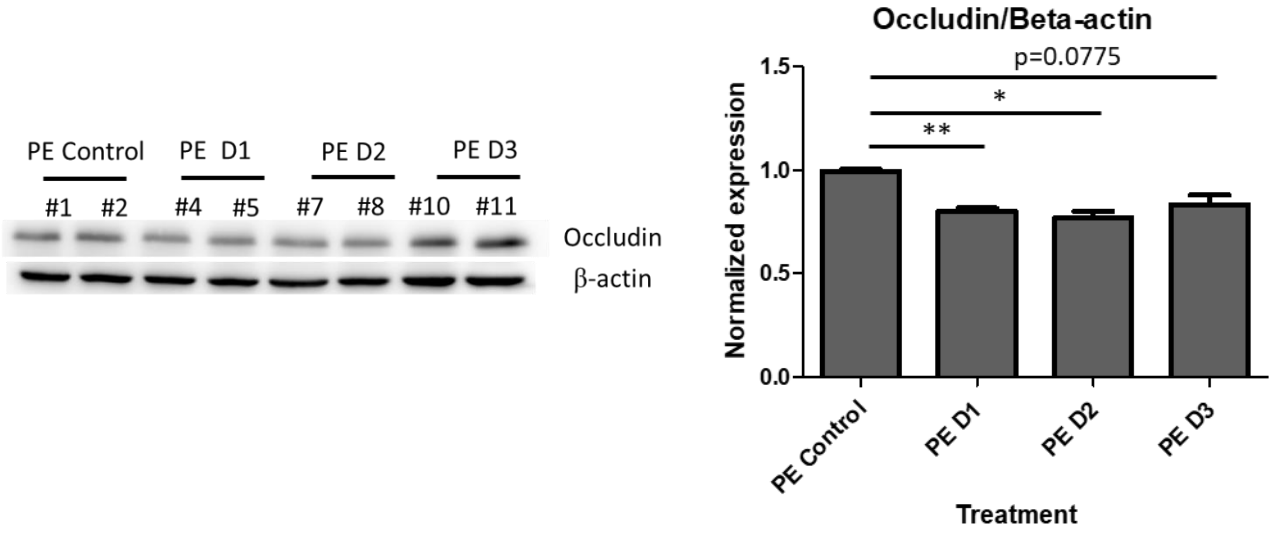

Figure 5.10. Protein expression of occludin in Caco-2 (t-test; data shown as mean +/- SEM; n=2; *p<0.05, **p<0.01 and ***p<0.005.)

Discussion

1. PE modified community composition of human gut microbiota

16S sequencing results showed that, in both batch culture and SHIME, addition of PE to microbiota fermentation promoted alpha diversities such as OTU counts and diversities. At the same time, community phylogenetic distances of PE-treated microbiota deviated from that of microbiota without PE treatment. Similar community diversity changes are consistent with a recent study about microbiota modification in murine model feeding with PE. Though higher diversity was observed in the gut microbiota exposed to PE, these PE-fed mice induced higher expressions of several pro-inflammatory receptor and transcription factors (TLR4, AP-1 and IRF5) in the duodenum and colon regions [213].

2. PE reduced epithelium-protecting taxa with small relative abundance

GI disorders such as IBD, IBS-D and CeD are commonly characterized by dysbiosis, leaky gut and local to systemic inflammations. Intestinal epithelial integrity is often found impaired in patients with these conditions. Modifications on relative abundance of different taxa by PE treatment were implicated in both beneficial and detrimental effects on health status reported in some microbiota studies. Enrichment of *Bifidobacterium* and *Blautia* was detected in PE batch fermenters. Numerous studies on *Bifidobacteria* have demonstrated beneficial effects to human health [214-217]. Genus *Blautia*, one of the SCFA producers in GI microbiota which shows anti-inflammatory ability on peripheral blood mononuclear cell cultures, was found negatively correlated with IBD and obesity [6, 218]. Meanwhile, reductions of pro-inflammatory species, *Alloprevotella* and *Prevotella*, were observed in all PE batch fermenters [29, 30, 154].

On the contrary, some other SCFA producers, *Roseburia* and *Faecalibacterium* were all reduced in PE batch fermenters. These taxa were reduced in inflamed GI microbiota [173, 203]. Some inflammation-

related taxa were also enriched. *Holdemanella*, genus correlated with upregulation of TNF-α, IL-1β and IL-6, and down-regulation of TJ adapter protein [219, 220]; and IBD/RA correlated genus, *Collinsella*, was found more abundant in PE batch fermenters [205, 207]. Limited research was performed on genus *Allisonella* about health and disease in human. However, *Allisonella* spp. utilizes histidine as energy source producing histamine as product. Enrichment of genus *Allisonella* could intensify the severity of local inflammation through histamine stimulation [16].

3. PE shifted distal colon microbiota composition

Batch culture provided a sketch and transient impact PE may have on the modification of gut microbiota, showing whether the presence of PE favors the growth of certain taxon of microbes. On the contrary, the setting of SHIME involved continuous culture flow, digestive enzymes, and real-time pH monitoring, all of which were controlled and monitored by the software of SHIME. The microbiota analysis in SHIME experiment allowed assessment of compositional change within a more realistic condition. Further tests were mainly focused on the DC chambers as DC contained the most abundant gut microbiota *in vivo* and there was significant TEER drop observed after treatment of DC-PE microbiota extract. More abundant *Megamonas, Bilophila, Acidaminococcus* were detected in DC-PE. In which genus *Megamonas* were described to harbor acetate- and propionate-producing abilities. Its low abundance was also correlated with Behcet's disease (multiple organ inflammation) implicating the relationship between this genus and immunoregulation [221, 222]. However, oral administration of *Bilophila wadsworthia* to mice stimulated serum amyloid A and IL-6 levels [223]. This bacterium was also found to be positively correlated with IBDs, and further promoted epithelium permeability, liver/ileum IFN-γ and TNF-α levels in high fat diet-fed mice [224, 225]. *Acidaminococcus* was significantly increased in IBD patient mucosal biopsy microbiota and positively correlated with pro-inflammatory diet [226, 227].

4. SHIME-DC-PE extract enhanced permeability and PE batch extracts reduced occludin in Caco-2

Occludin has long been studied due to its importance on epithelial integrities in various kind of organs such as vascular endothelium, kidney tubules and alveolar mucosa. Its upregulation promotes intestinal barrier function and prevent excessive antigens such as Gram-negative bacteria derived endotoxin LPS from crossing epithelium into circulatory system [34]. Microbiota derived extracts from PE batch culture did not alter Caco-2 electrochemical permeability as indicated in the TEER results but decreased the expression level of barrier-enforcing occludin. The inconsistent findings could possibly be due to slightly enrichment of several other TJ and AJ genes which compensated the loss of occludin. Interestingly, a more rapid drop of TEER in Caco-2 treated with SHIME-DC-PE extracts than control extract was detected, however, all selected major TJ/AJ genes remained stable or showed limited changes. The exact mediator(s) that affects the electrical resistance of Caco-2 monolayer remained unclear. TJ/AJ protein endocytosis and degradation pathways related genes or proteins may provide further evidence to elucidate this observation.

Summary

PE treatments in both batch culture and SHIME enhanced alpha and community phylogenetic diversities, enriched *Bifidobacterium* while slightly decreased *Prevotella*, however, some IBD-correlated taxa including *Holdemanella*, *Collinsella* and *Allisonella*, were enriched in the treatment groups. In addition to that, *Dorea*, *Roseburia* and *Faecalibacterium*, which are SCFA-producers and important for IBD remission, became less abundant in PE batch culture. The overall microbial extracts from all PE-fermenters reduced occludin expression. On the other hand, though mRNA levels of TJ/AJ proteins were stable, SHIME-DC-PE extract increased Caco-2 permeability as showed in TEER assay, showing the tendency towards leaky gut. Meanwhile, this extract was collected from the microbiota with more abundant *Bilophila* and *Acidaminococcus* that had been reported to involve in intestinal inflammation studies, implying PE may deteriorate the integrity of gut via alteration of gut microbiota. Our results showed that microbiota compositional changes in batch culture may induce down-regulation of *OCLN* and its protein level in epithelial cells. Consistently, alteration of microbiota of SHIME distal colon due to PE exposure promoted barrier permeability of enterocytes.

On top of being environmentally friendly, we should be aware of any detrimental effects on health brought by the long-term intake of MP. Oral intake is the most possible pathway for solid MPs. It is possible that ingested PE may accumulate and alter our GI microbiota, leading to dysbiosis and eventually leaky gut We should use less plastics, recycle and dispose properly, to minimize production and exposure of MP.

Supplementary information

Supplementary Table 5.1. Primers used for 16S sequence amplification and 16S rDNA sequencing

Primers names	Sequences (5'-3')
16S515F	GTGCCAGCMGCCGCGGTAA
16S806R	ATTAGATACCCSBGTAGTCC

Supplementary Table 5.2. Primers for RT-qPCR on gene expressions in Caco-2 (Adopted from [1]Putt, 2017 and [2]Suzuki, 2011 [33, 124])

Gene	Protein	Forward sequence (5'-3')	Reverse sequence (5'-3')
RPLP0	Ribosomal protein P0	ACTTCCTTAAGATCATCCAACT	TATGAGGCAGCAGTTTCTCCA
OCLN[1]	Occludin	CCAATGTCGAGGAGTGGG	CGCTGCTGTAACGAGGCT
CLDN1	Claudin-1	TGGTGGTTGGCATCCTCCTG	AATTCGTACCTGGCATTGACTGG
CLDN2[2]	Claudin-2	CTCCCTGGCCTGCATTATCTC	ACCTGCTACCGCCACTCTGT
CLDN4	Claudin-4	ATCATCGTGGCTGCTCTGG	ACACCGGCACTATCACCATAA
CLDN7	Claudin-7	TTTCATCGTGGCAGGTCTTG	CTCATACTTAATGTTGGTAGGG
JAMA	JAM-A	GATCACAGCTTCCTATGAGGA	ATGGAGGCACAAGCACGAT
CDH1	E-cadherin	AAGAGGACCAGGACTTTGACTT	CAGCCGCTTTCAGATTTTCATC
CTNNB1	Beta-catenin	GGAATGAGACTGCTGATCTTGG	ATCATCCTGGCGATATCCAAGG
TJP1[1]	ZO-1	CAAGATAGTTTGGCAGCAAGAGATG	ATCAGGGACATTCAATAGCGTAGC
TJP2	ZO-2	GCACAGAATGCAAGGATCGA	GTCTGGAACTCGTGTGCTGG
TJP3	ZO-3	GCGAGAAGCCAGTTTCAAGC	GTCCTGGACACAGTCTCTGCGA
TRIC	Tricellulin	GGCAAAATACCCTGTGATTCAGACAG	CATGGATTCTTGAAATTCTCTCATG
AFDN	Afadin	ACCGACAAGCAAGAGCACCACTAG	TGCCTGCGATAATCTGGCTGCTG
NECT2	Nectin-2	CAGAGTCATAGCCAAGCCCAAGAAC	GTCCAGGGATGAGAGCCAGGAG
NECT3	Nectin-3	TCTCCAGGCTCTGTGGTGCC	ATGGTGAACTGCAACAGTCTGTGAA

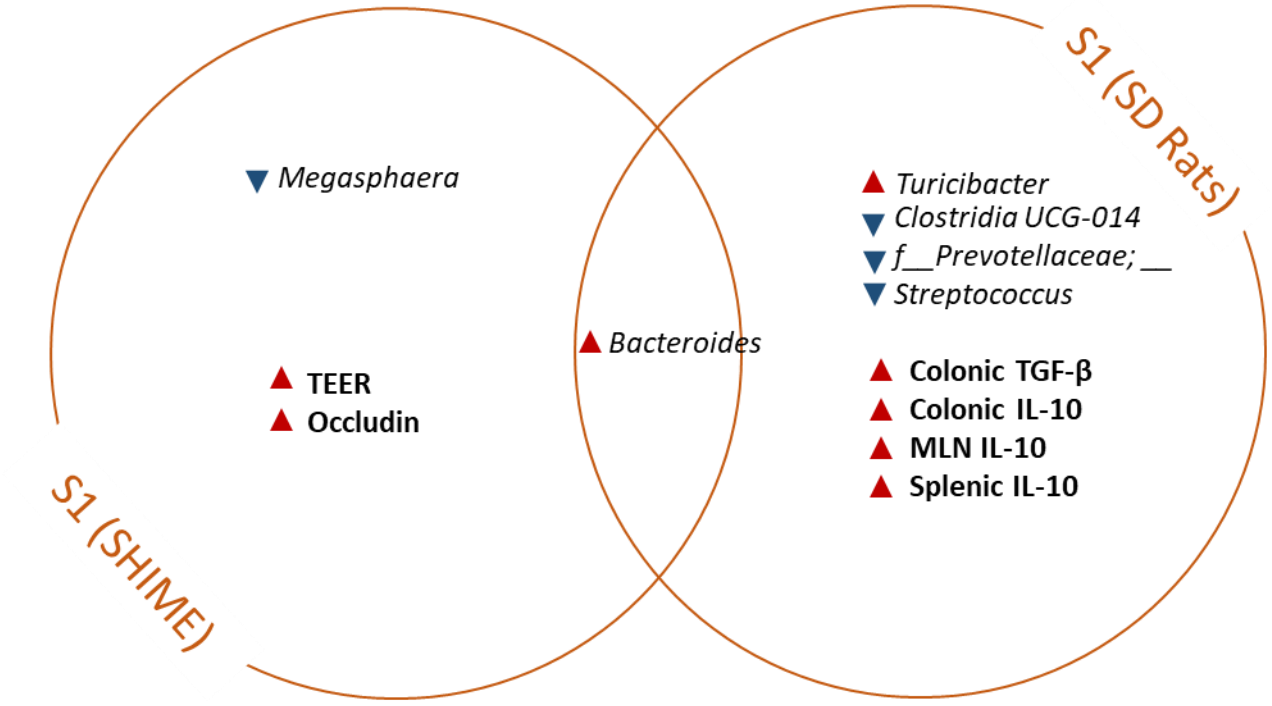

Figure 6.1 Major observation in experiments related to S1 treatment in SHIME and SD rats

Probiotics have been demonstrated to provide beneficial effects on host for long time. *Lactobacilli* are well-studied genera of probiotics and have been used in various kinds of natural and fermented food products. The local-isolated *L. rhamnosus* strain S1 reduced *Megasphaera* spp. while increased *Bacteroides* spp. especially in the distal colon region of SHIME. Resultant luminal extracts from S1-treated SHIME distal colon upregulated TJ sealing occludin expression in cultural intestinal epithelial cells and promoted epithelial integrity, which are possibly enhanced by up-regulation of occludin.

In-vivo reduction of *Bacteroides* spp. was consistent in both SHIME and animal experiment after treatment of S1. On top of that, an unclassified genus from family *Prevotellaceae, Clostridia* UCG-014 and *Streptococcus* spp. were decreased which have been shown to be positively associated with inflammations, productions of anti-inflammatory cytokine IL-10 by local colon tissue, mesenteric lymph node cells and splenic mononuclear cells were promoted in rats.

S1 reduced *Megasphaera* spp. in the SHIME microbiota, and pro-inflammatory taxa such as *Prevotellaceae* and *Streptococcus* spp. in SD rats. Meanwhile, extract from SHIME promoted cultural epithelial integrity, whereas anti-inflammatory cytokines in SD rats were increased. To sum up, *L. rhamnosus* S1 has potential in maintaining epithelial barrier function and ameliorating inflammatory diseases such as endotoxemia, IBDs and arthritis. Further study on usage of this novel strain in inflammation can be performed in the future.

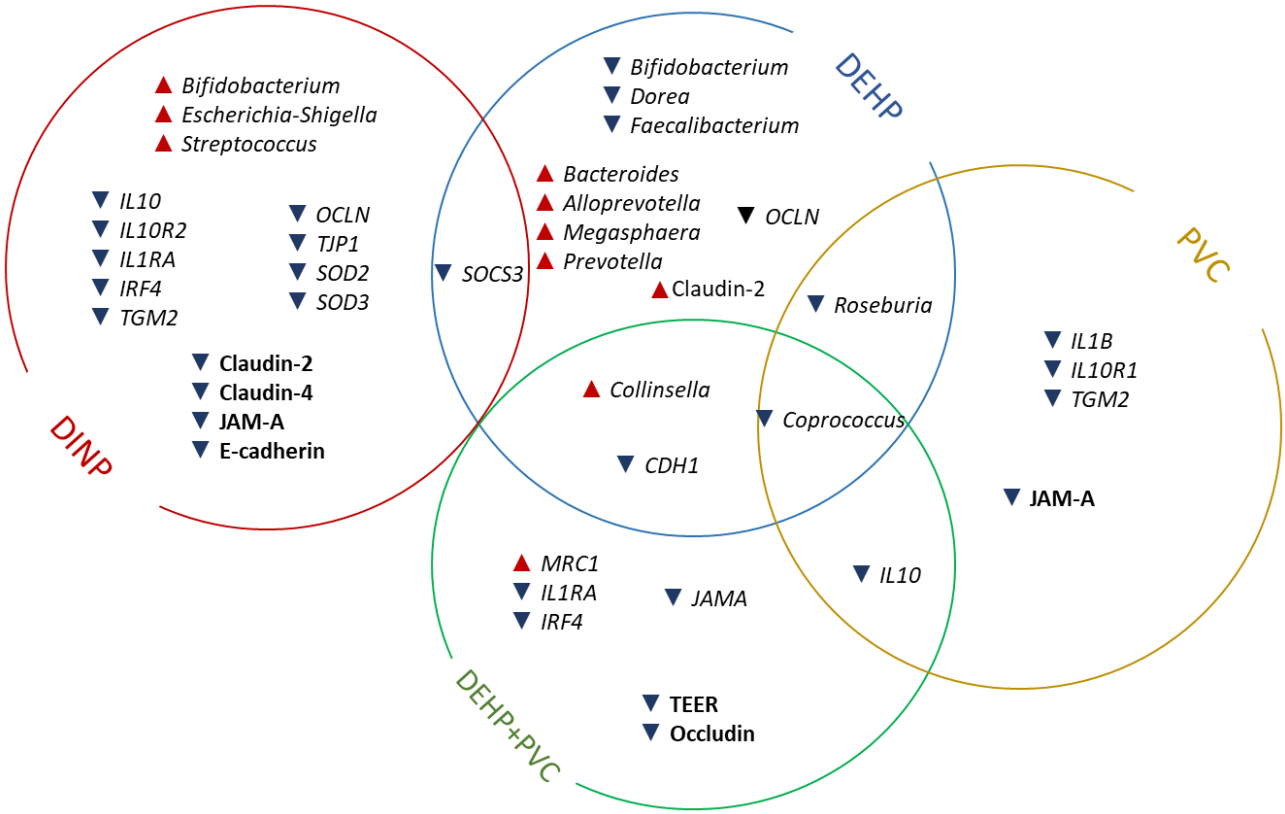

Figure 6.2 Major observation in experiments related to plasticizer (DEHP and DINP) and microplastic PVC which are often used together in food packing.

Microbial communities of microbiota treated with DINP had enriched *Escherichia-Shigella* and *Streptococcus*, and reduced *Megasphaera*. Extracts derived from these communities reduced the mRNA levels of several anti-inflammatory cytokines and TJ/AJ proteins in RAW264.7 and HT-29 cells, respectively. Interestingly, these extracts reduced pore-forming claudin-2 in HT-29. On the contrary, bearing more abundant taxa associated with intestinal disorders, DEHP treated microbiota produced mediators in extracts upregulated claudin-2 in HT-29.

Microbiota exposed to sole DEHP or PVC had less *Roseburia*, whereas all DEHP treated microbiota possessed more *Collinsella*. In addition to that, the relative abundance of *Coprococcus* was reduced in all fermenters treated to PVC or DEHP. These taxa changes are also observed in correlation studies on dysbiosis and inflammatory diseases. Consistently, downregulation of anti-inflammatory gene, *IL10*, in cultural macrophage were also observed in PVC and DEHP+PVC experiments. In conclusion, DEHP has a more significant adverse impact on the homeostasis of gut microbiota than DINP, in turn leading to more severe degree of compromised gut permeability and intestinal inflammation. Common changes were observed in DEHP and DEHP+PVC experiments. This suggests that DEHP is the major effector on community modification. The combinational use of both DEHP and PVC also shows negative influence on the intestinal permeability and reduced anti-inflammatory effects.

PVC and plasticizers (DINP and DEHP) modified microbiota compositions. DINP-modified microbial extracts reduced tissue-repairing M2 gene expressions, whereas DEHP- or PVC-modified microbiota decreased junction-sealing gene expressions. Among these batch cultures, inflammation-correlated *Collinsella* was enriched in those DEHP containing fermenters, while health-associated *Coprococcus* was reduced in all contaminated fermenters. Relationship between epithelial integrity / immunomodulation, and these two genera of bacteria can be further investigated in in-vivo model for verification. Moreover, *L. rhamnosus* S1 possesses anti-inflammatory ability as demonstrated in murine model. Bacteria under genus Lactobacillus have been found able to retain DEHP in feces instead of being absorbed. It is also possible that S1 could reduce plasticizer absorption from food and reduce oxidative and inflammatory stimulations of plasticizers.

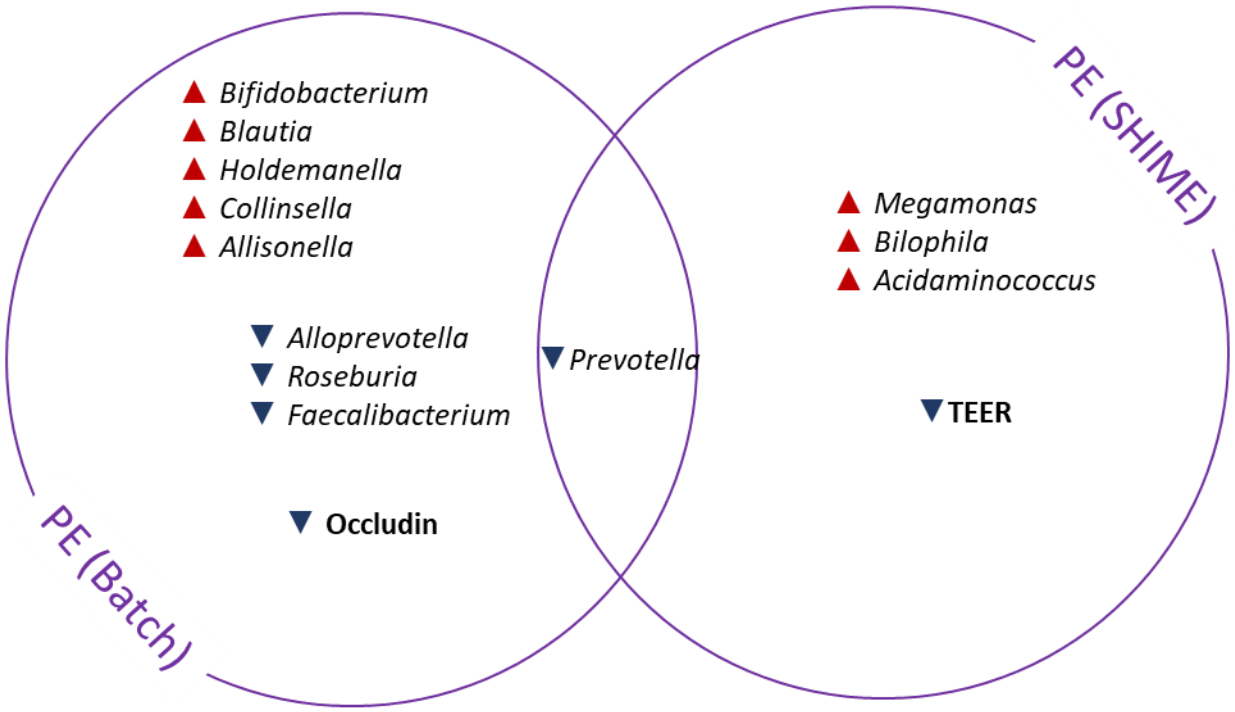

Figure 6.3 Major observation in experiments related to PE

Studies of gut microbiota research are commonly conducted in a batch culture setting, in which a bacterial consortium is introduced in a batch mode and allows for fermentation for a period of time, which ranges from 24 hours to couple days. The Simulator of Human Intestinal Microbial Ecosystem (SHIME) mimics the continuous fermentation of food components, contaminants, or other compounds of interests as they are in the human digestive system. In this study, we adopted both batch and SHIME settings to compare the similarity and difference of gut microbiota exposed to PE. Microbiota of batch and SHIME cultures differed from each other.

In the batch culture, microbiota exposed to PE have less abundant health associated *Roseburia* and *Faecalibacterium* regardless of dosages PE exposure. Meanwhile, enriched GI inflammation-related taxa *Holdemanella*, *Collinsella* and *Allisonella* was observed in PE treated fermenters. Though *Bifidobacteria*

and *Blautia* were enriched; and *Alloprevotella* and *Prevotella* were reduced, overall microbial extracts reduced occludin expression in cultural enterocyte. In SHIME, only distal colon region showed alteration after PE treatment. Among the three enriched taxa, namely *Megamonas*, *Bilophila* and *Acidaminococcus*, the latter 2 taxa were associated with GI permeability and inflammatory cytokine levels. Consistently, cultural enterocytes stimulated by extracts from PE contaminated microbiota has a higher transepithelial permeability compared with those treated with control extract.

Extracts from PE treatment groups in both batch culture and SHIME settings affected occludin expression and epithelium permeability in Caco-2, respectively. Though exact target(s) responsible for higher permeability in the treatment groups were not the same, these results still implied that both short-term and chronic exposure to PE induced compositional changes in human origin microbiota, which may impair GI barrier function.

In PE experiments, there were drops of occludin and TEER in PE batch culture extracts and SHIME distal colon extract treatment groups, respectively. Yet the exact mediator(s) causing TEER drop in Caco-2 after PE SHIME DC extract treatment cannot be explained by the expression levels of selected TJ or AJ genes from RT-qPCR. In this study, we did not include assays in testing internalization and location of junction proteins. Some studies have indicated that endocytosis with/without caveolin and clathrin transfers membrane-integrated occludin or claudin into the cytoskeleton impairing paracellular sealing function of barrier, which could be the candidates for testing in the future [228-231].

References

1. Morowitz, M.J., E.M. Carlisle, and J.C. Alverdy, *Contributions of intestinal bacteria to nutrition and metabolism in the critically ill.* Surg Clin North Am, 2011. **91**(4): p. 771-85, viii.
2. Pinu, F.R., et al., *Metabolite secretion in microorganisms: the theory of metabolic overflow put to the test.* Metabolomics, 2018. **14**(4): p. 43.
3. LeBlanc, J.G., et al., *Bacteria as vitamin suppliers to their host: a gut microbiota perspective.* Curr Opin Biotechnol, 2013. **24**(2): p. 160-8.
4. Youssef, O., et al., *Stool Microbiota Composition Differs in Patients with Stomach, Colon, and Rectal Neoplasms.* Dig Dis Sci, 2018. **63**(11): p. 2950-2958.
5. Li, J., et al., *Akkermansia Muciniphila Protects Against Atherosclerosis by Preventing Metabolic Endotoxemia-Induced Inflammation in Apoe-/- Mice.* Circulation, 2016. **133**(24): p. 2434-46.
6. Benitez-Paez, A., et al., *Depletion of Blautia Species in the Microbiota of Obese Children Relates to Intestinal Inflammation and Metabolic Phenotype Worsening.* mSystems, 2020. **5**(2).
7. Koliada, A., et al., *Association between body mass index and Firmicutes/Bacteroidetes ratio in an adult Ukrainian population.* BMC Microbiol, 2017. **17**(1): p. 120.
8. Stojanov, S., A. Berlec, and B. Strukelj, *The Influence of Probiotics on the Firmicutes/Bacteroidetes Ratio in the Treatment of Obesity and Inflammatory Bowel disease.* Microorganisms, 2020. **8**(11).
9. Rohlke, F. and N. Stollman, *Fecal microbiota transplantation in relapsing Clostridium difficile infection.* Therap Adv Gastroenterol, 2012. **5**(6): p. 403-20.
10. Levy, A.N. and J.R. Allegretti, *Insights into the role of fecal microbiota transplantation for the treatment of inflammatory bowel disease.* Therap Adv Gastroenterol, 2019. **12**: p. 1756284819836893.
11. Livanos, A.E., et al., *Intestinal Host Response to SARS-CoV-2 Infection and COVID-19 Outcomes in Patients With Gastrointestinal Symptoms.* Gastroenterology, 2021. **160**(7): p. 2435-2450 e34.
12. Hill, C., et al., *Expert consensus document. The International Scientific Association for Probiotics and Prebiotics consensus statement on the scope and appropriate use of the term probiotic.* Nat Rev Gastroenterol Hepatol, 2014. **11**(8): p. 506-14.
13. Todorov, S.D., et al., *Safety of Lactobacillus plantarum ST8Sh and Its Bacteriocin.* Probiotics Antimicrob Proteins, 2017. **9**(3): p. 334-344.
14. Huang, S.C., et al., *Metabolic Reprogramming Mediated by the mTORC2-IRF4 Signaling Axis Is Essential for Macrophage Alternative Activation.* Immunity, 2016. **45**(4): p. 817-830.
15. Ren, D.Y., et al., *Lactobacilli reduce chemokine IL-8 production in response to TNF-alpha and Salmonella challenge of Caco-2 cells.* Biomed Res Int, 2013. **2013**: p. 925219.
16. Kim, C.S., et al., *Probiotic Supplementation Improves Cognitive Function and Mood with Changes in Gut Microbiota in Community-Dwelling Older Adults: A Randomized, Double-Blind, Placebo-Controlled, Multicenter Trial.* J Gerontol A Biol Sci Med Sci, 2021. **76**(1): p. 32-40.
17. Pascal, V., et al., *A microbial signature for Crohn's disease.* Gut, 2017. **66**(5): p. 813-822.
18. Wilck, N., et al., *Salt-responsive gut commensal modulates TH17 axis and disease.* Nature, 2017. **551**(7682): p. 585-589.
19. Earley, H., et al., *The abundance of Akkermansia muciniphila and its relationship with sulphated colonic mucins in health and ulcerative colitis.* Sci Rep, 2019. **9**(1): p. 15683.
20. Ottman, N., et al., *Pili-like proteins of Akkermansia muciniphila modulate host immune responses and gut barrier function.* PLoS One, 2017. **12**(3): p. e0173004.

21. Plovier, H., et al., *A purified membrane protein from Akkermansia muciniphila or the pasteurized bacterium improves metabolism in obese and diabetic mice.* Nat Med, 2017. **23**(1): p. 107-113.
22. Hiippala, K., et al., *Isolation of Anti-Inflammatory and Epithelium Reinforcing Bacteroides and Parabacteroides Spp. from A Healthy Fecal Donor.* Nutrients, 2020. **12**(4).
23. Thorkildsen, L.T., et al., *Dominant fecal microbiota in newly diagnosed untreated inflammatory bowel disease patients.* Gastroenterol Res Pract, 2013. **2013**: p. 636785.
24. Shaw, K.A., et al., *Dysbiosis, inflammation, and response to treatment: a longitudinal study of pediatric subjects with newly diagnosed inflammatory bowel disease.* Genome Med, 2016. **8**(1): p. 75.
25. Hamer, H.M., et al., *Effect of butyrate enemas on inflammation and antioxidant status in the colonic mucosa of patients with ulcerative colitis in remission.* Clin Nutr, 2010. **29**(6): p. 738-44.
26. Soong, G., et al., *Staphylococcus aureus protein A mediates invasion across airway epithelial cells through activation of RhoA GTPase signaling and proteolytic activity.* J Biol Chem, 2011. **286**(41): p. 35891-8.
27. Sartingen, S., et al., *Aggregation Substance Increases Adherence and Internalization, but Not Translocation, of Enterococcus faecalis through Different Intestinal Epithelial Cells In Vitro.* Infection and Immunity, 2000. **68**(10): p. 6044.
28. Hooi, J.K.Y., et al., *Global Prevalence of Helicobacter pylori Infection: Systematic Review and Meta-Analysis.* Gastroenterology, 2017. **153**(2): p. 420-429.
29. Su, T., et al., *Altered Intestinal Microbiota with Increased Abundance of Prevotella Is Associated with High Risk of Diarrhea-Predominant Irritable Bowel Syndrome.* Gastroenterol Res Pract, 2018. **2018**: p. 6961783.
30. Iljazovic, A., et al., *Perturbation of the gut microbiome by Prevotella spp. enhances host susceptibility to mucosal inflammation.* Mucosal Immunol, 2020.
31. Chhibber-Goel, J., et al., *Linkages between oral commensal bacteria and atherosclerotic plaques in coronary artery disease patients.* NPJ Biofilms Microbiomes, 2016. **2**: p. 7.
32. Lu, P., et al., *Colonic gene expression patterns of mucin Muc2 knockout mice reveal various phases in colitis development.* Inflamm Bowel Dis, 2011. **17**(10): p. 2047-57.
33. Putt, K.K., et al., *Yogurt inhibits intestinal barrier dysfunction in Caco-2 cells by increasing tight junctions.* Food Funct, 2017. **8**(1): p. 406-414.
34. Zhou, Z., et al., *Progesterone decreases gut permeability through upregulating occludin expression in primary human gut tissues and Caco-2 cells.* Sci Rep, 2019. **9**(1): p. 8367.
35. Oshima, T., H. Miwa, and T. Joh, *Changes in the expression of claudins in active ulcerative colitis.* J Gastroenterol Hepatol, 2008. **23 Suppl 2**: p. S146-50.
36. Tsai, P.Y., et al., *IL-22 Upregulates Epithelial Claudin-2 to Drive Diarrhea and Enteric Pathogen Clearance.* Cell Host Microbe, 2017. **21**(6): p. 671-681 e4.
37. Hering, N.A., et al., *Transforming growth factor-beta, a whey protein component, strengthens the intestinal barrier by upregulating claudin-4 in HT-29/B6 cells.* J Nutr, 2011. **141**(5): p. 783-9.
38. Li, W., et al., *Glycine Regulates Expression and Distribution of Claudin-7 and ZO-3 Proteins in Intestinal Porcine Epithelial Cells.* J Nutr, 2016. **146**(5): p. 964-9.
39. Tanaka-Okamoto, M., et al., *Involvement of afadin in barrier function and homeostasis of mouse intestinal epithelia.* J Cell Sci, 2011. **124**(Pt 13): p. 2231-40.
40. Ebnet, K., et al., *Junctional adhesion molecules (JAMs): more molecules with dual functions?* J Cell Sci, 2004. **117**(Pt 1): p. 19-29.
41. Garrido-Urbani, S., P.F. Bradfield, and B.A. Imhof, *Tight junction dynamics: the role of junctional adhesion molecules (JAMs).* Cell Tissue Res, 2014. **355**(3): p. 701-15.

42. Mailer, R.K., et al., *IL-1beta promotes Th17 differentiation by inducing alternative splicing of FOXP3.* Sci Rep, 2015. **5**: p. 14674.
43. Wang, L., et al., *IL-6 induces NF-kappa B activation in the intestinal epithelia.* J Immunol, 2003. **171**(6): p. 3194-201.
44. Greving, C.N.A. and J.E. Towne, *A Role for IL-12 in IBD after All?* Immunity, 2019. **51**(2): p. 209-211.
45. Patrizia Puddu, L.F., Paola Borghi, Barbara Varano, Gabriella Rainaldi,, W.M. Eric Guillemard, Pascale Nicaise,Stanley F. Wolf, Filippo Belardelli,, and a.S. Cessani, *IL-12 Induces IFN-y Expression and Secretion in Mouse Peritoneal Macrophages.* The Journal of Immunology, 1997: p. 3490-3497.
46. Li, Y., et al., *Interleukin-12p35 deletion promotes CD4 T-cell-dependent macrophage differentiation and enhances angiotensin II-Induced cardiac fibrosis.* Arterioscler Thromb Vasc Biol, 2012. **32**(7): p. 1662-74.
47. Zhou, X., et al., *YAP Aggravates Inflammatory Bowel Disease by Regulating M1/M2 Macrophage Polarization and Gut Microbial Homeostasis.* Cell Rep, 2019. **27**(4): p. 1176-1189 e5.
48. Steinbach, E.C. and S.E. Plevy, *The role of macrophages and dendritic cells in the initiation of inflammation in IBD.* Inflamm Bowel Dis, 2014. **20**(1): p. 166-75.
49. J H Kwon, S.K., L Bassani, L F Mayer, A C Keates, *Colonic epithelial cells are a major site of macrophage inflammatory protein 3α (MIP-3α) production in normal colon and inflammatory bowel disease.* Gut, 2002. **51**: p. 818-826.
50. Wang, Z., et al., *Inulin alleviates inflammation of alcoholic liver disease via SCFAs-inducing suppression of M1 and facilitation of M2 macrophages in mice.* Int Immunopharmacol, 2020. **78**: p. 106062.
51. Kiri Honma, H.U., Tomoko Kohno, Kazuo Yamamoto, Asako Ogawa, Toshitada Takemori, Atsushi Kumatori, Shoichi Suzuki, Toshifumi Matsuyama, and Katsuyuki Yui, *Interferon regulatory factor 4 negatively regulates the production of proinflammatory cytokines by macrophages in response to LPS.* PNAS, 2005. **102**(44): p. 16001–16006.
52. Jun Eguchi, X.K., Masafumi Tenta, Xun Wang, Sona Kang, and Evan D. Rosen, *Interferon Regulatory Factor 4 Regulates Obesity-Induced Inflammation Through Regulation of Adipose Tissue Macrophage Polarization.* DIABETES, 213: p. 3394-3403.
53. El Chartouni, C., L. Schwarzfischer, and M. Rehli, *Interleukin-4 induced interferon regulatory factor (Irf) 4 participates in the regulation of alternative macrophage priming.* Immunobiology, 2010. **215**(9-10): p. 821-5.
54. Zhou, L., et al., *TGF-beta-induced Foxp3 inhibits T(H)17 cell differentiation by antagonizing RORgammat function.* Nature, 2008. **453**(7192): p. 236-40.
55. Sun, M., et al., *Microbiota-derived short-chain fatty acids promote Th1 cell IL-10 production to maintain intestinal homeostasis.* Nat Commun, 2018. **9**(1): p. 3555.
56. Li, B., et al., *IL-10 modulates DSS-induced colitis through a macrophage-ROS-NO axis.* Mucosal Immunol, 2014. **7**(4): p. 869-78.
57. Zigmond, E., et al., *Macrophage-restricted interleukin-10 receptor deficiency, but not IL-10 deficiency, causes severe spontaneous colitis.* Immunity, 2014. **40**(5): p. 720-33.
58. Gunasekera, D.C., et al., *The development of colitis in Il10(-/-) mice is dependent on IL-22.* Mucosal Immunol, 2020. **13**(3): p. 493-506.
59. Qasimi, P., et al., *Divergent mechanisms utilized by SOCS3 to mediate interleukin-10 inhibition of tumor necrosis factor alpha and nitric oxide production by macrophages.* J Biol Chem, 2006.

281(10): p. 6316-24.
60. Qin, H., et al., *SOCS3 deficiency promotes M1 macrophage polarization and inflammation.* J Immunol, 2012. **189**(7): p. 3439-48.
61. Meguro, K., et al., *SOCS3 Expressed in M2 Macrophages Attenuates Contact Hypersensitivity by Suppressing MMP-12 Production.* J Invest Dermatol, 2016. **136**(3): p. 649-657.
62. Qin, H., et al., *Signal transducer and activator of transcription-3/suppressor of cytokine signaling-3 (STAT3/SOCS3) axis in myeloid cells regulates neuroinflammation.* Proc Natl Acad Sci U S A, 2012. **109**(13): p. 5004-9.
63. Jiang, Z., et al., *Lack of SOCS3 increases LPS-induced murine acute lung injury through modulation of Ly6C(+) macrophages.* Respir Res, 2017. **18**(1): p. 217.
64. M J Carter, F.S.d.G., S Jones, J Mee, N J Camp, A J Lobo, G W Duff, *Association of the interleukin 1 receptor antagonist gene with ulcerative colitis in Northern European Caucasians.* Gut, 2001. **48**: p. 461-467.
65. Maeda, S., et al., *Mucosal imbalance of interleukin-1beta and interleukin-1 receptor antagonist in canine inflammatory bowel disease.* Vet J, 2012. **194**(1): p. 66-70.
66. Gabay, W.P.A.a.C., *Physiologic role of interleukin-1 receptor antagonist.* Arthritis Res, 2000. **2**: p. 245-248.
67. Eligini, S., et al., *Inhibition of transglutaminase 2 reduces efferocytosis in human macrophages: Role of CD14 and SR-AI receptors.* Nutr Metab Cardiovasc Dis, 2016. **26**(10): p. 922-30.
68. Scientific, T.F. *Macrophage Cell Overview*. n.d. December 18, 2021]; Available from: https://www.thermofisher.com/hk/en/home/life-science/cell-analysis/cell-analysis-learning-center/immunology-at-work/macrophage-cell-overview.html.
69. Novotna, K., et al., *Microplastics in drinking water treatment - Current knowledge and research needs.* Sci Total Environ, 2019. **667**: p. 730-740.
70. Schymanski, D., et al., *Analysis of microplastics in water by micro-Raman spectroscopy: Release of plastic particles from different packaging into mineral water.* Water Res, 2018. **129**: p. 154-162.
71. Smith, M., et al., *Microplastics in Seafood and the Implications for Human Health.* Curr Environ Health Rep, 2018. **5**(3): p. 375-386.
72. Liebezeit, G. and E. Liebezeit, *Non-pollen particulates in honey and sugar.* Food Addit Contam Part A Chem Anal Control Expo Risk Assess, 2013. **30**(12): p. 2136-40.
73. Powell, J.J., et al., *Origin and fate of dietary nanoparticles and microparticles in the gastrointestinal tract.* J Autoimmun, 2010. **34**(3): p. J226-33.
74. Tong, H., et al., *Occurrence and identification of microplastics in tap water from China.* Chemosphere, 2020. **252**: p. 126493.
75. Deng, Y., et al., *Tissue accumulation of microplastics in mice and biomarker responses suggest widespread health risks of exposure.* Sci Rep, 2017. **7**: p. 46687.
76. Leslie, H.A., et al., *Discovery and quantification of plastic particle pollution in human blood.* Environ Int, 2022. **163**: p. 107199.
77. I. Voronov, J.P.S., A. Hinek, J. W. Callahan, J. Sandhu, E. L. Boynton, *Macrophage phagocytosis of polyethylene particulate in vitro.* Journal of Biomedical Materials Research, 1998. **39**: p. 40-51.
78. T R Green, J.F., M Stone, B M Wroblewski, E Ingham, *Polyethylene particles of a 'critical size' are necessary for the induction of cytokines by macrophages in vitro.* Biomaterials, 1998. **19**(24).
79. E. L. Boynton, J.W., E. Meek,R. S. Labow,V. Edwards,J. P. Santerre, *The effect of polyethylene particle chemistry on human monocyte-macrophage function in vitro.* Journal of Biomedical

Materials Research, 2000. **52**(2): p. 239-245.
80. Palaniappan, S., C.M. Sadacharan, and B. Rostama, *Polystyrene and Polyethylene Microplastics Decrease Cell Viability and Dysregulate Inflammatory and Oxidative Stress Markers of MDCK and L929 Cells In Vitro.* Expo Health, 2021: p. 1-11.
81. Bahrami, N., et al., *Evaluating the protective effects of melatonin on di(2-ethylhexyl) phthalate-induced testicular injury in adult mice.* Biomed Pharmacother, 2018. **108**: p. 515-523.
82. Liang, F. and B. Yan, *Oxidative damage in the liver and kidney induced by dermal exposure to diisononyl phthalate in Balb/c mice.* Toxicol Ind Health, 2020. **36**(1): p. 30-40.
83. Kurchaba, N., et al., *Effects of MP Polyethylene Microparticles on Microbiome and Inflammatory Response of Larval Zebrafish.* Toxics, 2020. **8**(3).
84. Sun, H., et al., *Effects induced by polyethylene microplastics oral exposure on colon mucin release, inflammation, gut microflora composition and metabolism in mice.* Ecotoxicol Environ Saf, 2021. **220**: p. 112340.
85. Tsumura, Y., et al., *Estimated daily intake of plasticizers in 1-week duplicate diet samples following regulation of DEHP-containing PVC gloves in Japan.* Food Addit Contam, 2003. **20**(4): p. 317-24.
86. Wang, Y. and H. Qian, *Phthalates and Their Impacts on Human Health.* Healthcare (Basel), 2021. **9**(5).
87. CFS-HKSAR. *Plasticisers in food*. 2018 [cited 2019; Available from: https://www.cfs.gov.hk/english/consumer_zone/foodsafety_contaminants_DEHP_Q&A_4.html.
88. Cheng, J., et al., *Relative Influence of Plastic Debris Size and Shape, Chemical Composition and Phytoplankton-Bacteria Interactions in Driving Seawater Plastisphere Abundance, Diversity and Activity.* Front Microbiol, 2020. **11**: p. 610231.
89. Chung, H.C., et al., *Bacterial community succession and chemical profiles of subtidal biofilms in relation to larval settlement of the polychaete Hydroides elegans.* ISME J, 2010. **4**(6): p. 817-28.
90. Chen, H., et al., *Investigation of Microplastics in Digestion System: Effect on Surface Microstructures and Probiotics.* Bull Environ Contam Toxicol, 2022.
91. Nagpal, R., et al., *Comparative Microbiome Signatures and Short-Chain Fatty Acids in Mouse, Rat, Non-human Primate, and Human Feces.* Front Microbiol, 2018. **9**: p. 2897.
92. de Simone, C., *The Unregulated Probiotic Market.* Clin Gastroenterol Hepatol, 2019. **17**(5): p. 809-817.
93. Arora, M. and A. Baldi, *Regulatory categories of probiotics across the globe: a review representing existing and recommended categorization.* Indian J Med Microbiol, 2015. **33 Suppl**: p. 2-10.
94. TANAKA, H., *Current System for Regulation of Health Foods in Japan.* Journal of the Japan Medical Association, 2004. **126**(6): p. 792–805.
95. Kuda, T., et al., *Suppressive effect of Tetragenococcus halophilus, isolated from fish-nukazuke, on histamine accumulation in salted and fermented fish.* Food Chemistry, 2012. **130**(3): p. 569-574.
96. Borges, S., et al., *Effects of processing and storage on Pediococcus pentosaceus SB83 in vaginal formulations: lyophilized powder and tablets.* Biomed Res Int, 2013. **2013**: p. 680767.
97. Adriana Nowak, I.M., *In vitro anti-adherence effect of probiotic Lactobacillus strains on human enteropathogens.* Biotechnology and Food Science, 2017. **81**(2): p. 103-112.
98. Jayashree, S., et al., *Anti-adhesion Property of the Potential Probiotic Strain Lactobacillus fermentum 8711 Against Methicillin-Resistant Staphylococcus aureus (MRSA).* Front Microbiol, 2018. **9**: p. 411.

99. Li, C., et al., *Effect of Lactobacillus plantarum NCU116 on loperamide-induced constipation in mice.* Int J Food Sci Nutr, 2015. **66**(5): p. 533-8.
100. Xie, J., et al., *Effects of Lactobacillus plantarum NCU116 on Intestine Mucosal Immunity in Immunosuppressed Mice.* J Agric Food Chem, 2015. **63**(51): p. 10914-20.
101. Li, C., et al., *Cholesterol-lowering effect of Lactobacillus plantarum NCU116 in a hyperlipidaemic rat model.* Journal of Functional Foods, 2014. **8**: p. 340-347.
102. Darfeuille-Michaud, N.B.a.A., *Adherent-invasive Escherichia coli and Crohn's disease.* Current Opinion in Gastroenterology, 2007. **23**: p. 16-20.
103. Engevik, M.A., et al., *Bifidobacterium dentium Fortifies the Intestinal Mucus Layer via Autophagy and Calcium Signaling Pathways.* mBio, 2019. **10**(3).
104. Gao, J., et al., *A Novel Postbiotic From Lactobacillus rhamnosus GG With a Beneficial Effect on Intestinal Barrier Function.* Front Microbiol, 2019. **10**: p. 477.
105. Malin E. V. Johansson, M.P., Joel Petersson, Anna Velcich, Lena Holm, and Gunnar C. Hansson, *The inner of the two Muc2 mucin-dependent mucus layers in colon is devoid of bacteria.* PNAS, 2008. **15**(39): p. 15064–15069.
106. Macias-Rodriguez, M.E., et al., *Lactobacillus fermentum BCS87 expresses mucus- and mucin-binding proteins on the cell surface.* J Appl Microbiol, 2009. **107**(6): p. 1866-74.
107. Watanabe, M., et al., *An adhesin-like protein, Lam29, from Lactobacillus mucosae ME-340 binds to histone H3 and blood group antigens in human colonic mucus.* Biosci Biotechnol Biochem, 2012. **76**(9): p. 1655-60.
108. Miyoshi, Y., et al., *A mucus adhesion promoting protein, MapA, mediates the adhesion of Lactobacillus reuteri to Caco-2 human intestinal epithelial cells.* Biosci Biotechnol Biochem, 2006. **70**(7): p. 1622-8.
109. von Ossowski, I., et al., *Mucosal adhesion properties of the probiotic Lactobacillus rhamnosus GG SpaCBA and SpaFED pilin subunits.* Appl Environ Microbiol, 2010. **76**(7): p. 2049-57.
110. Nishiyama, K., et al., *Adhesion properties of Lactobacillus rhamnosus mucus-binding factor to mucin and extracellular matrix proteins.* Biosci Biotechnol Biochem, 2015. **79**(2): p. 271-9.
111. Pretzer, G., et al., *Biodiversity-based identification and functional characterization of the mannose-specific adhesin of Lactobacillus plantarum.* J Bacteriol, 2005. **187**(17): p. 6128-36.
112. Johnson-Henry, K.C., et al., *Lactobacillus rhamnosus strain GG prevents enterohemorrhagic Escherichia coli O157:H7-induced changes in epithelial barrier function.* Infect Immun, 2008. **76**(4): p. 1340-8.
113. Sollid, J.U., et al., *Staphylococcus aureus: determinants of human carriage.* Infect Genet Evol, 2014. **21**: p. 531-41.
114. Talaro, K.P., *Foundations in microbiology*. Ninth edition.. ed, ed. B. Chess. 2015, New York, NY: New York, NY : McGraw-Hill Education.
115. Hadjirin, N.F., et al., *Detection of livestock-associated meticillin-resistant Staphylococcus aureus CC398 in retail pork, United Kingdom, February 2015.* Euro surveillance : bulletin Europeen sur les maladies transmissibles = European communicable disease bulletin, 2015. **20**(24).
116. Murphy, J., et al., *Staphylococcus Aureus V8 protease disrupts the integrity of the airway epithelial barrier and impairs IL-6 production in vitro.* Laryngoscope, 2018. **128**(1): p. E8-E15.
117. Becker, K., et al., *The clinical impact of livestock-associated methicillin-resistant Staphylococcus aureus of the clonal complex 398 for humans.* Veterinary Microbiology, 2017. **200**(C): p. 33-38.
118. Foster, T.J. and M. Höök, *Surface protein adhesins of Staphylococcus aureus.* Trends in Microbiology, 1998. **6**(12): p. 484-488.
119. Wells, C.L., et al., *Inducible Expression of Enterococcus faecalis Aggregation Substance Surface*

Protein Facilitates Bacterial Internalization by Cultured Enterocytes. Infection and Immunity, 2000. **68**(12): p. 7190.
120. Isenmann, R., et al., *Aggregation substance promotes colonic mucosal invasion of Enterococcus faecalis in an ex vivo model.* J Surg Res, 2000. **89**(2): p. 132-8.
121. Kreft, B., et al., *Aggregation substance of Enterococcus faecalis mediates adhesion to cultured renal tubular cells.* Infection and Immunity, 1992. **60**(1): p. 25.
122. Olmsted, S.B., et al., *A Plasmid-Encoded Surface Protein on Enterococcus faecalis Augments Its Internalization by Cultured Intestinal Epithelial Cells.* The Journal of Infectious Diseases, 1994. **170**(6): p. 1549-1556.
123. Nallapareddy, S.R., et al., *Enterococcus faecalis Adhesin, Ace, Mediates Attachment to Extracellular Matrix Proteins Collagen Type IV and Laminin as well as Collagen Type I.* Infection and Immunity, 2000. **68**(9): p. 5218.
124. Suzuki, T., N. Yoshinaga, and S. Tanabe, *Interleukin-6 (IL-6) regulates claudin-2 expression and tight junction permeability in intestinal epithelium.* J Biol Chem, 2011. **286**(36): p. 31263-71.
125. Eckburg, P.B., et al., *Diversity of the human intestinal microbial flora.* Science (New York, N.Y.), 2005. **308**(5728): p. 1635.
126. Petrof, E.O., et al., *Bacteria-free solution derived from Lactobacillus plantarum inhibits multiple NF-kappaB pathways and inhibits proteasome function.* Inflamm Bowel Dis, 2009. **15**(10): p. 1537-47.
127. Jo, S.G., et al., *Lactobacillus curvatus WiKim38 isolated from kimchi induces IL-10 production in dendritic cells and alleviates DSS-induced colitis in mice.* J Microbiol, 2016. **54**(7): p. 503-9.
128. Sakai, F., et al., *Lactobacillus gasseri SBT2055 induces TGF-beta expression in dendritic cells and activates TLR2 signal to produce IgA in the small intestine.* PLoS One, 2014. **9**(8): p. e105370.
129. Wu, H., T.F. Shum, and J. Chiou, *Characterization of the Probiotic Potential of Lactic Acid Bacteria Isolated from Kimchi, Yogurt, and Baby Feces in Hong Kong and Their Performance in Soymilk Fermentation.* Microorganisms, 2021. **9**(12).
130. Halder, D., et al., *Indigenous Probiotic Lactobacillus Isolates Presenting Antibiotic like Activity against Human Pathogenic Bacteria.* Biomedicines, 2017. **5**(2).
131. Hassanzadazar, H., et al., *Investigation of antibacterial, acid and bile tolerance properties of lactobacilli isolated from Koozeh cheese.* Veterinary Research Forum, 2012. **3**(3): p. 181-185.
132. Damayanti, E., et al., *Characterization of Lactic Acid Bacteria as Poultry Probiotic Candidates with Aflatoxin B1 Binding Activities.* IOP Conference Series: Earth and Environmental Science, 2017. **101**.
133. Ren, D., et al., *Inhibition of Staphylococcus aureus adherence to Caco-2 cells by lactobacilli and cell surface properties that influence attachment.* Anaerobe, 2012. **18**(5): p. 508-15.
134. Song, A.X., et al., *Bifidogenic effects of Cordyceps sinensis fungal exopolysaccharide and konjac glucomannan after ultrasound and acid degradation.* Int J Biol Macromol, 2018. **111**: p. 587-594.
135. Zhao, G., M. Nyman, and J.A. Jonsson, *Rapid determination of short-chain fatty acids in colonic contents and faeces of humans and rats by acidified water-extraction and direct-injection gas chromatography.* Biomed Chromatogr, 2006. **20**(8): p. 674-82.
136. Rzepkowska, A., et al., *Safety assessment and antimicrobial properties of the lactic acid bacteria strains isolated from polish raw fermented meat products.* International Journal of Food Properties, 2017. **20**(11): p. 2736-2747.
137. Vijayakumar, P.P. and P.M. Muriana, *Inhibition of Listeria monocytogenes on Ready-to-Eat*

Meats Using Bacteriocin Mixtures Based on Mode-of-Action. Foods, 2017. **6**(3).
138. Matti Kankainena, L.P., Soile Tynkkynenb, Ingemar von Ossowskic, Justus Reunanenc, Pasi Partanena,, et al., *Comparative genomic analysis of Lactobacillus rhamnosus GG reveals pili containing a human-mucus binding protein.* PNAS, 2009. **106**(40): p. 17193–17198.
139. von Ossowski, I., et al., *Functional characterization of a mucus-specific LPXTG surface adhesin from probiotic Lactobacillus rhamnosus GG.* Appl Environ Microbiol, 2011. **77**(13): p. 4465-72.
140. Van den Abbeele, P., et al., *Butyrate-producing Clostridium cluster XIVa species specifically colonize mucins in an in vitro gut model.* ISME J, 2013. **7**(5): p. 949-61.
141. Garcia-Villalba, R., et al., *Gastrointestinal Simulation Model TWIN-SHIME Shows Differences between Human Urolithin-Metabotypes in Gut Microbiota Composition, Pomegranate Polyphenol Metabolism, and Transport along the Intestinal Tract.* J Agric Food Chem, 2017. **65**(27): p. 5480-5493.
142. Van den Abbeele, P., et al., *Incorporating a mucosal environment in a dynamic gut model results in a more representative colonization by lactobacilli.* Microb Biotechnol, 2012. **5**(1): p. 106-15.
143. Koper, J.E.B., et al., *Polyphenols and Tryptophan Metabolites Activate the Aryl Hydrocarbon Receptor in an in vitro Model of Colonic Fermentation.* Mol Nutr Food Res, 2019. **63**(3): p. e1800722.
144. Requile, M., et al., *Use of a combination of in vitro models to investigate the impact of chlorpyrifos and inulin on the intestinal microbiota and the permeability of the intestinal mucosa.* Environ Sci Pollut Res Int, 2018. **25**(23): p. 22529-22540.
145. Samah O Noor, K.R., Louise Scovell, E Katherine Kemsley, Elizabeth K Lund, Crawford Jamieson, Ian T Johnson, Arjan Narbad, *Ulcerative colitis and irritable bowel patients exhibit distinct abnormalities of the gut microbiota.* BMC Gastroenterology, 2010. **10**(10).
146. Chen, L., et al., *Megasphaera elsdenii Lactate Degradation Pattern Shifts in Rumen Acidosis Models.* Front Microbiol, 2019. **10**: p. 162.
147. Kenta Hashizume, T.T., Kouji Yamada, and H.K.a.K. Ushida, *Megasphaera elsdenii JCM1772T Normalizes Hyperlactate Production in the Large Intestine of Fructooligosaccharide-Fed Rats by Stimulating Butyrate Production.* Nutrient Metabolism-Research Communication, 2003. **133**: p. 3187–3190.
148. Sato, N., et al., *The relationship between cigarette smoking and the tongue microbiome in an East Asian population.* J Oral Microbiol, 2020. **12**(1): p. 1742527.
149. Wang, X., et al., *Microbial Community Analysis of Saliva and Biopsies in Patients With Oral Lichen Planus.* Front Microbiol, 2020. **11**: p. 629.
150. van Teijlingen, N.H., et al., *Vaginal dysbiosis associated-bacteria Megasphaera elsdenii and Prevotella timonensis induce immune activation via dendritic cells.* J Reprod Immunol, 2020. **138**: p. 103085.
151. Olmeda, D., et al., *Snail silencing effectively suppresses tumour growth and invasiveness.* Oncogene, 2007. **26**(13): p. 1862-74.
152. Jagle, S., et al., *SNAIL1-mediated downregulation of FOXA proteins facilitates the inactivation of transcriptional enhancer elements at key epithelial genes in colorectal cancer cells.* PLoS Genet, 2017. **13**(11): p. e1007109.
153. Gatti, S., et al., *Effects of the Exclusive Enteral Nutrition on the Microbiota Profile of Patients with Crohn's Disease: A Systematic Review.* Nutrients, 2017. **9**(8).
154. Kelly, T.N., et al., *Gut Microbiome Associates With Lifetime Cardiovascular Disease Risk Profile Among Bogalusa Heart Study Participants.* Circ Res, 2016. **119**(8): p. 956-64.
155. Boer, C.G., et al., *Intestinal microbiome composition and its relation to joint pain and*

inflammation. Nat Commun, 2019. **10**(1): p. 4881.
156. Kesavalu, L., et al., *Increased atherogenesis during Streptococcus mutans infection in ApoE-null mice.* J Dent Res, 2012. **91**(3): p. 255-60.
157. Zheng, L., et al., *Microbial-Derived Butyrate Promotes Epithelial Barrier Function through IL-10 Receptor–Dependent Repression of Claudin-2.* The Journal of Immunology, 2017. **199**(8): p. 2976-2984.
158. Hogberg, J., et al., *Phthalate diesters and their metabolites in human breast milk, blood or serum, and urine as biomarkers of exposure in vulnerable populations.* Environ Health Perspect, 2008. **116**(3): p. 334-9.
159. Rusyn, I. and J.C. Corton, *Mechanistic considerations for human relevance of cancer hazard of di(2-ethylhexyl) phthalate.* Mutat Res, 2012. **750**(2): p. 141-58.
160. Rowdhwal, S.S.S. and J. Chen, *Toxic Effects of Di-2-ethylhexyl Phthalate: An Overview.* Biomed Res Int, 2018. **2018**: p. 1750368.
161. Hao, C., et al., *The endocrine disruptor mono-(2-ethylhexyl) phthalate promotes adipocyte differentiation and induces obesity in mice.* Biosci Rep, 2012. **32**(6): p. 619-29.
162. Hines, C.J., et al., *Estimated daily intake of phthalates in occupationally exposed groups.* J Expo Sci Environ Epidemiol, 2011. **21**(2): p. 133-41.
163. Adamovsky, O., et al., *Evaluation of Microbiome-Host Relationships in the Zebrafish Gastrointestinal System Reveals Adaptive Immunity Is a Target of Bis(2-ethylhexyl) Phthalate (DEHP) Exposure.* Environ Sci Technol, 2020. **54**(9): p. 5719-5728.
164. Chiu, K.K., et al., *Isolation of DiNP-Degrading Microbes from the Mouse Colon and the Influence DiNP Exposure Has on the Microbiota, Intestinal Integrity, and Immune Status of the Colon.* Toxics, 2022. **10**(2).
165. Pereyra-Camacho, M.A., V.E. Balderas-Hernandez, and A. De Leon-Rodriguez, *Biodegradation of diisononyl phthalate by a consortium of saline soil bacteria: optimisation and kinetic characterisation.* Appl Microbiol Biotechnol, 2021. **105**(8): p. 3369-3380.
166. Yang, T., et al., *Biodegradation of Di-(2-ethylhexyl) Phthalate by Rhodococcus ruber YC-YT1 in Contaminated Water and Soil.* Int J Environ Res Public Health, 2018. **15**(5).
167. Li, F., et al., *Biodegradation of di-(2-ethylhexyl) phthalate by a halotolerant consortium LF.* PLoS One, 2018. **13**(10): p. e0204324.
168. Chang-Liao, W.L., et al., *Determination and pharmacokinetics of di-(2-ethylhexyl) phthalate in rats by ultra performance liquid chromatography with tandem mass spectrometry.* Molecules, 2013. **18**(9): p. 11452-66.
169. Koch, H.M. and J. Angerer, *Di-iso-nonylphthalate (DINP) metabolites in human urine after a single oral dose of deuterium-labelled DINP.* Int J Hyg Environ Health, 2007. **210**(1): p. 9-19.
170. McKee, R.H., et al., *Absorption, disposition and metabolism of di-isononyl phthalate (DINP) in F-344 rats.* J Appl Toxicol, 2002. **22**(5): p. 293-302.
171. Chang, J.W., et al., *Estimated Daily Intake and Cumulative Risk Assessment of Phthalates in the General Taiwanese after the 2011 DEHP Food Scandal.* Sci Rep, 2017. **7**: p. 45009.
172. Centre for Food Safety, F.a.E.H.D., The Government of the Hong Kong Special Administrative Region, *Risk Assessment Studies Report No. 57 Chemical Hazard Evaluation - Phthalates in Food.* 2018.
173. Gevers, D., et al., *The treatment-naive microbiome in new-onset Crohn's disease.* Cell Host Microbe, 2014. **15**(3): p. 382-392.
174. Chiodini, R.J., et al., *Microbial Population Differentials between Mucosal and Submucosal Intestinal Tissues in Advanced Crohn's Disease of the Ileum.* PLoS One, 2015. **10**(7): p.

e0134382.
175. Alam, M.T., et al., *Microbial imbalance in inflammatory bowel disease patients at different taxonomic levels.* Gut Pathogens, 2020. **12**(1).
176. Lo Presti, A., et al., *Fecal and Mucosal Microbiota Profiling in Irritable Bowel Syndrome and Inflammatory Bowel Disease.* Front Microbiol, 2019. **10**: p. 1655.
177. Gerasimidis, K., et al., *Decline in presumptively protective gut bacterial species and metabolites are paradoxically associated with disease improvement in pediatric Crohn's disease during enteral nutrition.* Inflamm Bowel Dis, 2014. **20**(5): p. 861-71.
178. Michael S. Caplan, R.M.C., Susan Kaup, Tanya Russell, Matthew Lickerman, Michael Amer, Yu Xiao, And Richard Thomson, Jr., *Bifidobacterial Supplementation Reduces the Incidence of Necrotizing Enterocolitis in a Neonatal Rat Model.* Gastroenterology, 1999. **117**(3): p. 577-583.
179. Felix Sommer, M.C.R., et al., *Microbiomarkers in inflammatory bowel diseases caveats come with caviar.* Gut, 2017. **66**(10): p. 1734-1738.
180. Martin Lipkin, P.S., Bertrand M. Bell, *Generation Time of Epithelial Cells in the Human Colon.* Nature, 1962. **195**.
181. Kucharzik, T., et al., *Neutrophil Transmigration in Inflammatory Bowel Disease Is Associated with Differential Expression of Epithelial Intercellular Junction Proteins.* The American Journal of Pathology, 2001. **159**(6): p. 2001-2009.
182. Taman, H., et al., *Transcriptomic Landscape of Treatment—Naïve Ulcerative Colitis.* Journal of Crohn's and Colitis, 2018. **12**(3): p. 327-336.
183. Liu, X., et al., *Microbial products induce claudin-2 to compromise gut epithelial barrier function.* PLoS One, 2013. **8**(8): p. e68547.
184. Shastri, S., et al., *Idebenone Protects against Acute Murine Colitis via Antioxidant and Anti-Inflammatory Mechanisms.* Int J Mol Sci, 2020. **21**(2).
185. Segui, J., et al., *Superoxide dismutase ameliorates TNBS-induced colitis by reducing oxidative stress, adhesion molecule expression, and leukocyte recruitment into the inflamed intestine.* J Leukoc Biol, 2004. **76**(3): p. 537-44.
186. Damiani, C.R., et al., *Oxidative stress and metabolism in animal model of colitis induced by dextran sulfate sodium.* J Gastroenterol Hepatol, 2007. **22**(11): p. 1846-51.
187. Martinez, F.O., et al., *Genetic programs expressed in resting and IL-4 alternatively activated mouse and human macrophages: similarities and differences.* Blood, 2013. **121**(9): p. e57-69.
188. Zhu, W., et al., *Baicalin ameliorates experimental inflammatory bowel disease through polarization of macrophages to an M2 phenotype.* Int Immunopharmacol, 2016. **35**: p. 119-126.
189. Cox, K.D., et al., *Human Consumption of Microplastics.* Environmental Science & Technology, 2019. **53**(12): p. 7068-7074.
190. Zhang, Z., et al., *Polyvinyl chloride degradation by a bacterium isolated from the gut of insect larvae.* Nat Commun, 2022. **13**(1): p. 5360.
191. Fang, H., J. Wang, and R.A. Lynch, *Migration of di(2-ethylhexyl)phthalate (DEHP) and di- n -butylphthalate (DBP) from polypropylene food containers.* Food Control, 2017. **73**: p. 1298-1302.
192. Moreira, M.A., L.C. Andre, and Z.L. Cardeal, *Analysis of phthalate migration to food simulants in plastic containers during microwave operations.* Int J Environ Res Public Health, 2013. **11**(1): p. 507-26.
193. Barakat, R., et al., *Germline-dependent transmission of male reproductive traits induced by an endocrine disruptor, di-2-ethylhexyl phthalate, in future generations.* Sci Rep, 2020. **10**(1): p. 5705.

194. Hart, R.J., et al., *The Possible Impact of Antenatal Exposure to Ubiquitous Phthalates Upon Male Reproductive Function at 20 Years of Age.* Front Endocrinol (Lausanne), 2018. **9**: p. 288.
195. Crobeddu, B., et al., *Di(2-ethylhexyl) phthalate (DEHP) increases proliferation of epithelial breast cancer cells through progesterone receptor dysregulation.* Environ Res, 2019. **173**: p. 165-173.
196. Jadhao, M., et al., *The Long-Term DEHP Exposure Confers Multidrug Resistance of Triple-Negative Breast Cancer Cells through ABC Transporters and Intracellular ROS.* Antioxidants (Basel), 2021. **10**(6).
197. Miao, Y., et al., *Lifetime cancer risk assessment for inhalation exposure to di(2-ethylhexyl) phthalate (DEHP).* Environ Sci Pollut Res Int, 2017. **24**(1): p. 312-320.
198. Hsin-Pao Chen, Y.-K.L., Shih Yin Huang, Pei-Chun Shi, Ping-Chi and H.a.C.-F. Chang, *Phthalate exposure promotes chemotherapeutic drug resistance in colon cancer cells.* Oncotarget, 2018. **9**(17): p. 13167-13180.
199. Busch, M., et al., *Investigations of acute effects of polystyrene and polyvinyl chloride micro- and nanoplastics in an advanced in vitro triple culture model of the healthy and inflamed intestine.* Environ Res, 2021. **193**: p. 110536.
200. Pei, D., et al., *DEHP chronic exposure disturbs the gut microbial community and metabolic homeostasis: Genderbased differences in zebrafish.* 2020.
201. Ma, Z.F., Y.S. Ibrahim, and Y.Y. Lee, *Microplastic Pollution and Health and Relevance to the Malaysia's Roadmap to Zero Single-Use Plastics 2018-2030.* Malays J Med Sci, 2020. **27**(3): p. 1-6.
202. Parada Venegas, D., et al., *Short Chain Fatty Acids (SCFAs)-Mediated Gut Epithelial and Immune Regulation and Its Relevance for Inflammatory Bowel Diseases.* Front Immunol, 2019. **10**: p. 277.
203. Vacca, M., et al., *The Controversial Role of Human Gut Lachnospiraceae.* Microorganisms, 2020. **8**(4).
204. Aden, K., et al., *Metabolic Functions of Gut Microbes Associate With Efficacy of Tumor Necrosis Factor Antagonists in Patients With Inflammatory Bowel Diseases.* Gastroenterology, 2019. **157**(5): p. 1279-1292 e11.
205. Swidsinski, A., et al., *Mucosal flora in inflammatory bowel disease.* Gastroenterology, 2002. **122**(1): p. 44-54.
206. Astbury, S., et al., *Lower gut microbiome diversity and higher abundance of proinflammatory genus Collinsella are associated with biopsy-proven nonalcoholic steatohepatitis.* Gut Microbes, 2020. **11**(3): p. 569-580.
207. Chen, J., et al., *An expansion of rare lineage intestinal microbes characterizes rheumatoid arthritis.* Genome Med, 2016. **8**(1): p. 43.
208. Raul Y. Tito, H.C., Marie Joossens,Ga€elle Varkas, Liesbet Van Praet, Elien Glorieus, Filip Van den Bosch, Martine De Vos, Jeroen Raes, and Dirk Elewaut, *Dialister as a Microbial Marker of Disease Activity in Spondyloarthritis.* ARTHRITIS & RHEUMATOLOGY, 2017. **69**(1): p. 114–121.
209. Ma, Y., et al., *Physical and chemical modifications of poly(vinyl chloride) materials to prevent plasticizer migration - Still on the run.* Reactive and Functional Polymers, 2020. **147**.
210. Jeongsoo Choi, S.-Y.K., *Hyperbranched Poly(E-caprolactone) as a Nonmigrating Alternative Plasticizer for Phthalates in Flexible PVC.* Environmental Science & Technology, 2007. **41**(10): p. 3763–3768.
211. Chen, Q., et al., *Lactic acid bacteria alleviate di-(2-ethylhexyl) phthalate-induced liver and testis*

toxicity via their bio-binding capacity, antioxidant capacity and regulation of the gut microbiota. Environ Pollut, 2022. **305**: p. 119197.
212. Mouafo Tamnou, E.B., et al., *Biodegradation of polyethylene by the bacterium Pseudomonas aeruginosa in acidic aquatic microcosm and effect of the environmental temperature.* Environmental Challenges, 2021. **3**.
213. Li, B., et al., *Polyethylene microplastics affect the distribution of gut microbiota and inflammation development in mice.* Chemosphere, 2020. **244**: p. 125492.
214. Cani, P.D., et al., *Changes in gut microbiota control inflammation in obese mice through a mechanism involving GLP-2-driven improvement of gut permeability.* Gut, 2009. **58**(8): p. 1091-103.
215. Moratalla, A., et al., *Protective effect of Bifidobacterium pseudocatenulatum CECT7765 against induced bacterial antigen translocation in experimental cirrhosis.* Liver Int, 2014. **34**(6): p. 850-8.
216. Underwood, M.A., et al., *Bifidobacterium longum subspecies infantis: champion colonizer of the infant gut.* Pediatr Res, 2015. **77**(1-2): p. 229-35.
217. Martin, R., et al., *Bifidobacterium animalis ssp. lactis CNCM-I2494 Restores Gut Barrier Permeability in Chronically Low-Grade Inflamed Mice.* Front Microbiol, 2016. **7**: p. 608.
218. Ozato, N., et al., *Blautia genus associated with visceral fat accumulation in adults 20-76 years of age.* NPJ Biofilms Microbiomes, 2019. **5**(1): p. 28.
219. Tang, W., et al., *Modulation of the Gut Microbiota in Rats by Hugan Qingzhi Tablets during the Treatment of High-Fat-Diet-Induced Nonalcoholic Fatty Liver Disease.* Oxid Med Cell Longev, 2018. **2018**: p. 7261619.
220. Hu, R., et al., *Dietary protocatechuic acid ameliorates inflammation and up-regulates intestinal tight junction proteins by modulating gut microbiota in LPS-challenged piglets.* J Anim Sci Biotechnol, 2020. **11**: p. 92.
221. Shimizu, J., et al., *Relative abundance of Megamonas hypermegale and Butyrivibrio species decreased in the intestine and its possible association with the T cell aberration by metabolite alteration in patients with Behcet's disease (210 characters).* Clin Rheumatol, 2019. **38**(5): p. 1437-1445.
222. Kieler, I.N., et al., *Gut microbiota composition may relate to weight loss rate in obese pet dogs.* Vet Med Sci, 2017. **3**(4): p. 252-262.
223. Feng, Z., et al., *A human stool-derived Bilophila wadsworthia strain caused systemic inflammation in specific-pathogen-free mice.* Gut Pathog, 2017. **9**: p. 59.
224. Natividad, J.M., et al., *Bilophila wadsworthia aggravates high fat diet induced metabolic dysfunctions in mice.* Nat Commun, 2018. **9**(1): p. 2802.
225. David, L.A., et al., *Diet rapidly and reproducibly alters the human gut microbiome.* Nature, 2014. **505**(7484): p. 559-63.
226. Altomare, A., et al., *Gut mucosal-associated microbiota better discloses inflammatory bowel disease differential patterns than faecal microbiota.* Dig Liver Dis, 2019. **51**(5): p. 648-656.
227. Zheng, J., et al., *Dietary inflammatory potential in relation to the gut microbiome: results from a cross-sectional study.* Br J Nutr, 2020. **124**(9): p. 931-942.
228. Marchiando, A.M., et al., *Caveolin-1-dependent occludin endocytosis is required for TNF-induced tight junction regulation in vivo.* J Cell Biol, 2010. **189**(1): p. 111-26.
229. Wang, H.Y., et al., *Occludin endocytosis is involved in the disruption of the intestinal epithelial barrier in a mouse model of alcoholic steatohepatitis.* J Dig Dis, 2019. **20**(9): p. 476-485.
230. Ares, G., et al., *Caveolin 1 is Associated with Upregulated Claudin 2 in Necrotizing*

Enterocolitis. Sci Rep, 2019. **9**(1): p. 4982.
231. Stamatovic, S.M., et al., *Endocytosis of tight junction proteins and the regulation of degradation and recycling.* Ann N Y Acad Sci, 2017. **1397**(1): p. 54-65.